Electrochemical Society

Columbus Meeting Program Issue

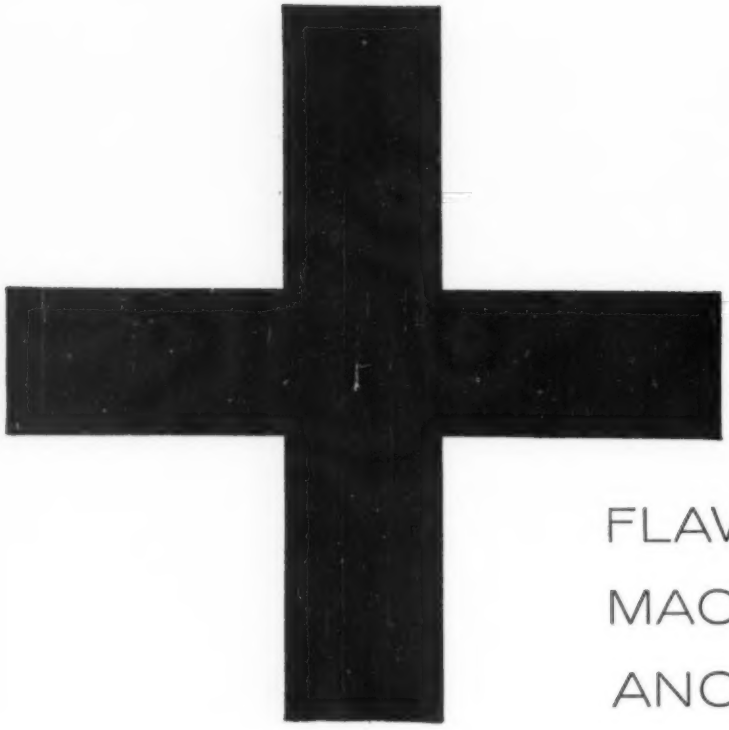

FLAWLESSLY MACHINED ANODES

are your assurance of trouble-free, cost-saving performance. Every GLC anode is custom made to your requirements and machined precisely to your engineering drawings.

This faithful observance of close tolerances is characteristic of a markedly superior product. Let comparisons prove this to you.

PRODUCTS ELECTRODE GLC DIVISION YOU CAN TRUST

GREAT LAKES CARBON CORPORATION

18 EAST 48TH STREET, NEW YORK 17, N. Y. OFFICES IN PRINCIPAL CITIES

EDITORIAL STAFF

H. H. Uhlig, Chairman, Publication Committee

Cecil V. King, Editor

Norman Hackerman, Technical Editor

Ruth G. Sterns, Managing Editor

U. B. Thomas, News Editor

H. W. Salzberg, Book Review Editor

Natalie Michalski, Assistant Editor

DIVISIONAL EDITORS

W. C. Vosburgh, Battery

Milton Stern, Corrosion, I

R. T. Foley, Corrosion, II

T. D. Callinan, Electric Insulation

Seymour Senderoff, Electrodeposition

H. C. Froelich, Electronics

Ernest Paskell, Electronics—Semiconductors

Sherlock Swann, Jr., Electro-Organic, I

Stanley Wawzonek, Electro-Organic, II

John M. Blocher, Jr., Electrothermics and Metallurgy, I

A. U. Seybolt, Electrothermics and Metallurgy, II

N. J. Johnson, Industrial Electrolytic

C. W. Tobias, Theoretical Electrochemistry, I

A. J. deBethune, Theoretical Electrochemistry, II

ADVERTISING OFFICE

ECS
1860 Broadway, New York 23, N. Y.

ECS OFFICERS

W. C. Gardiner, President
Olin Mathieson Chemical Corp., Niagara Falls, N. Y.

R. A. Schaefer, Vice-President
The Bunting Brass and Bronze Co., Toledo, Ohio

Henry B. Linford, Vice-President
Columbia University, New York, N. Y.

F. L. LaQue, Vice-President
International Nickel Co., Inc., New York, N. Y.

Lyle I. Gilbertson, Treasurer
Air Reduction Co., Murray Hill, N. J.

I. E. Campbell, Secretary
National Steel Corp., Weirton, W. Va.

Robert K. Shannon, Executive Secretary
National Headquarters, The ECS, 1860 Broadway, New York 23, N. Y.

Manuscripts submitted to the Journal should be sent, in triplicate, to the Editorial Office at 1860 Broadway, New York 23, N. Y. They should conform to the Instructions to Authors, published in this issue, pp. 232C-233C. Manuscripts so submitted become the property of The Electrochemical Society and may not be published elsewhere, in whole or in part, unless permission is requested and granted by the Editor.

Journal of the

Electrochemical Society

AUGUST 1959 **VOL. 106 • NO. 8**

CONTENTS

Editorial

NSF Will Help 185C

Technical Papers

The Silver/Silver Chloride/Chlorine Solid Electrolyte Cell. *D. M. Smyth* 635

Surface to Volume Considerations in the Palladium-Hydrogen-Acid System. *J. P. Hoare* 640

The Growth of Barrier Oxide Films on Aluminum. *W. J. Bernard and J. W. Cook* 643

Kinetics of the Dissolution of Copper in Oxygen-Containing Solutions of Various Chelating Agents. *J. Halpern, H. Milants, and D. R. Wiles* 647

Electrodeposition of Amorphous Selenium. *A. K. Graham, H. L. Pinkerton, and H. J. Boyd* 651

Electroclad Aluminum on Uranium. *J. G. Beach and C. L. Faust* 654

Electrolytic Iron Powder from a Caustic Soda Solution. *J. A. M. LeDuc, R. E. Loftfield, and L. E. Vaaler* 659

Electric Field Enhancement of Cathodoluminescence (Cathodoelectroluminescence). *P. M. Jaffe* 667

Influence of Hydrogen on the Red ZnS-Cu Fluorescence. *W. van Gool and A. P. D. M. Cleiren* 672

The Fluorescence of Binary and Ternary Germanates of Group II Elements. *H. Koelmans and C. M. C. Verhagen* 677

Thermoluminescence and Shallow Traps in ZnS:Cu:Co. *B. Goldstein and J. J. Dropkin* 682

Arrays of Inorganic Semiconducting Compounds. *A. J. Cornish* 685

Glycerol Baths for the Electrodeposition of Molten Indium or Indium-Cadmium Alloy. *A. J. Certa, T. J. Manns, G. L. Schnable, and H. S. Segal* 690

Potential Measurements during Jet Etching of P-Type Ge and P-Type Si. *P. F. Schmidt and M. Blomgren* 694

Junction Delineation on Silicon in Electrochemical Displacement Plating Solutions. *D. R. Turner* 701

Diffusion of Radioactive Antimony in Silicon. *J. J. Rohan, N. E. Pickering, and J. Kennedy* 705

The Relation of Gas Composition to Current Efficiency in an Aluminum Reduction Cell. *T. R. Beck* 710

Electromotive Force Series of Metals in Fused Salts and Activities of Metal Chlorides in 1:1 Molar KCl-NaCl Solutions. *S. N. Flengas and T. R. Ingraham* 714

The Oxygen-Evolution Reaction at Gold Anodes, I. Accuracy of Overpotential Measurements. *S. Barnartt* 722

Electrokinetic Measurements on Stainless Steel Capillaries. *B. Levy and A. R. Fritsch* 730

Brief Communications

Electron Diffraction of Zinc Silicate Phosphor. *S. Yamaguchi* 735

Influence of Crystallographic Orientation on the Pitting of Iron in Distilled Water. *J. Kruger* 736

Columbus Meeting Program 189C-213C

Feature Section

A Short Survey of the Status of the Society—Presidential Address. *S. Swann, Jr.* 214C

Current Affairs 216C-233C

Published monthly by The Electrochemical Society, Inc., from Manchester, N. H., **Executive Offices, Editorial Office** and **Circulation Dept.,** and **Advertising Office** at 1860 Broadway, New York 23, N. Y., combining the JOURNAL and TRANSACTIONS OF THE ELECTROCHEMICAL SOCIETY. Statements and opinions given in articles and papers in the JOURNAL OF THE ELECTROCHEMICAL SOCIETY are those of the contributors, and The Electrochemical Society assumes no responsibility for them. Nondeductible subscription to members $5.00; subscription to nonmembers $18.00. Single copies $1.25 to members, $1.75 to nonmembers.

Copyright 1959 by The Electrochemical Society, Inc.

Entered as second-class matter at the Post Office at Manchester, N. H., under the act of August 24, 1912.

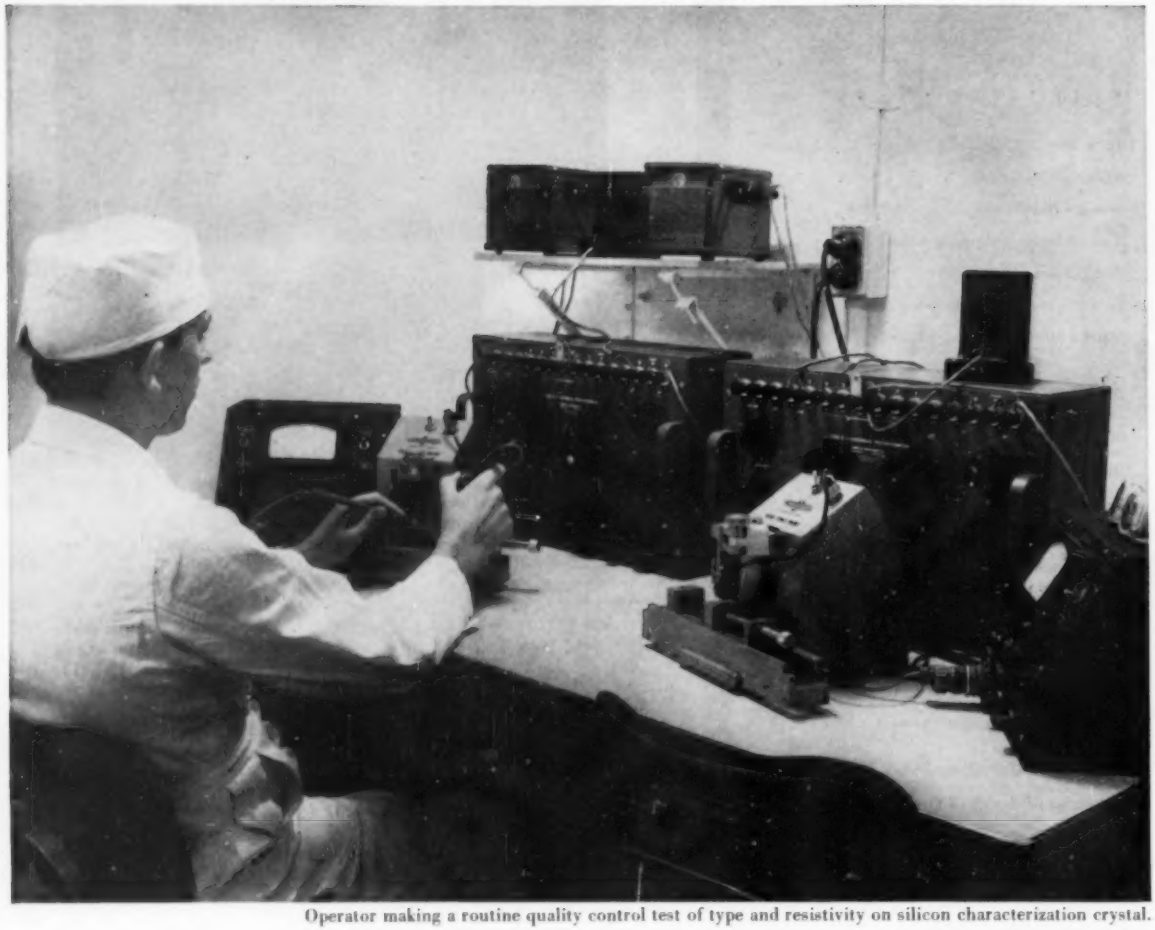

Operator making a routine quality control test of type and resistivity on silicon characterization crystal.

Round-the-clock operations at new Du Pont plant assure you of ample supplies of Hyperpure Silicon

Du Pont's new Brevard, N. C., HYPERPURE Silicon plant—with a 70,000 lbs./yr. capacity—is now operating at high production rate to assure you of a prompt supply of high-purity silicon in the form, grade and quantity you need. Du Pont is uniquely qualified to serve you because of its experience as pioneer producer of semiconductor grades of silicon. This experience includes installing the first full-scale commercial silicon plant in the world and frequent expansion of productive facilities since then.

Single crystals of Du Pont HYPERPURE Silicon are now available in a wide range of resistivities, thanks to Du Pont's new research and manufacturing techniques. Each has a specially prepared "spec. sheet."

Here's more news: Du Pont recently completed a $3,000,000 Technical Service Laboratory specifically designed, equipped and staffed to handle customer problems. Here, highly trained Du Pont Technical Specialists are available to discuss any difficulties in crystal growing or manufacture you may encounter.

Du Pont HYPERPURE Silicon is also available in densified cut rods . . . and rods specially designed for float-zone refining in Grades 1, 2 and 3, with carefully controlled purity levels. As an additional service, Du Pont offers doping material at no additional cost.

Free booklet is available upon request. It describes the manufacture, properties and uses of HYPERPURE Silicon. E. I. du Pont de Nemours & Co. (Inc.), Pigments Dept., Silicon Development Group, Wilmington 98, Delaware.

HYPERPURE SILICON

DU PONT

REG. U.S. PAT. OFF.

BETTER THINGS FOR BETTER LIVING
. . . THROUGH CHEMISTRY

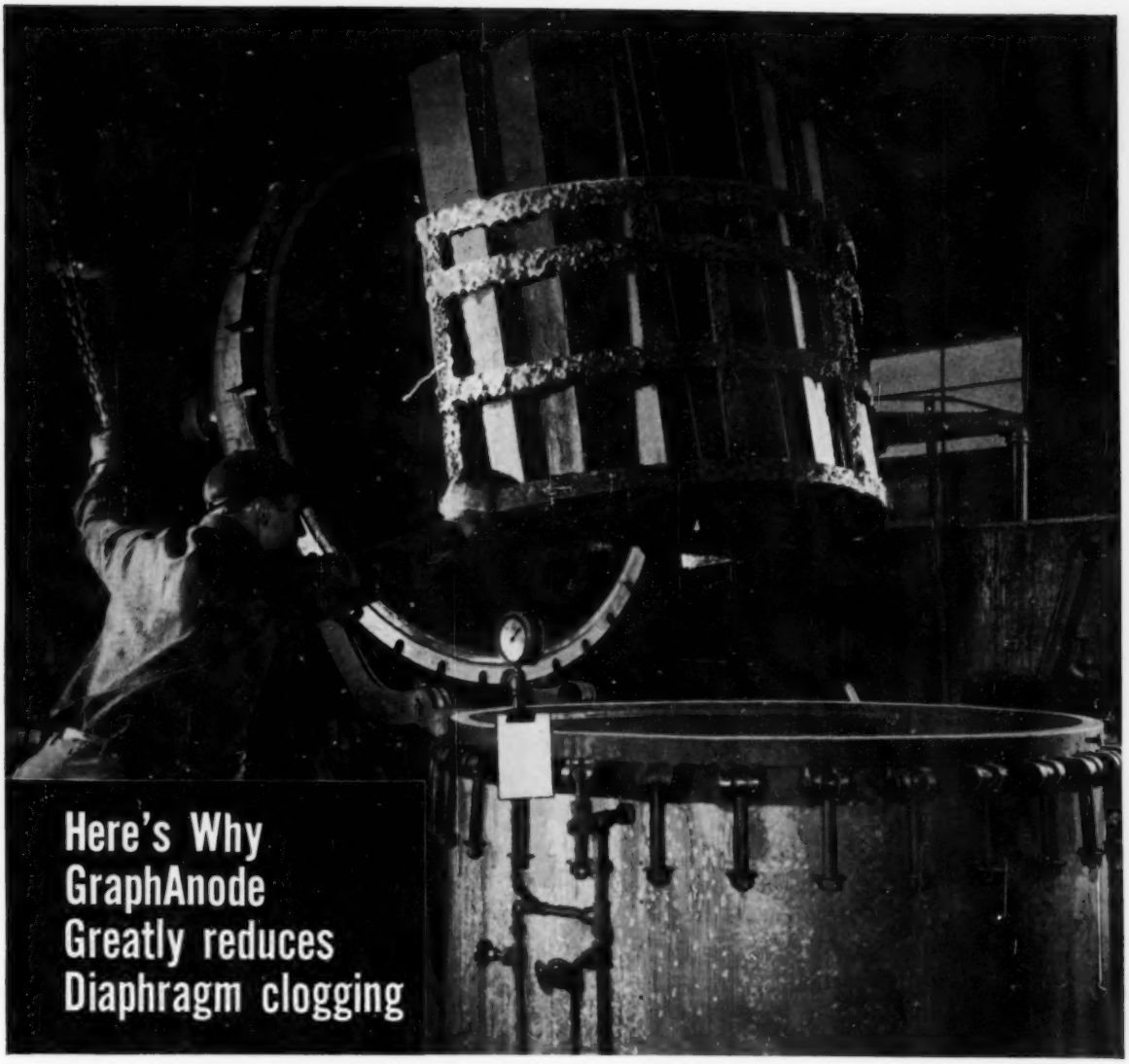

Here's Why GraphAnode Greatly reduces Diaphragm clogging

. . . and whack down cell maintenance costs accordingly

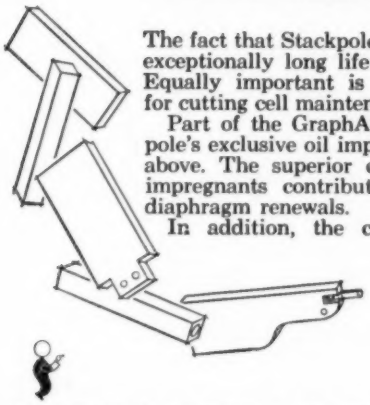

The fact that Stackpole GraphAnode anodes have exceptionally long life is only part of the story. Equally important is their enviable reputation for cutting cell maintenance costs.

Part of the GraphAnode "secret" is in Stackpole's exclusive oil impregnation process pictured above. The superior chemical resistance of the impregnants contributes substantially to fewer diaphragm renewals.

In addition, the carefully-machined GraphAnode anodes present outstandingly uniform, low-porosity surfaces to the electrolyte. The graphite is consumed slowly and evenly. It does not slough off to contaminate the cell.

Inevitably, the result is many more useful cell operating hours — and with the added advantage of low cell voltages. For a convincing demonstration on your own equipment, we suggest you get in touch with Stackpole now.

STACKPOLE CARBON CO., St. Marys, Pa.

CATHODIC PROTECTION ANODES • TUBE ANODES • BEARINGS • SEAL RINGS FLUXING & DE-GASSING TUBES • SALT BATH RECTIFICATION RODS • ELECTRODES & HEATING ELEMENTS • POROUS CARBON • WELDING CARBONS • ROCKET NOZZLES • VOLTAGE REGULATOR DISCS • MOLDS & DIES • "CERAMAGNET"® CERAMIC MAGNETS • ELECTRICAL CONTACTS • BRUSHES for all rotating electrical equipment • and many other carbon, graphite and electronic components

STACKPOLE

GraphAnode®

ELECTROCHEMICAL ANODES

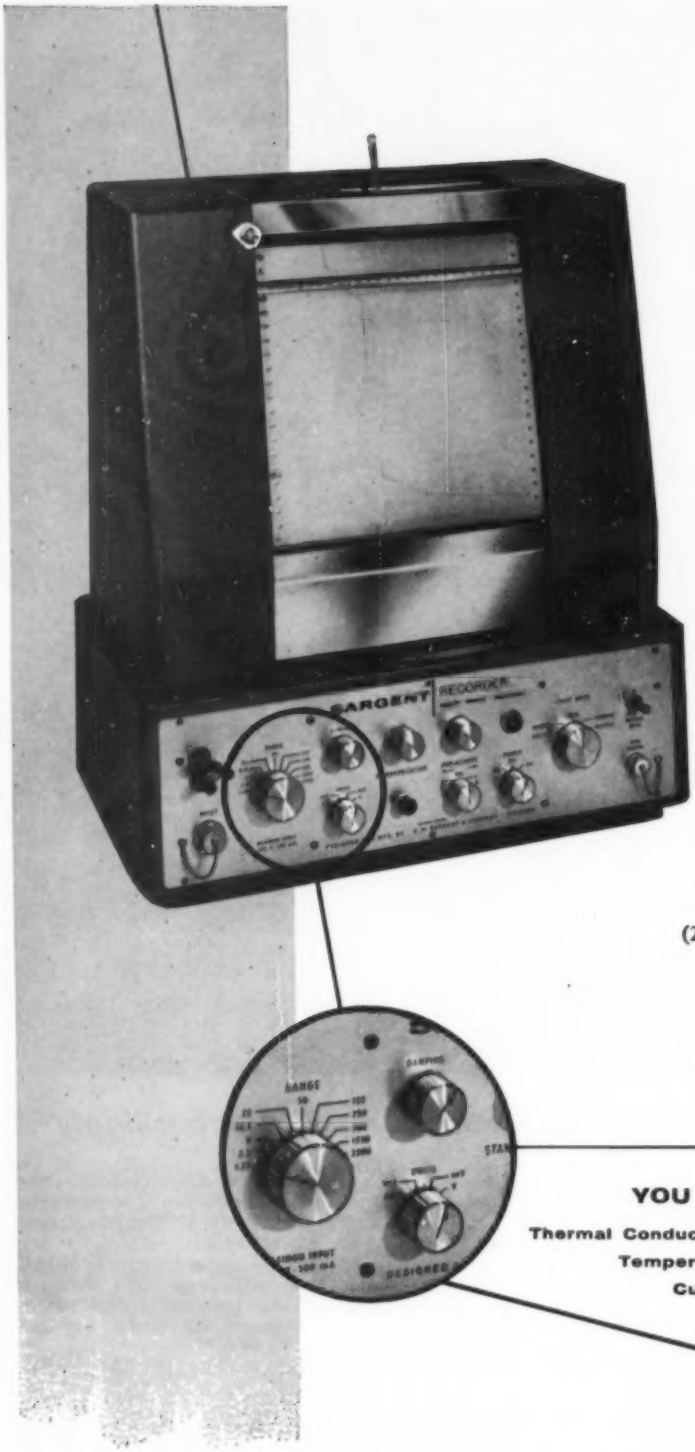

RECORD MANY VARIABLES with the SARGENT RECORDER

(PATENTS PENDING)

Here in one expertly designed instrument is a Multi-purpose Recorder that measures current and voltage and all other quantities which can be transposed into potential or current signals.

THIS RECORDER FEATURES:

18 Current Ranges—18 Potential Ranges—
9 Chart Speeds (Time Range)
(27 Chart Speeds with Multi-range Attachment)
—Designed for Bench Operation

Designed and Manufactured by
E. H. SARGENT & CO.

S-72150 SARGENT RECORDER.....$1725.00

YOU CAN RECORD:

Thermal Conductivity	Dielectric Constant
Temperature	Potential
Current	Conductance
	Light Intensity

For complete information write for Bulletin R.

SARGENT SCIENTIFIC LABORATORY INSTRUMENTS • APPARATUS • SUPPLIES • CHEMICALS

E. H. SARGENT & COMPANY, 4647 W. FOSTER, CHICAGO 30, ILLINOIS
DETROIT 4, MICH. • DALLAS 35, TEXAS • BIRMINGHAM 4, ALA. • SPRINGFIELD, N. J.

Editorial

NSF Will Help

THE National Science Foundation is financed by direct Congressional appropriations, and its budget and plans are scrutinized very carefully by the House and Senate Committees concerned. The tendency seems to be to allow the Foundation to increase its activities, but at a rather slow rate. For the current year, NSF asked for $205,000,000; this figure was cut to $160,000,000 by the Bureau of the Budget, in accordance with its balance-the-national-budget policy. Congress probably has done some further trimming, but left NSF with a few millions more than it had in 1958-1959.

The Foundation has amply demonstrated its ability to assist and encourage research and the training of scientific personnel. In addition to basic research grants and contracts, it provides funds for graduate fellowships, teacher training institutes, and various projects in science education. This year, it has provided $1,700,000 to make it possible for some 2000 undergraduate students to participate in research programs directed by college and university faculty members. It provides funds to assist in the publication of translations, on both a national and an international basis. Through its Office of Scientific Information Service, it attempts to assist in quicker publication and distribution of scientific material wherever possible.

During 1958, some 12 primary publication grants totaling more than $450,000 were made to enable various journals to reorganize or expand, to publish backlogs of manuscripts, or to issue indexes. Other grants were made to start experimental publications, such as the semimonthly *Physical Review Letters*, which is expected to be self-supporting after building up a subscription list. Another grant was made to assist in starting an international high-energy-physics newsletter, which is also supported by other nations including the U.S.S.R.

Could NSF help The Electrochemical Society with its publication problems? Fortunately, the JOURNAL is on a sound basis at the moment. However, as mentioned on this page last month, there is increasing pressure for other types of publication, such as the proceedings of symposia held at the semiannual meetings. The Society experience with Monographs has so far been distinctly successful, but there are some drawbacks: the time is too long, and the price is too high. Each Monograph has taken nearly two years to publish, and $18 is a high price even for a very well-done book. The delay would be intolerable in certain rapidly expanding fields.

In the near future, the Society may wish to investigate other methods of publication. For instance, the material might be set up for reproduction with the aid of special typewriters. If necessary, it would be appropriate to ask NSF to assist in purchasing the necessary equipment, including the wide variety of type needed, and in training operators. With insistence on prompt receipt of manuscripts from authors, a proper objective might be to trim publication time to six months, and to cut the retail price in half.

—CVK

dial any output from 0-1000V within 1%

KEITHLEY Model 240 High-voltage Supply combines convenience, accuracy, wide range

This convenient supply brings new speed, ease and accuracy to laboratory tests. Typical applications include calibration of meters and dc amplifiers, supplying potentials for photomultiplier tubes and ionization chambers. Other uses include furnishing potentials for high resistance measurements, and for diode and capacitor leakage resistance tests.

The Model 240 output delivers 0 to 1000 volts at up to 10 milliamperes. Three calibrated dials on the front panel select the desired output voltage in one volt steps, with accuracy of 1% or 100 millivolts. Greater accuracy may be obtained with a potentiometer provided for setting the output with an accurate voltmeter.

Polarity is selectable. The switch includes an "OFF" position, facilitating timed measurements. An overload relay cuts off the output at 12 milliamperes within 50 milliseconds. Connectors are provided on front and rear panels.

SPECIFICATIONS

DC OUTPUT VOLTAGE: Positive or negative, 0 to 1000 volts, in one volt steps.

OUTPUT CURRENT: 0 to 10 milliamperes.

ACCURACY: Within 1% above 10 volts, within 100 millivolts below 10 volts.

LOAD REGULATION: 0.02% for 0 to 10 ma.

RIPPLE: Less than 3 mv RMS above 5 cps.

OUTPUT IMPEDANCE: 0.15 ohms at 10 volts, rising linearly to 15 ohms at 1000 volts.

STABILITY: Within 0.02 volts ± 0.02% the first hour, or in subsequent 24-hour periods.

LINE REGULATION: Output change, less than 0.02 volts for a line change of 105 to 125 V.

RACK mounting, shown above with accessory end frames, bench mounting.

PRICE $325.00

SEND TODAY FOR COMPLETE DETAILS

KEITHLEY INSTRUMENTS, INC.
12415 EUCLID AVENUE • CLEVELAND 6, OHIO

GRACE Si

For

low boron

content . . .

GRACE SILICON

(ultra-high-purity)

"For want of a nail the battle was lost" becomes painfully true when translated to lack of purity in the semi-conductor material you choose for your transistors, diodes or other silicon devices.

The Pechiney process, used in the manufacture of Grace Silicon, is noted for a product with low boron content as well as overall high purity.

May we suggest that whenever top quality silicon is desired—silicon combining both high purity and uniform quality—you get in touch with GRACE ELECTRONIC CHEMICALS, INC., at PLaza 2-7699, 101 N. Charles Street in Baltimore.

GRACE ELECTRONIC CHEMICALS, INC.

101 N. Charles St., Baltimore, Maryland

Subsidiary of W. R. GRACE & CO.

FUTURE MEETINGS OF
The Electrochemical Society

Columbus, Ohio, October 18, 19, 20, 21, and 22, 1959

Headquarters at the Deshler Hilton Hotel

Sessions will be scheduled on

Batteries, Corrosion (including a joint Corrosion–Electronics-Semiconductors session),
Electrodeposition (including symposia on "Electrodeposition from Organic Solvents"
and "Electro- and Chemical-Polishing"),
Electronics (Semiconductors), Electro-Organics,
and Electrothermics and Metallurgy

★ ★ ★

Chicago, Ill., May 1, 2, 3, 4, and 5, 1960

Headquarters at the Lasalle Hotel

Sessions probably will be scheduled on

Electric Insulation (including a symposium on "Electrolytic Capacitors"),
Electronics (including Luminescence and Semiconductors),
Electrothermics and Metallurgy (including a symposium on "High-Purity Vanadium"
and a round table on "Methods of Reducing Iron Ores"), Industrial Electrolytics,
and Theoretical Electrochemistry

★ ★ ★

Houston, Texas, October 9, 10, 11, 12, and 13, 1960

Headquarters at the Shamrock Hotel

★ ★ ★

Indianapolis, Ind., April 30, May 1, 2, 3, and 4, 1961

Headquarters at the Claypool Hotel

★ ★ ★

Detroit, Mich., October 1, 2, 3, 4, and 5, 1961

Headquarters at the Statler Hotel

Papers are now being solicited for the meeting to be held in Chicago, Ill., May 1-5, 1960. Triplicate copies of each abstract (*not exceeding 75 words in length*) are due at Society Headquarters, 1860 Broadway, New York 23, N. Y., *not later than January 4, 1960* in order to be included in the program. *Please indicate on abstract for which Division's symposium the paper is to be scheduled, and underline the name of the author who will present the paper.* Complete manuscripts should be sent in triplicate to the Managing Editor of the JOURNAL at 1860 Broadway, New York 23, N.Y.

The Silver/Silver Chloride/Chlorine Solid Electrolyte Cell

Donald M. Smyth

Sprague Electric Company, North Adams, Massachusetts

ABSTRACT

A Ag/AgCl/Cl_2 solid electrolyte cell has been developed in which the chlorine is furnished by the dissociation of potassium tetrachloroiodide, $KICl_4$. These cells can be assembled into batteries which are extremely stable and compact and which deliver currents in the microampere range. The dissociation characteristics of the cathode salt influence the shelf-life, temperature dependence of the open-circuit voltage (OCV), and the change of OCV with aging. The ionic conductivity of the AgCl electrolyte controls the internal resistance of the battery and its temperature dependence. The shelf-life, OCV, and temperature dependence of OCV are strongly dependent on the cathode atmosphere since this can influence the electronic conduction of the electrolyte.

The development of electronic devices which can operate on currents in the microampere range has given rise to considerable interest in electrochemical cells with solid electrolytes. Such cells have potential shelf-lives many times those of conventional systems and lend themselves to extreme miniaturization. This paper describes a cell system with an indicated shelf-life in excess of 20 years and which is easily constructed in sizes of the order of 0.03 cm^3/v.

The choice of a solid electrolyte cell system is based on several factors: (*a*) the electrolyte should have a high ionic conductivity for current delivery and an infinitesimal electronic conductivity for long shelf-life; (*b*) the electrolyte must have suitable mechanical properties for the formation of strong, thin films; (*c*) the component parts must be chemically compatible; and (*d*) a high emf is desirable.

Requirement (*b*) excludes a large majority of ionic salts from consideration as electrolytes. The silver/silver halide/halogen systems meet these requirements quite well, and batteries based on the Ag/AgI/I_2 and Ag/AgBr/Br_2 systems have been described previously (1-3). The Ag/AgCl/Cl_2 system has the advantages of a higher emf [Ag-Cl_2, $E_\circ = 1.133$ v; Ag-Br_2, $E_\circ = 1.008$ v; Ag-I_2, $E_\circ = 0.788$ v (4)], an electrolyte with a smaller electronic conductivity (based on the evidence of silver-halogen tarnishing reactions), and an electrolyte with excellent mechanical properties. Use of potassium tetrachloroiodide, $KICl_4$ as a low pressure source of chlorine vapor has made possible the development of a Ag/AgCl/Cl_2 cell which is extremely stable. The cells have an open-circuit voltage (OCV) of 1.04 v at 25°C, and this does not vary more than ±5% over the temperature range +75° to −40°C. The theoretical shelf-life predicted by tarnishing experiments and the shelf-life obtained by extrapolation of accelerated aging data are both of the order of decades of years. The cells have an internal resistance of about 10^5 ohms/cm^2 area at 25°C and this increases by a factor of 60 as the temperature is reduced to −40°C.

Cell Structure

For a system such as the Ag/AgCl/Cl_2 cell which contains a corrosive vapor phase, the stability of the cell system depends on the extent to which this vapor can be sealed within the cell and, for this reason, a sealed cup structure has been developed. The cell is constructed from a small silver can which serves as the anode and as the main structural unit. An electrolyte film of AgCl a few microns thick is formed over the anode by exposure to Cl_2 at 200°-300° for about 30 min. The cathode is a conducting mixture of $KICl_4$ and carbon black in 6:1 weight ratio mixed with Kel-F #90 grease[1] to give a putty-like consistency. The cathode is extruded into the anode can which is then sealed with a compression fitted Teflon plug through which extends a tantalum wire that provides electrical contact to the cathode.

Open-Circuit Voltage (OCV)

The emf of the Ag/AgCl/Cl_2 system is related to the temperature, T, chlorine pressure, P_{Cl_2}, and the standard free energy, ΔF°, of the reaction

$$Ag + \tfrac{1}{2}\ Cl_2 = AgCl \qquad [1]$$

by the familiar expression

$$E = \frac{-\Delta F^\circ}{F} + \frac{RT}{2F} \ln P_{Cl_2} \qquad [2]$$

This expression yields a theoretical emf of 1.04 v at 25°C using thermodynamic data compiled by Quill (4) for ΔF° and the data of Smyth and Cutler (5) and Cornog and Bauer (6) for P_{Cl_2}. The observed OCV is in exact agreement with this theoretical value. If Eq. [2] is differentiated with respect to temperature, neglecting the variation of ΔF° with temperature and assuming that the chlorine pressure over $KICl_4$ can be expressed in the form

$$P_{Cl_2} = Ae^{-B/T} \qquad [3]$$

we obtain an expression for the temperature dependence of the emf,

[1] A product of M. W. Kellogg Co., Jersey City, N. J.

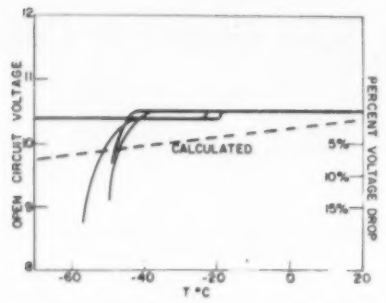

Fig. 1. Temperature dependence of open-circuit voltage. Behavior of several ten cell batteries compared with calculation from Equation IV.

$$\frac{dE}{dT} = \frac{R}{2F} \ln A \qquad [4]$$

in which R is the gas constant in coulombs per mole °K and A is a constant evaluated from the dissociation pressure data (5, 6). Evaluation of this relation gives a predicted temperature variation of OCV of 0.00092 v/°C assuming that the chlorine vapor is always in equilibrium with the solid phase. Figure 1 shows the actual temperature dependence of the OCV of several batteries together with the calculated dependence. It is seen that the observed OCVs lie above the predicted value down to about −50°C. In the vicinity of this temperature, the voltages start to drop off rapidly in many cases, although a few batteries show very little voltage drop even at −70°C. The rapid drop in OCV at very low temperatures is probably related to a relatively increasing importance of the electronic conductivity of the electrolyte with decreasing temperature.

The discrepancy between the observed and calculated temperature dependence of the OCV can be related to the nonreversible dissociation of the polyhalide cathode salt. It has been observed that equilibrium dissociation pressures are obtained only in the direction of increasing temperature for these salts (5). After a decrease in temperature, halogen pressures several times the equilibrium value may be maintained for several days. This is probably related to the formation of a film of solid recombination product over the decomposition residue, with the result that further recombination is hindered. Thus the assumption that the chlorine vapor is in equilibrium with the solid cathode phase is not valid when the temperature is decreased.

Attempts have been made to return the OCV to its equilibrium value by consuming the excess halogen pressure by current drain. The number of electrochemical equivalents of excess pressure is surprisingly high, however, and exceeds that estimated from the cell volume by more than a factor of ten. It is believed that the grease cathode binder and the carbon black act as reservoirs of excess halogen by dissolving and adsorbing large amounts of vapor. This fact reduces the hazard that a slight drop in OCV may result after a small amount of current has been drawn from the cell.

The full, theoretical emf of the electrochemical system will be observed across the cell terminals only for systems in which electronic conduction through the electrolyte phase is negligible compared with the ionic conduction. This requirement is always satisfied in aqueous electrolyte cells, since water solutions have immeasurably small electronic conductivities. Ionic crystals range all the way from essentially pure ionic conductors to essentially pure electronic conductors, however, and the relative magnitudes may depend on the purity and crystallinity of the material, the composition of the ambient atmosphere, and the nature of the electrodes.

As a result of the early work of Tubandt (7), the silver halides were long considered to be classic examples of materials having almost purely ionic conductivity. Wagner was able to show, however, that in the presence of 0.23 atm of bromine at 200°C the total conductivity of AgBr films formed by reaction of silver with bromine is 17% electronic, and that the electronic contribution increases rapidly with decreasing temperature (8). In recent years, Pfeiffer, Hauffe, and Jaenicke have shown that single crystal AgBr is an essentially pure electronic conductor and that the ionic contribution increases with the concentration of grain boundaries (9). Luckey and West (10) and Shamovskii, Dunina, and Gosteva (11) have shown that, in the presence of bromine vapor, single crystal AgBr has an "additional" conductivity which is proportional to the square root of the bromine pressure and which is thus considered to be due to the injection of electron holes into the AgBr in agreement with the theories of Wagner. These properties of AgBr and their possible extension to AgCl and AgI raise a question as to the suitability of the silver halides for electrolytes in solid-state cells of the silver-halogen type. It has been known for several years that such cells do have open-circuit voltages close to the theoretical emf (1-3), and it is necessary to reconcile this fact with the known electrical properties of the electrolytes. The following experiments clarify this point.

It has been found that a Ag/AgCl/Cl_2 cell with a cathode phase consisting of 1 atm of dry chlorine has an equilibrium OCV of about 0.75 v, whereas the theoretical emf is 1.13 v. The OCV also decreases rapidly with temperature. This indicates that a substantial electronic conduction through the AgCl electrolyte is partially short-circuiting the emf and that the relative electronic contribution is increasing with decreasing temperature. When undried chlorine is used, however, the OCV is the same as the thermodynamic emf, and the change of OCV with temperature is greatly reduced. The cell voltage changes rapidly and reversibly with changes in the moisture content of the chlorine. It appears that the moisture content of the chlorine atmosphere is suppressing the electronic conduction through the AgCl. Measurements of the internal resistance of the cell in wet and dry chlorine show that the water vapor has very little effect on the ionic conduction through the electrolyte. These findings led to an investigation of the effect of foreign

vapors on the tarnishing rate of silver in halogen vapor; this work is described in a separate publication (12). It was found that very small partial pressures of water or carbon tetrachloride vapor suppress the reaction rates drastically and that the rate-determining process is an interface phenomenon, since the reaction rate is independent of tarnish film thickness. The suppression of the reaction rate may be taken as an upper limit of the suppression of the electronic current.

It has since been found that cells made with cathodes consisting only of carbon black and $KICl_4$ have voltages less than the theoretical emf, and very poor low-temperature properties. Cells in which the cathode contains a hydrated salt as a source of water vapor or Kel-F grease have the theoretical emf and greatly improved low temperature properties. Thus the Kel-F grease binder used in the cathode serves to stabilize the cell voltage and to extend the theoretical shelf-life by decreasing the electronic conduction through the electrolyte. Tarnishing experiments indicate that the stabilizing vapor is not consumed during the formation of more silver halide.

The stability of the OCV with time as a function of temperature is of great interest for such a potentially long shelf-life item. The shelf-life under ideal conditions will be determined by the rate of consumption of the active materials by the internal tarnishing reaction whose rate is limited by the electronic leakage through the electrolyte. Thus a maximum attainable life of such a system can be estimated from tarnishing data and the amount of active materials in a cell. The reaction rates of silver foils of different purities with the equilibrium halogen atmosphere over $KICl_4$ at 60°C are shown in Fig. 2, in which the square of the weight increase is plotted against time. The two cadmium doped samples appear to follow a parabolic tarnishing expression, whereas high-purity and commercial purity silver have an even greater dependence of reaction rate on film thickness.

Chemical analyses of these films indicate a chloride:iodide atomic ratio of about 19.5:1 whereas the equilibrium dissociation vapor of $KICl_4$ at 60° has a Cl:I ratio of 14.5:1 (5). Thus there may be a slight preferential reaction of chlorine, and the films may be considered as a dilute solution of AgI in AgCl.

A calculation based on the assumption that the commercially pure silver reacts according to a parabolic rate expression gives a theoretical shelf-life of 25 years for continuous storage at 60°C for typical cell dimensions and an initial electrolyte thickness of 13 μ. This is a conservative estimate, since the actual reaction rate is decreasing with time more rapidly than indicated by a parabolic expression and also because the reactions were carried out in the room atmosphere without the presence of any rate-depressing vapors such as are present in actual cells. The initial electrolyte film of pure AgCl will also depress the reaction rate to a greater extent than would the same thickness of Ag-$KICl_4$ tarnishing product.

In actual practice, the shelf-life of a solid electrolyte cell is limited by the leakage of active cathode vapor from the cells and by electrical leakage through and over the surface of the encapsulating material. The magnitude of these effects may be determined from accelerated life tests carried out at elevated temperatures. Such tests have been performed with groups of 4-cell batteries stored at 125°, 110°, and 100°C. The end of the battery life has been defined arbitrarily as the time at which the room temperature open-circuit voltage of half the batteries in a group has dropped 5%. Results are summarized in Fig. 3, in which the shelf-life has been plotted logarithmically against the reciprocal absolute storage temperature. The relationship is merely an intuitive guess which seems to fit the extremely strong temperature dependence of shelf-life reasonably well. Although the extrapolation of these data to ordinary storage temperatures cannot be considered accurate, the indication is that satisfactory stability has been attained.

The aging characteristics of a typical battery are shown in Fig. 4, in which the room temperature voltage of a 4-cell battery stored at 100°C is plotted against storage time. It is seen that there are two stable voltage levels: an initial voltage of about

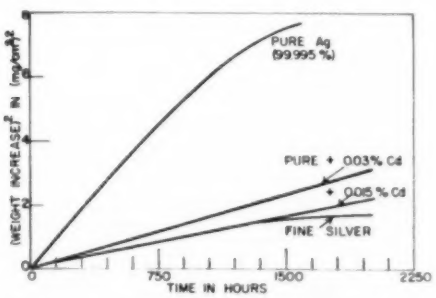

Fig. 2. Tarnishing rates of various silver samples with the dissociation vapor over $KICl_4$ at 60°C. Square of weight increase plotted against reaction time. (Fine silver is nominally 99.9% silver.)

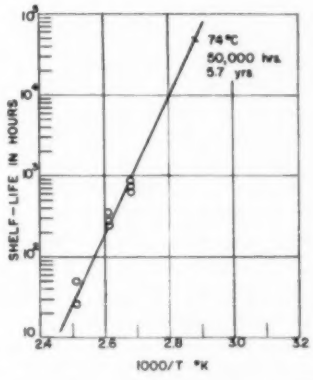

Fig. 3. Accelerated aging data of four-cell batteries, and a possible extrapolation to lower temperatures. Shelf-life defined as time prior to a 5% drop in open-circuit voltage (measured at room temperature) for half of the batteries in a group. The line was fitted to the data by the method of least squares.

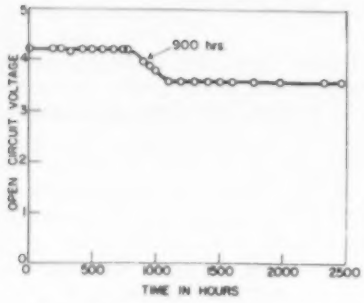

Fig. 4. Aging behavior of a four-cell battery stored at 100°C. Open-circuit voltage measured at room temperature.

1.05 v/cell which is related to a Ag/AgCl/Cl_2 cell in which the Cl_2 is furnished by the dissociation of $KICl_4$, and a subsequently stable plateau at 0.89 v/cell. It has been shown that this latter voltage is that of a Ag/AgCl/ICl cell in which the ICl is furnished by the dissociation of $KICl_2$. An earlier publication (5) has shown that $KICl_4$ dissociates in two steps:

$$KICl_4 \rightarrow KICl_2 + Cl_2 \qquad [5]$$

$$KICl_2 \rightarrow KCl + ICl \qquad [6]$$

and that the equilibrium vapor is predominantly chlorine which is thus consumed or lost faster than the ICl. When the chlorine has all been lost, there is still sufficient $KICl_2$ left to maintain the voltage at 0.89 v/cell for a period which is generally longer than the duration of the initial voltage. Note that this second voltage plateau has not been included in the shelf-life definition and thus represents a substantial safety factor for applications that can tolerate a 15% voltage drop. The internal resistances of the cells do not increase appreciably until near the end of the second voltage plateau.

The Internal Resistance

The internal resistance, R_s, is defined here by the expression

$$V = E_s \frac{R}{R+R_s} \qquad [7]$$

in which E_s is the OCV and V is the terminal voltage with load R. The relatively small ionic conductivity of the AgCl electrolyte determines the general magnitude of the resistance and also its temperature dependence. Data reported by Compton (13) show a conductivity of about 3×10^{-9} to 2×10^{-8} ohm^{-1} cm^{-1} at 25°C for undoped AgCl. For a cell area of 0.24 cm^2 and an electrolyte thickness of 0.0013 cm, this gives a calculated resistance range of 2.7×10^5 to 1.8×10^6 ohms which is to be compared with an observed range of 5×10^5 to 5×10^6 ohms for cells with these dimensions. The single-crystal conductivity data reported by Compton may contain an unknown electronic contribution which could account for the observed resistances being slightly higher than the calculated values. The conductivity data predict a resistance increase by a factor of 60 between 25° and −40°. Seventeen 10-cell batteries selected at random showed an average increase by a factor of 57 over this range although there was considerable variation among the group (average deviation of factor = 20).

Compton's conductivity data lie in the impurity-sensitive range below 100°C rather than in the intrinsic range, and the correlation between the temperature coefficients of resistance and resistivity indicate that the cell behavior should also be typical of the impurity-sensitive range. Thus small additions of impurities to the AgCl electrolyte might have considerable influence on the resistance. It is well established that the principal ionic charge carriers in silver halides in this temperature range are silver ion vacancies and that the cation vacancy content of the silver halides can be enhanced by the addition of divalent metallic halides such as those of cadmium or lead. The divalent foreign cation enters the lattice in place of a monovalent silver ion, and another silver ion position is left vacant to maintain electrical neutrality. It has also been established that the impurity content of halide films formed by tarnishing reactions is related to the metallic impurity content of the base silver. Cells have been made from silver anode cans containing various amounts of cadmium, and it was found that a cadmium content of 0.02% causes a reduction in the cell resistance by a factor of three to five over the entire temperature range of battery operation. Larger amounts of cadmium cause the AgCl film to become brittle and less adherent. Aging characteristics, low temperature properties, and other operating characteristics are as good or better for these batteries as for the undoped cells.

In addition to the ionic conductivity of the electrolyte, other factors may influence the apparent resistance of cells during long periods of heavy current drain. The rate of dissociation of the polyhalide salt and the rate of diffusion of the liberated halogen to the electrolyte-cathode interface may eventually limit the current. The importance of these secondary factors may be surmised from a comparison of heavy current drain data with ideal behavior, which takes into account only conductivity effects. In particular it is necessary to allow for the fact that the electrolyte thickness increases with current drain due to the formation of additional AgCl.

The rate of increase in electrolyte thickness with current drain may be expressed as

$$\frac{dx}{dt} = \frac{V}{\mathbf{F}} \frac{\sigma E}{x} \qquad [8]$$

where x is the thickness of the electrolyte, t the time, V the volume of AgCl per equivalent weight, $\mathbf{F}$ Faraday's constant, σ the ionic conductivity of the AgCl, and E the voltage drop across the electrolyte (essentially the emf for near short-circuit conditions). It has been assumed that the current can be expressed as

$$i = \frac{\sigma A E}{x} \qquad [9]$$

where A is the active electrolyte area, and that the product of current drain is essentially pure AgCl.

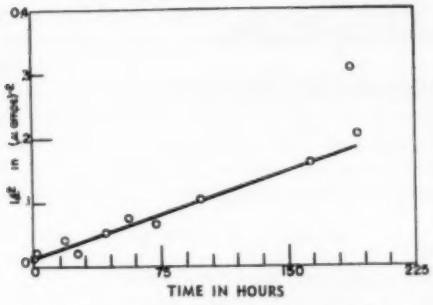

Fig. 5. Short-circuit current of a ten-cell battery at room temperature plotted according to Eq. [10].

Integrating [8] and using [9] to relate thickness to current and expressing σ in terms of i_o and x_o (the initial current and electrolyte thickness) gives

$$\frac{1}{i^2} = \frac{2V}{\mathbf{F}x_oAi_o} \cdot t + \frac{1}{i_o^2} \qquad [10]$$

Thus a plot of $1/i^2$ vs. t should give a straight line of slope $2V/\mathbf{F}x_oAi_o$ and an intercept of $1/i_o^2$, if the electrolyte conductivity is the principal determining factor. An example of this type of treatment is shown in Fig. 5. It is seen that ideal behavior is followed for about 150 hr, after which the current decreases quite abruptly. The scatter of the data is due mainly to fluctuations in room temperature; smoothed discharge data give precise linearity. At the end of 150 hr, the cell had delivered a total of 2 coulombs; after 265 hr of continuous drain the load was removed from the cell and its OCV returned to 85% of its original value in 3 sec and to 95% of its original value in 25 min. When current drain was resumed the current was 5.5 μa, decaying after about a day to the 1.5 μa level reached prior to the initial removal of the load. A more detailed study of the first few minutes of discharge discloses a brief period of high current which amounts to about 0.005 coulombs of charge more than would correspond to a linear $1/i^2$ vs. t plot extrapolated to $t=0$. An evaluation of the slope of this plot gives $x_o = 11.6$ μ and $\sigma = 3.7 \times 10^{-6}$ ohm^{-1} cm^{-1} which agrees remarkably well with the x_o of 13 μ estimated from the time and temperature of the chlorination of the silver cans and with the conductivity range previously quoted from the work of Compton. This correlation is a good indication that the current drain is conductivity controlled even in the near short-circuit range for periods up to about a week.

Typical current drain performance of 10-cell batteries at room temperature and −40°C are shown in Fig. 6 and 7. Voltage recovery after removal of the load is almost instantaneous.

Acknowledgment

The author gratefully acknowledges the advice and guidance of Dr. Kurt Lehovec and the valuable assistance of Mr. Matthew Stefanski.

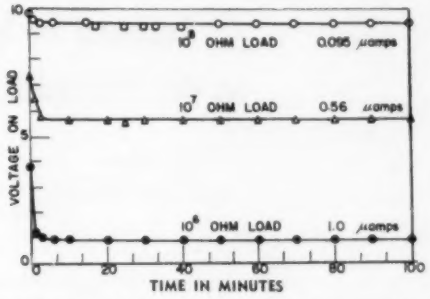

Fig. 6. Terminal voltage of a ten-cell battery with various loads at room temperature (undoped cells).

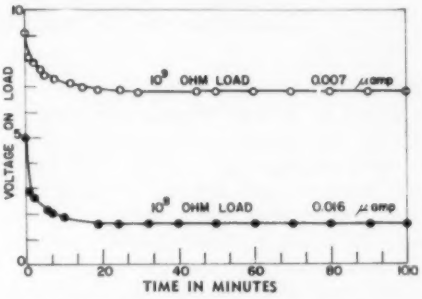

Fig. 7. Terminal voltage of a ten-cell battery with various loads at −40°C (undoped cells).

This work was sponsored by the U.S. Army Signal Research and Development Laboratories under contracts DA-36-039-sc-63151 and DA-36-039-sc-72349.

Manuscript received Jan. 12, 1959. This paper was prepared for delivery before the Ottawa Meeting, Sept. 28-Oct. 2, 1958.

Any discussion of this paper will appear in a Discussion Section to be published in the June 1960 JOURNAL.

REFERENCES

1. K. Lehovec and J. Broder, *This Journal*, **101**, 208 (1954).
2. W. J. van der Grinten, *ibid.*, **103**, 201C (1956).
3. J. L. Weininger, *ibid.*, **105**, 439 (1958).
4. Nat'l. Nuclear Energy Series, Div. 4, *19B*, "Chemistry and Metallurgy of Miscellaneous Materials, Thermodynamics", pp. 76-192, McGraw-Hill Book Co., New York (1950).
5. D. Smyth and M. Cutler, *J. Am. Chem. Soc.*, **80**, 4462 (1958).
6. J. Cornog and E. Bauer, *ibid.*, **64**, 2620 (1942).
7. C. Tubandt and F. Lorenz, *Z. physik. Chem.*, **B7**, 513 (1914).
8. C. Wagner, *ibid.*, **B32**, 447 (1936).
9. I. Pfeiffer, K. Hauffe, and W. Jaenicke, *Z. Elektrochem.*, **56**, 728 (1952).
10. G. Luckey and W. West, *J. Chem. Phys.*, **24**, 879 (1956).
11. L. Shamovskii, A. Dunina, and M. Gosteva, *Soviet Physics, JETP*, **3**, 511 (1956).
12. D. Smyth and M. Cutler, *This Journal*, **106**, 107 (1959).
13. W. Compton, Thesis, University of Illinois (1955).

Surface to Volume Considerations in the Palladium-Hydrogen-Acid System

James P. Hoare

Scientific Laboratory, Ford Motor Company, Dearborn, Michigan

ABSTRACT

The open-circuit potential against a Pt/H_2 electrode in the same 2*N* sulfuric acid solution of a series of palladium electrodes of different sizes and shapes was recorded as a function of time. The electrical resistance in certain cases was also followed as a function of time. It is shown that the time required for charging the palladium with hydrogen is sensitive to the surface-to-volume ratio of the electrode. Charging mechanisms are discussed.

It has been shown (1) that pure palladium metal, when placed in an acid solution saturated with hydrogen gas, will absorb the hydrogen until the maximum α-Pd concentration (~0.03 H/Pd atomic ratio) has been reached and will exhibit a potential of 50 mv more noble than a Pt/H_2 electrode placed in the same solution. It was stated also that under open-circuit conditions the Pd would not absorb additional hydrogen beyond this maximum α-Pd limit and that the 50-mv potential could be maintained indefinitely in the absence of impurities. The potential of 50 mv has been associated with an atomic-hydrogen potential-determining reaction (2) on the Pd as opposed to the molecular hydrogen reaction on the Pt/H_2 electrode. The solubility limit at H/Pd atomic ratios of about 0.03 has been described (3) in terms of a blocking mechanism due to a variation in the point of zero charge of the Pd as hydrogen was absorbed.

Recently, Ratchford and Castellan (4) have reported that Pd electrodes made from thin metal wires or foils behaved somewhat differently. Such electrodes did not give open-circuit-potential-vs-time curves with a plateau at 50 mv of indefinite length; instead, the plateau at 50 mv was less than 10 hr long after which the potential dropped to a steady value of zero volt. Another interesting feature about these curves is the initial overshooting of the 50 mv value with an immediate return to the 50 mv plateau, analogous to a supercooling curve. Electrodes, which had gone to zero potential vs. a Pt/H_2 electrode, were analyzed for the hydrogen content with ceric sulfate (5) and found to have absorbed hydrogen to the β-phase concentration of about 0.6 H/Pd atomic ratio.

It is the purpose, then, of this investigation to study possible surface to volume effects important to the solution of hydrogen by palladium.

Experimental

Electrodes were made from Pd foil and wire 99.5+% pure. In the first set of experiments the following electrodes were used: (*a*) a 1 cm^2 piece of Pd foil 2 mils thick; (*b*) a 1 cm^2 piece of foil 4 mil thick; (*c*) a 1 cm^2 piece of 4 mil foil whose surface was nine-tenths covered with a polyethylene film; (*d*) a 3 cm length of wire, 5 mil in diameter; and (*e*) a Pd bead 0.057 in. in diameter and half way covered with polyethylene so that a hemisphere was exposed to the solution.

The Teflon cell was similar to those used before (6). All electrodes were cleaned in hot concentrate HNO_3 and the cell was rinsed repeatedly with water triply distilled in an all-quartz still as described before (6). All measurements were made in 2*N* H_2SO_4 solution made with triply distilled water and saturated with hydrogen purified by a standard multistage purification-train. The hydrogen flow was maintained approximately at a constant rate night and day. Final purification of the solution and electrodes was done by pre-electrolysis overnight with an auxiliary Pt electrode which was removed while the pre-electrolysis current was flowing. The open-circuit potential between the test electrode and a Pt/H_2 electrode in the same solution was recorded as a function of time. At no time in this complete investigation was any electrode cathodized.

A second series of experiments was done in which wires of approximately the same length but of varying diameters were used. These wires were about 11 cm long and had diameters of 5, 10, 15, 20, and 25 mils. Each wire was cleaned as described above and mounted diagonally in a virgin polyethylene cell 19 cm long and 2.5 cm in diameter from the top on one side to the bottom on the other side. Platinum leads were welded to the Pd wire and the weld area as well as about 3 or 4 mm of Pd wire penetrated through the cell wall and was well covered with polyethylene. This was done to assure adequate protection against contact between the weld area or the Pt and solution and against contact between Pd and the external atmosphere. It is to be noted that in all cases throughout this investigation the entire Pd electrode was maintained submerged beneath the solution level so that the Pd was never in contact with the external atmosphere. After a given wire was cleaned electrolytically overnight, the hydrogen stirring was begun and the open-circuit potential vs. a Pt/H_2 electrode in the same solution as well as the electrical resistance of the wire was recorded as a function of time. Zero time is taken when hydrogen flow is begun. The resistance was measured

with a General Electric Portable Double Bridge which is designed to measure resistance from 0.0001 to 22Ω.

These same experiments were repeated with these same wires wound in the form of a toroid on a polyethylene ring and placed in the Teflon cell. The results of this series of experiments were similar to those done in the polyethylene cell.

Results and Discussion

Figure 1 shows the open-circuit potential vs. a Pt/H_2 electrode in the same $2N$ H_2SO_4 solution for a series of Pd electrodes having different values for the ratio of the exposed apparent surface area to the total volume of the Pd as a function of time. The surface area was determined by geometric measurement and the volume by weight measurements using a value of 12.01 g cm^{-3} for the density of Pd. As was observed by Ratchford and Castellan, the open-circuit potential falls from the high positive value produced by anodization to a very flat plateau at about 50 mv. After a time, the potential falls along a sigmoid curve to zero and remains there. The length of the 50 mv plateau and the transition time from the 50 mv plateau to the zero volt plateau are found to be sensitive to the ratio, area/volume (A/V).

In Fig. 2 and 3 are shown the relative resistance-vs.-time curves for a series of Pd wires. Figure 3 shows the initial part of the curves in greater detail. It is seen that a plateau of varying length occurs at about a value of R/R_0 of 1.05. Using Fischer's expression (7), $R = R_0(1.0292 + 0.000668\ V)$, where V is the relative volume of the dissolved hydrogen, this resistance value corresponds to about 31 relative volumes or a H/Pd atomic ratio of about 0.03, the upper limit of the α-phase (1, 7, 8).

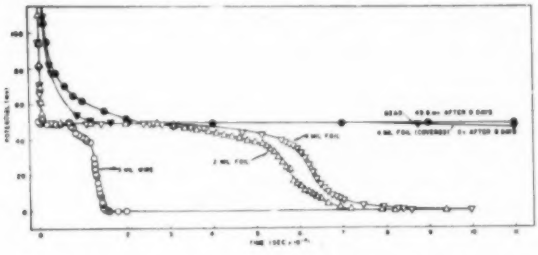

Fig. 1. Open-circuit potentials of Pd electrodes of various sizes in 2N H_2SO_4 solution plotted as function of time. Potential measured with reference to Pt/H_2; temperature, 24°±1°C.

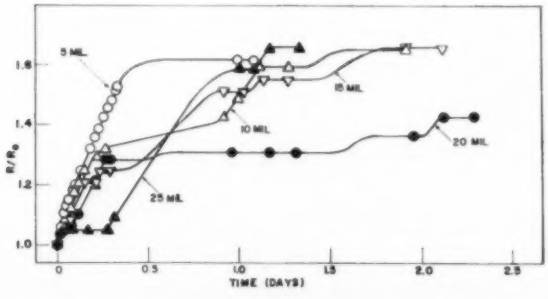

Fig. 2. Relative resistance-vs.-time curves for Pd wires of different diameter; temperature, 24°±1°C.

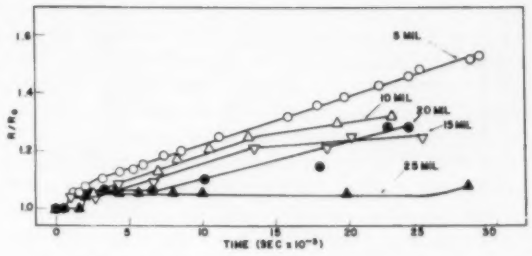

Fig. 3. Initial part of relative resistance-vs.-time curves of Fig. 2 for Pd wires on open circuit in H_2-saturated acid solution.

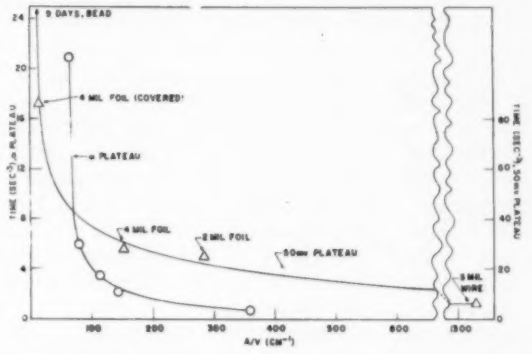

Fig. 4. Length of α plateau found on resistance-time curves for Pd wires is shown by circles and is plotted vs. surface-to-volume ratio. Length of 50 mv plateau found on potential curves for Pd electrodes of various shapes is shown by triangles and also is plotted as function of surface-to-volume ratio.

In general after the α-phase-plateau the resistance increases uniformly to about a value of 1.27 for R/R_0 which corresponds to a H/Pd atomic ratio of 0.29. In Fig. 5 is shown the potential-time curve with the accompanying relative resistance-time curve for only the 5 mil wire case, for the sake of simplicity. Similar curves were obtained for all the other wires. When the relative resistance reaches a value of about 1.35, corresponding to a H/Pd atomic ratio of 0.37, the potential begins to drop away from the 50 mv plateau in all cases. This is in good agreement with the data reported when the wire was charged with hydrogen cathodically (1, 2). When the potential finally reaches a steady value of zero volts, the resistance has come to a steady value somewhat over 1.6 for R/R_0. This is a higher value than was reported for a wire charged with hydrogen cathodically (1, 2) and corresponds to a H/Pd atomic ratio near 0.7.

In order to check the hydrogen content of a wire which had reached zero volts, the amount of hydrogen absorbed was determined using ceric sulfate solution and was found to contain about 0.6 H/Pd atomic ratio.

A plot of the length of the 50 mv plateau vs. A/V is found in Fig. 4. The curve is hyperbolic. Although the experiment with the bead was terminated for convenience after 9 days, it is believed that the potential would have fallen to zero after a sufficiently long time.

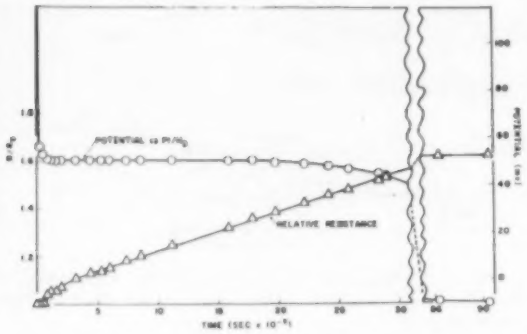

Fig. 5. Potential vs. time and R/R_o time curve recorded simultaneously for 5 mil wire; temperature, 24°±1°C; solution, hydrogen saturated 2N H_2SO_4.

The length of the α-Pd plateau for the wires is plotted in Fig. 4 as a function of A/V. This plot is also hyperbolic. If the data in Fig. 4 are plotted as a function of V/A instead of A/V, indeed, straight lines are obtained. This indicates that the length of the plateau is directly proportional to the volume and inversely proportional to the area. It is to be noted, though, that the values for the bead and for the 25 mil wire deviate from the respective straight lines toward higher values.

One may conclude from the data in Fig. 5 that hydrogen does not enter the Pd metal until the oxide is removed from the surface. This is indicated by the fact that the resistance does not change until the potential drops from a high positive value to that of 50 mv which is the potential associated with the exposed α-Pd surface of maximum concentration. This same behavior was found in all cases. Once the surface is clear the hydrogen is dissolved by the Pd.

The potential remains at 50 mv until an H/Pd atomic ratio of about 1.37 is reached. At this point, the amount of β-Pd has increased at the expense of the α-phase until now the mixed potential (2), which had, up until now, been dominated by the α-phase potential-determining reaction, is beginning to be dominated by the β-phase reaction. Of course, when the wire reaches a potential of zero volt, it is now a β-phase electrode and the potential determining reaction is the same as that on Pt.

Because of the fact that both the length of the plateau of 50 mv on the potential curves and the length of the α-phase plateau on the resistance curves are sensitive to the ratio, A/V, it is suggested that the penetration of the surface skin of the metal is the rate-determining step in the solution of hydrogen by Pd. This proposal is also supported by the lack of a thickness effect in the transport of hydrogen through a Pd bielectrode (9). Once the hydrogen enters the interior of the metal, it is quite mobile as shown by the nuclear magnetic resonance work of Norberg (10) and spreads evenly throughout the metal. It is postulated here that the β-phase cannot nucleate until the entire body of Pd is converted to the α-phase of maximum hydrogen concentration (H/Pd at ratio ~0.03). It is interesting to note that the resistance makes a very rapid jump to an R/R_o-value of about 1.05 and remains at this value for a length of time dependent on the value of A/V according to the curve shown in Fig. 4. It would appear, then, that the resistance is not a linear function of the hydrogen content until the maximum α-phase concentration is reached throughout the metal. As a matter of fact, Fischer makes this statement, and it appears in the intercept value of 1.0292 in his equation. It is assumed here that the length of the α-phase plateau is the time it takes to change the entire bulk of Pd to the α-phase of maximum concentration and that the resistance is not a linear function of hydrogen content until at least some β-phase is present.

After the α-phase plateau the resistance increases at the same linear rate of 1.67×10^{-5} units sec^{-1} up to a value of about 1.27 for R/R_o in all cases regardless of the value of A/V. From then on, as shown in Fig. 2, the resistance increases in steps, increasing in length with decreasing values of A/V, except for the 25 mil case. This would seem to suggest that the β-phase nucleates at various centers throughout the metal and then grows according to a domain-type mechanism at the expense of the α-phase. The steps in the resistance may be due to a coalescing of these domains. The rate at which the β-phase nucleates and grows seems to be a function of the history of the electrode preparation as exemplified by the rapid charging of the 25 mil wire. Such steps are not found in the open-circuit potential curves for these wires. These curves are not shown here, but they are similar to the smooth curves shown in Fig. 1. This may have been expected since the resistance is a bulk quantity while the potential is a function of a surface quantity and surface conditions may not necessarily vary linearly with those occurring in the bulk material.

In the case of a very small wire, these effects are at a minimum because of the high surface area and consequently the high rate of penetration of the hydrogen to the interior of the metal. It is with this type of electrode, one with a very high value of A/V, that Ratchford and Castellan worked and so they worked on the right-hand branch of the hyperbolas shown in Fig. 4. On the other hand, Schuldiner and Hoare worked on the left-hand branch by using small beads and pieces of foil

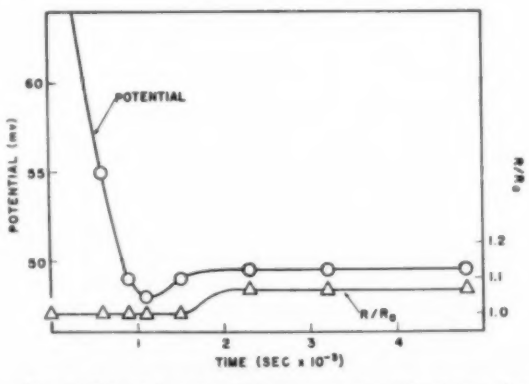

Fig. 6. Potential and resistance curves for 20 mil wire that exhibited overshoot in potential. Potential is measured against Pt/H_2 electrode in same solution.

highly covered with polyethylene films. In this way it is possible to resolve the differences between the two investigations. Even though it is not necessary to resort to a change in the point of zero charge to explain the α-phase plateau, it is still held that the hydrogen enters the metal by way of a hydrogen atom in the double layer being transported to the metal surface through an adsorbed water molecule as described before (3).

It was observed neither by Schuldiner and Hoare nor in this investigation that an electrode made from Pd foil or bead gave a potential time curve with a minimum similar to a supercooling curve. This effect was not observed for the wires stretched along a straight line in the polyethylene cell nor for the same wire wound as a toroid on a polyethylene ring in the Teflon cell. However if the wire was wound in the form of a loose air-cored helix, a minimum may be found as shown in Fig. 6. It is important to note that the resistance does not change from the original hydrogen free value of R_0 until the potential has returned to the 50 mv value. It would appear, then, as the hydrogen removes the oxygen from the surface, by some chance condition of the surface film brought about by an accidental stage in the history of its preparation the surface becomes more platinum-like, that is, a noble metal that does not dissolve hydrogen readily and the potential strives toward zero volt. However, the potential never reaches zero because the hydrogen gradually destroys this unusual surface film. After the film is destroyed and the true Pd surface exposed, the hydrogen begins to dissolve, the resistance increases and the potential returns to the 50 mv plateau. Although the nature of this surface film has not been determined at this time, it is seen that it is reduced by hydrogen, it is conducting, it is a catalyst for the hydrogen reaction, and it most likely contains oxygen since it occurs only after strong anodization.

In view of the results presented here it may be necessary to differentiate between three types of hydrogen-charging mechanisms in the Pd-H system. In previous work (3), it was shown that hydrogen-charged Pd that was obtained from dry Pd exposed to dry hydrogen gas had different properties from that obtained by the cathodic charging of a Pd electrode in an acid solution. A difference was in the hydrogen content of the final stable product which seemed to be a function of the amount of lattice distortion. In the first case the H/Pd atomic ratio was about 0.6 while in the second case it was about 0.36. In the present work, the final product contains hydrogen at 0.6 H/Pd atomic ratio but which exhibits a relative resistance which seems to be much too high and does not lose hydrogen as in the cathodized case. This may indicate that in this case the lattice is distorted in a different manner in absorbing a quantity of hydrogen necessary to raise the H/Pd atomic ratio to 0.6 than in the two previous cases cited above. Apparently the domain-like charging process described here was not permitted in the cathodically charged Pd due to the forcing of the hydrogen into the Pd by electrochemical means as shown by the linear curve in Ref. (1).

One may say, then, that Pd charged with hydrogen to the β-phase by standing on open circuit in a hydrogen-stirred acid solution gives a final result more similar to the dry Pd-H charging than to the cathodic charging. Also, if one wishes to study the properties of α-phase Pd one must use an electrode configuration (e.g., beads) in which the A/V value is such that the rate of change to the β-phase is very slow.

Manuscript received Feb. 20, 1959. This paper was prepared for delivery before the Philadelphia Meeting, May 3-7, 1959.

Any discussion of this paper will appear in a Discussion Section to be published in the June 1960 JOURNAL.

REFERENCES

1. J. P. Hoare and S. Schuldiner, *J. Phys. Chem.*, **61**, 399 (1957).
2. S. Schuldiner, G. W. Castellan, and J. P. Hoare, *J. Chem. Phys.*, **28**, 16 (1958).
3. J. P. Hoare, S. Schuldiner, and G. W. Castellan, *ibid.*, **28**, 22 (1958).
4. R. J. Ratchford and G. W. Castellan, *J. Phys. Chem.*, **62**, 1123 (1958).
5. F. A. Lewis and A. R. Ubbelohde, *J. Chem. Soc.*, 1710 (1954).
6. J. P. Hoare and S. Schuldiner, *This Journal*, **102**, 485 (1955).
7. F. Fischer, *Ann. Physik*, **20**, 503 (1906).
8. D. P. Smith, "Hydrogen in Metals," p. 126, Univ. Chicago Press, Chicago (1948).
9. J. P. Hoare and S. Schuldiner, *ibid*, **104**, 564 (1957).
10. R. E. Norberg, *Phys. Rev.*, **86**, 745 (1952).

The Growth of Barrier Oxide Films on Aluminum

W. J. Bernard and J. W. Cook

Sprague Electric Company, North Adams, Massachusetts

ABSTRACT

The growth of anodically formed barrier oxide films on aluminum has been followed by weight, capacitance, and rate measurements. The increase of film thickness at constant voltage has been calculated and compared to the values obtained by optical measurements. The results have been shown to obey the law $i = \alpha e^{\beta V}$.

Several papers in recent years (1-6) which have dealt with the thickness of anodically formed barrier oxide films on aluminum lead to the conclusion that the thickness is determined precisely by the voltage impressed on the oxide film. This conclusion ignores the generally accepted theory of anodic ox-

ide growth first advanced by Mott (7) and covered more specifically in the case of aluminum by Charlesby (8) and by Nagase (9). It is the purpose of the present paper to show that the relationship between current and field $i = \alpha e^{\beta V/s}$, where α and β are constants, correctly expresses the dependence of the thickness, s, of the oxide film on both ionic current density, i, and the applied voltage, V. It is probably the failure to define the current density in the cited papers, rather than the use of different electrolytic solution, which has led to the variations in reported values of oxide thickness, ranging from 12.7 to 16.5 Å/v. Although it is pointed out by van Geel and Schelen (2) that film growth may continue at constant voltage, they suggest that it is sufficient only to permit the current to decrease to a low (but unspecified) value in order to define the thickness.

In this investigation we have calculated oxide film thicknesses by measurement of the weight of oxide and by the direct measurement through the use of interference fringes. This latter method has been employed previously by Nagase (1).

Barrier films can be formed on Al in any of several different aqueous solutions, most commonly in solutions of boric acid or alkali borates. However, aqueous solutions are characterized by generally poor current efficiency of oxide formation, as a result of oxygen evolution and anodic dissolution of Al. These effects make it difficult to examine only that component of the current which leads to film growth, and we have, therefore, found it convenient to work with solutions of ammonium pentaborate in ethylene glycol. The particular composition chosen by us (30% by weight of salt) is not useful for oxidizing Al to high voltages, but it is characterized by a high current efficiency of formation up to 150 v; within the error of the measurements the efficiency is 100%. The films found in this solution appear to be identical to those found in aqueous solutions of boric acid, as shown by the capacitance of films formed under the same conditions of temperature, voltage, and current density in the two electrolytes.

In order to determine the thickness of a formed film by weight measurements, the density of the oxide and the surface area of the formed metal must be known. The density of such films of Al_2O_3 is not necessarily the same as that of the bulk oxide, and values varying from 3.0 to 5.0 g/cm³ have been reported. We have, therefore, also carried out a determination of this quantity. The "roughness factor" of the metal surface has been estimated by comparing the formation charge required for foil to that of highly polished Al surfaces where the true area is assumed to be equal to the geometrical area. We have verified the equation for oxide growth by obtaining straight-line plots of log i vs. 1/W (W = oxide film weight), and log i vs. capacitance, over the current density range of 10^{-8} to 10^{-7} amp/cm² for films maintained at a constant voltage of 150 v.

Experimental

Formations were carried out at 25°C on Alcoa foil of 99.99% purity, with an apparent surface area of 97 cm². Before forming the foil was cleaned briefly with cold potassium dichromate-sulfuric acid cleaning solution and washed thoroughly with high-purity water, rinsed in methanol, and dried. The negative electrodes of the formation cell, which were platinized, also served as the subsidiary electrodes for capacitance measurements of the formed films.

The roughness factor of the foil was measured by comparing its formation charge to that of electrodes which were assumed to have a factor of unity. These latter electrodes were prepared by machining high-purity Al plates in the form of disks 2 in. in diameter. One face of each disk was drilled and tapped to accommodate a brass rod which served as an electrical contact. The opposite face was polished, cleaned, and then formed, along with the cylindrical surface, to 400 v in aqueous boric acid. The formed face was repolished to a mirror finish and then given a brief chemical polish in Alcoa "R-5 Bright Dip" solution. The heavy formation on the cylindrical surface of the electrode protected that portion from chemical attack and defined the area for subsequent formation. Several such electrodes were formed to 150 v at 1.0 ma/cm², and from the charge passed it was determined that the roughness factor of our foil specimen was 1.03. This low roughness factor is probably not a true measure of the state of the surface before formation but is a result of the smoothing effect of anodizing. This effect has been discussed by Lewis and Plumb (10).

Oxide films were detached from the underlying metal by dissolving the Al in a methanol-bromine solution (11), filtered, washed, and dried at 105°C. All weighings were made on a Brinkmann-Sartorius microbalance.

Density measurements were made by hydrostatic weighing in toluene. About 100 mg of sample was sufficient to give the desired accuracy.

Capacitance readings were made 10 min after removal of voltage, at which time the change in capacity with time is negligible.

Direct determinations of the thickness of films were made by the measurement of the displacement of interference fringes produced by a standard air wedge. Detached flakes of oxide, prepared by Strohmaier's method (12), were mounted on an optical flat and covered with an evaporated layer of silver about 600Å thick. Since the step thus produced on the surface of the optical flat is the same height as the thickness of the oxide film, the observed displacement is the same as that which would be due to the film itself. The displacement was measured at a magnification of 32X with a traveling microscope which was calibrated to read to 0.001 mm. The light source was the Hg 5460Å line.

A constant-current generator[1] was used for the measurement of formation rates at constant current. The range of current of this instrument limited the measurements to between 2.0×10^{-6} and 2.0×10^{-4} amp/cm². During the period of measurement the current could be held constant to better than 0.5%.

[1] Constructed by the Test Equipment Department, Sprague Electric Co.

Table I. Current efficiency of oxide formation based on weight measurements

Current density, amp/cm²	10^{-7}	10^{-6}	10^{-5}	10^{-4}	10^{-3}
Total charge, coulombs/cm²	0.388	0.363	0.339	0.318	0.299
Measured wt. gain, μg/cm²	31.9	30.0	28.3	26.8	25.0
Calculated wt. gain, μg/cm²	32.2	30.3	28.1	26.3	24.8
Measured wt. of oxide, μg/cm²	68.0	63.6	59.8	56.5	53.4
Calculated wt. of oxide, μg/cm²	68.4	64.0	59.6	56.0	52.8

Results

The validity of the results is dependent on a knowledge of the current efficiency of oxide formation, i.e., the fraction of the total current which is ionic. Preliminary work with the glycol-borate electrolyte showed a linear rise in voltage with time to slightly higher than 150 v when a constant current of 10^{-3} amp/cm² was maintained. Therefore, an end voltage of 150 v was chosen as a convenient value for our formations. Formations were made at a constant current density with a silver coulometer in series with the cell, the voltage being adjusted manually during formation. At the end voltage, the voltage was held constant, and the current was allowed to decrease to the desired value. Therefore, in each formation 0.299 coulomb/cm² (see Table I) was passed at 10^{-3} amp/cm², the remainder of the charge being passed at a constantly decreasing current density. The measured weight gain of the anode was compared to that calculated from the amount of charge passed, assuming that the production of Al_2O_3 was the only anodic process. In addition, the oxide was removed from the foil, and its weight was also compared to the calculated value. Table I shows that the agreement between the two values is generally within 1%, which is the estimated error of the experiments.

Heating of the oxide to 600°C resulted in no change in weight, indicating that the film contained neither water nor glycol, and the presence of borates could not be detected by chemical analysis. Furthermore, there was no apparent oxygen evolution at any time during formation, nor did the electrolyte contain Al after formation. On the basis of these analyses, we have concluded that the anodic product was solely Al_2O_3 and that the conditions of formation led to 100% current efficiency of oxide formation.

Figure 1 is a plot of log i vs. $1/W$ (the reciprocal of the weight of oxide per unit area), where each point represents the average value of at least three separate measurements. The data at the higher current densities were corrected for iR losses in the electrolyte so that each point corresponds to an applied anodic voltage of 150 v. The slope of the line is $150\beta\rho/2.303$ where ρ is the density of the anodic oxide. Four separate density measurements resulted in an average value for ρ of 3.17 ± 0.03 g/cm³. β is then calculated to be 4.8×10^{-6} cm/v. A similar plot of log i vs. capacitance per unit area measured at 120 cps is given in Fig. 2. The slope in this case is equal to $150\beta/2.04 \times 10^{-13}\epsilon$. From the thickness measurements, ϵ is calculated to be 8.4 ± 0.2, and β from this plot has a value of 5.4×10^{-6} cm/v. Extrapolation of the two plots permits an estimation of α, giving 10^{-22} and 10^{-24} amp/cm² in Fig. 1 and 2, respectively. Charlesby (8) reported $\beta = 3 \times 10^{-6}$ and $\alpha = 10^{-18}$, while Nagase (9), who obtained his values from rate measurements, is in better agreement with our figures, giving 4.3×10^{-6} and 10^{-20} for β and α.

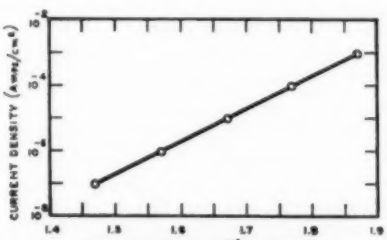

Fig. 1. Current density vs. reciprocal weight of aluminum oxide films maintained at a constant potential of 150 v at 25°C.

Table II shows the thickness, s, calculated for some of the points and compared with those obtained from interferometric measurements, the latter being reliable to about 30Å. Satisfactory agreement was obtained between the two methods.

The increase in oxide thickness which is possible at constant voltage explains the variation in the reported values for anodic aluminum oxide. In the range of currents discussed here, a 150-v film may vary in thickness from 11.3 to 14.4 Å/v. Clearly, then, both voltage and ionic current density must be defined if the value of thickness at some specified voltage is to be significant.

In a recent paper, Winkel, Pistorius, and van Geel (13) suggest a modification of the existing theory for anodic growth. Support for their view is given by their observation that the constant β apparently varies with field. However, the aqueous electrolyte used in their experiments required them to correct the total current for the electronic component, and large corrections of this nature lead to an appreciable degree of uncertainty in the final results. We, on the other hand, have measured these rates in our electrolyte of high current efficiency and plotted in the same manner as Winkel, *et al.*, as shown in Fig. 3. A straight line is produced as predicted by theory. From the slope β may again be calculated and gives the value 4.4×10^{-6}, in good

Table II. Comparison of film thickness at constant voltage as determined by weight and optical measurements

Current density, amp/cm²	Film thickness, cm × 10^6	
	Weight measurement	Optical measurement
10^{-3}	1.68	1.72
10^{-5}	1.89	1.93
10^{-7}	2.15	2.14

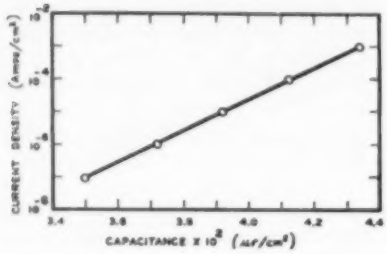

Fig. 2. Current density vs. 120 cps capacitance of aluminum oxide films maintained at a constant potential of 150 v at 25°C.

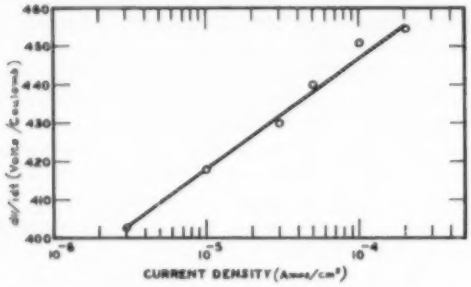

Fig. 3. Increase of voltage per unit charge as a function of the current density of formation at 25°C.

agreement with the values obtained from weight and capacitance measurements.

Rates at all current densities were measured in the voltage range of 120–150 v by first forming at 10^{-3} amp/cm² to 120 v and then reducing the current to the desired level. In this way all rates were measured under the same conditions of surface roughness since nearly the same thickness of oxide was present before the initial readings were taken.

All the work presented here is based on the assumption that even at the lowest current densities used we are dealing solely with ionic current. It may be argued that since the experiments which led to this conclusion were based on formations during which the major portion of the charge was passed at 10^{-3} amp/cm², an appreciable contribution by electronic current would have been unnoticed at the lower currents. If such were the case, however, we would not expect such a good fit to the plots over the whole range. Furthermore, the rate curve (Fig. 3) would then be expected to have the shape obtained by Winkel, *et al.*, rather than a straight line.

Acknowledgments

The authors wish to acknowledge the assistance of Mr. Stanley Szpak, who prepared the special electrodes for surface roughness measurements, and Mrs. Concetta Duval, who carried out the density determinations.

Manuscript received Jan. 19, 1959.
Any discussion of this paper will appear in a Discussion Section to be published in the June 1960 JOURNAL.

REFERENCES

1. K. Nagase, *Mem. Inst. Sci. Ind. Research, Osaka Univ.*, **10**, 66 (1953).
2. W. Ch. van Geel and B. J. J. Schelen, *Philips Research Repts.*, **12**, 240 (1957).
3. M. Hennig, *Z. Physik*, **144**, 296 (1956).
4. W. Walkenhorst, *Naturwissenschaften*, **34**, 373 (1947).
5. G. Hass, *J. Opt. Soc. Amer.*, **39**, 532 (1949).
6. R.C. Plumb, *This Journal*, **105**, 498 (1958).
7. N. F. Mott, *Trans. Faraday Soc.*, **43**, 429 (1947).
8. A. Charlesby, *Proc. Phys. Soc.*, **66B**, 317 (1953).
9. K. Nagase, *Mem. Inst. Sci. Ind. Research, Osaka Univ.*, **12**, 67 (1955).
10. J. E. Lewis and R. C. Plumb, *Intern. J. Appl. Radiation and Isotopes*, **1**, 33 (1956).
11. T. J. Nurse and F. Wormwell, *J. Appl. Chem. (London)*, **2**, 550 (1952).
12. K. Strohmaier, *Z. Naturforsch.*, **6a**, 508 (1951).
13. P. Winkel, C. A. Pistorius, and W. Ch. van Geel, *Philips Research Repts.*, **13**, 277 (1958).

Kinetics of the Dissolution of Copper in Oxygen-Containing Solutions of Various Chelating Agents

J. Halpern,[1] H. Milants,[2] and D. R. Wiles[3]

Department of Mining and Metallurgy, The University of British Columbia, Vancouver, British Columbia

ABSTRACT

The kinetics of the dissolution of copper in stirred oxygen-containing solutions of ethylenediamine and several amino acids have been examined and compared with those found earlier for ammonia. In each case, provided that the partial pressure of oxygen exceeds a critical value (below which its transport to the copper surface may be rate limiting), the rate was found to be zero-order in oxygen and first-order in the complexing agent. The rate-determining process is believed to be the chemical attack of the oxygen-covered copper surface by the complexing agent. At 25°, the rate constants for dissolution by ethylenediamine, glycinate, α-alaninate, and β-alaninate were found to be 2.3×10^2, 49, 59, and 11 mg Cu cm^{-2} hr^{-1} M^{-1}. These follow the same order as the stability constants of the corresponding cupric complexes. In each system there is also another reaction path, independent of the first, which involves the protonated species, i.e., the ethylenediaminium ion and the neutral amino acids. The corresponding rate constants are 5.1×10^2, 31, 36, and 3.5 mg Cu cm^{-2} hr^{-1} M^{-1}.

A kinetic study of the dissolution of copper in oxygen-containing aqueous solutions of ammonia and ammonium salts was described earlier (1, 2). It was shown that the reaction proceeded by two independent paths whose rate-determining steps are the chemical attack on the oxygen-covered copper surface by an NH_3 molecule and an NH_4^+ ion, respectively. Both rates are independent of the oxygen concentration above a critical value when the transport of oxygen to the surface is no longer rate-limiting. Under these conditions the kinetics are of the form

$$\text{Rate} = k_A[NH_3] + k_{AB}[NH_4^+] \qquad [1]$$

At lower oxygen partial pressures a different rate law, first-order in oxygen and independent of the concentrations of ammonia or ammonium salts, was observed; this was attributed to rate control by oxygen transport.

The present paper describes similar measurements using several other complex-forming reagents, notably the chelating agents ethylenediamine, glycine, α-alanine, and β-alanine. These were selected with a view to providing further insight into the role of complex formation in the mechanism of the dissolution process and to correlating the rate of dissolution with the structure and stability of the complexes formed.

Experimental

The apparatus and experimental procedure were similar to those employed earlier (1, 2) with the following minor variations: Agitation was effected by means of a turbine-type impeller whose blades, generally rotating at 770 rpm, swept a cylindrical volume of 8 cm diameter. The exposed surface (generally about 2 cm^2) of the Bakelite-mounted copper specimen was positioned in a vertical plane tangential to this cylindrical volume.

Most of the measurements were made using conductivity-grade (99.97%) copper; no difference in the rate of dissolution was noted when Johnson-Matthey high-purity (99.999%) copper was used instead. Different annealing pretreatments, which resulted in grain sizes ranging from 0.035 to 0.12 mm, were also without effect on the dissolution rate. Before each experiment the copper surface was etched lightly with an ammonia-ammonium persulfate solution, but this procedure also did not appear to be critical.

Ethylenediamine (99%) was obtained from Carbon and Carbide Chemicals Corp. Purification by fractional distillation did not affect the dissolution rate. Glycine, α-alanine, and β-alanine, of Reagent Grade, were obtained from Nutritional Biochemical Corp.

Dissolution rates were determined by analyzing the leaching solution periodically for copper using the carbamate colorimetric method (3). All experiments were performed at 25.0° ± 0.1°C. To avoid the complications due to salt effects found in the previous study (1), the total electrolyte concentration of all the solutions was adjusted (in most cases to 0.1M) with sodium perchlorate.

Results

The chelating agents used and their properties are listed in Table I. Typical rate plots for the various complexing agents are shown in Fig. 1. In all cases these were found to be linear, and the dissolution rates, corresponding to the slopes of the plots, were generally reproducible to about ±2%. It was established that the total dissolution rates were proportional to the copper surface area and independent of the solution volume (generally 2 liters). No cuprous species could be detected in the solutions, the dis-

[1] Department of Chemistry, University of British Columbia.
[2] Present address: Union Minière du Haut Katanga, Jadotville, Belgian Congo.
[3] Present address: Department of Chemistry, Carleton University, Ottawa, Ont.

Table I. Properties of complexing agents and first order rate constants for the dissolution of copper at 25°C

Complexing agent	A or A⁻	Formula	pK* HA⁺	pK* H_2A^{++}	Stability constant of Cu^{++} complex* $\log K_1$	Stability constant of Cu^{++} complex* $\log K_2$	Rate constant (mg cm^{-2} hr^{-1} M^{-1}) k_A	Rate constant (mg cm^{-2} hr^{-1} M^{-1}) k_{AH}
Ammonia	A	NH_3	9.26	—	4.3	3.6	84†	1550†
Ethylenediamine	A	$NH_2CH_2CH_2NH_2$	10.2	7.47	10.7	9.3	2.3×10^2	5.1×10^2
Glycinate	A^-	$NH_2CH_2COO^-$	9.78	2.35	8.4	6.9	49	31
α-Alaninate	A^-	NH_2CHCOO^- (CH₃)	9.87	2.34	8.4	6.9	59	36
β-Alaninate	A^-	$NH_2CH_2CH_2COO^-$	10.4	3.60	7.1	5.5	11	3.5

* From Ref. (4).
† From Ref. (1).

solved copper apparently being predominantly in the form of the tetracoordinated cupric chelate complex, e.g., $Cu(en)_2^{++}$, $Cu(gl)_2$, etc.

For each of the complexing agents, the dependence of the rate of dissolution on the concentration of the reagent and on the oxygen partial pressure (shown for ethylenediamine in Fig. 2) was found to conform qualitatively to the same pattern as observed previously for ammonia. This pattern is characterized by two distinct kinetic regions. At low oxygen pressures, the rate is first order in oxygen and independent of the concentration of the complexing agent. In the case of ammonia, evidence was found that the rate in this region is determined by transport of oxygen to the copper surface. While this interpretation also may apply to the present systems, it appears superficially at variance with the observations that the rate for ethylenediamine in this region (as well as in the region of high oxygen pressure) was unaffected by varying the stirring rate from 550 to 810 rpm and that the rates for solutions of different complexing agents (e.g., ethylenediamine and glycine) differed by as much as 25%. This point was not investigated further, and all the kinetic results to be considered here refer to the region of higher oxygen pressure, where the rate was found to be zero-order in oxygen and first-order in the complexing agent. In this region the rate-determining step is obviously chemical in nature.

In the ethylenediamine system, kinetic measurements extended over ethylenediamine (en) concentrations of 0.05 to 0.5M, ethylenediaminium (enH^+) perchlorate concentrations of 0.00 to 0.03M and oxygen partial pressures of 0 to 7.5 atm. The results are summarized in Table II and Fig. 2 to 4 and, in the high oxygen pressure region, conform to a rate-law analogous to Eq. [1], i.e.,

$$\text{Rate} = k_A[\text{en}] + k_{AH}[\text{enH}^+] \qquad [2]$$

Values of k_A and k_{AH}, given in Table I, were computed from the data in Table II.

Addition of sodium hydroxide to a solution of ethylenediamine resulted in a slight decrease in the rate of dissolution (Table II). This is attributed to passivation of the copper surface by oxide or hydroxide films.

In the glycine, α-alanine, and β-alanine systems, kinetic measurements were made at concentrations ranging from 0.0 to 0.3M each of the free amino acid (AH) and of the corresponding anion (A^-). The results are summarized in Table II. Both

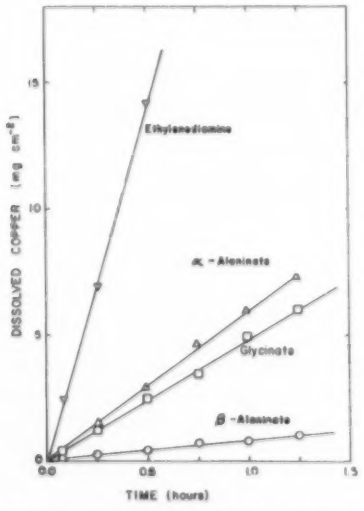

Fig. 1. Typical rate plots for the dissolution of copper in 0.1M solutions of various complexing agents at 25°, 6.5 atm O_2.

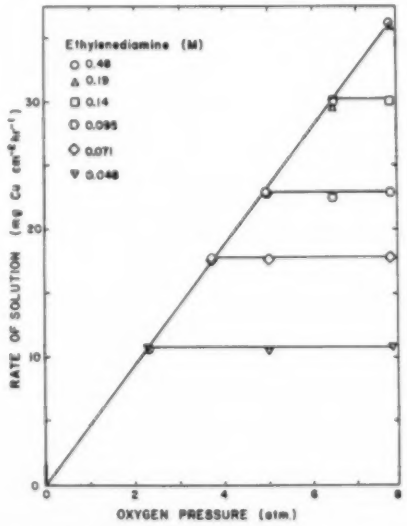

Fig. 2. Dependence of the dissolution rate on the ethylenediamine concentration and the oxygen partial pressure.

Table II. Summary of kinetic data (25°)*

Chelating agent	Concentration (M) A†	AH⁺†	AH_2^{++}†	NaOH (M)	pH	Ionic strength‡	Rate of solution (mg Cu $cm^{-2}hr^{-1}$)
Ethylenediamine	0.045	0.002	0.00	0.00	11.5	0.1	11.7
	0.068	0.003	0.00	0.00	11.5	0.1	17.2
	0.091	0.004	0.00	0.00	11.6	0.1	22.8
	0.138	0.005	0.00	0.00	11.7	0.1	31.3
	0.0475	0.010	0.00	0.00	10.9	0.1	17.0
	0.0475	0.020	0.00	0.00	10.6	0.1	22.0
	0.0475	0.030	0.00	0.00	10.4	0.1	27.0
	0.0950	0.00	0.00	0.01	11.8	0.1	20.0
	0.0950	0.00	0.00	0.02	12.2	0.1	19.4
	0.0950	0.00	0.00	0.03	12.4	0.1	18.5
Glycinate	0.097	0.003	0.00	0.00	11.3	0.1	4.8
	0.146	0.004	0.00	0.00	11.3	0.2	9.8
	0.194	0.006	0.00	0.00	11.3	0.3	14.8
	0.00	0.10	0.00	0.00	6.0	0.1	3.2
	0.00	0.15	0.00	0.00	6.0	0.1	4.6
	0.00	0.20	0.00	0.00	6.0	0.1	6.2
	0.00	0.10	0.01	0.00	4.2	0.1	0.2
	0.00	0.10	0.02	0.00	2.7	0.1	0.0
α-alaninate	0.096	0.0037	0.00	0.00	11.3	0.1	5.9
	0.193	0.0074	0.00	0.00	11.3	0.2	11.7
	0.29	0.011	0.00	0.00	11.3	0.3	17.3
	0.00	0.10	0.00	0.00	6.3	0.1	3.6
	0.00	0.20	0.00	0.00	6.3	0.2	7.5
	0.00	0.30	0.00	0.00	6.3	0.3	10.8
	0.00	0.10	0.01	0.00	4.2	0.1	0.2
	0.00	0.10	0.02	0.00	2.7	0.1	0.0
β-alaninate	0.094	0.006	0.00	0.00	11.6	0.1	1.0
	0.187	0.013	0.00	0.00	11.6	0.2	2.2
	0.281	0.019	0.00	0.00	11.6	0.3	3.6
	0.00	0.10	0.00	0.00	6.6	0.1	0.34
	0.00	0.20	0.00	0.00	6.6	0.1	0.69
	0.00	0.30	0.00	0.00	6.6	0.1	1.11
	0.00	0.10	0.01	0.00	4.7	0.1	0.00

* O_2 partial pressure = 7.8 atm for ethylenediamine and 6.5 atm for the other systems.
† [A^-], [AH], and [AH_2^+] in the case of the amino acids.
‡ Adjusted with $NaClO_4$.

species are apparently active in promoting dissolution and the oxygen-independent rate law in each system was found to be of the form

$$\text{Rate} = k_A[A^-] + k_{AH}[AH] \qquad [3]$$

Values of k_A and k_{AH}, computed from these data, are listed in Table I. By analogy with the interpretations accorded to the ammonia and ethylenediamine system it may be concluded that these are the rate constants for the independent attack of the anion and acid species, respectively, on the oxygen-covered copper surface, either process leading to the dissolution of a cupric ion.

The neutral amino acids are present in solution in two forms (5), the zwitterion (e.g., $^+NH_3CH_2COO^-$) and the molecular form (e.g., NH_2CH_2COOH). Since the ratio of the concentrations of the two forms is constant for each acid, the kinetic data provide no information about the relative contributions of the two species to the rate. However, in view of the predominance of the zwitterion form, it is reasonable to conclude that k_{AH} refers essentially to the reaction of this species.

No passivation effect was evident with solutions containing appreciable concentrations of the free amino acid and/or the anion. However, the addition of an excess of H^+, resulting in formation of some protonated amino acid, H_2A^+, was found to inhibit dissolution completely. This is attributed to passivation of the copper surface by an oxide film due to suppression of complex formation in the solution

$$CuA_2 + 2H_2A^+ \rightleftharpoons Cu^{++} + 4AH \qquad [4]$$

[Similarly it was found (2) that copper does not dissolve in a solution containing NH_4^+ if the free NH_3 concentration is very low, despite the fact that the rate constant for the reaction of NH_4^+ is higher than for NH_3 when both are present.] Because of this restriction, measurements could be made only in solutions in which the concentration of the pro-

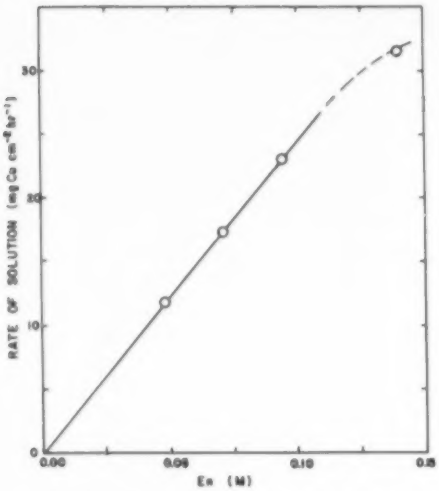

Fig. 3. Dependence of the rate at 7.8 atm O_2 on the ethylenediamine concentration.

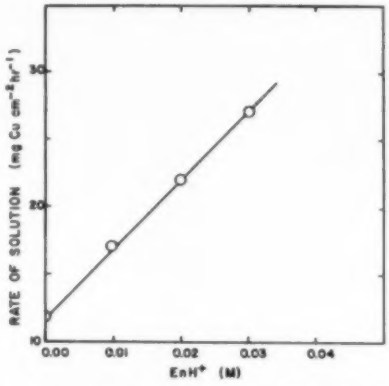

Fig. 4. Dependence of the rate at 7.8 atm O_2 on the ethylenediaminium perchlorate concentration. Solutions also contain 0.048M free en. Ionic strength held constant at 0.1M with sodium perchlorate.

tonated amino acid (e.g., $^{+}NH_3CH_2COOH$) was very low and the rate constant for the reaction of this species could not be determined.

Under the conditions employed in these studies (25°, 6.5 atm O_2) the dissolution of copper in solutions of acetic acid and/or sodium acetate was found to be very slow. This is probably also due to passivation of the copper since the pH of these solutions is relatively high and the complexing of Cu^{++} weak.

Conclusions

The same type of mechanism as proposed earlier for the dissolution of copper by ammonia also appears to be applicable to the present systems. This mechanism involves the following sequence of steps

$$\text{(i)}\quad Cu + \tfrac{1}{2}\,O_2 \xrightarrow{\text{fast}} Cu\ldots O$$

$$\text{(ii)}\quad Cu\ldots O + NH_2R \xrightarrow{\text{slow}} \left[\begin{array}{c} NH_2R \\ | \\ {}^{++}Cu \\ \diagdown \\ O^{=} \end{array}\right]$$

$$\xrightarrow[\text{fast}]{HOH} Cu(NH_2R)^{++} + 2\,OH^- \qquad [5]$$

or

$$Cu\ldots O + {}^{+}NH_2R \xrightarrow[\text{slow}]{} \left[\begin{array}{c} NH_2R \\ | \\ {}^{++}Cu \quad H^{+} \\ \diagdown \\ O^{=} \end{array}\right]^{+}$$

$$\xrightarrow{\text{fast}} Cu(NH_2R)^{++} + OH^- \qquad [6]$$

Examination of the data in Table I reveals the following points of interest:

1. The reactivities of the amines (NH_3 and en) in dissolving copper appear to be significantly higher than those of the amino acids.

2. The higher reactivities of ethylenediamine relative to ammonia, and of α-alanine relative to β-alanine suggest the influence of a chelate effect in the rate-determining step. This implies that both coordinating groups of the chelating agent interact with the metal surface in this step.

3. The rate constants for the four chelating agents follow approximately the same order as the stability constants of the corresponding cupric complexes.

4. In the case of both ammonia and ethylenediamine the protonated species is more reactive than the neutral base ($k_{AH^+} > k_A$). This has previously (1) been attributed to stabilization of the activated complex in the dissolution process by interaction between the extra proton and the incipient oxide ion (Eq. [6]). However, this explanation does not accommodate the present observation that the reactivities of the amino acids are enhanced by *removal* of a proton (i.e., $k_{A^-} > k_{AH}$). It may be of significance that in both cases the higher reactivity is associated with the ionic species.

5. A comparison of the rates of reaction of α- and β-alanine fails to reveal any indication that the presence of a methyl group on the α- position of the amino acid interferes sterically with the reaction.

6. Somewhat unexpectedly, the ratio $k_{NH_4^+}/k_{NH_3}$ (18.5) is much greater than k_{enH^+}/k_{en} (2.1). A possible explanation of this is that dissolution by ethylenediamine involves concerted interaction with the surface of both amine groups and hence is assisted only slightly by protonation of one of the groups.

Acknowledgment

The authors are grateful to the National Research Council (Canada) for financial support.

Manuscript received Dec. 9, 1958.

Any discussion of this paper will appear in a Discussion Section to be published in the June 1960 JOURNAL.

REFERENCES

1. J. Halpern, *This Journal*, **100**, 421 (1953).
2. J. I. Fisher and J. Halpern, *ibid.*, **103**, 282 (1956).
3. E. B. Sandell, "Colorimetric Determination of Traces of Metals," p. 204, Interscience Publishers, Inc., New York (1950).
4. "Stability Constants," Special Publications Nos. 6 and 7. The Chemical Society, London, 1957, 1958.
5. N. Bjerrum, *Z. phys. Chem.*, **104**, 149 (1923).

Electrodeposition of Amorphous Selenium

A. K. Graham, H. L. Pinkerton, and H. J. Boyd

Graham, Savage & Associates, Inc., Jenkintown, Pennsylvania

ABSTRACT

Amorphous selenium coatings have been electroplated in thicknesses up to 30 μ (1.2 mils) on bright nickel cathodes (and thicker coatings can be prepared). Data are given for studies leading to the selection of the optimum bath and operating conditions for the formation of reproducible, uniform, and adherent deposits. It is shown that the plating baths employed and the amorphous deposits obtained are extremely sensitive to a variety of conditions, thus emphasizing the need for further study of the electrodeposition of selenium in the amorphous form.

During recent years an electrophotographic process called xerography (1) has been developed. It is used for the rapid reproduction of photographs. As a photographic process, xerography employs a reusable plate consisting of a thin layer of a photoconductive material, having a high dark resistivity, on an electrically conductive base. The plate is sensitized by electrostatic charging immediately before use and an electrical image formed by exposure of the plate to a light image. The electrical image then is transformed to a powder image by subjecting the plate to an electrically charged powder dispersed in air. Prints are made by transferring the powder image to paper or other material suitable for handling or use.

The photographic plates in use today are composed of a 50 μ (2.0 mils) thick layer of amorphous selenium on an aluminum base. The selenium layers are deposited on the basis metal by a vacuum evaporation process.

This paper presents the results of a research investigation undertaken to produce by electrodeposition amorphous selenium films having the required properties for use as electrophotographic plates.

Both electronegative and electropositive ions of selenium can exist together in alkaline solutions. Crystalline allotropes of selenium include two monoclinic forms and one hexagonal form. The monoclinic variety consists of 8-membered ring molecules (2), and the hexagonal form is built up from chain-molecule spirals (3). The amorphous and monoclinic forms of selenium are nonconductors and are dark red to black and red, respectively. The hexagonal modification is a semiconductor and is generally gray in color.

The semiconducting hexagonal form of selenium has reportedly been electrodeposited both cathodically (4) and anodically (5). However, there is little information concerning the formation of uniform, dense, and adherent amorphous selenium electrodeposits. Von Hippel and Bloom (4) in their work on the electrodeposition of metallic selenium stated that under certain conditions nonconductive selenium was formed which interrupted current flow. They also reported that the electrodeposition of amorphous selenium practically ceases in the dark but could be continued under strong illumination until a thickness of about 0.12 μ was reached. Sella (6) reported obtaining, by electrodeposition, the allotropic forms of selenium by varying the deposition temperature with low temperature (0° - 62°C), apparently producing the amorphous form of the element.

The baths previously reported for electrodepositing selenium ranged from alkaline (for anodic deposition) to strongly acid and, except for anodic deposition, were solutions containing Se IV. It appears from polarographic evidence (7) that Se VI is not reduced in acid media.

Experimental

Plating solutions were prepared in distilled water, using selenium dioxide of high purity.[1] When a wetting agent was used, it was important to follow the sequence of adding the agent to the water first, and then adding the desired amount of selenium dioxide in order to obtain satisfactory reproducibility. The solution was digested 30 min at 80°C, cooled, and filtered through a cellulose filter aid.

The range of spectrographic analyses of three lots of selenium dioxide is shown in Table I.

Except in the preliminary work, the plating so-

[1] Obtained from A. D. Mackay Inc., New York, N.Y.

Table I. Analysis of SeO_2
Range of three lots, %

Cu	-0.005	-0.01
Pb	-0.02	-0.05
Fe	-0.01	-0.1
Si	-0.005	-0.01
Al	-nd*	-0.01
Mg	-0.01	-0.05
Cr	-nd	-0.001
Ca	-0.01	-0.03
Bi	-0.0001	
As	-0.001	
Ag	-0.0005	-0.005
B	-0.0001	-0.0005
Hg	-nd	-0.001
Te	-0.2	
Sb	-nd	-0.001

Sought but not detected—Ni, Mn, Sn, Au, Ga, Ti, V, Mo, Co, Zn.
* Not detected.

lutions were contained in a Lucite Haring cell provided with a ceramic diaphragm. The anolyte was placed in the smaller section; for acid plating baths, 10% (vol) H_2SO_4 was used with lead anodes; stainless steel anodes were used in NaOH solution of bath strength when alkaline plating baths were being studied. Most of the work was done in a cell 17.7 x 10 x 11 cm deep, although a smaller, geometrically similar cell also was used.

The plating solutions were circulated through Tygon tubing by means of a Sigmamotor pump, providing mild agitation of the catholyte. Temperature control was obtained by immersing a considerable length of the Tygon tubing in a constant temperature bath. Storage batteries were used as the current source to provide direct current with zero ripple.

Provision was made for varying the degree of illumination of the cathode from very strong to complete darkness. The very strong illumination was obtained by focusing three 500-w photospot lamps on the cathode surface from a distance of 12½ in. Under these conditions, considerable cooling was required to maintain bath temperatures, especially those below room temperature.

Temperatures from 5° to 40°C were investigated; no higher temperature was studied, since it was deemed inadvisable to approach the transformation temperature amorphous → crystalline too closely.

Exploratory work was done on a beaker scale with a Pt cathode and with the anodes in porous cups. Deposits were made with normal illumination and no agitation at room temperature. In one series, the solution contained 211 g/l SeO_2 and the pH, originally about 0.8, was raised successively to 1.5, 2.6, 7.8, 12.8, and 13.7 with NaOH. At the two higher pH values, little or no deposit was obtained. From the other baths, at moderate current densities of 0.1 to 0.2 amp/dm², uniform, adherent, glossy deposits were obtained ranging from glossy slate or black below pH 3 to dark red above this pH. In another series, 350 g/l SeO_2 was dissolved in water or in 1, 2, or 5*N* H_2SO_4. Deposits made in the same way showed the solution without added acid to be the most promising. Further work was confined to the pH region of 0.8 to 8.0.

Solutions of selenious acid attack a great many metals, including lead, silver, and gold. Platinum is not attacked, and the attack on rhodium or chromium, if any, is slow. The rate of attack diminishes, naturally, as the pH is raised. In all the work reported here, the cathode was connected to the current source before immersion in the plating solution to minimize the effect of the chemical attack.

Using the two baths at the extremes of the selected pH range, the limiting current densities on platinum were found to be as shown in Table II. Above these current densities, the deposits became redder, pulverulent, and nonadherent.*

Alkaline bath.—Because of its higher limiting current density and the reduced attack on metals other than platinum, the alkaline bath of Table II was chosen initially for evaluation in the Haring cell. The temperature was varied from 5° to 25°C,

Table II. Preliminary work with selenium deposits on Pt cathodes for 15 min at 25°C with normal illumination

	Bath	Composition	pH	Limiting C. D., amp/dm²	Deposit description below limiting C. D.
A	Acid	350 g/l SeO_2	0.7-0.9	0.4	Amorphous,* uniform dark red to black
B	Alkaline	211 g/l SeO_2 in 2.6*N* NaOH	7.5-8.0	0.85	Amorphous,* uniform, red

* By x-ray diffraction.
Note: The deposits tended to be pulverulent, the more so at the higher current densities.

the current density from 0.05 to 0.25 amp/dm², and strong illumination of the cathode was used. The character of the deposit, as judged by appearance, was extremely sensitive to the cathode material used, which included buffed sheet copper, and electrodeposits thereon of lead, Watts nickel, bright nickel, bright chromium, black chromium, rhodium, and gold. Generally speaking, the limiting current density was lower (about 0.4 amp/dm²) on these cathodes than on platinum. The deposits were redder, with a tendency to be pulverulent, and on copper a black, nonadherent deposit was obtained. With the sole exception of the deposit on platinum, which was amorphous, all deposits from this bath were crystalline, by x-ray diffraction.[2] The addition of wetting agent, the addition of citrate ion, and/or the substitution of ammonium ion for sodium were without effect. No further work was done with alkaline baths.

Acid bath.—From various modifications of the acid bath of Table II, a large number of deposits were obtained which were amorphous according to x-ray diffraction. These varied widely in appearance, and surprisingly, deposits up to 30 μ (1.2 mils) thick were obtained, with no indication that this was an upper limit. Spectrographic analysis of two such deposits showed contamination with copper, nickel, and lead, minor in one case and in major amounts in the other. Possibly because of such contamination, none of the amorphous deposits would retain an electrical charge, and were therefore unsuitable for xerographic purposes. The physical character of many such deposits, however, was excellent, being smooth, glossy black, and adherent. Because of this it is considered worth while to report on their preparation.

The best deposits were obtained from a solution of 350 g/l SeO_2 in distilled water, containing 1 g/l Duponol ME (sodium lauryl sulfate) prepared as described above. The cathode was plated with an undercoat of bright nickel about 0.25 mil thick and was introduced into the bath with the current on, at a current density of 0.1 to 0.4 amp/dm². Room temperature up to 40°C was found to be the best range. Moderate to strong illumination favored the formation of glossy black deposits; the deposits were less glossy and grayer in normal illumination or in total darkness.

[2] Since the authors were interested only in amorphous selenium, the existence of any crystalline diffraction pattern at all amounted to a rejection. No attempt was made to characterize the actual structure of the crystalline deposits from the diffraction data.

Results

At acidities varying between 5*N* H_2SO_4 up to pH 1.5, over temperatures from 5° to 40°C, with illumination varying from total darkness to very strong white light, amorphous deposits were obtained, varying only in appearance, on bright nickel-plated cathodes from baths containing wetting agent from 0.01 to 10 g/l. From baths without wetting agent, deposits were sometimes amorphous and sometimes crystalline, for causes not clearly established.

None of these amorphous deposits would retain an electrical charge. Seeking the reason for this, two of the best-looking amorphous deposits and two samples of vacuum-deposited selenium suitable for xerography were sent out for spectrographic analysis, with rather startling results:

	Spec. A	Spec. B	Vacuum-deposited
Ni	0.5	>10.0	nd*
Cu	0.5	>10.0	0.005-0.5
Pb	0.01	1-10	nd-0.0002
Fe	0.001	nd*	0.005-0.01
Ag	0.02	<0.01	nd-0.01

Notes:

1. Specimen B was analyzed by a different laboratory, and the results are believed to be order-of-magnitude only, rather than quantitive.
2. Specimen A was produced in a bath without wetting agent at pH 0.7; Specimen B was produced under similar conditions of temperature, current density, and illumination, but the bath contained wetting agent.
* nd, not detected.

An attempt was made to obtain purer deposits by purifying the bath before use and by taking extra precautions to avoid accidental contamination of the bath. Graphite anodes were substituted for the lead anodes previously used; the porous diaphragm of the cell was replaced by a fresh one, and all metallic connections close to the bath were coated heavily with stop-off lacquer, leaving the face of the nickel cathode as the only exposed metal. The freshly prepared bath was carefully neutralized with ammonium hydroxide. The white precipitate which was obtained was filtered off and the pH was readjusted to 0.8 with H_2SO_4. Another portion of fresh bath was passed through a bed of Amberlite IR-120,[3] a strong acid cation exchange resin. Baths with and without wetting agents were treated thus. After plates were prepared under conditions presumed to be optimum, the purified baths were purposely contaminated with 10 mg/l each of Cu and Ni and 30 mg/l of Pb as soluble salts, and further plates were made. Plates also were made from a freshly prepared control bath (i.e., untreated) with and without additions of contaminating metals. Generally speaking, the appearance of the deposits from purified baths was less satisfactory than from the control; those from the contaminated baths were slightly improved. Time was not available for x-ray or spectrographic analyses, but retention-of-charge tests showed some very weak ability to hold a charge in about half the plates, but in an entirely haphazard and inconsistent manner from which no conclusions could be drawn.

[3] Rohm & Haas Co. analytical grade.

Effect of substrate.—It has already been observed that from the alkaline bath deposits on platinum were amorphous, but on all the other basis metals tried, they were crystalline. Except on copper, the deposits were dense, uniform, and dark red to reddish black. Copper was so reactive that good deposits could not be obtained.

From the acid bath, deposits on lead and dull nickel were smooth and black; glossy black on bright nickel, but orange-red and pulverulent over chromium and bright nickel that had been passivated by a dichromate dip. All these deposits were amorphous. Black deposits were obtained on platinum, which were amorphous when prepared at room temperature, but crystalline when prepared from the bath at 5°C.

Defective Deposits.—All the remarks above apply to deposits which were not visibly defective. Especially in the early work, good deposits were difficult to obtain reproducibly. During the long plating runs necessary to obtain the thicker deposits, a defect frequently occurred which at the onset appeared like pitting in nickel but as plating progressed, these pits erupted into large crater-like areas of powdery red selenium. These areas invariably gave x-ray evidence of crystallinity, although the good black areas remained amorphous. It was surmised that hydrogen evolution was responsible for the pitting and likewise for the chemical reduction of selenious acid to the metal. Addition of the wetting agent improved the situation and it was found that, if the fresh bath was made up in the manner which has been described, good deposits could be obtained reproducibly until the bath had been operated for no more than about 6 amp-hr/l, when the defect reappeared. All attempts to determine the cause and cure for this behavior were futile. There had been no measurable loss of wetting agent, and depletion of the selenium content of the bath was insignificantly small. During plating, a certain amount of red selenium invariably formed in the bath; when no wetting agent was present, this could be removed by filtration, but in the presence of wetting agent some of it must have been in colloidal form, since even after heavy carbon treatment and filtration through filter aid, the bath had a red tinge. This treatment, followed by replacement of the wetting agent, also failed to restore the bath's ability to produce good plates. Considering what was later learned of the presence of impurities in the deposits, it is thought possible that the depletion by deposition of some of these impurities from the bath may have been responsible. The results of the later attempts to purify the bath in part support this explanation, although replacement of the three major impurities did not again cause good plates to be produced. Time did not permit a fuller exploration of this problem.

Summary

1. Although the production of relatively thick amorphous selenium electrodeposits with photosensitive retention-of-charge properties was not achieved, thick, sound, amorphous deposits were obtained from a bath containing 350 g/l SeO_2 and

wetting agent at current densities of 0.05 to 0.2 amp/dm^2 and temperatures of 20°-40°C.

2. Spectrographic analysis of two of the best-looking amorphous deposits showed metallic contamination, in one case serious, but relatively minor in the other. It was not determined whether this contamination occurred in all cases.

3. A serious drawback was the short life of the bath before defective deposits were obtained. More work needs to be done to discover the cause and cure for this behavior.

4. Equally sound crystalline deposits were obtained from a bath containing 211 g/l SeO_2 and wetting agent in 2.6*N* NaOH (8.0 pH) under similar conditions, but this area was not as extensively investigated.

5. Illumination varying from zero to very strong had no very profound effect.

6. The nature of the cathode material exerts a profound influence on the appearance and structure of the deposits. Bright nickel plating was the best of the substrates examined, which also included lead, silver, gold, rhodium, copper, dull nickel, bright chromium, and black chromium electrodeposits and sheet platinum.

Acknowledgment

The authors wish to express their appreciation to Dr. Harold J. Read, Pennsylvania State University, University Park, Pa., under whose direction the x-ray diffraction and spectrographic analyses were performed, and personnel of the Fort Monmouth Laboratory for several spectrographic determinations.

Manuscript received Oct. 20, 1958. Project carried out under Contract DA-36-039-SC-71228 with U. S. Army Signal Corps, Fort Monmouth, N. J.

Any discussion of this paper will appear in a Discussion Section to be published in the June 1960 JOURNAL.

REFERENCES

1. R. M. Schaffert and C. D. Oughton, *J. Opt. Soc. Am.*, **38**, 991 (1948).
2. P. H. Keck, *ibid.*, **41**, 53 (1951).
3. A. J. Bradley, *Phil. Mag.*, **48**, 447 (1924).
4. A. von Hippel and M. C. Bloom, *J. Chem. Phys.*, **18**, 1243 (1950).
5. M. C. Bloom, U. S. Pat. 2,414,438, Jan. 21, 1947.
6. G. Sella, *Ricerca sci.*, **10**, 1143 (1939).
7. J. J. Lingane and L. W. Niedrach, *J. Am. Chem. Soc.*, **71**, 196 (1949).

Electroclad Aluminum on Uranium

John G. Beach and Charles L. Faust

Battelle Memorial Institute, Columbus, Ohio

ABSTRACT

Electroplating of aluminum was studied at Battelle in 1953-55 as an alternative method for aluminum cladding of uranium fuel elements. Uranium electroclad with 12 mils of aluminum over a 0.5-mil nickel or nickel-plus-copper electroplate resisted corrosion for more than 100 hr in boiling water. Hot pressing the electroclad composite improved the corrosion resistance. Many of the results obtained with aluminum electrocladdings paralleled those obtained with wrought aluminum claddings on uranium.

One method of cladding uranium fuel elements with wrought aluminum involves an intermediate braze layer of aluminum-12.5% silicon alloy (AlSi) or a nickel plate. The purpose of the intermediate layer is to aid bonding, to prevent rapid interdiffusion, and/or to provide a secondary barrier to rapid corrosion by hot water in case of penetration of the aluminum cladding. However, during dip brazing excessive solution of the aluminum cladding in the molten AlSi and selective penetration of the AlSi into the cladding may result if the temperature and time of AlSi dip brazing are not carefully controlled, and porosity of the AlSi brazing layer and unbonded area can also result in an inferior cladding.

This research was undertaken at Battelle to evaluate the possibilities of electrocladding uranium with aluminum. The electrodeposition of aluminum had been developed to the point where commercial applications were technically feasible, but electrocladding of reactor materials had not been explored. New techniques for preparing metal surfaces to be plated with adherent aluminum were needed. The principal characteristics of the electrocladding investigated were the diffusion and the corrosion protection afforded by aluminum plated directly on uranium and also over intermediate coatings plated on uranium. The studies were useful in showing the role of barrier-metal electroplates in preventing deleterious diffusion of uranium with the aluminum and the importance of good bonds between the barrier metal, the uranium, and the aluminum.

Selection of an Aluminum Plating Process

Two types of aluminum electroplating baths were available: fused salt (1) and organic. In this work, the need for deposits thicker than 10 mils (0.010 in.) obviated more than a few cursory tests with fused-salt baths. Two organic-type baths, the ethyl pyridinium bromide bath and the hydride bath, were investigated.

The ethyl pyridinium bromide-aluminum chloride-toluene bath was discovered by Weir and Hurley (2, 3, 4) and developed by Safranek, Schick-

ner, and Faust (5, 6). The following plating bath and conditions are recommended: *bath composition*: Ethyl pyridinium bromide-aluminum chloride fusion product, 32%; toluene (sp gr 0.866), 67%; methyl t-butyl ether, 1%; *plating conditions*: temperature, 86° ± 2°F; current density, 10-20 amp/ft² (superimposed a.c.); agitation nitrogen diffuser.

The lithium hydride-aluminum chloride-ethyl ether bath (composition and operating conditions are given later) was discovered by Couch and Brenner (7-9). The hydride bath is relatively easy to prepare. The ether content makes the bath flammable and safety precautions must be followed rigorously. Although explosions with systems containing lithium hydride and ether have been reported (10, 11), the presence of aluminum chloride tends to suppress the volatility of the ether and thus reduces the fire hazard.

Both nonaqueous organic processes produce smooth, dense, mat-type deposits, but electroformed foils, prepared for this work from the hydride bath, were more resistant to boiling water than those made in the ethyl pyridinium bromide bath. After 8 days' exposure to boiling distilled water, 2S aluminum foils and foils deposited in the hydride bath gained about 0.4 mg/cm² in weight. The absence of appreciable lithium in the hydride-bath deposit, in view of the high lithium content of the bath and the low weight change, suggests little or no occlusion of the bath constituents in the electrodeposited aluminum. On the other hand, foils deposited in the ethyl pyridinium bromide bath gained 2.0 mg/cm² in weight after exposure to distilled water. This greater weight gain is attributed to the hydration of occluded organic matter. Table I shows the results of spectrographic analyses of the aluminum deposits from the two organic plating baths. The aluminum produced in the hydride bath was of somewhat higher purity than that produced in the other bath.

Based on the ease of plating-bath preparation and operation and the higher purity and greater corrosion resistance of the electrodeposited aluminum, the hydride bath was selected for these studies of electrocladding aluminum on uranium.

Table I. Per cent of impurities in aluminum deposits

Contaminant	Ethyl pyridinium bromide bath	Hydride bath
Antimony	*	<0.01†
Arsenic	*	<0.01†
Calcium	*	0.03
Cobalt	*	<0.001†
Chromium	<0.005	0.001
Copper	0.005-0.05	*
Gallium	*	0.0005
Iron	0.05-0.10	0.008
Lead	0.005-0.05	0.001
Lithium	*	<0.005†
Magnesium	0.005-0.05	0.002
Manganese	*	0.001
Molybdenum	*	<0.005†
Nickel	*	0.001
Potassium	*	<0.1†
Silicon	0.05-0.10	0.001
Sodium	*	<0.01†
Tin	*	0.005
Titanium	*	0.003
Tungsten	*	<0.02†
Uranium	*	<0.05*
Zinc	*	0.01

* Not determined.
† Lower limit for this spectrographic analysis.

Adherent Plating of Aluminum on Various Metals

Good adhesion between the aluminum and the uranium is an important factor for satisfactory claddings. But, as shown later, the good as-plated adhesion of aluminum directly on uranium is degraded by diffusion. Thus, adherent plating of aluminum on metals other than uranium was investigated. Adherent plating of aluminum on wrought metals was done preparatory to electrocladding aluminum over intermediate coatings plated on the uranium.

Treatment of clean metal surfaces by rinsing in alcohol, dipping in oleic acid (12), and plating with aluminum produced fairly adherent aluminum deposits on many metals. Wrought metal surfaces were first cleaned and activated by conventional means for aqueous plating and then treated by rinsing in alcohol and oleic acid.

Fatty acids other than oleic acid, such as linoleic acid and ethereal solutions of palmitic acid, were also successfully used to promote adherent plate of aluminum. Since pelargonic acid was not effective, a fatty acid with carbon chain longer than nine carbon atoms apparently is necessary.

Solutions of stearato chromic chloride[1] in isopropyl alcohol were even more effective than oleic acid in promoting adhesion of aluminum to iron and nickel. However, the stearato chromic chloride carried into the plating bath shortened the bath life. Subsequently rinsing in oleic acid was helpful in preventing bath contamination. Oleic acid per se did not shorten the life of the aluminum plating bath noticeably.

Preparation of Metal Surfaces for Plating with Adherent Aluminum

Aluminum.—Preparation of aluminum surfaces was by application of a conventional zincate replacement film and rinsing in water before rinsing in alcohol and oleic acid. The adhesion of the aluminum electroplates on 3S aluminum was tested by peening and by soldering. Peening of the surface was done by a rounded tip tool mounted in a vibrating marking tool. In the second test, the aluminum electrodeposit was copper plated, and a rod was soldered perpendicular to the surface and then pulled loose. Neither peening nor solder testing broke the aluminum-zincate-aluminum bond. The distortion of the peened aluminum plate is apparent in Fig. 1.

Copper.—Clean copper surfaces were activated in a sodium cyanide solution and then rinsed in water before rinsing in alcohol and oleic acid.

Nickel.—Nickel was activated by electropolishing[2]

[1] Quinol, E. I. du Pont de Nemours and Company, Inc.

[2] Proprietary nickel electropolishing process, Battelle Development Corp. U.S. Pat. 2,440,715, May 4, 1948.

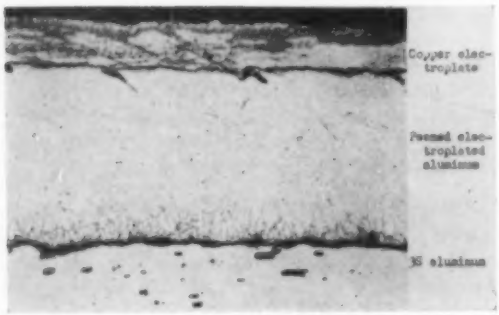

Fig. 1. Aluminum electroplate on 35 aluminum after peening and plating with copper. HF etch. Magnification 50X before reduction for publication.

Fig. 2. Aluminum electroplate on SAE 1020 steel. HF etch. Magnification 250X before reduction for publication.

or anodic etching and strike plating in the high-chloride "Woods" nickel bath and then rinsed in water prior to rinsing in alcohol and oleic acid.

Stainless steel.—Stainless steel was activated by anodic etching and nickel strike plating in the high-chloride "Woods" nickel bath and then rinsed in water before rinsing in alcohol and oleic acid.

Carbon steel.—Carbon steel, Type 1020, was electropolished and then rinsed in water prior to rinsing in alcohol and oleic acid. Chemical etching in hydrochloric acid or anodic etching in sulfuric acid was less satisfactory than electropolishing. Aluminum on carbon steel is shown in Fig. 2.

Electroplating of Aluminum over Metals Electroplated on Uranium

Electroplating of aluminum over electroplated metals on uranium was complicated by the fact that uranium was exposed through discontinuities in the intermediate plated layers which prevented optimum activation of the surface. Nickel, copper, and iron electrodeposits, ½ mil thick, plated adherently on uranium, were not impervious. The thickness of the intermediate metal coating was limited in this study to about ½ mil because of the higher thermal-neutron cross section of nickel, copper, and iron as compared with aluminum.

The best methods for activating solid nickel and steel specimens prior to the organic activation steps were not applicable to nickel- or iron-plated uranium, because these acid treatments attacked the underlying uranium. Therefore, aluminum was electroplated directly on nickel- or iron-plated uranium following rinsing in alcohol and oleic acid. The method for activating clean copper surfaces by immersion in a cyanide solution prior to the organic activation steps was effective in promoting adherent aluminum electroplating over uranium plated with copper or nickel.

The as-plated bond of the aluminum to the nickel or iron plates was inferior to that of aluminum to electroplates of copper or copper over nickel on uranium. Subsequent hot pressing or vacuum heat treating of electroclad specimens having aluminum on nickel- and copper-plated uranium improved the as-electroplated bonds. However, hot pressing of aluminum plate on iron-plated uranium produced brittle alloys that resulted in doubtful adherence.

Electrocladding Uranium with Aluminum

Uranium samples.—Alpha-rolled uranium plate was cold rolled to 90-mil sheet and cut into samples ¾ by ¾ in. square. The edges and corners were rounded to minimize edge buildup. Surfaces were cleaned by grinding or by grit blasting to remove scale. Samples were held in racks made of stainless steel with two point-type contacts on opposite edges. The contact areas were not plated, and thus there were discontinuities in the electrocladding. The racks were coated with Synthetasine,[2] a synthetic resin preparation, which was inert in the bath.

Aluminum-Plating Bath

Preparation.—The lithium hydride-ethyl ether bath was prepared under nitrogen atmosphere in a three-neck flask provided with a stirrer and a cooling bath of dry ice and acetone. Ethyl ether was stirred in the flask while $AlCl_3$ was added through a gooch rubber tube. Next, the LiH was added similarly. Considerable heat was liberated during these additions; however, the temperature was maintained between −25° and −10°C to minimize ether evaporation. The final composition was 400 g $AlCl_3$, 6 g LiH, and ether to make 1 liter.

Baths of 2.5 liters were contained in glass jars and covered with an aluminum dry box into which dry nitrogen gas was bled slowly. Two sets of doors were provided in the dry box for insertion and removal of the cathodes. Figure 3 shows the electroplating setup.

Bath life.—The longest time a hydride type of aluminum bath was operated was 30 days, or 190 amp-hr/liter. About 160 g of aluminum had been deposited from the 2-½-liter bath, or 80% of the amount in the original $AlCl_3$. The bath was then discarded because the electrodeposited aluminum had become brittle, nodulated, and spongy. The cathode current efficiency had increased to 115%. No attempt was made to recondition the bath.

Generally, at the beginning of their use, aluminum plating baths produced ductile, mat aluminum. As the baths grew older the plates tended to become smoother. In some cases, the smoothness was accompanied by small cracks and fissures in the plates. As the plates became smoother they usually tended to loose ductility. Finally, many baths began to produce dark, streaky deposits when they had outlived their usefulness.

[2] Synthetasine Protective Coatings, Inc., New York, N.Y.

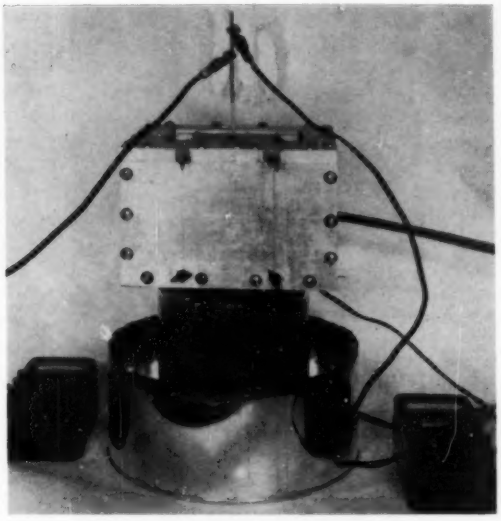

Fig. 3. Aluminum plating bath with dry box and plating rack in place.

Fig. 4. Surface view of crystalline electrodeposited aluminum. Magnification approx. 1000X before reduction for publication.

In some cases the aluminum tended to become satin surfaced, due to aluminum crystals. Figure 4 shows one of these flat surfaces. The tendency to form regular hexagons was outstanding. In Fig. 4 cubic crystals can be seen also.

Aluminum Plated Directly on Uranium

The preparation of uranium for aluminum plating was the same as for conventional aqueous plating, as discussed later. An extra requirement for aluminum plating was that after activation the uranium was dried in alcohol and ether before being immersed in the anhydrous plating bath. As-plated aluminum on uranium is shown in Fig. 5.

Heat treatment of aluminum-plated uranium easily diffused the two metals. The extent of diffusion occurring in 24 hr at temperatures of 200°, 250°, and 300°C is illustrated in Fig. 6, 7, and 8. The diffusion in 24 hr at 300°C was enough to destroy the as-plated bond.

Diffusion of aluminum and uranium at 250°C, and possibly at 200°C, was unexpected based on the observed diffusion between wrought aluminum and uranium. The interface of aluminum plated on uranium probably has less oxides than mechanically

Fig. 5. Aluminum electroplate on uranium as-plated (aluminum thickness, 12 mils). As-polished. Magnification 500X before reduction for publication.

Fig. 6. Aluminum electroplate on uranium after 24-hr diffusion at 200°C (aluminum thickness, 12 mils). As-polished. Magnification 500X before reduction for publication.

Fig. 7. Aluminum electroplate on uranium after 24-hr diffusion at 250°C (aluminum thickness, 12 mils). As-polished. Magnification 500X before reduction for publication.

Fig. 8. Aluminum electroplate on uranium after 24-hr diffusion at 300°C (aluminum thickness, 12 mils). As-polished. Magnification 500X before reduction for publication.

prepared diffusion samples, and this difference could explain the difference in diffusion across the aluminum-uranium interface.

Aluminum Plated over Electroplated Metals on Uranium

The observed deleterious diffusion of electroplated aluminum and uranium in 24 hr at 250° and 300°C pointed out the need for an interfacial diffusion barrier. A barrier metal was desired that would prevent diffusion, would be well bonded to both the aluminum and the uranium, and would provide secondary corrosion protection to the uranium when exposed to boiling water through discontinuities in the aluminum. Nickel, copper, and iron electroplates were tried as barrier layers.

The procedure for activating and plating on uranium was as follows:

Descale uranium: (a) surface grind, (b) abrasive blast, or (c) chemical pickle.

Alkaline clean: immersion for 2 min at 180°F.

Rinse

Nitric pickle: 8*N* HNO_3, 80 ± 10°F, 5-10 min.

Rinse

Anodic pickle: 22*N* H_3PO_4, 0.2*N* HCl, 100°F, 50 amp/ft², 10 min

Cold rinse

Nitric pickle: 8*N* HNO_3, 80° ± 10°F, 3-5 min.

Electroplate: (a) Copper (0.5 mil), copper sulfate, $CuSO_4 \cdot 5H_2O$, 210 g/l; sulfuric acid, H_2SO_4, 82.5 g/l; molasses, 2.5 g/l; 20° ± 10°F, 50 amp/ft², 1 min, 25 amp/ft², 20 min.

(b) Iron (0.5 mil), ferrous sulfate, $FeSO_4 \cdot 7H_2O$, 300 g/l; ferrous chloride, $FeCl_2 \cdot 4H_2O$, 40 g/l; sodium formate, NaCOOH, 15 g/l; ammonium sulfate, NH_4SO_4, 15 g/l; boric acid, H_3BO_3, 30 g/l; wetting agent, DuPonol M. E.,[4] 1 g/l; pH 4.1 ± 0.1, 140°F, 60 amp/ft², 1 min, 30 amp/ft², 19 min.

(c) Nickel (0.5 mil), nickel sulfate, $NiSO_4 7H_2O$, 145 g/l; magnesium sulfate, $MgSO_4 \cdot 7H_2O$, 75 g/l; ammonium chloride, NH_4Cl, 15 g/l; boric acid, H_3BO_3, 15 g/l; wetting agent, XXXD,[5] 20 mil/liter; pH 5.5 ± 0.1, 100°F, 30 amp/ft², 1 min, 15 amp/ft², 30 min.

Rinse

Activate: (a) ethyl alcohol rinse, (b) oleic acid rinse.

Aluminum plate (12 mils), aluminum chloride, $AlCl_3$, 400 g/l; lithium hydride, LiH, 6 g/l; ethyl ether, balance; 75° ±5°F, 10 amp/ft², 24 hr.

Rinse and dry.

Treatment after electrocladding.—Heat treating of aluminum-electroclad samples for 5 min at 950°F and hot pressing for 5 min at 950°F with ram pressures up to 5.1 tsi were done to promote diffusion and improve the as-plated adhesion. Heat treating was done in a vacuum tube furnace with a pressure of less than 10 μ.

Hot pressing was done in a closed die. The hot-press assembly, Fig. 9, consisted of a frame and two cover plates of 3S aluminum in which the electroclad sample was encased. A 1-½-mil iron foil was included as a parting compound. The 1-7/16-in.-diameter by ⅜-in. thick assemblies were hot pressed in a tubular die with the ram pressure applied on one face. The 3S aluminum deformed under pressure and heat to fill the contours of the aluminum-electroclad sample. After being hot pressed, the aluminum-electroclad core was peeled off the 3S aluminum casing. A small hydraulic press[6] furnished the pressure.

Corrosion Testing of Aluminum-Plated Uranium

Samples of aluminum-plated uranium were immersed in boiling distilled water for 24-hr intervals or less. The corrosion trend was followed by the weight change and the progressive change in appearance. The relative corrosion resistances of the various cladding systems were based on the hours in test before a weight change of ± 1 mg/cm² was noted. Corrosion for the most part occurred only at contact areas in the aluminum electrocladding. If the bond of the aluminum cladding was not good, corrosion also occurred over the barrier-coated uranium because of penetration of water along the aluminum-barrier metal interface. The best samples

[4] E. I. du Pont de Nemours and Co., Inc.

[5] Harshaw Chemical Company.

[6] Carver Laboratory Press, Fred S. Carver Inc., Summit, N.J.

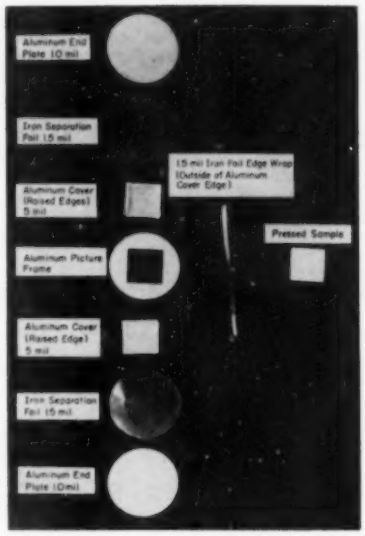
Aluminum End Plate (0 mil)
Iron Separation Foil (5 mil)
(5 mil Iron Foil Edge Wrap (Outside of Aluminum Cover Edge))
Aluminum Cover (Raised Edges) 5 mil
Pressed Sample
Aluminum Picture Frame
Aluminum Cover (Raised Edge) 5 mil
Iron Separation Foil (5 mil)
Aluminum End Plate (0 mil)

Fig. 9. Assembly for hot-pressing aluminum-clad uranium samples.

Table II. Relative corrosion resistance of aluminum-electroclad uranium specimens having various barrier-metal coatings and postcladding treatments (aluminum 12 mils in thickness)

Barrier metal	Thickness, mil	Postcladding treatment	Corrosion resistance, hr*
Ni	0.5	Hot pressed	63
Ni	0.5	Heat treated	39
Ni + Cu	0.4 + 0.1	Hot pressed	104
Ni + Cu	0.4 + 0.1	Heat treated	64
Ni + Cu	0.25 + 0.25	Hot pressed	50
Ni + Cu	0.25 + 0.25	Heat treated	38
Ni + Cu	0.1 + 0.4	Hot pressed	26
Ni + Cu	0.1 + 0.4	Heat treated	23

* Hours in boiling water until weight change of ±1 mg/cm² occurred. Average of four samples.

Table III. Effects of barrier-metal coating, activity of uranium surface for plating, and pressure applied during postcladding hot pressing on the relative corrosion resistance of aluminum-electroclad uranium (aluminum, 12 mils in thickness)

Barrier metal	Coating thickness, mil	Activity of uranium*	Pressure, tons/in.²	Corrosion resistance, hr†	
Fe	0.5	Active	3.5-4.3	144-77	(95)
Fe	0.5	Passive	0.2-2.2	31-1	(16)
Cu	0.5	Active	3.3-3.9	108-46	(77)
Cu	0.5	Passive	3.5-5.1	46-1	(23)
Ni	0.5	Active	0.6-1.2	38-1	(19)
Ni	0.5	Passive	0.0-4.8	7-86	(46)
Ni + Cu	0.4 + 0.1	Active	1.0-5.1	138-327	(232)
Ni + Cu	0.4 + 0.1	Passive	1.4-4.4	109-80	(94)
Ni + Fe	0.4 + 0.1	Active	2.8-3.5	49-84	(66)
Ni + Fe	0.4 + 0.1	Passive	2.6-4.5	36-1	(18)

* *Active* uranium was that which was pretreated for good as-plated adherence. *Passive* uranium was just pickled in nitric acid and plated with an envelope of the barrier metal. Bonding of the electroplated metal to the uranium depended on the diffusion that occurred during hot pressing.

† Hours in boiling water until weight change of ±1 mg/cm² occurred. Number in parentheses is average of two samples.

showed slight corrosion only at the electroplating contact areas.

Tables II and III show the relative corrosion resistance of uranium electroclad with various barrier metals plus 12 mils of aluminum. The best corrosion resistance was observed for uranium that was plated with adherent 0.4 mil of nickel plus 0.1 mil of copper plus aluminum and hot pressed at 950°F with a ram pressure of 5.1 tsi. This system provided the best adhesion of the aluminum cladding and also provided desirable alloying of the uranium with the nickel as a secondary corrosion barrier. Samples that were not hot pressed nor heated after electrocladding corroded rapidly (within a few hours) along the uranium-electroplate interface.

Manuscript received Feb. 13, 1959. This paper was prepared for delivery before the Ottawa Meeting, Sept. 28-Oct. 2, 1958. Work on this paper was performed under AEC Contract W-7405-eng-92.

Any discussion of this paper will appear in a Discussion Section to be published in the June 1960 JOURNAL.

REFERENCES

1. F. R. Collins, *Iron Age*, **169** (3), 100 (Jan. 17, 1952).
2. F. H. Hurley and T. P. Weir, *This Journal*, **98** (5), 203 (1951).
3. T. P. Weir and F. H. Hurley, U. S. Pat. 2,446,349, Aug. 3, 1948.
4. T. P. Weir, U. S. Pat. 2,446,350, Aug. 3, 1948.
5. W. H. Safranek, W. C. Schickner, and C. L. Faust, *This Journal*, **99** (2), 53 (1952).
6. W. H. Safranek, *et al.*, U. S. Pat. 2,692,850.
7. D. C. Couch and A. Brenner, *This Journal*, **99** (6), 234 (1952).
8. D. C. Couch, *et al.*, U. S. Pat. 2,651,608, Sept. 8, 1953.
9. J. H. Conner and A. Brenner, *This Journal*, **103** (12), 657 (1956).
10. G. Barbaras, *et al.*, *J. Am. Chem. Soc.*, **70**, 877 (1948).
11. Anonymous, *Chem. and Eng. News*, **31**, 2334 (1953).
12. W. C. Schickner, *Steel*, **135**, 125 (Nov. 2, 1953).

Electrolytic Iron Powder from a Caustic Soda Solution

J. Adrien M. LeDuc[1] and Richard E. Loftfield

Electro Chemicals Division, Research Department, Diamond Alkali Company, Painesville, Ohio

and Luther E. Vaaler[2]

Electrochemical Engineering Division, Battelle Memorial Institute, Columbus, Ohio

ABSTRACT

Conditions for electrolytic deposition of iron powder from a slurry of iron III oxide in caustic soda solutions were investigated. The variables that influence the deposition the most were temperature (90°C), caustic soda concentration (600-800 g/l), and low current densities. Results from pilot-plant studies were in good agreement with laboratory findings. Several photomicrographs of the deposits are included. Physical and chemical properties of the powders are listed. Results show that a ductile, dendritic deposit was obtained that could be ground up easily. The size of the dendrites was influenced greatly by conditions of deposition. Particle size distribution, particle shape, ductility, flow rate, purity, and compactability of several powders were examined. Tensile strength and elongation of sintered compacts were also studied.

Iron III hydroxide is soluble to a limited extent in strong caustic soda solution from which metal powder may be deposited in a dentritic and ductile form. The solution is kept saturated by employing an excess of finely divided iron oxide maintained in suspension by agitation.

Estelle (1) first patented such a process in which he recommended a bath consisting of 30% iron III hydroxide, 35% sodium hydroxide, and 35% water, maintained at 100°C. He stated that a gray metallic deposit can be obtained from this solution. Angel (2) showed that finely divided iron ore could be used in place of the pure hydroxide in the same type of medium. Estelle's and Angel's patents defined very few conditions for electrodepositing the iron and did not describe the characteristics of the powder produced. Little attention has been given to this method of producing iron powder. Ljungberg (3) described it in a review of electrolytic methods for making powders and concluded that further work would be necessary to change it from the status of a laboratory curiosity. He considered the method attractive, since the powder is obtained directly from the ore. Mehl (4) stated that a brittle deposit, suitable for crushing, is obtained by Estelle's process, and patented a process (5) in which soluble iron anodes were employed in 50% caustic solution at 100°C. A very fine, dentritic powder was obtained.

The experimental work described in this paper was undertaken to determine conditions of electrolysis, yields, and characteristics of the iron powder produced in an alkaline iron oxide medium.

Experimentation

Laboratory Electrolytic Studies

A bath was prepared consisting of equal parts of water, caustic soda, and finely divided C.P. iron III oxide. This was electrolyzed at cathode current densities ranging from 30 to 90 amp/ft^2 and a tem-

[1] Present address: Exploratory Research Department, Research & Development Laboratories, M. W. Kellogg Co., Jersey City, N.J.

[2] Present address: Research Laboratories, National Carbon Co., Parma, Ohio.

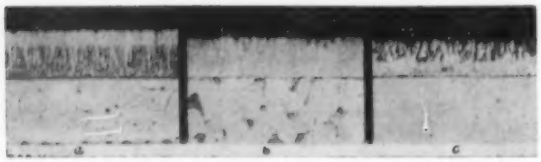

Fig. 1. Effect of agitation: a, iron deposited on flat panel cathode; b, iron deposited on rotating cathode; c, iron deposited from agitated bath. Magnification 500X before reduction for publication.

perature of 120°C in an iron container used as the anode. Gray, metallic deposits were formed from which it was difficult to remove all of the adhering oxide, so that the current efficiencies calculated from the gain in weight were 120%. A photomicrograph of the cross section of a typical deposit is shown in Fig. 1a. Oxide inclusions are evident, except near the surface, where they were washed out. However, if a rotating cathode was used, the calculated current efficiency was reduced to 92%. Figure 1b is a photomicrograph of this deposit, and the amount of oxide occluded is seen to be less than previously. If, in addition, a high-speed impeller was used to agitate the viscous bath, oxide inclusions were further eliminated, as shown in Fig. 1c, and a current efficiency of 70% was obtained.

In addition to its tendency to give deposits containing occluded oxide, the bath was so viscous that drag out was excessive. The viscosity was considerably reduced by decreasing the amount of suspended oxide, and deposition at high current efficiency was still possible if the bath was vigorously agitated. Further experiments were carried out in 1- and 4-liter containers. Nickel or iron anodes 0.5 in. in diameter or larger and 6-7 in. long were used. The iron anodes were corroded slowly during electrolysis. The cathodes consisted of mild-steel sheets that had been slightly roughened. The deposits adhered well to the surface but were easily removed from the electrode by flexing or scraping. The removed chips were reduced to powder by mild grinding. Air agitation was tried in a few experiments but had the disadvantages of producing a large amount of spray and introducing carbon dioxide into the bath. Agitation with a 2.5 in. diameter impeller revolving at about 700-800 rpm was found to be more satisfactory.

Bath stability during electrolysis.—The cathode current efficiency of a freshly prepared bath was found to decrease upon continued electrolysis. In a typical experiment a current efficiency of 90% was obtained during the first few hours of electrolysis, but after 24 hr the current efficiency had decreased to a steady value in the range of 60-80%. The high current efficiency of a freshly prepared solution may be due to the fact that the iron oxide contains an easily soluble fraction that dissolves shortly after the addition to the caustic soda solution.

The character of the deposits also changed during the stabilization period. Deposits from freshly prepared baths were loose and powdery but became more compact as electrolysis was continued. In the progress of the experimental work, successive experiments were run until the bath had reached a stable state.

Table I. Effect of bath temperature on current efficiency. Fe_2O_3-50 g/l; current density, 40 amp/ft²

Temp, °C	NaOH, g/l	Cathode current efficiency, %
30	400	30
35	600	45
50	600	75
60	400	45
70	600	85
80	600	90
90	400	60
90	600	90-95
120	400	70

Effect of temperature.—The effect of temperature was investigated in a bath containing 200-600 g/l of caustic soda and 25-75 g/l of iron III oxide. Electrolysis was carried out at a cathode current density of 40 amp/ft² over a temperature range from 30° to 120°C. The highest temperature was still below the boiling point of the bath.

Results are shown in Table I and indicate a current efficiency of well over 80% in several instances. The effect of temperature was investigated before the need for extensive electrolysis to obtain a stable condition was realized. While the results are generally consistent with one another, some of the values are inconsistent with later work.

The best current efficiency was obtained at the highest temperature for any given caustic concentration. The nature of the deposit also changed with the temperature. As the temperature increased the deposited dendrites increased in size, as shown in Fig. 2a to 2d inclusive. These figures are photomicrographs of polished cross sections of the deposits. The deposit made at 60°C was dispersed somewhat when mounted prior to polishing.

The variation in dendrite size with temperature was even more clearly shown by grinding deposits to −325 mesh, mounting in Lucite, and polishing.

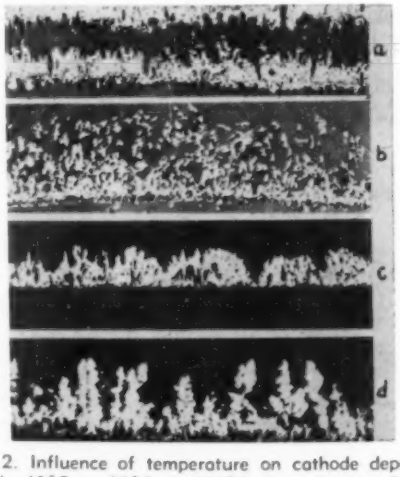

Fig. 2. Influence of temperature on cathode deposits: a, 35°C; b, 60°C; c, 90°C; d, 120°C. Magnification 100X before reduction for publication.

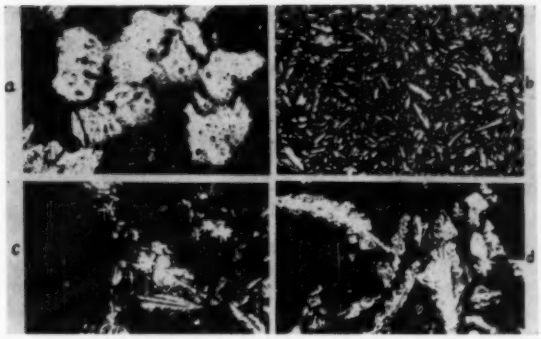

Fig. 3. Effect of bath temperature on iron deposit (caustic soda, 400 g/l; Fe_2O_3, 50 g/l): a, 35°C; b, 60°C; c, 90°C; d, 120°C. Magnification 500X before reduction for publication.

Photomicrographs of the specimens are shown in Fig. 3a to 3d. The large particles appearing in the photomicrograph of the powder deposited at 35°C are not individual dendrites but rather clumps made up of many smaller dendrites. This powder had very poor flow characteristics and balled up on the screen rather than passing through it. The dendrites from the 60°C deposit easily passed a −325 mesh screen. At higher temperatures some of the dendrites were too large to pass a −325 mesh screen and had to be distorted first, requiring a much more severe grinding treatment. However, the flow properties of the powder tended to improve as the temperature of deposition increased.

In all of the photomicrographs, except that of the powder produced at 35°C, fragments with a hexagonal symmetry can be observed, resulting from sectioning through the width rather than the length of the dendrite. Therefore, the dendrites consist of six longitudinal ridges spaced around a longitudinal axis with hexagonal symmetry.

Effect of caustic concentration.—Electrodeposition of iron from iron III oxide slurries in caustic soda solutions of varying concentrations showed that a high caustic soda concentration, in excess of 400 g/l, is required to obtain a current efficiency of over 50%. Representative results are shown in Table II. A bath containing 200 g/l of caustic soda and 50 g/l of iron III oxide was held at a temperature of 90°C and electrolyzed at 36 amp/ft². The first deposits from this bath were obtained at a current efficiency in excess of 60%, but the current efficiency dropped continually as more ampere-hours were put through the bath. Apparently, caustic soda present in a concentration of 200 g/l is not able to solubilize all of the iron oxide.

Table II. Effect of caustic soda concentration. Fe_2O_3-50 g/l; temp, 90°C; current density, 40 amp/ft²

200 g/l NaOH		465 g/l NaOH		765 g/l NaOH	
Amp-hr/l	C.E., %	Amp-hr/l	C.E., %	Amp-hr/l	C.E., %
3.1	68	3.1	91	4.7	80
15.6	40	15.6	86	17.2	85
28.0	22	28	65	26.6	73
50.0	13	47.0	54	36.0	68
59.5	13	50	52	39.2	67

With 465 g/l of caustic soda in the bath, a stable current efficiency of about 55% was obtained. With 765 g/l of caustic soda in the bath, deposits were produced at a current efficiency of 70%.

Effect of iron III oxide concentration.—The slurry concentration of iron III oxide in caustic soda solution was varied to determine whether its concentration affected the current efficiency of electrodeposition and the type of deposit produced. A finely divided, chemically pure iron oxide was selected for use in the bath. Baths containing 25, 50, and 75 g/l of iron oxide and 400-765 g/l of caustic soda were operated at 90°C and a cathode current density of 35-40 amp/ft². The results in Table III indicate that the concentration of oxide could be varied without significantly affecting the electrolysis.

Use of commercial hematite ores containing as high as 86% Fe_2O_3 in place of pure iron oxide gave somewhat inconsistent results. However, the current efficiencies were generally 20-30% lower than with the pure oxide. The use of a magnetite ore (Fe_3O_4) gave current efficiencies below 5%.

Effect of current density.—The effect of increasing the current density was to decrease both the current efficiency of deposition and the size of the dendrites deposited. Current efficiency values are given in Table IV. The decrease in the average size of the dendrites deposited is evident from the photomicrographs of deposit cross sections shown in Fig. 4a to 4g. At 2400 amp/ft² the deposit appears to have been torn off by the hydrogen evolved, except for a thin layer.

As expected, the effect of increasing the current density is opposite to the effect of increasing the temperature. Increasing the current density decreases the concentration of iron in the cathode film, leading to a decrease in the current efficiency and

Table III. Effect of iron oxide concentration on cathode current efficiencies. C.D., 40 amp/ft²; temp, 90°C

400 g/l NaOH						765 g/l NaOH			
25 g/l Fe_2O_3		50 g/l Fe_2O_3		75 g/l Fe_2O_3		25 g/l Fe_2O_3		50 g/l Fe_2O_3	
Amp-hr/l	C.E., %	Amp-hr/l	C.E., %	Amp-hr/l	C.E., %	Amp-hr/l	C.E., %	Amp-hr/l	C.E., %
1.39	46	1.4	66	1.4	74	3.13	83	3.13	73
7.1	55	2.8	63						
8.5	50	31	54	33	57	28.2	68	28.2	64
9.9	60							43.8	73
15.4	68			40	58	94	83		
25.2	60			46	61	163	80	163	73
				49	63	191	73	191	78
				52	48	269	68	269	75

Table IV. Effect of current density on current efficiency. Fe_2O_3, 50 g/l; temp, 90°C

Current density	Current efficiency, %	
Amp/ft²	at 400 g/l NaOH	at 765 g/l NaOH
40	55	80
72	—	75
80	45	—
145	—	68
160	35	—
300	20	—
600	15	—
1200	15	—
2400	3	—

more nucleation. Thus, finer dendrites are formed. An increase in temperature increases the rate of diffusion in the cathode film and probably increases the solubility of the oxide. The result is a higher current efficiency and a tendency to deposit on dendrite surfaces already established, rather than to start new ones.

Conclusions

The experimental results have shown that it is possible to prepare iron powder with an average particle size that can be varied over a wide range. The variables that most influence the electrodeposition of iron from an alkaline bath are temperature, caustic soda concentration, and current density. High temperatures of the order of 90°C are desirable for maintaining current efficiency and producing coarser dendritic deposits. Similarly low current densities, in addition to producing high current efficiencies, bring about coarse dendrites. High caustic soda concentrations in excess of 400 g/l and preferably between 600-800 g/l effect the best current efficiencies. The laboratory scale experiments established the feasibility of depositing dendritic iron from a caustic soda-iron oxide medium.

It is probable that the iron was deposited by the reduction of the soluble sodium ferrite in the solution. The solubility of the ferrite is rather low and deposition would soon cease without constant replenishment of the solution by the suspended oxide. The presence of more oxide particles than are needed to maintain the ferrite ion concentration should not change the results, which explains why the oxide concentration is not critical, at least above a certain minimum value.

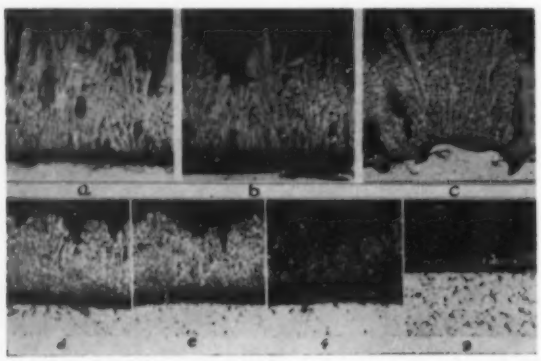

Fig. 4. Effect of current density on cathode deposit: a, 40 amp/ft²; b, 80 amp/ft²; c, 160 amp/ft²; d, 300 amp/ft²; e, 600 amp/ft²; f, 1200 amp/ft²; g, 2400 amp/ft². Magnification 500X before reduction for publication.

Pilot-Plant Electrolytic Studies

On the basis of the laboratory findings establishing the feasibility of the deposition process, pilot-plant studies were undertaken. Pilot-plant studies were to aid in determining the best conditions for continuous electrolysis, to verify efficiencies, to furnish a basis for an economic study of the process, and to make available sufficient quantities of iron powder for chemical and physical property studies, commercial applications and evaluations.

Large-scale studies also offered the possibility for investigating other sources of iron oxide in place of the chemically pure material used in the laboratory. They further aided in determining the technical advantages and disadvantages of the electrodeposition process and gave some knowledge on the design of the cell, grinding equipment, and the over-all production process.

Equipment and procedure.—The cell was constructed of 0.125 in. nickel sheet with base dimensions 18 x 9 in. and a height of 29 in., and had a 20-gal capacity. An inlet and outlet were provided on the side of the cell for the introduction and removal of liquor. Agitation was provided by a high-speed impeller rotating from 1000 to 1500 rpm. The solution was heated from the outside by strip heaters. The walls of the cell served as one anode, and a second anode was hung in the center of the cell. Two cathodes 10 x 24 in. made of 0.25-in. steel plate were inserted on either side of the center nickel anode. The total cathode area was 5.5 ft². D.C. current was supplied by a selenium rectifier.

Caustic soda flakes were dissolved in water to make 16.5 gal of 50% liquor. This electrolyte was used throughout a run, which sometimes extended from 6 to 8 days, with only periodic additions of water to replace evaporation loss. The iron was added as 9 lb of C.P. iron oxide or commercial ores. Periodic additions of approximately 2 lb of oxide were made every 4 hr throughout the run, assuming a current efficiency of 85%.

The cell was operated at 275 amp with an average cell potential of about 2.3 v. The bath temperature was maintained at 85°-90°C, and the solution was agitated to assure intimate mixing of the iron oxide and the alkaline bath.

After each 24 hr of operation the cathodes were removed from the cell. The deposited iron was washed thoroughly with water to remove any excess alkali and metallic oxides adhering to the surface and then scraped off. After the iron was ground in a ball mill, the oxide was removed. The powder was oven dried, sifted through a U. S. Standard 120 screen, and weighed. Samples of each day's production were analyzed for hydrogen loss, total iron, and particle size distribution according to standard MPA methods.

Process evaluation.—Pilot-scale runs were made at conditions which had proven most successful in the laboratory. The correlation between the laboratory work at Battelle Memorial Institute and Dia-

Table V. Pilot Plant Data. 82°-88°C, 275 amp, 45 amp/ft², 2.3 v, 16.5 gal. Capacity cell, 9 lb initial Fe_2O_3 charge followed by 2 lb additions every 4 hr

Run No.	Fe_2O_3 Ore	Current efficiency	Time, hr	Bath age, days	Amp-hr / liter	Ease of stripping deposit	Product analysis: Fe	Product analysis: H_2 loss
17	C.P.	75	8	New	35	Easy		
18	C.P.	80	11	1	83	Easy		
25	C.P.	46	20	New	88	Easy		0.4
26	C.P.	81	20	1	176	Easy	99.66	0.30
27	C.P.	76	21	2	268		99.60	0.33
28	C.P.	72	23	3	369		99.49	0.69
						Composite	99.57	0.43
19	Oolitic hematite	50	12	New	53	Easy when fresh, hard after standing.		
20	Oolitic hematite	52	12	1	106			
21	Oolitic hematite	46	12	2	159			
22	Oolitic hematite	58	24	6	273			
23	Oolitic	59	20	New	88	Easy when fresh, hard after standing.		
24	Oolitic	41	20	1	176		98	2.0

mond Alkali Company and the pilot-plant runs made at Diamond Alkali was excellent. As shown on Table V, using C. P. Fe_2O_3 as a raw material, current efficiencies were in the range of 75-80% and were not appreciably affected by the age of the bath as long as the Fe_2O_3 concentration was maintained by the addition of ore. The chemical quality of the product was excellent, analyzing 99.57% iron and 0.43% hydrogen loss. The type of deposit is shown in Fig. 5, which is similar to that found in bench scale work.

Pilot operation verified that a very simple cell design was sufficient. It was shown that a bath could be used for several days without detrimental effects. It was also shown that after several days of operation the cell could set dormant for several days and be put back in operation without a reduction in current efficiency.

The use of oolitic hematite in place of C.P. ore reduced the current efficiency to approximately 50%. The product quality was also reduced, showing 2% hydrogen loss. The nature of the deposit was altered slightly, and although it was easily removed while fresh, it became difficult to remove if allowed to cool and dry. This was probably due to the presence of silicate, which cemented the deposit. It is possible that with some additional work to improve the technique and by selection of a more suitable natural ore results could be considerably improved.

Fig. 5. Iron deposited on pilot plant cathode, cross section of cathode deposit. Magnification 90X before reduction for publication.

In general, it was shown that the electrodeposition of dendritic iron from a caustic soda bath containing a suspended Fe_2O_3 is chemically and economically feasible. The raw materials are low in cost and can be handled easily. The electrolysis proceeded as planned. And finally, the product could be removed from the cathodes with a minimum of effort, yielding a deposit that could be easily ground in a ball mill.

Physical and Chemical Properties of Iron Powders

A determination of the physical and chemical properties of powders made under all of the conditions tried would be extremely laborious, since there are so many properties of significance in powder metallurgy and other powder uses. However, many of the properties are related inherently to the shape and size distribution of the powder. Therefore, detailed determinations could be restricted to a few representative powders covering the shapes and size distributions encountered during the experimental production of powders. In most of the deposition experiments on a laboratory scale less than 30 g of powder were produced. This amount of material is insufficient to determine several important properties, such as flow rate. Therefore, most of the powders that were examined in detail were made on a

Table VI. Chemical analysis of iron powder. L-Laboratory; P-Pilot plant

Sample No.	Fe_2O_3	H_2 loss, %	Fe, %	FeO, %	Fe_2O_3, %	Total Fe, %
L-82	C.P.	0.05	98.77	0.65	0.49	99.62
L-83	C.P.	0.38	94.22	6.50	0.49	99.62
L-84	C.P.	0.00	97.08	3.05	0.25	99.62
L-85	C.P.	0.12	98.28	2.16	0.05	99.96
L-86	C.P.	0.58	97.08	3.05	0.00	99.45
P-25	C.P.	0.40	—	—	—	—
P-26	C.P.	0.30	—	—	—	99.66
P-27	C.P.	0.33	—	—	—	99.60
P-28	C.P.	0.69	—	—	—	99.49
#8		0.76	—	—	—	—
L-87	Oolitic hematite	1.08	—	—	0.73	96.58
L-88	Oolitic hematite	1.39	—	—	0.47	96.07
P-24	Oolitic hematite	2.0	90.6	7.3	0.6	—

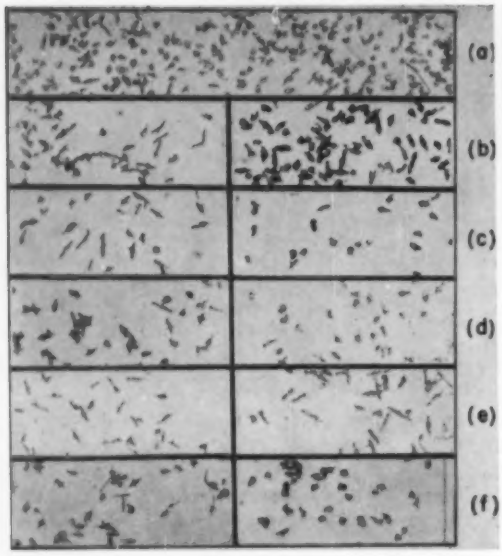

Fig. 6. Photomicrographs of various powders; left, unground; right, ground. a, powder No. 8; b, powder No. 9; c, powder No. 10; d, powder No. 11; e, powder No. 12; f, powder No. 13. Magnification 24X before reduction for publication.

pilot-plant scale. In several cases the operations of stripping from the starting sheet and washing with vigorous agitation were sufficient to reduce most of the deposit to powder. The product is referred to as "unground" powder as distinct from "ground" powder resulting from further comminution in a ball mill or mortar.

Analytical data.—Determinations were made of powders prepared from baths containing either C.P. iron oxide or a commercial iron oxide ore (hematite). Typical results of several experiments are shown in Table VI. Little difficulty was experienced in obtaining a hydrogen loss[a] (oxygen content) of less than 1% when pure oxide was used. However, with oolitic hematite ore the oxygen content was as high as 2%.

Ductility.—All deposits and powders were extremely ductile. When struck with a hammer a deposit was easily deformed without fracture. It was difficult or impossible to fracture particles by grinding. Even a relatively mild grinding deformed the particles as evidenced by the photomicrographs, Fig. 6a-6f, of the same powder, before and after milling. Extensive grinding caused severe deformation. Evidence that the powder is fully ductile as formed and that an annealing treatment does not increase the ductility was obtained as follows: A green compact prepared from powder No. 1 had a density of 5.51 when pressed at 38.7 t.s.i. A green compact made from powder No. 1 annealed in hydrogen at 1,000°C for 1 hr had a density of 5.57, or essentially the same value as the unannealed powder. Had the annealing increased the ductility to any extent, the density of the corresponding compact should have increased.

[a] The term "hydrogen loss" is the loss due to the removal of oxygen during the heating of the specimen in an atmosphere of hydrogen. Procedure in MPA-Standard 2-48 was followed.

Fig. 7. Electron micrograph showing pattern of growth. Magnification 24,750X before reduction for publication.

Comminution.—The deposits were adherent, and, after they were removed from the bath, excess electrolyte and oxide could be eliminated by spray rinsing. The size of the dendrites and their adherence to each other increased with the temperature of deposition. Many of the 90°C deposits were converted to powder by the stripping and washing operations, particularly the deposits prepared on a pilot-plant scale. A further mild grinding treatment separated the few remaining dendrite agglomerations except for the large nodules formed at the corners and edges of the cathodes. The deposits prepared at 120°C in the laboratory showed a different behavior than the lower temperature deposits. Dendrites were generally too large to pass a 100 mesh screen, and the agglomerates tended to deform under the impact in the ball mill rather than to separate into individual dendrites.

Particle shape.—The dendrites as formed tended to be needle-like, and the particles appeared to become narrower and longer as the current density and temperature were lowered. Powder particles of No. 12, as shown in Fig. 6e, had perhaps the largest length to width ratio of any of the samples examined. Even mild grinding tended to flatten the particles, and extensive grinding distorted the particles into flattened platelets. Individual particles were also examined at higher magnifications. Electron-micrographs in Fig. 7 show the pattern of growth. Growth appears to take place by budding off from a parent stalk.

Particle size distribution.—Sieve analyses were made of powders prepared in both the laboratory and pilot plant. The laboratory results are shown in Table VII. A high proportion of fines was found in all the powders. As the temperature of deposition was increased, more grinding was required to break up the deposit, and the amount of fines became less. At 120°C a firm deposit was obtained that required extensive grinding and resulted in powder particles having a flat, disk-like shape. Similar results were obtained with pilot-plant powders as shown in Table VIII. Again the powders were on the fine side. The results for −325 mesh fractions would appear to be erratic, and this is related to the deformability of the particles on grinding. Table IX indicates this effect clearly. In four of the five examples the frac-

Table VII. Properties of powders prepared in the laboratory

Sample No.	Temp, °C	Current density, amp/ft²	NaOH conc, g/l	Weight of powder, g	Green density, g/cc	Size distribution, Tyler Equivalent					
						+100 %	−100 +150 %	−150 +200 %	−200 +250 %	−250 +325 %	−325 %
1	90	86	400	49.4	5.2	8.8	—	—	5.3	—	85.9
2	90	40	600	26.4	5.5	1.02	0.38	22.6	16.9	23.4	35.7
3	105	40	600	26.2	5.5	0.23	1.5	4.8	5.3	14.7	73.5
4	112	40	600	26.8	5.8	1.06	14.7	13.6	8.3	15.3	47.1
5	116	40	600	24.8	5.8	0.14	17.9	15.3	6.56	14.0	46.2
6	120	40	600	35.7	5.7	12	12.3	18.6	9.6	21.6	26.0
7	120	80	600	49.6	5.4	19.7	2.3	10.7	7.5	19.3	39.8

Notes:
No. 1. Deposits average 0.1 in. in thickness and were ground wet for 2 hr with 1-in. diameter steel balls. Several large pieces from edges and corners of the deposits were not broken up. The large pieces account for most of the 100 mesh material.
No. 2. Deposit loose and crumbly. Ground for 5 min with ½-in. diameter steel balls. Particles were needle-like and tended to agglomerate so that particle size is probably much finer than indicated by sieve analysis.
No. 3. Ground with 0.5 in. diameter ceramic balls, sizing after 5, 15, 30, and 45 min and returning 100 mesh material to the ball mill. Powder definitely dendritic but less so than No. 2.
No. 4. Deposit was firm and adherent but easily ground in a mortar. Particles dendritic but considerably less so than No. 2 and No. 3.
No. 5. More grinding required than with lower temperature deposits and particles were more irregular in shape.
No. 6. Deposit very firm and compact. Ground with 0.625 in. diameter steel balls for 3 hr, removing −100 mesh material frequently. Particles were severely deformed and flattened.
No. 7. Deposit very firm and compact and required over 10 hr of grinding to reduce the bulk to −100 mesh powder. Particles severely deformed and flattened.

Table VIII. Properties of powders prepared on a pilot-plant scale

Sample No.	Current density, amp/ft²	Time, hr	Temp, °C	Thickness, in.	Sieve analysis of ground powders, Tyler screen size					
					+100 %	−100 +150 %	−150 +200 %	−200 +250 %	−250 +325 %	−325 %
8	—	—	—	—	0.06	1.63	11.72	10.52	14.82	61.25
9	45	24	93	3/32	15.1	7.9	11.7	9.1	27.0	29.2
10	45	8	93	1/32	0.5	0.5	2.8	5.5	33.2	57.0
11	90	12	93	1/8	13.4	3.7	6.9	7.1	33.3	35.6
12	33	24	88	3/32	4.6	1.9	7.2	8.2	29.5	48.6
13	45	24	77	3/32	5.0	2.4	5.5	5.4	28.6	53.1
14	45	24	93	—	Trace	8.0	15.3	(37.6)		39.1*

* Part of the fines were removed so that the powder would flow.

tion of fines is decreased by grinding, as the needle-shaped particles are flattened and unable to pass through as fine a screen. Therefore, the amount of grinding is very critical in determining size distribution, since breaking up of agglomerates, tending to reduce screen size, and flattening, tending to increase screen size, occur simultaneously.

The −325 fraction of a laboratory sample was further analyzed by air elutriation (infrasizer) with the results shown in Table X. The results can be considered only very approximate, since the instrument is calibrated for spherical rather than needle-like particles. The average nominal diameter for the particles in the fines appears to be in the range of 20-40 μ, with less material below 10 μ.

Flow rate.—Flow rate tests were carried out on sized fractions of powders prepared in the pilot plant with the results shown in Table XI. None of the powders flowed prior to screening, but all the −325 fractions flowed after screening. Powder No. 14 originally contained much more than 39% fines, but when the fines above this amount were removed, the powder flowed with a standard time of 35 sec, which is commonly accepted in powder specifications.

Apparent density.—The apparent densities of powder No. 8 and No. 14 were 2.29 g/cc and 2.47 g/cc, respectively. The higher value for the latter powder may be because a part of the fines were removed. The values for apparent density are acceptable for metallurgical powders.

Compactability.—Green compacts were made in a single plunger die with a 0.5 in. diameter cylinder. Unless otherwise stated, the pressure used was 30 t.s.i., and 0.5-1% of zinc stearate was added to the powder as a lubricant. In most cases the green density was in the range 5.5-6.0 g/cc (Fig. 8). A

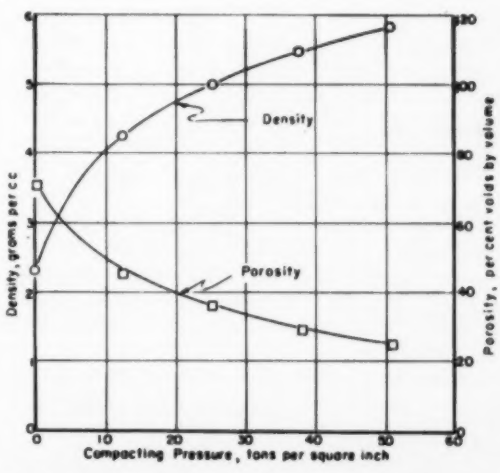

Fig. 8. Green density and porosity of iron powder compacts

Table IX. Change in amount of fines with grinding

Sample No.	Fraction of −325 mesh sample		Grinding time, min
	Unground	Ground	
9	42.5	29.2	40
10	49.5	57.0	30
11	45.5	35.6	60
12	59.4	48.6	25
13	71.2	53.1	30

Table X. Particle size distribution of −325 mesh fraction by air elutriation, powder No. 1

Particle size, microns	Weight fraction, %
0.9	56-84
16.0	42-70
30.6	28-56
25.2	15-42
15.2	9-30
6.7	5-18
3.5	3-15

green density of at least 6.5 would be preferable to meet existing specifications, although tensile tests indicated that such a high density is not necessarily required for strength and ductility.

Green strength.—The standard MPA rattler test was carried out with green compacts of powder No. 8. The value was 2.29% loss, well above minimum requirements.

Tensile strength and elongation of sintered compacts.—Tensile specimens were compacted, sintered, and tested according to MPA standard 10-50 T. Results for two experimental powders are shown in Table XII and are compared with several commercially available materials. Powder No. 12 had very long, jagged particles and did not flow. Its sintered compacts had strengths and ductilities comparing favorably with much higher density compacts from other powders. The results with powder No. 14 illustrate the risk in using a standard evaluation test. At a pressure of 30 t.s.i., commonly used for evaluation, results were very poor, but at 50 t.s.i., which is still a practical pressure, much higher strength and ductility were obtained.

A photomicrograph of a sintered compact made from an experimental powder is shown in Figure 9.

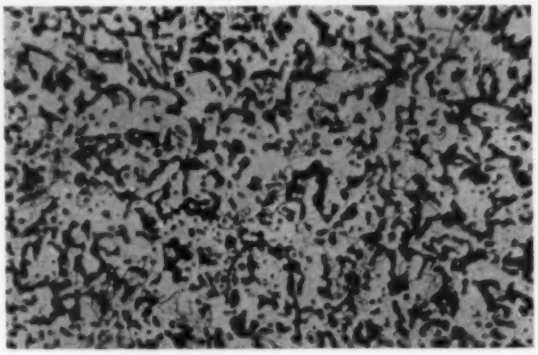

Fig. 9. Sintered powder compact. Magnification 250X before reduction for publication.

Table XI. Properties of powders prepared on a pilot-plant scale

Sample No.	Minus 325 mesh powder, %	Flow rate, sec					Green density, g/cc
		Tyler screen −100 +150	−150 +200	−200 +250	−250 +325	−325	
8	61.25	33.8	33.1	33.5	31.9	NF	5.9
9 (A)	29.2	43.0	39.8	36.8	32.5	NF	5.5
10 (B)	57	—	40.6	40.1	33.5	NF	5.5
11 (C)	35.6	57.3	51.1	44.9	35.2	NF	5.7
12 (D)	48.6	95.3	63.5	55.6	43.9	NF	5.6
13 (E)	53.1	45.8	44.1	41.1	34.7	NF	5.7
14	—	35					—

Table XII. Tensile strength and elongation of iron powder compacts

Powder	Lubricant	Compacting pressure, tsi	Density, g/cc	Tensile strength, psi	Elongation, %
Diamond No. 12	0.5% Zn stearate	30	5.8	22,000	9
		40	—	24,000	10
Diamond No. 14	0.5% Zn stearate	30	6.06	11,100	2.3
		50	6.64	28,000	6.1
British	none	40	6.8	23,000	10.5
	1% stearin	40	7.0	16,000	2.5
European I	—	25.8	6.8	18,000	—
		38.7	7.2	24,000	—
		51.6	—	27,000	—
European II	—	25.8	6.5	24,000	—
		38.7	7.0	31,000	—
		51.6	—	34,000	—
Japanese	—	30	6.4	20,045	10.4
U. S. I	0.5% Zn stearate	30	6.7	21,300	—
		50	7.2	29,200	20
U. S. II	—	18	6.6	23,000	7
		31	7.0	31,000	7
		45	7.3	37,000	10

Intermeshing of particles and grain growth are evident, as are the interstices.

The investigation just discussed was carried out at the Diamond Alkali Laboratories and at Battelle Memorial Institute under the sponsorship of the former.

Acknowledgment

Acknowledgment is expressed to the persons that have carried out the experimental work as follows: Battelle Memorial Institute, Messrs. W. Buckingham, R. Lindsey, and R. Wylle; Diamond Alkali Company, Messrs. A. Barbato, N. Daugherty, D. Goens, C. Hardman, P. Locotosh, T. Norris, and J. Parker. Appreciation is also extended to the Analytical and Metallurgical Departments of both institutions.

Manuscript received Oct. 28, 1958. This paper was prepared for delivery before the Buffalo Meeting, Oct. 6-10, 1957.

Any discussion of this paper will appear in a Discussion Section to be published in the June 1960 JOURNAL.

REFERENCES

1. Estelle, Swedish Pat. 42,849, (1915); U. S. Pat. 1,275,-161, Aug. 16, 1918.
2. Angel, U.S. Pat. 2,622,063, June 30, 1945.
3. Ljungberg, *Stahl u. Eisen*, **74**, 279 (1954).
4. Mehl, *Metal Treatment and Drop Forging*, **117**, 118 (1950).
5. Mehl, U. S. Pat. 2,389,734, Nov. 27, 1945.

Electric Field Enhancement of Cathodoluminescence (Cathodoelectroluminescence)[1]

Philip M. Jaffe

Research Department, Westinghouse Electric Corporation, Bloomfield, New Jersey

ABSTRACT

The application of an alternating electric field to certain cathode-ray excited ZnCdS:Mn,Cl powder phosphors causes the cathodoluminescence to be enhanced. Enhancement is a function of the frequency and strength of the applied field, the beam current density, and the accelerating potential. The indications are that the effect is in reality cathode-ray induced electroluminescence. Similar testing of a ZnCdS:Mn,Au,Cl phosphor results in either enhancement or quenching depending upon the exciting conditions.

Destriau has shown that the Roentgenoluminescence of certain ZnCdS:Mn,Cl (1) and ZnCdS:Mn,-Au,Cl(2) phosphors is enhanced by the application of an alternating electric field. Since then, several similar enhancement effects have been reported (3-14). One of these, described by Cusano (3-5), utilizes a thin film of ZnS phosphor activated by either manganese, arsenic, or phosphorus and coactivated by chlorine. On exciting the film with 3650Å radiation, x-rays, or cathode-rays, the simultaneous application of a d-c field produces an increase in the light output. A similar effect has been reported by Thornton using a wide variety of powdered ZnS phosphors with u.v. radiation and either a-c (6) or d-c (7) fields and by Woods (8) using single crystals. Halsted's enhancement effect (9) has been observed using a-c fields and 2537Å excitation of ZnS:Cu,Al and ZnS:Ag,Cl and 3650Å excitation of ZnCdS (35, 50, 85% Cd): Ag,Cl and ZnSSe (20% Se): Cu,Al phosphor powder samples. Gobrecht and Gumlich (10) have studied the effect of a-c fields on u.v.-excited ZnS:Mn,Cl powder phosphor, while Mattler (11) investigated the same phosphor using excitation by α particles. Neumark (12) has studied the enhancement of thermoluminescence by electric fields. Mention also should be made of the work of Woods and Wright (13) on the enhancement of the cathodoluminescence of MgO by the application of a d-c field.

The present paper deals with a-c field enhancement of the cathodoluminescence of certain ZnCdS:Mn,Cl, and ZnCdS:Mn,Au,Cl powder phosphors. The simultaneous effect of a-c fields and cathode-rays on ZnS:Cu,Al and ZnS:Mn powder phosphors has been reported on by Gobrecht and co-workers (14).

Experimental

The composition of the phosphor mainly used in this work was (70Zn·30Cd)S:0.14Mn,0.5NaCl[2] and is similar to that used by Destriau in his studies on x-ray enhancement (1). Some observations also were made with a (50Zn·50Cd)S:0.5Mn,10^{-4}Au (added as the respective chlorides) phosphor, supplied by Destriau, which shows greater x-ray enhancement than the phosphor without gold (2). In addition, silver-activated ZnS and ZnCdS(30,-70, 85 wt % Cd), Zn_2SiO_4:Mn and a good electroluminescent ZnS:Cu,Cl phosphor were tested. The silver-activated phosphors generally showed quenching of the cathodoluminescence on application of the field. No field response was found for the willemite phosphor, i.e., no enhancement or quenching.

[1] The sections of this paper which deal with the ZnCdS:Mn, Cl phosphor were presented at the Washington, D.C., Meeting of The Electrochemical Society, May 1957, under the title "Electrocathodoluminescence." F. E. Williams in his keynote speech before the Luminescence Symposium of this Society in 1955 suggested that in phenomena of this sort the first prefix indicate the controlling source and the second prefix the power source. As will be shown later, the experimental results indicate that the effect reported on here should be called "Cathodoelectroluminescence" in keeping with Williams' suggestion.

[2] All compositions are on a weight basis. Normally Destriau adds the activators as the chlorides but the presence of the halide is not necessary, at least for Mn alone. He finds, however, that the phosphors without chlorine are not as good as those containing chlorine.

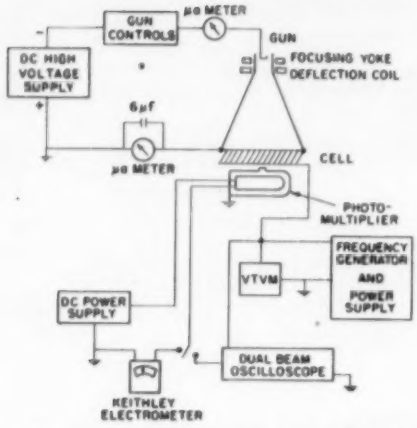

Fig. 1. Block diagram of the circuit used in the cathodoelectroluminescent studies.

The phosphors were made into cells 1 x 1 in. and approximately 2 mils thick using Nylon (DuPont FM6501) as the dielectric. The cells were prepared by coating the conducting surface of tin oxide-coated glass with a clear coat of Nylon, 0.5 mil thick (as measured with a micrometer), on which was superimposed a 1 to 1.5 mil thick layer of Nylon plus phosphor in a volume ratio of 1:1. The cell was completed by evaporating an approximately 1500Å thick layer of aluminum on the Nylon-phosphor layer. The cells were first tested under x-rays for uniform enhancement. The satisfactory cells then were examined in a continuously pumped, demountable cathode-ray tube. The tube was operated with the gun at negative high voltage while the aluminum electrode of the cell and the internal conducting coating of the tube were connected to ground. The gun was of the magnetically focused type, and a constant raster of approximately 5 cm^2 was used in all the measurements. The light output from the cell was detected with an RCA 1P22 photomultiplier and a Keithley electrometer. Provisions also were made for visual observations of the photomultiplier output on a dual-beam oscilloscope in order to study phase relationships. A block diagram of the test circuit is shown in Fig. 1.

Results

Studies of the enhancement effect were made as a function of accelerating potential, beam current density, and the frequency and strength of the applied field. The results of these measurements as well as several miscellaneous measurements and observations are given below. The results are reported in terms of the enhancement factor, ρ, which is defined by the expression

$$\rho = B/B_{cl} + B_{el}$$

where B is the light output under the action of both cathode rays and the field, B_{cl} is the normal cathodoluminescence and B_{el} is the electroluminescence, if any.

Enhancement as a function of frequency.—The enhancement effect was studied extensively over the range of 60-6000 cps; some measurements were also made between 20 and 60 cps using the ZnCdS:Mn,-Cl phosphor. With the Mn,Cl phosphor, ρ goes through a maximum around 30 cps and decreases toward a limiting factor of unity with increasing frequency (Fig. 2). Also, ρ decreases with increasing frequency for the Mn,Au,Cl phosphor, and, depending on the beam current density and field strength, may be less than unity, i.e., the output is quenched (Fig. 3).

Enhancement as a function of field strength.—The enhancement effect was studied over the range of approximately 10,000 to 60,000 v/in. since the use

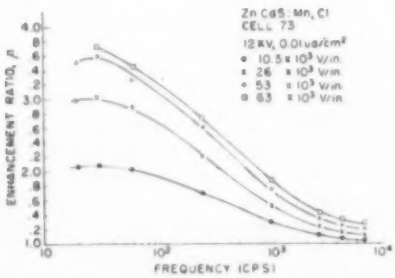

Fig. 2. Enhancement ratio, ρ, as a function of frequency for the (70Zn·30Cd)S:Mn,Cl phosphor at different field strengths.

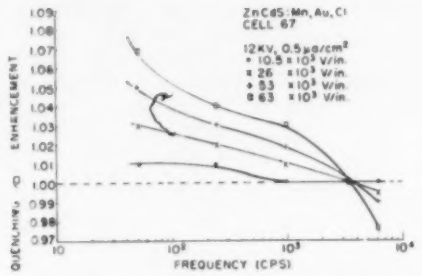

Fig. 3. Enhancement ratio, ρ, as a function of frequency for the (50Zn·50Cd)S:Mn,Au,Cl phosphor at different field strengths. At 12 kv, 0.5$\mu a/cm^2$ and field strengths between 26,000 and 63,000 v/in., quenching is found at frequencies above 3600 cps. Quenching is also found at 4 and 8 kv as discussed in the text.

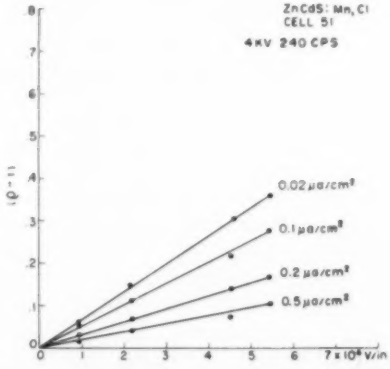

Fig. 4. $(\rho - 1)$ as a function of field strength for the (70Zn·30Cd)S:Mn,Cl phosphor. Notice the decrease in ρ with increasing beam current density over the range 0.02-0.5 $\mu a/cm^2$.

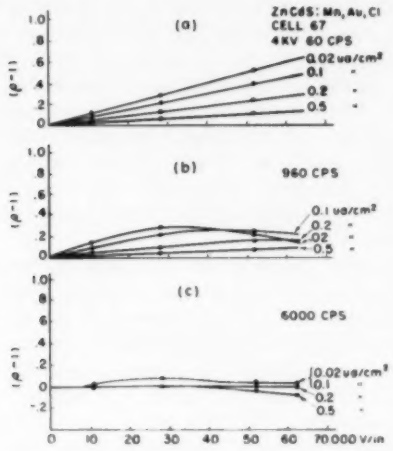

Fig. 5. $(\rho - 1)$ as a function of field strength for the (50Zn·50Cd)S:Mn,Au,Cl phosphor. Note the decrease in ρ with increasing frequency, field strength, and beam current density.

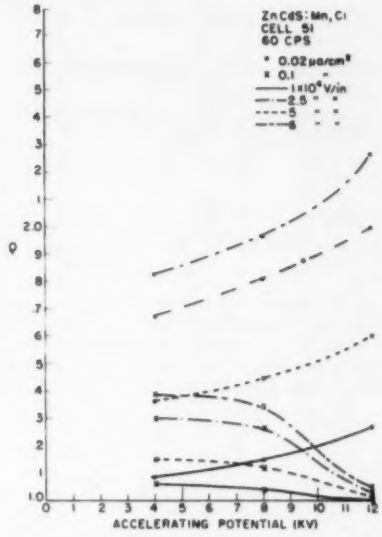

Fig. 6. Enhancement ratio, ρ, as a function of accelerating potential for the (70Zn·30Cd)S:Mn,Cl phosphor. At low beam current densities ρ increases with increasing accelerating potential over the range 4-12 kv; at high beam current densities ρ decreases with increasing accelerating potential. The value of the beam current density at the cross-over point between the two kinds of behavior varies from cell to cell. A similar behavior is observed for the (50Zn·50Cd)S:Mn,Au,Cl phosphor.

of higher fields resulted in arcing which deteriorated the cells. With the Mn,Cl phosphor the quantity $(\rho-1)$ increases linearly with field strength (Fig. 4). The quantity $(\rho-1)$ also increases linearly with increasing field strength for the Mn,Au,Cl phosphor at low frequency (60 cps) and 4 kv. As the frequency increases there is a negative deviation from linearity; the curves obtained at 0.02 and 0.1 μa/cm^2 first show the deviation, but as the frequency increases the 0.2 and 0.5 μa/cm^2 curves also deviate. In the frequency range of 3800-6000 cps there is quenching at high field strengths. This behavior is shown in Fig. 5. At 8 and 12 kv the quantity $(\rho - 1)$ is linear except at 6000 cps where quenching is observed at a beam current density of 0.2 and 0.5 μa/cm^2 and high field strengths.

Enhancement as a function of beam current density.—The effect of beam current density on the enhancement factor was studied over the range of 0.01 to 0.5 μa/cm^2 for the Mn,Cl phosphor and 0.02 to 0.5 μa/cm^2 for the Mn,Au,Cl phosphor. At higher current densities, or for long times of bombardment at the lower current densities there is some decomposition of the Nylon as evidenced by its acquiring a brown discoloration. Because of this, measurements at high current densities were taken after those at lower densities. Between measurements, the current was either lowered or turned off.

The enhancement factor is strongly dependent on the beam current density as can be seen in Fig. 4 and 5. Maximum enhancement occurs at the lower densities and decreases with increasing current density. This decrease in enhancement with increasing incident energy is not limited to the present studies but also is found with several of the other enhancement effects mentioned earlier (3-7, 9).

Enhancement as a function of accelerating potential.—The effect of accelerating potential was studied over the range of 4-12 kv. The results are a little erratic and depend on the beam current density, field strength, and frequency. In general the enhancement factor increases with increasing accelerating potential for low current densities and decreases for high current densities (Fig. 6). The value of the beam current density at the cross-over point between the two kinds of behavior varies from cell to cell, the range being from 0.1-0.5 μa/cm^2.

Brightness waves.—Brightness waves from cells made with the Mn,Cl phosphor were observed on a dual-beam oscilloscope. These were displayed in two different ways. In one method, the photomultiplier output was fed into one set of vertical deflection plates and the alternating voltage across the cell into the other set. The two channels were locked together so that the signals were synchronized. This resulted in a linear trace that showed the time relationship of the two curves. In the second method a trace similar to a Lissajous figure was obtained. This was accomplished by connecting the photomultiplier output to one set of vertical plates and the alternating voltage across the cell to both sets of horizontal plates. The two channels were locked together and the horizontal traces superimposed. In this way one channel, the one having only the horizontal signal, acts as a zero reference while the other shows the brightness wave form as a function of voltage.

The study of the wave form was made at beam current densities of 0.01 and 0.02 μa/cm^2 at variable frequency, field strength, and accelerating potential. The brightness waves show two peaks per cycle of applied voltage, with one peak generally larger than the other (Fig. 7 and 8). The brightness peaks appear after the voltage maxima, as can be seen in the figures. This is similar to the brightness waves obtained during the electroluminescence of Mn-

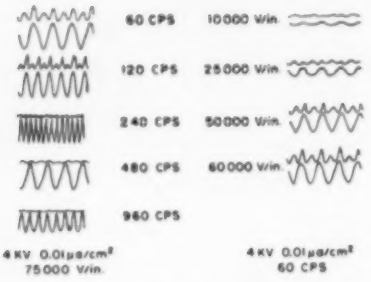

Fig. 7. Linear display of brightness and voltage wave forms for the (70Zn·30Cd)S:Mn,Cl phosphor. The curves on the left showe the influence of frequency and those on the right the influence of field strength. The bottom curve of each pair of curves is the voltage wave form.

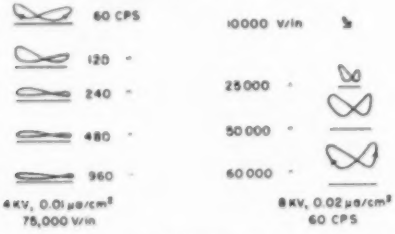

Fig. 8. Lissajous-type of display showing, on the left, the influence of frequency and, on the right, the influence of field strength on the brightness waves of the (70Zn·30Cd)S:Mn,Cl phosphor. The transparent conducting electrode is negative to the left and positive to the right. The direction of the trace is shown by arrows.

activated zinc sulfide phosphors (15). On increasing the field strength both peaks generally increased proportionally. In general the larger peak occurred after the transparent electrode became positive. On increasing the frequency of the applied field, the brightness waves shift slightly to later times, the magnitude of the shift varying from cell to cell. There also appears to be some field strength dependence of the brightness peaks, but the dependence is very erratic. The shift with increasing field strength is also to later times. Variations in beam current density and accelerating potential seem to have little, if any, effect on the waveform relationships.

Examination of the wave form shows the presence of two components, an a-c component superimposed upon a d-c component (Fig. 8). On increasing the field strength, at constant frequency, both the a-c and the d-c components increase, with the amplitude of the former increasing the faster. On increasing the frequency at constant field strength, the d-c component decreases slightly while the amplitude of the alternating component decreases fairly rapidly.

Miscellaneous observations.—In addition to the enhancement effect there is also a Gudden-Pohl effect. Immediately after the application of the field to a cell under cathode-ray excitation there is a rapid increase in brightness to some maximum value followed by a rapid decrease to a constant value which is higher than the initial cathodoluminescence. This permanent increase in light output here has been called the enhancement effect. Removal of the field also causes a transient brightness increase which decreases rapidly to the original field-off value. Both the magnitude and the decay time of the transient component increase with increasing field strength. Equilibrium was usually obtained within 5 sec after the application or removal of the field.

Relative brightness obtained with the enhancement effect.—In order to compare the relative brightness obtained with cathodoelectroluminescence with that of the usual P4 phosphor,[3] cells were prepared using a P4 phosphor (RCA #33Z259). Table I shows the results of brightness measurements (no field) for different beam current densities and accelerating potentials. An RCA 1P22 photomultiplier corrected for eye sensitivity was used in making these measurements. The enhancement ratio used for a given exciting condition is the maximum that was obtained under those conditions, i.e., for any value of frequency. The brightness with field acting was obtained by multiplying the brightness of the ZnCdS:Mn,Cl phosphor, no field acting, by the selected value of the enhancement ratio. As can be seen from Table I, depending on the exciting conditions,

[3] The phosphor used in black-and-white television, designated P4, is in reality a mixture of two phosphors, one (ZnS:Ag) having a blue emission and the other (ZnCdS:Ag) a yellow emission.

Table I. Relative brightness of (70Zn·30Cd)S:Mn,Cl phosphor, with and without field acting, compared to a standard P4 phosphor

Phosphor	Current density, μA/cm²	4 kv ρ_{max}*	4 kv Brightness (B)†	4 kv B Enhanced = $\rho_{max}B$	8 kv ρ_{max}	8 kv B	8 kv $\rho_{max}B$	12 kv ρ_{max}	12 kv B	12 kv $\rho_{max}B$
RCA P4	0.01	—	14.7	—	—	176	—	—	750	—
	0.02	—	24	—	—	480	—	—	1,420	—
	0.1	—	163	—	—	2,500	—	—	7,900	—
	0.2	—	310	—	—	4,900	—	—	15,000	—
	0.5	—	770	—	—	11,170	—	—	30,000	—
(70Zn·30Cd)S: Mn, Cl	0.01	2.36	1.16(12.7)‡	2.74(5.38)	3.07	7(25.2)	21.4(8.23)	4.03	25(30)	100.7(7.4)
	0.02	1.99	1.95(12.3)	3.88(6.2)	2.4	17(27.2)	42.3(11.2)	2.36	60(23.5)	141.3(10.0)
	0.1	1.38	7.7(21.2)	10.6(15.4)	1.5	82(30.5)	122.8(20.4)	1.33	220(35.9)	292(27.0)
	0.2	1.26	12.7(24.4)	16(24.2)	1.26	145(33.8)	182.15(26.9)	1.23	360(41.6)	444(33.7)
	0.5	1.13	27.5(28.8)	31.1(28.0)	1.13	300(39)	339(33.0)	1.06	800(37.6)	848(35.4)

* The value of ρ is the maximum under the given accelerating potential and current density.
† Brightness in arbitrary units with no field acting.
‡ The number in parenthesis is the ratio $B_{Fl}/B_{ZnCdS:Mn,Cl}$.

Table II. Maximum values of ρ for the ZnCdS:Mn,Cl and the ZnCdS:Mn,Au,Cl phosphors

Accelerating potential, kv	Beam current density, $\mu a/cm^2$	(70Zn 30Cd)S: Mn, Cl ρ	(50Zn·50Cd)S: Mn, Au, Cl ρ
4	0.01	2.36	—
	0.02	1.99	1.85
	1.0	1.38	1.59
	0.2	1.26	1.24
	0.5	1.13	1.14
8	0.01	3.07	—
	0.02	2.40	1.48
	0.1	1.50	1.20
	0.2	1.26	1.15
	0.5	1.13	1.08
12	0.01	4.03	—
	0.02	2.36	1.59
	0.1	1.33	1.18
	0.2	1.23	1.16
	0.5	1.06	1.07

the P4 phosphor is approximately 5-35 times brighter than the field-enhanced ZnCdS:Mn,Cl phosphor.

Discussion

An increase in light output is observed when an alternating electric field is applied to a 2-mil thick cell made with (70Zn·30Cd)S:Mn,Cl phosphor or, under certain conditions, with (50Zn 50Cd)S:Mn,-Au,Cl phosphor which is under cathode-ray excitation. As can be seen from Fig 9, the total light output (B) is greater than the sum of the electroluminescence (B_{el}) and the cathodoluminescence (B_{cl}). The enhancement ratio, ρ, is found to depend on several factors, the most important being the frequency and strength of the applied field, the accelerating potential, and the beam current density. The Mn,Cl phosphor has the brighter cathodoluminescence and also the larger enhancement factor (Table II).

In many respects the behavior of the ZnCdS:-Mn,Au,Cl phosphor is similar to the ZnCdS:Mn,Cl phosphor. The major differences are: (a) quenching occurs with the former phosphor at 4, 8, and 12 kv at high beam current densities, high field strengths, and high frequencies. (b) The quantity (ρ -1) as a function of field strength is linear for the Mn,Cl phosphor but may have a negative deviation from linearity at 4, 8, and 12 kv for the Mn,Au,Cl phosphor depending on the frequency, field strength, and beam current density.

Several characteristics of this effect are similar in nature to ordinary electroluminescence, i.e., the shape and number of brightness waves per cycle of applied field, the increase in ρ with field strength, the effect of frequency on the a-c component of the light output, and the possible shift of the brightness peaks with frequency (16). There are also some dissimilarities, the main ones being the decrease in ρ with increasing frequency and the apparent shift of the brightness waves to later times with increasing field strength.

This new enhancement effect is somewhat similar to some of the other enhancement effects in that there is a decrease in enhancement with increasing high exciting intensity (3-7, 9). The x-ray and

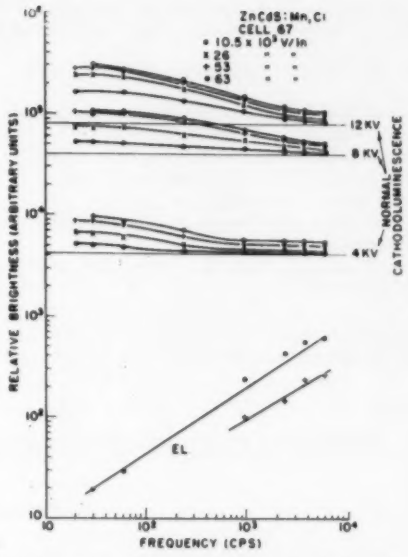

Fig. 9. Relative brightness of the enhanced cathodoluminescence and the electroluminescence of (30Zn·30Cd)S:Mn,Cl phosphor. Beam current density 0.01 $\mu a/cm^2$.

cathode-ray enhancement effects differ with respect to frequency in that there appears to be little frequency dependence for x-ray enhancement. This may be related to the difference in penetration between x-rays and cathode-rays.

Because of the preliminary nature of this work no conclusive theory can be developed at this time for the cathodoelectroluminescent effect. From the general behavior of this effect and the similarity to ordinary electroluminescence, it would appear that the effect is fundamentally radiation-controlled electroluminescence and is similar to the mechanism proposed by Williams for Cusano's and Destriau's enhancement effects (17). Recently, however, Curie (18), Destriau, (19), and Ivey (20) have concluded that the field-enhancement effect observed by Destriau does not have the same mechanism as that observed by Cusano. This presumably can be extended to the effect reported on here. Because of the complexity of cathodoluminescence in general and of the present effect, it may be extremely difficult to elucidate the enhancement mechanism.

Acknowledgments

The writer would like to thank Mr. E.G.F. Arnott and Dr. H. F. Ivey for suggesting this project (21) and Professor G. Destriau for supplying the information relating to the preparation of the ZnCdS:Mn,Cl phosphor and for the sample of the ZnCdS:Mn,Au,-Cl phosphor. Thanks also are due to Mr. G. Scanlon for his help in cell preparation and for obtaining some of the measurements. Acknowledgment should also be made to Drs. H.F. Ivey and W.A. Thornton for their advice and aid in solving some of the circuit problems and for the many valuable discussions held with them.

Manuscript received Dec. 15, 1958. This paper was prepared for delivery before the Washington Meeting, May 12-16, 1957.

Any discussion of this paper will appear in a Discussion Section to be published in the June 1960 JOURNAL.

REFERENCES

1. G. Destriau, J. Mattler, M. Destriau, and H. E. Gumlich, *This Journal*, **102**, 682 (1955).
2. G. Destriau, *Compt. rend.*, **245**, 1913 (1957).
3. D. A. Cusano, *Phys. Rev.*, **98**, 546 (1955).
4. D. A. Cusano, *ibid.*, **106**, 604 (1957).
5. D. A. Cusano, *IRE Trans. Nuclear Science*, NS3, #4, November 1956.
6. W. A. Thornton, *Bull. Am. Phys. Soc.*, **3**, 273 (1958) Abstract SP-1.
7. W. A. Thornton, *ibid.*, Abstract V-11.
8. J. Woods, *J. Electronics and Control*, **3**, 531 (1957).
9. R. E. Halsted, *Phys. Rev.*, **90**, 1807 (1955).
10. H. Gobrecht and H. Gumlich, *J. phys., rad.*, **17**, 754 (1956).
11. J. Mattler, *ibid.*, **17**, 758 (1956).
12. G. Neumark, *Phys. Rev.*, **103**, 416 (1956).
13. J. Woods and J. Wright, *Proc. Phys. Soc. (London)*, **68B**, 566 (1955).
14. H. Gobrecht, H. E. Gumlich, H. Nelkowski, and D. Langer, *Z. Phys.*, **149**, 504 (1957).
15. J. Mattler, *J. Phys., rad.*, **17**, 725 (1956).
16. W. A. Thornton, *Phys. Rev.*, **102**, 38 (1956).
17. F. E. Williams, *ibid.*, **98**, 547 (1956).
18. D. Curie, "Progress in Semiconductors," Vol. 2, 249, John Wiley, New York (1957).
19. G. Destriau, *Compt. rend.*, **245**, 1797 (1957).
20. H. F. Ivey, International Conference on Solid-State Physics, Brussels, 1958.
21. E. G. F. Arnott and H. F. Ivey, U. S. Pat. 2,863,084, Dec. 2, 1958.

Influence of Hydrogen on the Red ZnS-Cu Fluorescence

W. van Gool and A. P. D. M. Cleiren

Philips Research Laboratories, N. V. Philips' Gloeilampenfabrieken, Eindhoven, Netherlands

ABSTRACT

Self-coactivated ZnS-Cu phosphors were made by firing in different atmospheres. When H_2S/H_2 mixtures were used, the red fluorescence decreased with increasing amounts of hydrogen. With A/S_2 or with N_2/S_2 atmospheres no red fluorescence was obtained. These experimental results can be summarized by stating that, in order to obtain the red fluorescence, hydrogen must be incorporated into the phosphor and the sulfur pressure must be sufficiently high. The hydrogen either forms a part of the red center or it destroys or replaces a killer center that prevents the occurrence of red fluorescence when hydrogen is absent. In connection with the high sensitivity of the red fluorescence to small amounts of impurities it is suggested that the concentration of the red centers is much smaller than the amount of incorporated copper.

Some years ago Froelich (1) made an extensive study of the red fluorescence obtained by activating ZnS with Cu without coactivators such as chlorine or trivalent ions. Recently new data on the preparation of these powders and their properties were reported by Aven and Potter (2). In spite of this work it is as yet not possible to give a model of the structure of the centers which would account for this red fluorescence.

In our own investigations, which confirmed the more important facts given by the above-mentioned authors, we wanted to make sure that hydrogen had no influence on the red fluorescence. In view of the fact that most powders had been in contact with an atmosphere containing hydrogen in one way or another, the role of hydrogen should not be disregarded entirely. The experiments indicate that indeed hydrogen must be incorporated into the lattice in order to obtain the red fluorescence, as is described in the next sections.

Preparation of Powders and Firing Conditions

Several phosphors were made in gas atmospheres containing H_2S, S_2, and H_2. A fluorescent grade ZnS, precipitated from an acid $ZnSO_4$ solution, was used. By chemical analysis about 0.4% SO_4 and 0.003% Cl were found in the starting material. Spectrographical analysis showed 0.0005-0.0010% Pb and the other impurities were below their detection limit (all percentages are given by weight). The ZnS was wetted with a $CuSO_4$ solution, dried at 90°C, and mixed. The concentration in these phosphors was 10^{-4} gram atom Cu per mole ZnS.

The H_2S was taken from tanks. In the earlier stages of this research the H_2S was washed with an acid $CrCl_2$ solution to eliminate O_2 (3), with a solution of NaHS to eliminate HCl, and then dried over P_2O_5. At a certain stage of this investigation the red ZnS-Cu emission could not be reproduced. A careful investigation of the working conditions indicated that a change-over from one tank of H_2S to another was the cause of this failure. Further investigation showed that some tanks contained only small amounts of CO_2, whereas others contained about 1% CO_2. For this reason the H_2S was also washed with $Ba(OH)_2$ solution in the later stages of this research. The H_2S gas may contain small amounts of methylene chloride that are not removed by the purification technique used in these experiments. There was, however, no indication from the fluorescence of the powders that this impurity interfered with the result.

Hydrogen, nitrogen, and argon were taken from tanks and were of the purest quality available. In some experiments they were washed with an acid $CrCl_2$ solution, with a KOH solution, and then dried over P_2O_5. In other cases traces of oxygen were re-

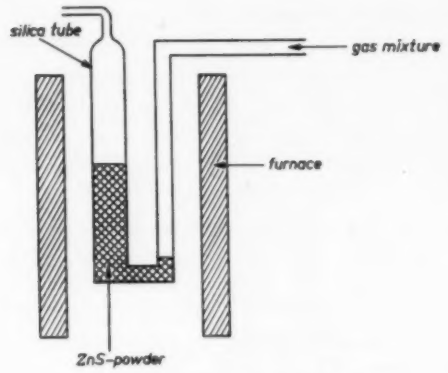

Fig. 1. Firing method used normally

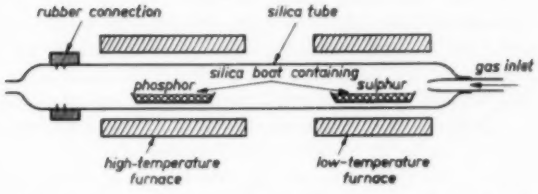

Fig. 2. Firing method used for producing sulfur-containing atmospheres.

moved from the nitrogen by means of a copper oven. When necessary the gases were mixed first and then passed through one purifying set. The sulfur used was of high purity: the only impurity found by spectrographical analysis was 0.00003% (by weight) of Cu.

Two different firing techniques were used. The first one, which was used in most of our experiments, is shown in Fig. 1. The second one, shown in Fig. 2, was used when addition of sulfur to the gases was necessary. By changing the temperature of the sulfur-containing part of the silica tube and the gas-flow rate, different sulfur pressures were obtained. In both firing techniques the tubes with powder were placed in the furnace after the furnace had reached the required temperature; thus the powders reached the firing temperature within a few minutes.

All powders were cooled as rapidly as possible. In the first firing technique this was done by immersing the firing tube in water; in the second one the outside tube was flooded with water.

Several cross experiments were made. Some powders were fired with both setups in order to make sure that no unexpected factors were important. Except for the case already mentioned, no significant differences were found.

Table I. ZnS-10^{-4} Cu fired in H_2S [not passed through $Ba(OH)_2$] 2 hr 1100°C

Phosphor	Firing method	Gas flow, ml/min*
AC 497	Fig. 1	75
AC 510	Fig. 2	200
AC 538	Fig. 2	200

* The gas flow was always measured at room temperature.

Table II. ZnS-10^{-4} Cu, fired in H_2S/H_2, 2 hr 1100°C

Phosphor	Firing method	Gases [no $Ba(OH)_2$ used]	Total gas flow, ml/min	Ratio H_2S/H_2
AC 499	Fig. 1	H_2 not purified	100	7/93
AC 532	Fig. 1	H_2 purified	100	7/93
AC 511	Fig. 2	H_2 not purified	200	7/93
AC 503	Fig. 1	H_2 not purified	100	20/80
AC 501	Fig. 1	H_2 not purified	100	44/56
AC 531	Fig. 1	H_2 purified	100	44/56

Three powders were fired in pure H_2S; some details of the firing conditions are given in Table I.

A second set of fluorescent powders was obtained by firing in H_2S/H_2 mixtures, as detailed in Table II.

A third series of phosphors was made by firing in H_2S/S_2 mixtures (Table III; AC 535, AC 536, and AC 537).

One single phosphor was made by passing pure H_2 over sulfur (Table III, AC 543).

In a fourth series nitrogen or argon were used as carrier gases. Powders AC 528, AC 529, AC 530, and AC 550 were obtained by passing the nitrogen over sulfur. AC 549 was fired in argon carrier gas (Table IV). The powders AC 533 and AC 534 were made by passing a N_2/H_2 mixture over sulfur.

In order to eliminate the effect of contaminations originating from the silica walls, ZnS-10^{-4} Cu was fired in two new vessels (Fig. 1). In each tube four firings were made in purified hydrogen. One tube was cleaned in the normal way after each firing. The second tube was not cleaned between the firings, the powder was merely shaken out (AC 551-AC 557).

Observations and Measurements

The fluorescence of the powders described in the preceding section was studied with 3650Å excitation. Although the relative brightness of the powders could be established easily by visual inspection of the powders, the measurement of the red fluores-

Table III. ZnS-10^{-4} Cu, fired in H_2S/S_2 or H_2/S_2, 1100°C, 200 ml gas/min, firing setup Fig. 2

Phosphor	Gas	Firing time	Evaporated sulfur, g
AC 535	H_2S no $Ba(OH)_2$ used	2 hr	3.418
AC 536	H_2S no $Ba(OH)_2$ used	2 hr	7.228
AC 537	H_2S no $Ba(OH)_2$ used	45 min	7.217
AC 543	H_2 purified	45 min	7.284

Table IV. ZnS-10^{-4} Cu, fired in N_2, N_2+H_2 or A, 1100°C

Phosphor	Gases used	Total gas flow, ml/min	Firing time	Evap. sulfur, g
AC 528	N_2 (copper oven)	200	2 hr	0.0245
AC 529	N_2 (copper oven)	200	2 hr	2.712
AC 530	N_2 (copper oven, P_2O_5)	200	2 hr	3.879
AC 550	N_2 ($CrCl_2$, KOH, P_2O_5)	100	45 min	9.177
AC 549	A ($CrCl_2$, KOH, P_2O_5)	200	2 hr	4.355
AC 533	N_2/H_2 70—30 (N_2 + H_2 — $CrCl_2$, P_2O_5; N_2-copper oven)	200	2 hr	4.575
AC 534	N_2/H_2 90—10 (N_2 + H_2 — $CrCl_2$, P_2O_5; N_2-copper oven)	200	2 hr	4.463

Table V. Relative luminance of phosphor layers, measured with Schott RG1 red filter

Fired in	H_2S		H_2S/S_2		H_2S/H_2		$N_2/S_2/H_2$		H_2, N_2/S_2, A/S_2	
	No. of phosphor	Lum.	No. of phosphor	Lum.	No. of phosphor	Lum.	No. of phosphor	Lum.	No. of phosphor	Lum.
	AC 497	73	AC 535	89	AC 543	38	AC 533	14	AC 551-557	<6
	AC 510	44	AC 536	94	AC 501	25	AC 534	8-10	AC 528-530	
	AC 538	100	AC 537	71	AC 531	19			AC 550	
					AC 503, AC 499, AC 532, AC 511	<6			AC 549	

cence was difficult owing to the weakness of the red light emitted. The best method was to compare the luminance of a phosphor layer with that of a mat surface by means of a Lommer-Brodhun photometer containing a Schott red RG1 filter in the eyepiece. The mat surface was illuminated by an incandescent lamp, and the lamp voltage was varied so as to match the luminance of both surfaces. Every measurement was repeated two or three times, and the average of the lamp voltages was used in the calculation. The red luminance (as seen through a Schott red RG1 filter) of the mat surface at different voltage settings was calibrated with a laboratory luminance meter. The luminance of one phosphor layer (AC 538) arbitrarily was given the value 100. Calculated values of the luminance of the phosphor layers are summarized in Table V.

Phosphors made in low sulfur pressure or made in atmospheres without hydrogen did not show any red fluorescence; this corresponds to the values below the minimum value detectable with the luminance meter (about 6 units). They had a weak green or green-blue fluorescence. This fluorescence was killed when infrared light was shone on the phosphors together with the u.v. at room temperature. No stimulation of an afterglow was found with infrared radiation. At low temperature (77°K) these phenomena were reversed: the fluorescence was not influenced by infrared, but a stimulation of the afterglow was found. During the stimulation, the emitted light had the same color as during u.v. excitation, and not the slightest indication of any red fluorescence was found.

It is well known that the red Cu-fluorescence has the important property that it is much more sensitive to impurities than the fluorescence of normally activated ZnS powders; small amounts of O_2, CO_2, or H_2O all disturb the red fluorescence (1, 2). When adding aluminum in the order of 10 mole % of the added amount of Cu, one finds a blue emission as strong as the red emission. We have confirmed these observations.

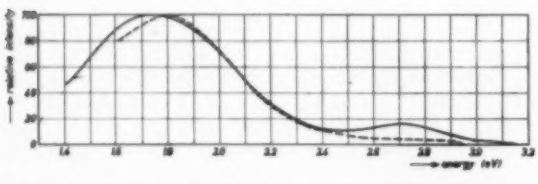

Fig. 3. Spectral distribution of red ZnS-Cu phosphor. ——— AC 538; measured at room temperature; - - - - - spectral distribution measured by Aven and Potter (2), Fig. 3 (x=0).

The spectral energy distribution was measured with the aid of a Leiss (Berlin) double mirror-monochromator with sodium chloride prisms. The 800 cps chopped radiation of the phosphor was imaged on the entrance slit of the monochromator. The output of the detector, amplified by a tuned a-c amplifier with synchronous detection, was recorded automatically as a function of the wave length.

The phosphor was excited by the radiation of a high-pressure mercury discharge lamp (the inner part of a Philips HP 125W lamp with stabilized discharge) from which the long wave length u.v. radiation was isolated by a combination of Schott filters UG11 and BG18. The BG18-filter was used to remove the transmission of the UG11 filter in the red part of the spectrum.

As a detector for the spectral region from 3.5 about to 1.65 ev a selected RCA photomultiplier (type IP28) was used with very high sensitivity in the red. For radiation of lower frequencies a Philips photomultiplier type 51CVP with Cs-O-Ag photocathode was used.

The relative emitted power of the phosphor was found from the recorded photocurrent by calibrating the equipment with the aid of a tungsten ribbon lamp with known spectral distribution. In Fig. 3 the spectral distribution of AC 538 is reported together with one of the distributions given by Aven and Potter (2).

Discussion

In describing the equilibrium system ZnS-sulfur vapor, the sulfur pressure is sufficient to define the oxidation-reduction state of the ZnS crystal. In that case the zinc pressure can be derived from the sulfur pressure according to the equation

$$p_{Zn} \cdot p_{S_2}^{1/2} = K_{ZnS} \qquad [1]$$

When hydrogen is also present in the atmosphere and when hydrogen is incorporated into the ZnS, the value of the hydrogen pressure must also be known in order to define the state of the ZnS powders. In equilibrium it is unimportant whether the presence of the hydrogen is defined by the hydrogen pressure itself, by the H_2S pressure, or by the pressure of some other hydrogen compounds, because these pressures are correlated by a relation of type [2]

$$\frac{p_{H_2}^{x} \cdot p_{S_2}}{(p_{H_2S})^{x}} = K_{H_2S} \qquad [2]$$

A third equation is obtained from the condition that the total pressure is 1 atm, thus

$$p_{Zn} + p_{H_2} + p_{H_2S} + p_{S_2} = 1 \qquad [3]$$

A fourth equation is obtained from the relative amounts of gases or sulfur used during the experiment. In the case of pure H_2S this equation is

$$p_{H_2} = 2p_{S_2} \qquad [4a]$$

When 1 mole gas mixture, introduced in the firing vessel, contains p moles H_2 and $(1-p)$ moles H_2S and when, after establishment of the equilibrium, x moles S_2 have been formed, then we have

$$p_{H_2} = \frac{p + 2x}{1 + x}$$

$$p_{S_2} = \frac{x}{1 + x}$$

Thus, after elimination of x

$$p_{H_2} = p + (2 - p) \cdot p_{S_2} \qquad [4b]$$

In the same way a similar additional equation can be formulated for every experiment. We used $K_{H_2S} = 17 \cdot 10^{-3}$ atm (4) at 1100°C.[1]

The value $K_{ZnS} = 5.4 \cdot 10^{-5}$ atm$^{3/2}$ at 1100°C was calculated from reference (6). Recent measurements by Spandau and Klanberg (7) and Neuhaus and Retting (8) do not permit the calculation of the dissociation constant K_{ZnS}. The total pressures of ZnS, as measured by Spandau and Klanberg, deviate from the values used in (6), but there is no important influence on the main aspects of these calculations. Calculated pressures are given in Table VI.

p_{Zn} is always so small that one can use the equation

$$p_{H_2} + p_{H_2S} + p_{S_2} = 1 \qquad [3a]$$

instead of [3] when only H_2, H_2S, S_2, and Zn are present in the atmosphere. The relation obtained by eliminating p_{H_2S} from Eq. [1] and [3a] is represented by the heavily drawn line in Fig. 4. In the same figure the pressure points of the fired powders are indicated. All pressures were calculated with the assumption that all equilibria were actually established. In some cases the sulfur pressure was lower than the minimum sulfur sublimation pressure of ZnS ($9.1 \cdot 10^{-4}$ atm) and thus the zinc pressure higher than the minimum zinc pressure. Then the question arises whether the gas flow is slow enough to provide sufficient time for the equilibria to be established (9). If this is not the case, the pressure will be stabilized on the minimum sublimation line. This has been indicated in Fig. 4 by arrows pointing to some powders (AC 499, AC 532, AC 511, AC 551-AC 557, and AC 528). As none of these powders has any red fluorescence (see below), the question of the exact localization of the firing conditions in the pressure diagram is not important.

[1] From the tables of (5) a value of $K_{H_2S} = 18.5 \cdot 10^{-3}$ atm was calculated. The difference between this constant and the one we used results in a relatively unimportant change in the pressure calculations.

Table VI. Calculated H_2 and S_2 pressures under equilibrium conditions, $T = 1100$°C

Powder	Gas introduced into the firing vessel	p_{H_2} (atm)	p_{S_2} (atm)
AC 497, AC 510, AC 538	H_2S	0.24	0.12
AC 535	H_2S/S_2	0.21	0.15
AC 536	H_2S/S_2	0.19	0.18
AC 537	H_2S/S_2	0.15	0.26
AC 543	H_2S/H_2	0.46	$2.1 \cdot 10^{-3}$
AC 501-531	H_2S/H_2	0.55	$1.0 \cdot 10^{-2}$
AC 503	H_2S/H_2	0.80	$1.0 \cdot 10^{-3}$
AC 499, AC 532, AC 511	H_2S/H_2	0.93	$1.0 \cdot 10^{-4}$
AC 533	$N_2/S_2/H_2$	0.18	$7.4 \cdot 10^{-3}$
AC 534	$N_2/S_2/H_2$	$4.1 \cdot 10^{-2}$	$3.4 \cdot 10^{-2}$
AC 551-557	H_2		
AC 528	N_2/S_2	—	$3.6 \cdot 10^{-4}$
AC 529	N_2/S_2	—	$3.8 \cdot 10^{-2}$
AC 530	N_2/S_2	—	$5.4 \cdot 10^{-2}$
AC 550	N_2/S_2	—	0.42
AC 549	A/S_2	—	$6.0 \cdot 10^{-2}$

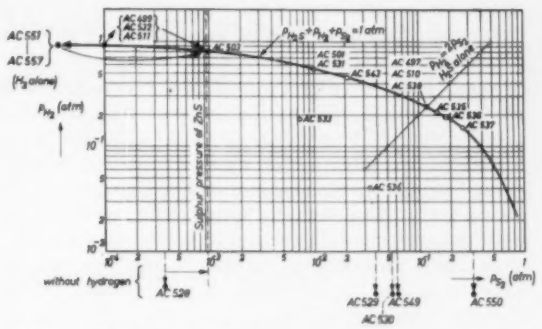

Fig. 4. Sulfur and hydrogen pressures used during preparation of the powders at 1100°C.

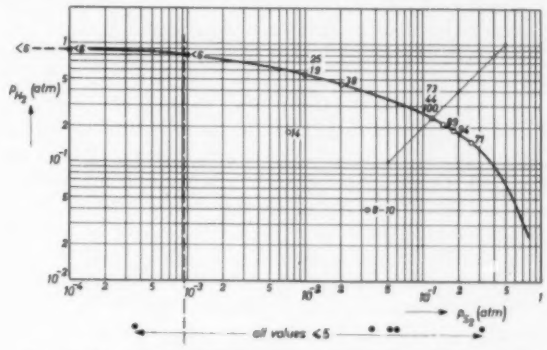

Fig. 5. Measured red fluorescence (in arbitrary units). The location in the pressure diagram corresponds with Fig. 4.

In order to facilitate the review of experimental results, the measured red fluorescence of the powders is inscribed at the respective pressure points in Fig. 5. From this figure it is immediately clear that two conditions had to be fulfilled in order to obtain the red fluorescence: (*a*) there must be hydrogen in the atmosphere, and (*b*) the sulfur pressure must be sufficiently high.

Unless these results are caused by impurity effects (see below), the first condition means that hydrogen is incorporated into the ZnS powders. At this time it is not possible to decide whether the hydrogen forms really a part of the red fluorescent center. The other explanation would be that without hydrogen the red centers would be present but that some other center kills the red fluorescence. Adding hydrogen then would transform the killer center into a harmless one. As there is, however, no evidence in our

work for the presence of the red centers in the powders fired without hydrogen, we prefer the first explanation.

Some doubt may be thrown on this conclusion on the basis of a few experiments described by Aven and Potter (2). They reported that firing ZnS-Cu in hydrogen first gave a blue fluorescence, but that repeated firings in the same vessel finally gave a red fluorescence. The authors interpreted their results with the transfer of a certain impurity (for instance aluminum) from the silica wall to the powder. We have found in some cases that the outside of the sintered powders did show a different fluorescence than the core, but this was restricted to a thin outer shell and the bulk of the powders was always homogeneous. Firing in hydrogen alone produced no red fluorescence, although the firings were repeated four times in the same vessel. Moreover, comparison of the powders AC 499, AC 503, AC 501, AC 543, and AC 497 (Table II) shows that the change in hydrogen pressure is rather small (by a factor of 4), but that the sulfur pressure changes at least by a factor of 100. The red fluorescence disappears completely at lower sulfur pressures in this series, and it seems improbable that a large change in impurity transfer should be brought about by a rather small change in hydrogen pressure. Therefore we believe that in the interpretation of our results we have to assume a direct influence of the sulfur pressure on the formation of the red fluorescence centers.

An important cross experiment is represented by the powders AC 533 and AC 534. With nitrogen no red fluorescence was found and with hydrogen the red fluorescence is decreased, as has been described above. Considering the great sensitivity of the red fluorescence to impurities it would be possible for some harmful impurity to have been introduced by each gas individually. But in using both gases together the red fluorescence was present again and thus the assumption about harmful gas impurities is made very improbable.

Some of the red fluorescent powders mentioned in (1) were made in a CS_2 atmosphere. This result is in conflict with the interpretation given in this paper. However, the experiments in (1) and (2) were not performed with the thought in mind that hydrogen in any form had to be removed carefully, and the experimental details necessary to settle this question are lacking in these papers.

Although the weakness of the red fluorescence as compared with that of strong red phosphors (for example color television phosphors) can be explained by assuming a small recombination coefficient in the kinetic mechanism, the assumption seems more probable that the concentration of the red centers is much smaller (by a factor of 10 to 100) than the added amount of Cu. Hence the occurrence of the red fluorescence centers results only in a minor change in the mechanism by which Cu is built into the lattice without hydrogen. This has three consequences. In the first place, the red fluorescence as such does not provide much useful information about the incorporation of Cu. In the second place, it is difficult to say anything definite about the structure of the red fluorescence centers so long as we do not know exactly the built-in mechanism of Cu. The diamagnetism of these ZnS-Cu phosphors, as found by Bowers and Melamed (10), can be interpreted as a diamagnetism of the majority of the built-in copper atoms. As long as we do not know the concentration of the red fluorescence centers the possibility that these centers are paramagnetic can not be excluded. Finally, this assumption can explain the high sensitivity of the red centers to impurities in a simple manner.

Perhaps one conclusion about the structure of the red fluorescence centers can be reached by comparing the red ZnS-Cu fluorescence with that of ZnS-Ag. According to the results published by Aven and Potter the red silver fluorescence has a spectral distribution different from that of Cu. Since hydrogen is also necessary for the red silver fluorescence the center must contain at least one metal (Ag or Cu) and one hydrogen atom or ion. As to the real nature of the center several possibilities arise depending on whether the impurities occupy substitutional or interstitial positions and on the valencies of these impurities.

In spite of the careful control of the preparative conditions a rather large spread in the luminance of the red phosphors was found, as can be seen from the powders fired in pure H_2S alone. Therefore it is impossible to give quantitative relationships between this luminance and the pressures used. Further investigations are necessary in order to find these quantitative relationships. In our opinion it is premature to give models for the red fluorescent centers as long as the experimental material is scarce and even partly contradictory.

Acknowledgments

The authors wish to express their thanks to Mr. H. J. M. Heyligers for his aid in the gas purifications and furnace construction. The assistance of Dr. P. M. van Alphen and Mr. A. H. C. Vliegen with the luminance measurement and of Dr. A. Bril with the measurement of the spectral distribution is gratefully acknowledged.

Manuscript received Jan. 7, 1959. This paper was prepared for delivery before the Philadelphia Meeting, May 3-7, 1959.

Any discussion of this paper will appear in a Discussion Section to be published in the June 1960 JOURNAL.

REFERENCES

1. H. C. Froelich, *This Journal*, **100**, 280 (1953).
2. M. H. Aven and R. M. Potter, *ibid.*, **105**, 134 (1958).
3. Gmelins Handbuch, Systemnummer 9 (Schwefel) Teil B Lieferung 1, S. 14, Verlag Chemie GmbH (1953).
4. *Ibid.*, p. 6.
5. W. H. Evans and D. D. Wagman, *J. Research Natl. Bur. Standards*, **49**, 141 (1952).
6. Gmelins Handbuch, Ergänzungsband Zink, 8. Auflage Verlag Chemie GmbH, S. 920 (1956).
7. H. Spandau and F. Klanberg, *Z. anorg u. allgem. Chem.*, **295**, 309 (1958).
8. A. Neuhaus and W. Retting, *Z. Elektrochem.*, **62**, 33 (1958).
9. J. Bloem and F. A. Kröger, *Z. Phys. Chem.*, **7**, 15 (1956).
10. R. Bowers and N. T. Melamed, *Phys. Rev.*, **99**, 1781 (1955).

The Fluorescence of Binary and Ternary Germanates of Group II Elements

H. Koelmans and C. M. C. Verhagen

Philips Research Laboratories, N. V. Philips' Gloeilampenfabrieken, Eindhoven, Netherlands

ABSTRACT

The fluorescence of binary and ternary germanates of Ca, Sr, Ba, Mg, and Zn with different activators was investigated. Germanate phosphors activated with Pb, Ti, and Mn are described. The ternary composition triangles are given together with the x-ray powder-diagrams of 23 hitherto unknown germanates.

A great deal of the research on inorganic phosphors has been concentrated on silicates. In contrast to this the germanates, which are closely related to the silicates, have drawn little attention. Only the orthogermanates of Mg, Zn, and Be have been investigated to some extent (1). For this reason it seemed worth while to investigate the fluorescence of germanates, also because nowadays pure GeO_2 is commercially available.

The work described in this article was done along the same lines and in close connection with the work of Klasens, Hoekstra, and Cox (2) on binary and ternary silicates. Most of the new germanates found are isomorphous with the corresponding silicates.

Preparation.—The starting materials used were reagent grade $CaCO_3$, $SrCO_3$, $BaCO_3$, $MgCO_3$, ZnO, and GeO_2. The activators, which included Pb, Ti, Mn, Sn, Ce, Bi, and Re, in form of solutions of their salts, were added in the required amounts to the raw materials. The suspension formed was evaporated to dryness and milled in a runner mill for 15 min. The blends were then heated in alundum crucibles in air at 1050°-1250° for 1 or 2 hr. In all cases 2 or 4% of the Ca-, Sr-, or Ba-carbonates used as base materials were substituted by the corresponding fluorides.

X-ray diagrams showed that this fluoride substitution greatly aided in quickly completing the reaction. It was shown by chemical analysis that after firing only a negligible amount of the fluoride was retained in the phosphors. The activator content was usually about 0.5 mole %. In order to prepare efficient phosphors an excess of free GeO_2 had to be avoided because GeO_2 absorbs u.v. radiation below 3150Å without giving any appreciable luminescence. The same is true for several of the germanates, especially those with a high GeO_2 content. This complication necessitated a careful choice of the composition with the aid of the phase diagrams to be discussed in section 3. X-ray diagrams of the fired powders were made with a North American Philips Geiger counter x-ray diffractometer using Co-K_α radiation.

Binary germanates.—The binary germanates found are listed in Table I together with the known binary silicates. The compounds labeled with the same letter in Table I are isomorphous. Our x-ray powder diagrams of the orthogermanates (2-1) of Ca, Sr, Ba, and Mg essentially correspond to those published by Ludekens (3). In contrast to Ludekens, who obtained only orthogermanates irrespective of the ratio of basic to acid oxides, we also found other compounds. Our mixtures were probably more reactive, especially because of the fluoride flux. The x-ray powder diagrams of the new 1-1, 2-3 and 1-2 germanates are given in Table II.

Ternary germanates.—The ternary germanates found are given in Table III together with the known ternary silicates. Table III shows that with the exception of the 2-1-2 BaMg- and BaZn-germa-

Table I. Binary germanates and silicates of Ca, Sr, Ba, Mg, and Zn. Identical letters in the columns denote that the corresponding compounds are isomorphous. Temperatures given are the firing temperatures in °C

Component oxides		Mole ratios of base to acid oxides									
		2-1		3-2	1-1		2-3		1-2	
CaO	GeO_2	a	1150°	—	d*	1200°	e	1100°	f	1150°
	SiO_2	b		c	d*		—		—	
SrO	GeO_2	g	1125°	—	h	1150°	—		i	1150°
	SiO_2	g		—	h		—		—	
BaO	GeO_2	g	1100°	—	h	1100°	—		i	1075°
	SiO_2	g		—	h		—		j	
MgO	GeO_2	k	1150°	—	m	1150°	—		—	
	SiO_2	l		—	n		—		—	
ZnO	GeO_2	o	1050°	—	—		—		—	
	SiO_2	o		—	—		—		—	

* $CaGeO_3$ is isomorphous with $\beta CaSiO_3$ (wollastonite); no other modifications of $CaGeO_3$ were found.

Table II. X-ray data of the binary germanates

$CaGeO_3$		$SrGeO_3$		$BaGeO_3$		$MgGeO_3$		$CaGe_2O_5$		$SrGe_2O_5$		$BaGe_2O_5$		$Ca_2Ge_3O_8$	
d (Å)	I	d (Å)	I	d (Å)	I	d (Å)	I	d (Å)	I	d (Å)	I	d (Å)	I	d (Å)	I
5.10	20	3.65	30	3.80	30	4.75	40	5.10	40	3.65	100	3.66	100	4.95	25
4.10	10	3.45	60	3.60	25	4.41	40	4.00	27	3.27	6	3.21	20	4.65	12
3.90	15	3.00	100	3.12	100	3.35	90	3.58	24	2.83	70	2.90	65	3.42	10
3.85	5	2.63	30	2.72	25	3.22	95	2.84	100	2.70	90	2.73	80	3.20	45
3.60	20	2.13	20	2.22	30	3.00	65	2.75	16	2.43	20	2.48	10	3.13	50
3.57	5	2.09	45	2.20	70	2.95	100	2.67	13	2.09	16	2.17	14	3.00	100
3.37	30	1.95	10	2.05	25	2.91	25	2.42	13	1.95	18	1.98	18	2.77	6
3.27	25	1.82	10	1.90	15	2.79	15	2.36	14	1.82	20	1.83	14	2.64	80
3.17	25	1.71	10	1.80	25	2.58	100	2.31	13	1.76	22	1.79	16	2.60	35
3.05	100	1.63	10	1.71	20	2.53	55	2.22	9	1.64	25	1.67	14	2.53	25
2.98	15	1.57	15	1.64	30	2.48	20	2.00	7	1.49	10	1.52	10	2.32	12
2.68	10	1.49	5	1.56	20	2.05	15	1.79	5	1.415	12	1.43	8	2.28	6
2.56	20	1.38	5	1.44	10	2.02	30	1.77	13	1.345	10	1.37	10	2.05	8
2.39	5	1.32	10	1.39	30	1.73	15	1.75	15					2.03	10
2.21	5					1.65	15	1.67	13					1.70	15
1.98	5					1.64	15	1.60	9					1.69	25
1.88	10					1.55	15	1.555	9					1.65	18
1.81	10					1.52	30	1.515	9					1.64	18
1.76	5					1.49	20	1.485	9					1.575	15
1.66	10					1.42	15	1.42	11					1.535	10
1.58	5							1.315	12					1.50	8
1.57	5													1.485	6
1.53	10													1.36	8

Table III. Ternary germanates and silicates of Ca, Sr, Ba, Mg, and Zn. Identical letters in the columns denote that the corresponding compounds are isomorphous. The temperatures given are the firing temperatures in °C

Component oxides		Mole ratios of base to acid oxides							
		2-1-2		1-1-1		1-2-2	3-1-2		1-1-2	
CaO, MgO	GeO_2	—		q	1100°	—	—	s	1100°
	SiO_2	p		q		—	v	s	
CaO, ZnO	GeO_2	p	1150°	—		—	—	s	1100°
	SiO_2	p		—		—	—	—	
SrO, MgO	GeO_2	p	1100°	—		—	v 1150°	s	1100°
	SiO_2	p		—		—	v	—	
SrO, ZnO	GeO_2	p	1150°	—		—	—	t	1050°*
	SiO_2	p		—		u	—	—	
BaO, MgO	GeO_2	p	1100°	—		—	v 1100°	t	1100°
	SiO_2	v		—		w	v	—	
BaO, ZnO	GeO_2	p	1100°	x	1100°	w*	—	—	
	SiO_2	v		x		w	—	—	

* $BaZn_2Ge_2O_7$ and $SrZnGe_2O_6$ are rather unstable. Lines of other compounds, especially of Zn_2GeO_4, also occur in the x-ray diagrams of these powders.

nates all corresponding germanates and silicates are isomorphous. This was confirmed by the formation of uninterrupted series of solid solutions. The x-ray powder data of the new ternary germanates are given in Tables IV-VII. The 2-1-2 germanates (Table IV) are all isomorphous with $Ca_2ZnSi_2O_7$ (hardystonite) and $Ca_2MgSi_2O_7$ (akermannite) which are tetragonal. The diagrams could readily be indexed. Cell dimensions are given in Table VIII in which it is seen that the corresponding Zn- and Mg-compounds have practically the same cell dimensions.

The 3-1-2 compounds occur only in the systems containing magnesium. $Sr_3MgGe_2O_8$ and $Ba_3MgGe_2O_8$ are isomorphous with $Ca_3MgSi_2O_8$ (merwinite) which is orthorhombic. With this knowledge the x-ray diagrams could be indexed (Table V) and the unit cell dimensions could be calculated.

$Sr_3MgGe_2O_8$	a = 5.5	b = 9.6	c = 7.3
$Ba_3MgGe_2O_8$	a = 5.7	b = 10.0	c = 7.4

$CaMgGe_2O_6$, $CaZnGe_2O_6$, and $SrMgGe_2O_6$ (Table VI) are isomorphous with $CaMgSi_2O_6$ (diopside), which is the only compound with this structure in the ternary silicate systems. $SrZnGe_2O_6$ and $BaMgGe_2O_6$ are isomorphous but have no diopside structure.

Sufficient firings were made to construct the composition phase triangles shown in Fig. 1. The final phases produced by the firing of compositions falling on conjugation lines are given by the compounds at the end of the lines. The final phases produced by the firing of compositions falling within the triangles are given by the compounds at the apexes of the triangles.

Activation with Pb.—The binary germanates did not give efficient phosphors with Pb activation. Of the ternary compounds the 2-1-2 BaMg-, SrMg-, BaZn-, and SrZn-germanates gave u.v. emitting phosphors. The emissions are given in Fig. 2 together with those of the corresponding silicates. The phosphors are excited strongly only with 2537Å. It is

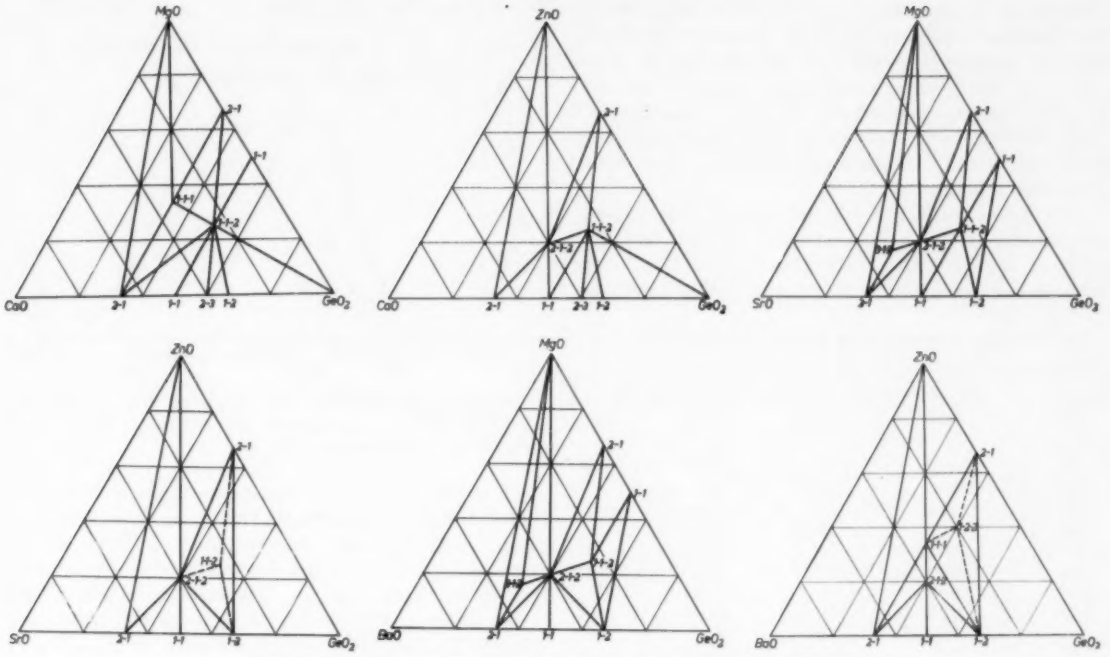

Fig. 1. Composition phase diagrams of the ternary germanate systems.

seen from Fig. 2 that the peak of the Pb emission in the germanates is at several hundred Å longer wave lengths than it is in the silicates. The 2-1-2 Pb-activated BaMg- and SrMg-germanates can be made with about the same efficiency as the corresponding silicates. The efficiency of the Pb-activated 2-1-2 BaZn-, SrZn-, and CaZn-germanates is much lower. An explanation for this can be given easily with the aid of Fig. 3, where the shaded parts are the triangles which contain one or more phases with an inefficient u.v. absorption. These phases are given by circles at the apexes. This means that compositions falling in the shaded areas have a low efficiency due to the presence of those undesired phases. It is also seen from Fig. 3 that in the Zn-containing compounds the whole area around the 2-1-2 com-

Table IV. X-ray data of the 2-1-2 germanates

Indices	$Ca_2ZnGe_2O_7$		$Sr_2MgGe_2O_7$		$Sr_2ZnGe_2O_7$		$Ba_2MgGe_2O_7$		$Ba_2ZnGe_2O_7$	
hkl	d (Å)	I	d (Å)	I	d (Å)	I	d (Å)	I	d (Å)	I
110	5.15	40	5.80	22						
101	4.35	8	4.49	5						
111	3.79	9	3.93	9	3.90	10	4.18	10	3.15	5
210	3.54	20								
201	3.15	20	3.25	20	3.20	22	3.30	20	3.35	12
211	2.92	100	3.04	100	3.00	100	3.10	100	3.10	100
220	2.80	6	2.90	3	2.87	8				
002	2.58	12	2.67	10	2.65	12	2.76	8	2.80	12
310	2.50	48	2.59	26	2.57	30	2.64	17	2.65	40
221	2.46	10	2.53	6	2.52	7				
301	2.34	5	2.42	7	2.40	3	2.50	5	2.50	12
311	2.26	30								
212	2.03	2	2.15	4	2.14	3	2.23	10	2.24	10
400	1.99	2	2.04	18	2.03	4	2.09	9	2.09	8
410	1.90	10	1.96	4	1.95	5	2.03	9	2.03	10
330	1.87	7	1.93	20	1.92	6	1.97	10	1.97	11
312	1.80	40	1.85	32	1.84	36	1.92	22	1.92	27
411							1.90	21	1.90	15
420	1.77	8	1.83	3	1.82	7	1.86	5	1.87	10
103, 322	1.68	4	1.72	3						
213	1.55	2	1.595	15	1.59	11	1.66	26	1.66	20
332			1.56	6	1.55	4	1.61	16	1.61	12
223	1.47	7	1.51	6	1.505	4	1.57	5	1.57	9
521	1.42	7	1.46	19	1.45	13	1.50	25	1.50	20
512					1.39	3	1.395	5	1.395	18
531			1.36	7	1.355	4				
004			1.32	7	1.32	5	1.365	11	1.37	12

position is shaded. Since in our firing experiments the reaction was never entirely complete, nonluminescent absorbers could not be avoided in these cases. In the systems containing Mg there are unshaded triangles around the 2-1-2 composition. In fact the efficient Mg-containing phosphors were made by firing compositions falling within these favorable triangles.

Activation with Ti.—Of the binary and ternary germanates only $Ca_2Ge_2O_6$ gave an efficient emission with Ti. The spectral distribution with 2537Å excitation is given in Fig. 4 which shows that the emission of the $Ca_2Ge_2O_6$-Ti closely corresponds to that of blue-emitting, Sb-activated calcium halophosphate (Cl/F = 1). The quantum efficiency of the germanate phosphor is the same as that of the halophosphate or slightly better. The activator was added from a solution of $TiCl_4$ in a mixture of alcohol and water. The intensity of the emission does not vary much between 0.05 and 0.5 mole % of Ti, a concentration of about 0.1 mole % being the optimum. In the preparation of the phosphor a slight excess of GeO_2 was taken, because the occurrence of small amounts of the 2-1 germanate (cf. Fig. 1), which also gives a fairly strong emission, is less harmful than the occurrence of the 1-1 compound which does not give an appreciable emission with Ti. The phosphor was made in one single firing at 1150°C for 1 hr. The $Ca_2Ge_2O_6$-Ti is not efficiently excited by cath-

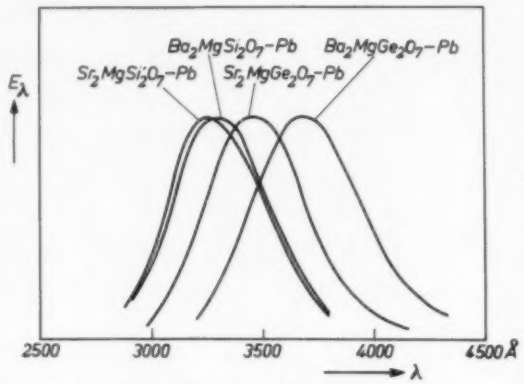

Fig. 2. Spectral distribution curves of Pb-activated 2-1-2-BaMg- and SrMg- germanates and silicates. Excitation with 2537Å at room temperature.

Table V. X-ray data of the 3-1-2 germanates

Indices	$Sr_3MgGe_2O_8$		$Ba_3MgGe_2O_8$	
hkl	d (Å)	I	d (Å)	I
111	4.00	22	4.15	36
002	3.50	15	—	—
012	3.25	15	—	—
102	3.02	25	3.10	18
112, 022	2.86	85	2.98	80
130	2.80	100	2.88	100
040	2.48	15	—	—
013	2.35	18	2.46	12
221	2.29	20	2.35	20
222	2.00	45	2.06	40
310			1.86	20
241			1.82	8
	1.685	9	1.73	12
	1.62	27	1.67	35
	1.605	28	1.655	30
			1.55	6
			1.48	12
			1.43	16
	1.39	15	1.41	12
			1.37	10
			1.35	10
			1.31	16

Table VI. X-ray data of the 1-1-2 germanates

$CaMgGe_2O_6$		$CaZnGe_2O_6$		$SrMgGe_2O_6$		$SrZnGe_2O_6$		$BaMgGe_2O_6$	
d (Å)	I	d (Å)	I	d (Å)	I	d (Å)	I	d (Å)	I
4.90	24	4.90	4	—	—	3.60	25	3.65	8
—	—	4.50	13	4.65	4	3.20	100	3.35	100
3.43	45	3.40	12	3.50	17	2.91	75	3.03	75
3.30	16	3.30	7	3.40	30	2.84	15	2.96	25
3.06	100	3.06	100	3.12	100	2.70	30	2.79	37
3.00	25	3.00	21	3.02	60	2.47	30	2.66	23
2.63	47	2.63	60	2.68	30	2.37	15	2.46	12
2.60	60	2.60	80	2.65	95	1.97	20	2.04	20
2.44	5	2.43	5	2.47	15	1.85	80	1.91	30
2.40	12	2.40	3	2.42	20	1.74	18	1.80	18
2.30	7	2.30	6	2.32	10	1.56	25	1.60	27
2.25	6	2.25	5	2.26	8	1.49	10	1.53	10
2.08	10	2.08	13	2.13	28				
2.06	15	2.06	6	2.10	12				
2.01	6	—	—	—	—				
1.91	8	1.91	3	1.92	10				
1.77	7	1.77	4	1.79	6				
1.71	10	1.70	7	1.73	10				
1.67	18	1.67	13	1.69	20				
1.585	5	1.58	10	1.615	10				
1.575	6	1.57	5	1.60	18				
1.545	7	1.54	5	1.58	13				
1.47	8	1.47	6	1.49	10				
1.44	7	1.44	6	1.465	17				
1.43	7	1.43	7	1.45	6				
1.375	8	1.38	8	1.39	12				
1.33	5	1.33	5	1.34	12				

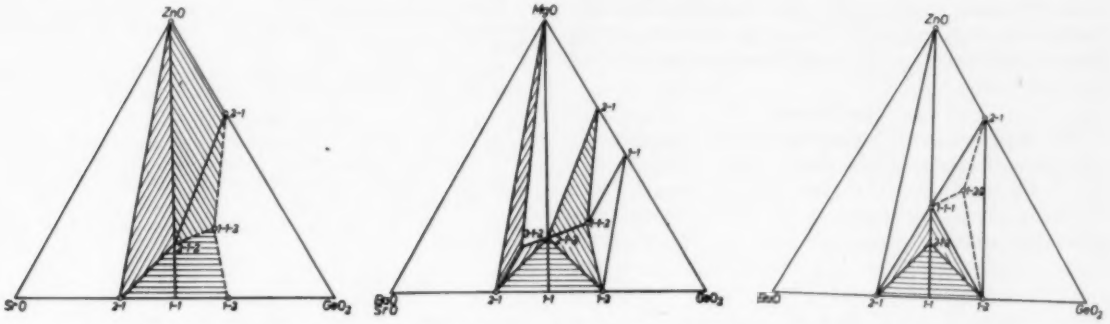

Fig. 3. Part of the phase diagram around the 2-1-2 compounds. Shaded parts contain one or more phases with an inefficient u.v. absorption given by circles at the apexes.

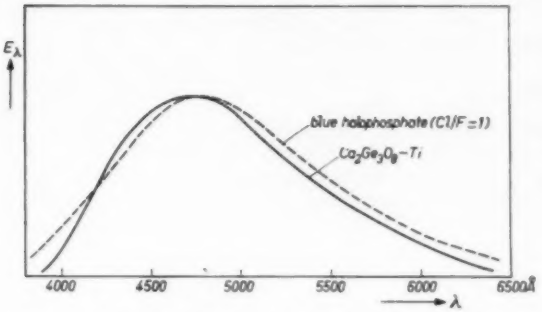

Fig. 4. Spectral distribution curve of the fluorescence in $Ca_2Ge_2O_8$-Ti with 2537Å excitation at room temperature.

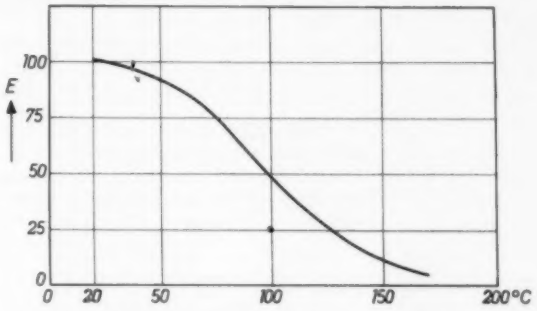

Fig. 5. Temperature dependence of the Ti-emission in $Ca_2Ge_2O_8$-Ti. Excitation 2537Å.

Table VII. X-ray data of the 1-1-1 and 1-2-2 germanates

$CaMgGeO_4$		$BaZnGeO_4$		$BaZn_2Ge_2O_7$	
d(Å)	I	d(Å)	I	d(Å)	I
5.61	25	4.75	15	3.30	100
4.55	25	4.15	30	3.23	75
4.25	70	3.21	100	3.06	75
3.95	25	3.12	20	2.94	18
3.75	25	2.68	85	2.56	45
3.23	30	2.49	40	2.48	15
3.05	20	2.06	45	2.33	33
2.73	100	1.99	20	2.16	21
2.64	70	1.82	10	1.98	21
2.58	30	1.71	40	1.80	9
2.43	15	1.65	20	1.70	10
2.28	20	1.63	60	1.64	6
2.07	5	1.60	5	1.60	25
1.86	20	1.55	15	1.535	6
1.78	15	1.51	5	1.425	8
1.73	25	1.40	10	1.41	6
1.69	10	1.37	15	1.31	12
1.61	30	1.34	10		
1.59	15	1.29	10		
1.52	10				
1.42	10				

Table VIII. Cell dimensions of the tetragonal 2-1-2 germanates

	a(Å)	b(Å)
$Ca_2ZnGe_2O_7$	7.94	5.16
$Sr_2MgGe_2O_7$	8.18	5.28
$Sr_2ZnGe_2O_7$	8.13	5.27
$Ba_2MgGe_2O_7$	8.40	5.46
$Ba_2ZnGe_2O_7$	8.40	5.46

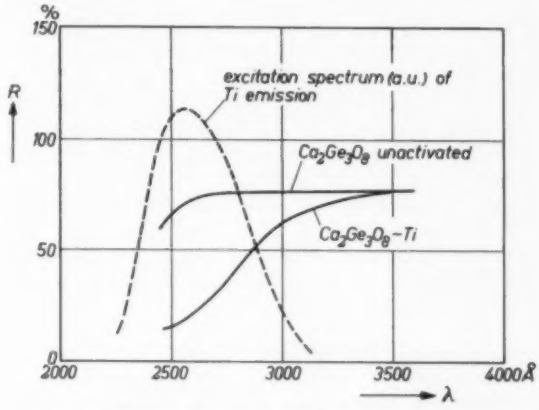

Fig. 6. Reflection spectra (solid lines) of unactivated and Ti-activated $Ca_2Ge_2O_8$ at room temperature. Excitation spectrum (dashed curve, arbitrary units) of $Ca_2Ge_2O_8$-Ti at room temperature.

ode rays or long-wave u.v. In samples activated with Ti and Mn no sensitization of a Mn emission by the Ti was found. The temperature dependence of the Ti emission is shown in Fig. 5. The reflection spectrum of the unactivated and activated phosphor together with the excitation spectrum of the Ti emission are given in Fig. 6.

Activation with Mn.—Of the other activators tried in the binary and ternary germanates, e.g., Mn, Sn, Ce, Bi, and Re, only Mn gave a noticeable emission in $Ca_2Ge_2O_8$ with cathode-ray excitation. The peak of the emission is in the orange-yellow region; the en-

ergy efficiency is about 2%. The optimum Mn concentration is about 0.8 mole %. In order to obtain proper incorporation of the Mn the phosphors had to be fired in N_2.

Conclusions

The fluorescence of binary and ternary germanates of group II elements has been investigated. $Sr_2MgGe_2O_7$-Pb and $Ba_2MgGe_2O_7$-Pb proved to be good u.v. emitting phosphors. $Ca_2Ge_2O_6$-Ti was found to be a good blue emitting phosphor.

Manuscript received Jan. 28, 1959. This paper was prepared for delivery before the Philadelphia Meeting, May 3-7, 1959.

Any discussion of this paper will appear in a Discussion Section to be published in the June 1960 JOURNAL.

REFERENCES

1. H. W. Leverenz, "An Introduction to Luminescence of Solids," John Wiley & Sons, New York (1950).
2. H. A. Klasens, A. H. Hoekstra, and A. P. M. Cox, *This Journal*, **104**, 93 (1957).
3. W. L. W. Ludekens, *J. Inorg. Nucl. Chem.*, **3**, 281 (1956).

Thermoluminescence and Shallow Traps In ZnS:Cu:Co

B. Goldstein[1] and J. J. Dropkin

Polytechnic Institute of Brooklyn, Brooklyn, New York

ABSTRACT

Trapping states of the hexagonal ZnS:Cu 10^{-4}:Co 10^{-6} phosphor were investigated by thermoluminescence as functions of the time and temperature of ultraviolet (u.v.) excitation and of the time and temperature of spontaneous or *IR* induced decay. The main copper (chloride) and cobalt peaks are complex, and retrapping takes place in both.

In connection with some work on photoconductivity, quenching, and stimulation of the ZnS:Cu-10^{-4} mole %:Co 10^{-6} mole % phosphor, we found it advisable to investigate the shallow trap structure and used thermoluminescence as one of the methods(1-4). This paper reports the results of the glow curve work on the nature of the shallow trap distribution. Some estimate of the trap energies is obtained from the initial slope of the glow curves (4). The presence of retrapping was shown by temperature recycling experiments(3). Some of the properties of the *IR* sensitivity of the traps were studied. A measure of the complexity of the trap distribution was obtained by varying the time and temperature of excitation as well as by introducing a delay time for decay of the trap population before running the glow curves.

Experimental Details

The apparatus used in our glow curve work is illustrated in Fig. 1. This was a metal-glass Dewar with a thin layer of the phosphor powder mounted in the vacuum in contact with a brass block which was cooled or heated by liquid nitrogen or a nichrome heater. The heating rate was 3.6°C/min.

The Dewar was so situated that the phosphor and a photomultiplier were located at conjugate foci of a spherical mirror. The phosphor was excited by 3650A u.v. radiation or stimulated by *IR* from a monochromator through a hole in the mirror. The luminescence reaching the photomultiplier first was filtered so that only the characteristic green Cu emission was measured.

The phosphors used were prepared by firing at 1100°C with NaCl flux in an atmosphere of H_2S to eliminate the effect of oxygen on the trap structure (4).

[1] Present address: Radio Corp. of America, Princeton, N. J.

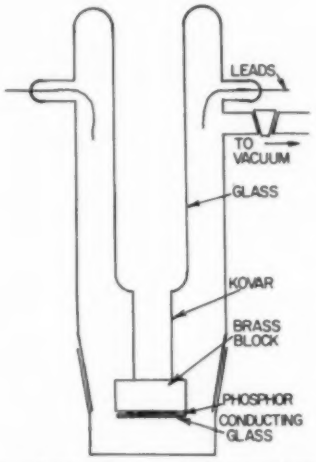

Fig. 1. Thermoluminescence and photoconductivity Dewar

Results

Effect of time and temperature of excitation.—Figure 2 shows some typical glow curves taken under saturation conditions of excitation for excitation at −178° and at −60°C. Curve A is the glow curve after 30-min excitation and 13 min of decay at −178°C. The low-temperature peak, attributable to copper (3) or to chloride (4),[2] is at −123°C and seems simple as in Hoogenstraaten's work (4). The high-temperature peak, attributable to Co (5), is at +60°C and shows some structure. The activation energies derived from the initial rising portions of these peaks under the assumption either of trap saturation or of no retrapping are 0.16 ev and 0.20 ev, respectively. With the phosphor excited at −60°C, cooled to −178°C, and then warmed, curve

[2] In what follows, we will refer to the lower temperature glow peak found in ZnS:Cu (NaCl flux) as the Cu peak.

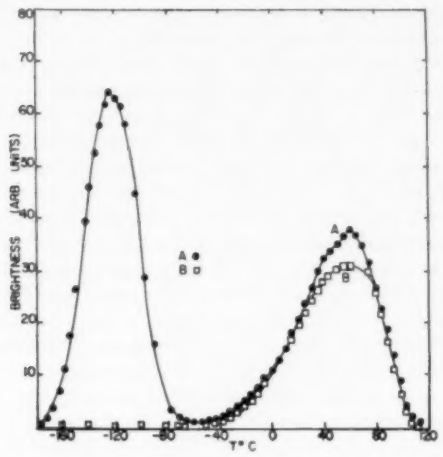

Fig. 2. ZnS:Cu:Co glow curves. A, Excitation: —178°C for 30 min, decay of 13 min at —178°C before glow curve run; B, excitation: —60°C for 30 min, cooled to —178°C before glow curve run.

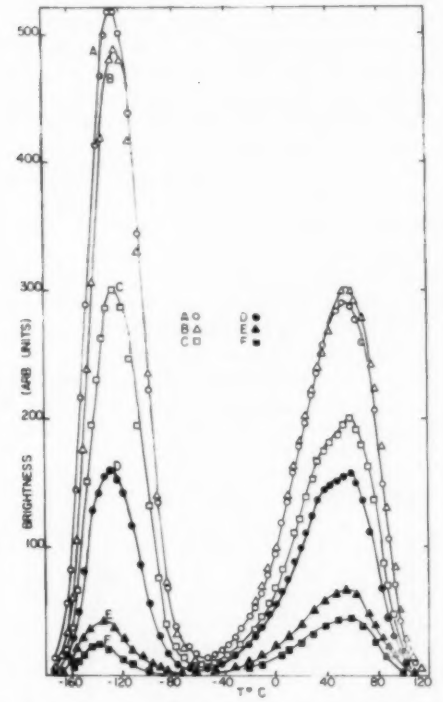

Fig. 3. Effect of time of excitation on ZnS:Cu:Co glow curves: A, 60 min; B, 5 min; C, 1 min; D, 10 sec; E, 5 sec; F, 2 sec (all at —178°C).

B is obtained. The first peak has disappeared, and now with no interference from the trailing edge of the lower temperature peak, the rising portion of the Co peak gives an activation energy of 0.38 ev.

When we studied how this trap or group of traps fills under excitation and empties under decay or *IR* stimulation, the simple structure apparent in the smooth shape of the Cu peak turned out to be nonexistent.

We investigated first the trap filling process by exciting the phosphor at —178°C for various lengths of time from 2 sec to 60 min. The results are given in Fig. 3. Saturation is seen to occur in approximately 5 min. We note that, as the excitation time was reduced, the Cu peak shifted to lower temperatures and the ratio of the Cu peak area to the Co peak area decreased.

The latter point seems to indicate either that the Co trap has a larger cross section for u.v. excited electrons than the Cu trap or that Co traps retrap electrons released from Cu traps. The former suggests that the Cu glow peak is due to a trap distribution rather than a single trap. A single trap which did not retrap liberated electrons would produce an unchanged glow peak. A single trap which did retrap liberated electrons would have a *higher* temperature glow peak when only partly filled than when completely filled. Activation energies obtained from the initial portions of the respective glow curves vary from 0.11 ev for 2-sec excitation to 0.16 ev for saturation.

The Co peak does not shift with excitation time. Activation energies obtained from the leading edge do vary from 0.21 ev for saturation to 0.23 ev for 2-sec excitation, but the effect of the trailing edge of the Cu peak could not be eliminated in any of these cases.

In order to study the trap distribution of the Cu peak by another means, the phosphor was excited at successively higher temperatures and then cooled to —178°C before warming. Figure 4 shows the glow curves obtained with excitation at —178°, —140°, —120°, and —100°C before running the glow curves from —178°C. These glow peak temperature shifts could be consistent with the behavior of a partly filled set of traps all of the same energy if they could retrap released electrons. However, in view of the previous results these

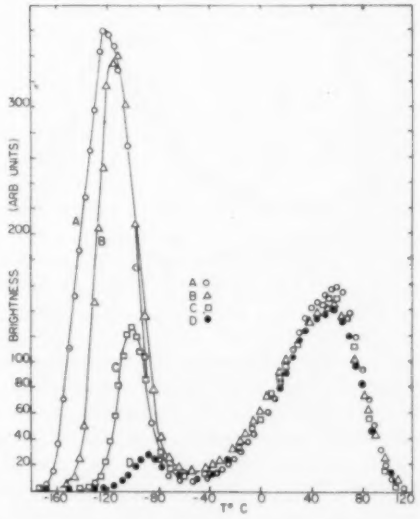

Fig. 4. Effect of temperature of excitation on ZnS:Cu:Co glow curves. Temperature of excitation for: A, —178°C; B, —140°C; C, —120°C; D, —100°C (all glow curves run from —178°C).

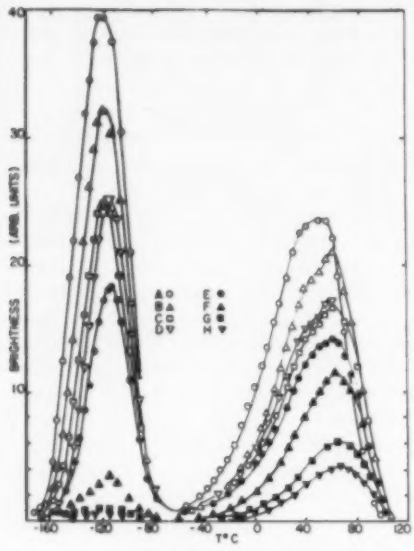

Fig. 5. Effect of infrared radiation on ZnS:Cu:Co glow curves. Wave length of IR for: A, No IR; B, 1.6μ; C, 1.4μ; D, 1.2 μ; E, 1.0 μ; F, 0.9 μ; G, 0.8 μ; H, 0.7 μ.

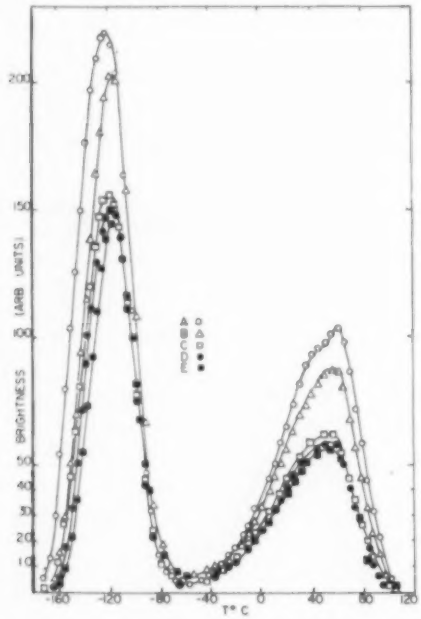

Fig. 6. Effect of decay time on ZnS:Cu:Co glow curves. Decay time at −178°C for: A, 11 min; B, 21 min; C, 36 min; D, 64 min; E, 122 min.

curves are better interpreted by the presence of a distribution of traps of different energy. The effect of higher temperatures of excitation is to leave occupied only those deeper traps of the distribution which are relatively more stable at the higher temperatures. The Co peak is unchanged throughout.

Effect of infrared radiation.—The wave-length dependence of the effect of *IR* on the thermoluminescence curves was studied by exciting the phosphor to saturation with u.v. for 30 min at −178°C and then irradiating the phosphor for 5 min with *IR* of a particular wave length at −178°C prior to running the glow curve. This was repeated for a number of *IR* wave lengths, keeping the incident *IR* intensity constant. Results are shown in Fig. 5. These curves seem to indicate that electrons trapped in either the Cu or the Co traps may absorb *IR*. All we observe, however, is the decrease of luminescence. The actual emptying of either or both traps may be an absorption of *IR* by the electron or alternatively may be part of an indirect process (such as one involving the luminescent center).

Effect of time of decay.—In the thermoluminescence obtained by allowing the phosphor to stand for a time after excitation before running the glow curves, we observed an interesting anomaly which also may indicate that both traps are linked to the luminescent center. Figure 6 shows the glow curves obtained by allowing the phosphor to decay for successively longer times at −178°C after excitation for 30 min at −178°C. The Cu peak temperature shifts slightly from −123°C after 11 min decay to −119°C after 21 min decay, and remains unchanged thereafter, except for a decrease in area for all longer decay times. There is little change in area from 36-min decay time to 120-min decay time. What is unusual, however, is that, although the decay takes place at −178°C, the Co peak, which should be stable, decreases in area also. In fact, the ratio of Cu peak area to Co peak area remains constant to within 2% over the entire decay time interval. This ratio was also found to be constant for these same decay times after excitation of 1 min, i.e., below saturation. This effect is not consistent with the removal of electrons from traps, but more likely with the filling of ionized luminescent centers by electronic transitions to these centers.

Effect of CdS.—We repeated the work of Hoogenstraaten (4) and found that both glow peaks shifted linearly to lower temperatures as CdS was added.

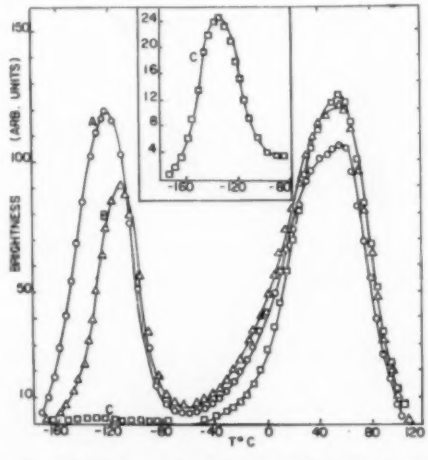

Fig. 7. Retrapping of electrons released by infrared. ZnS:Cu:Co glow curves: A, u.v. 1 min at −178°C, no IR; B, u.v. 1 min at −178°C, IR 1 min at −178°C; C, u.v. 1 min at −60°C, IR 1 min at −178°C. Insert: Portion of curve C replotted with enlarged scale.

In addition, the emission during thermal glow shifted to longer wave lengths with increased CdS content.

Retrapping.—After exciting at −60°C so that the Cu traps were empty (see Fig. 2), and for only 1 min so that the Co traps were only partially filled (see Fig. 3), the phosphor was cooled to −178°C and then irradiated with intense 1.2-μ radiation.[8] Results shown in Fig. 7 indicate that retrapping can occur in either the Cu or the Co trap. The insert shows the retrapping in the Cu peak on a larger scale. A comparison of curve A with curve B shows that retrapping occurs in the Co traps as well. It should be noted that this increase in the Co peak by retrapping of electrons released from the 1.2-μ deep trap occurs over and above the *IR* sensitivity of the Co traps shown in Fig. 5.

Summary

The shallow trap structure of ZnS:Cu 10^{-4}:Co 10^{-4} which produces thermoluminescence consists of two different groups of traps, one associated with copper or chloride, the other with cobalt. Each of these is capable of retrapping electrons that are released. The copper traps have a distribution of energy levels.

[8] In connection with photoconduction studies, we have found a 1.2-μ sensitive storage center in ZnS:Cu:Co. (See final report N6onr 26313, "Photoconduction in Phosphors.")

Acknowledgment

The authors wish to thank Professor E. Banks and his assistant, A. Ferretti, of the Chemistry Department of the Polytechnic Institute of Brooklyn, for the preparation of the samples used in this work.

Manuscript received Jan. 19, 1959. This paper was prepared for delivery at the Chicago Meeting, May 2-6, 1954, and is part of the Ph.D. dissertation of one of the authors (B. G.). Work on this paper was supported by the Office of Naval Research Contract N6onr 26313.

Any discussion of this paper will appear in a Discussion Section to be published in the June 1960 JOURNAL.

REFERENCES

1. F. Urbach, *Sitz. Ber. Akad. Wiss., Wien, Math. Naturw. Klasse*, **139**, 353 (1930).
2. J. T. Randall and M. H. F. Wilkins, *Proc. Roy. Soc., London*, **A184**, 366 (1945).
3. G. F. J. Garlick and D. E. Mason, *J. (and Trans.) Electrochem. Soc.*, **96**, 90 (1949).
4. W. Hoogenstraaten, Electron Traps in Zinc-Sulfide Phosphors, Thesis of Univ. of Amsterdam (1958).
5. E. S. Krylova, *Doklady Akad. Nauk S.S.S.R.*, **64**, 495 (1949).

Arrays of Inorganic Semiconducting Compounds

A. J. Cornish

Research Laboratories, Westinghouse Electric Corporation, Pittsburgh, Pennsylvania

ABSTRACT

Arrays of compounds related to the periodic chart of the elements can be prepared. These arrays aid in estimating the physical and chemical properties of compounds, including semiconducting properties. Many compounds included in the arrays may not exist; however, if the compound does exist, the value of its melting point, energy gap, and electron mobility generally fit into a uniform pattern related to adjacent compounds. The crystal structure of semiconducting compounds is shown to be of only second-order importance. Grouping semiconducting compounds by crystal types loses the over-all relations that exist between many compounds.

Braun (1) observed the rectifying action of metallic sulfides, and since then many attempts have been made to relate the phenomena of semiconductivity to chemical bonds and structure for the purpose of discovery of new semiconducting compounds. In 1925 Wherry (2), using a copper cat's whisker, a simple crystal set, and a mineral collection, found 75 minerals capable of being used as radio detectors. Since 1925 numerous tables of inorganic semiconducting compounds have been published (3-5); however, the number of compounds has not increased materially. Winkler's (3) list published in 1955 contains slightly under 100 inorganic semiconducting compounds. The reason for the lack of greatly expanded tables of semiconducting compounds is not because workers in the field are unaware of the large number that exist, but rather the lack of experimental work confirming the existence of a large number of suspected semiconducting compounds.

The recent expansion of semiconductor materials into the infrared detector, thermoelectric device, and other fields of application has led to a new interest in expanding the list of available compounds. Such an expansion involves the selection of compounds likely to be semiconductors, the careful preparation, and the measurement of properties of these compounds. Arrays of compounds, related to the periodic chart of the elements, serve a very useful purpose in the selection, preparation, and estimation of properties of semiconducting compounds. With these arrays, it is possible to estimate melting points, energy gaps, and possibly electron mobilities.

Crystal structure.—The idea that semiconductivity is found in only a few different types of crystal structures has been disproved during the past few years. Table I lists over 35 crystal structures containing inorganic semiconducting compounds. Many more are known to exist. Fischer and Pearson (6) and Mooser and Pearson (7) have shown relation-

Table I. Structures of semiconducting compounds

Structure	System	Semiconducting compounds
B1* (NaCl)	Cub.	PbS, SrS, $AgSbSe_2$, etc.
B3 (ZnS)	Cub.	AlSb, In_2Te_3, $CdZnSe_2$, etc.
B4 (ZnO)	Hex.	ZnO, CdS, ZnS, AgI, etc.
B8 (NiAs)	Hex.	MnTe, FeS, CrSe, etc.
B9 (HgS)	Hex.	HgS
B18 (CuS)	Hex.	CuS, CuSe
B29 (SnS)	Ortho.	GeS, SnS, $PbSnS_2$
B32 (NaTl)	Cub.	Li_2MgSn
B37 (TlSe)	Tet.	TlSe
C1 (CaF_2)	Cub.	Mg_2Pb, $GeLi_2P_2$, LiZnN, etc.
C2 (FeS_2)	Cub.	FeS_2, CoAsS, $MnSe_2$
C3 (Cu_2O)	Cub.	Cu_2O
C4 (TiO_2)	Tet.	TiO_2, SnO_2
C6 (CdI_2)	Hex.	SnS_2
C13 (HgI_2)	Tet.	HgI_2
C18 (FeS_2)	Ortho.	$FeAs_2$, $CoAs_2$, $NiAs_2$
C33 (Bi_2Te_3)	Rhomb.	Bi_2Te_3, Bi_2Te_2S, Sb_2Te_3
D0$_3$ (BiF_3)	Cub.	Li_3Bi
D0$_{21}$ (Cu_3P)	Hex.	Cu_3As
D5$_1$ (Al_2O_3)	Rhomb.	Fe_2O_3
D5$_2$ (La_2O_3)	Hex.	Mg_3Sb_2, Mg_3Bi_2
D5$_3$ (αMn_2O_3)	Cub.	Mg_3As_2
D5$_9$ (Zn_3P_2)	Tet.	Zn_3P_2, Cd_3As_2
E0$_1$ (FeAsS)	Mon.	FeAsS, FeSbS
E1$_1$ ($CuFeS_2$)	Tet.	AgInTe$_2$, $ZnGeP_2$, etc.
E3$_1$ (Ag_2HgI_4)	Tet.	Cu_2HgI_4, $HgIn_2Te_4$, etc.
E3$_3$ ($FeSb_2S_4$)	Ortho.	$FeSb_2S_4$
F5$_3$ ($CuSbS_2$)	Ortho.	CuSbS$_2$, $PbSb_2S_4$, etc.
H1$_1$ ($MgAl_2O_4$)	Cub.	Fe_3O_4, $HgIn_2S_4$
H2$_4$ (Cu_3VS_4)	Cub.	Cu_3VS_4
H2$_5$ (Cu_3AsS_4)	Ortho.	Cu_3AsS_4, Cu_3SbS_4
H2$_6$ (Cu_2FeSnS_4)	Tet.	Cu_2FeSnS_4

* "Strukturbericht" symbols.

ships between many of the different structures. It now appears that semiconductivity could be found in any crystal structure except the close-packed, high coordination number structures. In the latter structures, the large number and nearness of neighboring atoms generally insures an overlapping of the bands and therefore metallic characteristics.

Too much emphasis has been placed on the relationship between semiconductivity and crystal structure. The crystal structure which a compound assumes is a minimum energy orientation of atoms in space satisfying a particular bond scheme. The bond scheme is determined by the distribution of electrons between atoms in the compound; this same distribution determines the position of the valence and the conduction band. Although it is true that certain crystal structures commonly exhibit semiconductivity, the more basic property is the nature of the bonds. As the bonds change in a series of compounds, different crystal structures become preferred. In some examples an increase or decrease in ionic contribution to the bond changes the structure; in other examples radius ratio rules forbid certain orientations. However, in a chemically related series of compounds, even these structural changes form a more or less continuous spectrum, the crystal structures of adjacent compounds being the same as, or related to, the crystal structure of its neighbors. Thus listing and discussing semiconductors by crystal structure types hides the over-all relationships of properties that exist between structure types.

Melting points.—Attempts have been made to correlate the melting points of semiconducting compounds with bond strength and energy gap. Considerable caution should be taken in such work. The melting point of a compound may or may not be related to the strength of the bonds providing semiconducting properties. When germanium melts, covalent bonds are broken and the liquid becomes a denser metallic material. In tin, metallic properties appear following a solid-state phase change. The melting point is a transition from a metallic solid to a metallic liquid. Weak van-der Waal bonds are broken at the melting point of selenium; the covalent bonds giving rise to semiconductivity exist at temperatures well above the melting point. Compounds frequently behave like tin or selenium. The occurrence of phase changes and low melting points greatly reduce the number of usable semiconducting compounds. For chemically related compounds we expect melting points to decrease as the molecular weight increases. When this trend is reversed we look for a complicated bond structure.

Energy gaps.—At the present time it is not possible to predict satisfactorily the energy gap of a compound chosen at random. For related compounds, however, Pauling and Goodman have provided us with a means of understanding many of the measured values. Pauling (8) proposed that bond energies were inversely proportional to the equilibrium interatomic distance for the Group IVB elements C, Si, Ge, and αSn as well as groups using covalent bonds other than sp^3.

Goodman (9), in a speculative paper, assumed that the bond energy was proportional to energy gap. He also assumed the measured energy gap was the sum of two terms: a covalent contribution which is a function of the interatomic distance, and an ionic contribution which is a function of the electronegativity differences. The Group IVB elements, having no ionic contribution, gave values of the "covalent" energy gap as a function of interatomic distance. Values of the second term can be obtained for Group III-V compounds knowing the interatomic distance and the measured energy gap. Goodman was then able to show that an increase in the ionic contribution to the energy gap was proportional to an increase in the ionicity. When a series of chemically related compounds are compared the energy gap increases when: (*a*) the compounds become more ionic or less metallic, (*b*) the covalent bond length decreases, (*c*) the molecular weight decreases.

Electron mobilities.—The experimental values of electron mobilities are so sensitive to crystal perfection that it is difficult to put much faith in the present values. They appear to increase with increasing molecular weight and reach a maximum value in compounds possessing a small ionic component to the binding.

Periodic Arrays of Compounds

Knowing only the general trends of the melting points, energy gaps, and electron mobilities as the molecular weights, ionicities, and bond lengths change, we should look for some method of tabulat-

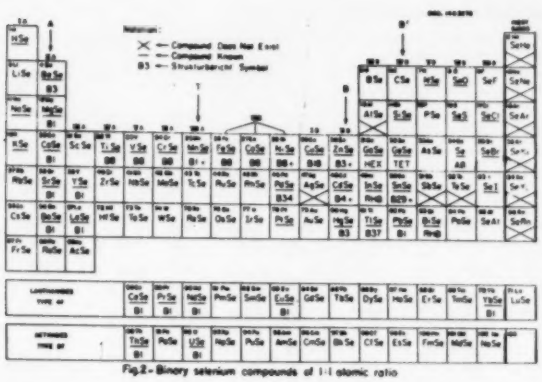

Fig. 1. Binary selenium compounds of 1:1 atomic ratio

ing or arranging compounds in order to make maximum use of this knowledge. The periodic chart of the elements is such an arrangement for the elements. Similar charts can be constructed for compounds. One such chart, a periodic chart of binary selenium compounds of 1:1 atomic ratio is shown in Fig. 1. The complete chart illustrates the principles involved but does not conveniently permit the listing of physical properties. Reduced charts or arrays of compounds including crystal structures, melting points, energy gaps, and electron mobilities will be used to discuss semiconducting compounds. Obviously many charts similar to Fig. 1 may be drawn considering that there are 102 elements and a large number of common stoichiometric ratios. The number of possible arrays increase rapidly when ternary and higher component systems are considered.

Figure 1 is similar to the elemental periodic chart in many ways. Cations occupy their normal positions as in the periodic chart of elements. The number of electrons increases as it does for the elements, and electronegativity differences between positions in the table are the same as for the elements. Definite trends in properties should and do exist as adjacent compounds in the same group (column) or period (row) are compared. These trends are more uniform in an array of binary compounds, such as Fig. 1, than in the periodic chart of elements. The common element, selenium, in this chart tends to moderate the effect of a change in the cation. In higher component systems where more than one atom is constant throughout the table this moderating effect is even more pronounced.

The compounds underlined in Fig. 1 are known to exist. Many not underlined probably exist, but sufficient work has not been done to establish the compound. When the phase diagram is known and a compound of 1:1 atomic ratio does not occur an x is placed in the appropriate square.

Relationships between crystal structures of adjacent compounds can be shown. In the alkaline earth column (IIA) the B1 (NaCl) structure occurs except for BeSe where the radius ratio forces a lower coordination number structure. The hexagonal B8 (NiAs) structure taken by many transition metals acts as a bridge structure, adjusting its c/a ratio in such a manner that it forms an almost continuous transition between adjacent compounds. Many compounds lying close to the tetrahedrally bonded B3 and B4 structures have related structures such as the B37 (TlSe) and B18 (CuSe). Similar relations exist between other physical properties which depend primarily on the bond between the cation and nearest selenium atoms.

Since selenium requires two electrons to fill its outer shell, selenium compounds are most stable when the element forming the cation can, by losing or sharing two electrons, form a stable kernel. This occurs whenever the element possesses two electrons above a stable electron configuration such as a filled or half-filled shell. Most semiconductors are compounds which obey this rule of stability and can conveniently be written as normal ionic compounds. A few important exceptions do exist, e.g., CuSe and BiSe. These would be missed if we limited ourselves to the abbreviated arrays that follow. They do appear on a periodic chart of compounds of the type shown in Fig. 1.

Columns A, T, B, and B′ in Fig. 1 indicate some of the places where this maximum stability occurs. Elements in Column A can lose 2 electrons and leave a stable filled p-shell (an s-shell in the case of Be). These elements form compounds which are largely ionic as their outer electrons are easily lost. Elements in Column T are transition metals. They are able to lose two electrons and have remaining a stable half-filled d-shell. Column B contains the usual B Group elements which tend to share two electrons leaving a filled d-shell, the two shared electrons being s-electrons. The B′ column elements are capable of losing two electrons leaving filled s- and d-shells. Many elements in other columns show a valence of two, but only those in columns designated A, T, B, and B′ are discussed in this paper.

The arrays that follow are, therefore, portions of periodic charts of compounds. The other anions in each anion group are included in such a manner that maximum use can be made of the relations that exist between chemically similar compounds.

It is obvious from Fig. 1 that, if we were forming compounds with a Group VB anion (N, P, As, Sb, or Bi) which require three electrons to fill their outer shells, the column marked A, T, B, and B′ would move one space to the right. In like manner, columns of other valence can be designated.

Table II shows an array of Group II-VI compounds with melting points, crystal structures, energy gaps, and electron mobilities taken from the literature. Compounds of beryllium, radium, and carbon have been omitted since they are not at present of great interest as semiconductors. Using the general relations discussed in the previous section, estimates can be made to fill in many of the missing experimental values. In the A column we generally expect the melting points to decrease with increasing molecular weight thus mp MgO > mp MgS > mp MgSe > mp MgTe and mp MgO > mp CaO > mp SrO > mp BaO. Similar series should

Table II. Properties of group II VI compounds

A					T					B					B'				
Comp.	mp, °C	Str.	ΔEg, ev	$\frac{\mu_e, cm^2}{v. sec}$	Comp.	mp, °C	Str.	ΔEg, ev	$\frac{\mu_e, cm^2}{v. sec}$	Comp.	mp, °C	Str.	ΔEg, ev	$\frac{\mu_e, cm^2}{v. sec}$	Comp.	mp, °C	Str.	ΔEg, ev	$\frac{\mu_e, cm^2}{v. sec}$
MgO	2800	B1	6												SiO				
MgS		B1													SiS		?		
MgSe		B1													SiSe		?		
MgTe		B4													SiTe		Cub.		
CaO	2572	B1			MnO	1650	Cub.	0.5		ZnO	1975	B4	3.4	1000	GeO	700			
CaS		B1			MnS	1580	B3+			ZnS	1850	B3+	3.6	100	GeS	530	B16	1.8	
CaSe		B1			MnSe		B1	0.1		ZnSe		B3	2.58	~100	GeSe	680	Tet.		
CaTe		B1			MnTe	1175	B8			ZnTe	1238	B3	2.2		GeTe	725	B1+		
SrO	2430	B1			TcO					CdO		B1		120	SnO		B10		
SrS		B1	4.1		TcS					CdS	1750	B3	2.42	210	SnS	882	B29		
SrSe		B1			TcSe					CdSe	>1350	B3	1.74	700	SnSe	860	B29		
SrTe		B1			TcTe					CdTe	1041	B3	1.4	300	SnTe	790	B1		
BaO	1923	B1	4.20		ReO					HgO		RHB			PbO	888	B11+		
BaS		B1	3.6		ReS					HgS	583	B3+		700	PbS	1114	B1	0.34	800
BaSe		B1			ReSe					HgSe	690	B3	0.16	15,000	PbSe	1088	B1	0.25	1200
BaTe		B1			ReTe					HgTe	650	B3	0.1	25,000	PbTe	905	B1	0.22	2100

exist for the T column. Occasionally in the B column and more frequently in the B′ column we find deviations from this general rule. These deviations are attributed to a more complicated bonding picture than simple cation-anion interaction. The B′ group elements, and to some extent, the B group elements are capable of forming covalent bonds between themselves. This means a competition between bonding types exist in the solid. Many of these compounds melt to give covalent liquids. Their melting points are irregular.

Energy gaps follow the general rules already discussed. The gaps in the A group of Table II are too large to be classed as semiconductors; they are ionic insulators. The decrease in energy gaps with increasing molecular weights leads to predictions such as 6 ev > Eg (CaO) > Eg (SrO) > 4.2 ev, and 3.6 ev > Eg (BaSe) > Eg (BaTe). In the T group the gap of MnO of about 0.5 ev indicates that all the other compounds that exist in that group will have a gap of less than 0.5 ev. In fact it might indicate the ReSe and ReTe, if they exist as compounds, could be metallic. In the B group, the gaps are quite regular with the exception that ΔEg (ZnO) < ΔEg(ZnS). This inversion of the general rule could possibly be the 2nd order effect of crystal structure. In the B group the measured gap of 1.8 ev for GeS indicates that 1.8 ev > Eg GeSe > Eg GeTe and also 1.8 ev > Eg SnS > 0.34 ev.

Mobilities of compounds in Table II follow the rules except for the high value of ZnO and the low value of CdTe. It should be pointed out again that electron mobilities are so dependent on crystal perfection that all measured values are open to question. The large mobilities of HgSe and HgTe confirm the statement that maximum mobilities occur with slight ionicity.

Table III shows an array of Group III_2VI_3 compounds; boron and nitrogen compounds have been omitted. The trends in melting points and energy gaps are similar to those for the Group II-VI compounds. The value of 2.3 ev for the energy gap of Fe_2O_3 and 2.5 ev for Al_2O_3 indicates that the remaining compounds in both groups will have energy gaps below 2.3 and 2.5 ev, respectively. The energy gap of As_2Se_3 should be above 1.2 ev, the value for Sb_2Se_3, and below 2.2 ev, the value for As_2Se_3. It is expected that higher mobilities will be found, especially in the lower portion of the B group of compounds.

Ternary compounds and higher component systems require elaborate arrays if all possibilities are to be included. Figure 2 shows the possible substitutions that can be made to form compounds of the type I III VI_2. All possibilities do not exist, however many of the compounds do occur. In a single array, the effect of having more than one atom in

Table III. Properties of group III_2 VI_3 compounds

A					T					B					B'				
Comp.	mp, °C	Str.	ΔEg, ev	$\frac{\mu_e, cm^2}{v. sec}$	Comp.	mp, °C	Str.	ΔEg, ev	$\frac{\mu_e, cm^2}{v. sec}$	Comp.	mp, °C	Str.	ΔEg, ev	$\frac{\mu_e, cm^2}{v. sec}$	Comp.	mp, °C	Str.	ΔEg, ev	$\frac{\mu_e, cm^2}{v. sec}$
										Al_2O_3	2050	$D5_1$+	2.5		P_2O_3	23.8	Mon.		
										Al_2S_3	1100	Hex.			P_2S_3	290			
										Al_2Se_3	950	B_{4}'			P_2Se_3				
										Al_2Te_3	890				P_2Te_3				
Sc_2O_3		$D5_3$			Fe_2O_3	1565	$D5_1$+	2.3		Ga_2O_3	1740	$D5_1$			As_2O_3	315	Cub.+		
Sc_2S_3		?			Fe_2S_3		?			Ga_2S_3	1255	$B3_1$			As_2S_3	310	Mon.	2.2	
Sc_2Se_3		?[1]			Fe_2Se_3					Ga_2Se_3	1020	~B3			As_2Se_3	307			
Sc_2Te_3		?			Fe_2Te_3	780	B8			Ga_2Te_3	790	~B3			As_2Te_3	360	Mon.	1.0	170
Y_2O_3	2410	$D5_3$			Ru_2O_3		?			In_2O_3	>2000	$D5_3$			Sb_2O_3	652	$D5_{11}$+		
Y_2S_3	1600	Mon.			Ru_2S_3					In_2S_3	1095	$H1_1$+			Sb_2S_3	550	$D5_8$	1.7	
Y_2Se_3	?	?[1]			Ru_2Se_3					In_2Se_3	890	~B3	1.2	30	Sb_2Se_3	575	$D5_8$	1.2	15
Y_2Te_3					Ru_2Te_3					In_2Te_3	667	~B3	1.0		Sb_2Te_3	629	C33	0.3	
La_2O_3	2315	$D5_2$			Os_2O_3	?	?			Tl_2O_3	717	$D5_3$		>100	Bi_2O_3	860	$D5_{12}$+		
La_2S_3	2150	$D7_3$			Os_2S_3					Tl_2S_3	260				Bi_2S_3	745	$D5_8$	1.3	200
La_2Se_3		?[2]			Os_2Se_3					Tl_2Se_3	274				Bi_2Se_3	706	C33	0.35	600
La_2Te_3					Os_2Te_3					Tl_2Te_3	—	—			Bi_2Te_3	573	C33	0.15	800

[1] Isomorphous with Er_2Se_3, Yb_2Se_3.
[2] Isomorphous with Ce_2Se_3, Pr_2Se_3, Nd_2Se_3.

Table IV. Properties of Group I(Cu) III VI_2 compounds

A					T					B					B'				
Comp.	mp, °C	Str.	ΔEg, ev	$\frac{\mu e, cm^2}{v. sec}$	Comp.	mp, °C	Str.	ΔEg, ev	$\frac{\mu e, cm^2}{v. sec}$	Comp.	mp, °C	Str.	ΔEg, ev	$\frac{\mu e, cm^2}{v. sec}$	Comp.	mp, °C	Str.	ΔEg, ev	$\frac{\mu e, cm^2}{v. sec}$
$CuBO_2$															$CuNO_2$				
$CuBS_2$															$CuNS_2$				
$CuBSe_2$															$CuNSe_2$				
$CuBTe_2$															$CuNTe_2$				
$CuAlO_2$															$CuPO_2$				
$CuAlS_2$		El_1	~2.4												$CuPS_2$				
$CuAlSe_2$		El_1													$CuPSe_2$				
$CuAlTe_2$		El_1													$CuPTe_2$				
$CuScO_2$					$CuFeO_2$					$CuGaO_2$					$CuAsO_2$				
$CuScS_2$					$CuFeS_2$	950	El_1	0.53		$CuGaS_2$		El_1			$CuAsS_2$	625	~B3	>1	
$CuScSe_2$					$CuFeSe_2$	800		0.16		$CuGaSe_2$	1040	El_1	1.6		$CuAsSe_2$	415	~B3	>1	
$CuScTe_2$					$CuFeTe_2$	773		0.10		$CuGaTe_2$	840	El_1	1.0		$CuAsTe_2$	360			
$CuYO_2$					$CuRuO_2$					$CuInO_2$					$CuSbO_2$				
$CuYS_2$					$CuRuS_2$					$CuInS_2$		El_1	1.2		$CuSbS_2$	535	$F5_6$	>1	
$CuYSe_2$					$CuRuSe_2$					$CuInSe_2$	990	El_1	1.07	1000	$CuSbSe_2$	460		>1	
$CuYTe_2$					$CuRuTe_2$					$CuInTe_2$	700	El_1	0.95		$CuSbTe_2$	520			
$CuLaO_2$					$CuOsO_2$					$CuTlO_2$					$CuBiO_2$				
$CuLaS_2$					$CuOsS_2$					$CuTlS_2$		El_1			$CuBiS_2$		$F5_6$	0.6	
$CuLaSe_2$					$CuOsSe_2$					$CuTlSe_2$	405	El_1			$CuBiSe_2$	590			
$CuLaTe_2$					$CuOsTe_2$					$CuTlTe_2$	375				$CuBiTe_2$	510			

common moderates the trends in properties to a greater degree than in the binary systems.

Table IV shows an array of Group I III VI_2 compounds in which copper is used as the Group I element. Similar arrays exist for each of the other Group I elements. The few measured properties shown in Table IV confirm in general the trends expected. A similar chart with the Group I element silver instead of copper should have very similar properties with slightly lower melting points, energy gaps, and higher mobilities.

Similar arrays can be drawn up for other stoichiometric ratios of binary, ternary, and higher component systems following a pattern similar to that shown in Fig. 2.

One guide to other possible arrays could be a list of semiconducting compounds similar to Table I. For example Zn_3P_2 suggests II_3V_2, ZnGeP$_2$ suggests II IV V_2 and $HgIn_2Te_4$ suggests II III_2 VI_4. Goodman (10) has outlined a procedure which would aid in the selection of types of compounds which could be expanded into arrays. If the properties of some of the compounds in an array are known, the properties of others can be estimated.

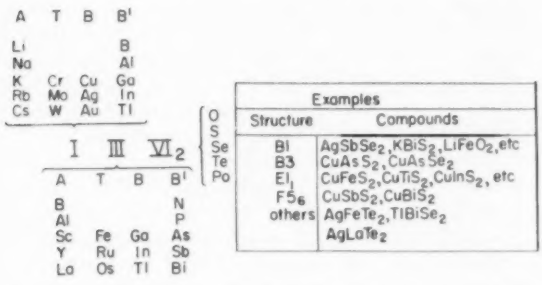

Fig. 2. Possible Group I III VI_2 semiconducting compounds

Acknowledgment

The author is indebted to Dr. R. L. Longini for his encouragement and helpful comments on this work.

Manuscript received Feb. 9, 1959. This paper was prepared for delivery before the Ottawa Meeting, Sept. 28-Oct. 2, 1958.

Any discussion of this paper will appear in a Discussion Section to be published in the June 1960 JOURNAL.

REFERENCES

1. F. Braun, *Pogg. Ann.*, **153**, 556 (1874).
2. E. Wherry, *Amer. Mineral.*, **10**, 28 (1925).
3. U. Winkler, *Helv. Phys. Acta.*, **28**, 633 (1955).
4. E. Mooser and W. B. Pearson, *J. Chem. Phys.*, **26**, 893 (1957)
5. R. L. Sproull, Section 5e, "American Institute of Physics Handbook," McGraw-Hill Book Co., New York (1957).
6. G. Fischer and W. B. Pearson, Compound Semiconductors, Proceedings of the Symposium on the Role of Solid State Phenomena in Electric Circuits, Polytechnic Institute of Brooklyn (1957).
7. E. Mooser and W. B. Pearson, *Phys. Rev.*, **101**, 1608 (1956).
8. L. Pauling, *J. Phys. Chem.*, **58**, 662 (1954).
9. C. H. L. Goodman, *J. Elect.*, **1**, 115 (1955).
10. C. H. L. Goodman, *Physics and Chem. Solids*, **6**, 305 (1958).

Glycerol Baths for the Electrodeposition of Molten Indium or Indium-Cadmium Alloy

A. J. Certa, T. J. Manns, G. L. Schnable, and H. S. Segal[1]

Lansdale Tube Company, Division of Philco Corporation, Lansdale, Pennsylvania

ABSTRACT

Plating baths employing glycerol as a solvent are described, from which ellipsoidal beads of molten indium or indium-cadmium alloy of approximately eutectic composition are electrodeposited onto whisker wires used as leads to electrodes of transistors. The In-Cd eutectic consists of 75% In and 25% Cd by weight and melts at 123°C. The glycerol baths for electrodepositing molten In-Cd alloy, which are solutions of $InCl_3$, $CdCl_2$, and NH_4Cl (and in some cases ethylenediaminetetraacetic acid) in glycerol, are usually operated at 140°C. Carbon anodes are used. With 24 v d.c. applied, a 15 μg ellipsoidal bead of In-Cd alloy of approximately eutectic composition can be electrodeposited on the end of a 0.05-mm nickel wire in about 2 sec. The effects of bath composition and of plating conditions on alloy composition, plating rate, and bath life are discussed. The plating baths are capable of serving as effective fluxes during soldering of whisker wires to electrodes of transistors.

In the manufacture of many types of semiconductor devices, electrical connections must be made to the electrodes. Indium metal, mp 156°C, is a convenient solder for devices where a soldering temperature of about 170°C can be employed.

In the fabrication of surface-barrier transistors, electrical connections must be made to indium emitter and collector electrodes. Indium-cadmium eutectic alloy (75% In, 25% Cd, by weight), which melts at 123°C (1), can be used to solder whisker wires to emitter and collector electrodes without melting the In metal. Soldering temperatures of about 140°C are employed. Indium-cadmium alloys in the approximate range from 50% In-50% Cd to 80% In-20% Cd by weight have been found to flow at temperatures below 130°C and thus are considered satisfactory solders for In metal. The advantages of In-Cd alloys as solders for semiconductor devices have been described previously (2).

Electrodeposition of Molten Solders

Metals electrodeposited in molten form are smooth, dense, and nonporous (2, 3). When molten metal or alloy is electrodeposited on a small wire, a bead forms at the end of the wire in a location highly suitable for a subsequent soldering operation (3). Deposition can be very rapid since high current densities can be used. Such current densities would generally cause dendritic growths in ordinary aqueous electroplating solutions.

The glycerol baths for electrodepositing molten In or In-Cd alloy are particularly suitable for rapidly plating small amounts of metals or alloys which may readily be used as solders. In contrast to the fused salt bath described previously (2), the glycerol bath is capable of acting as a soldering flux in the temperature range from room temperature to about 200°C. Thus in some applications, for example, on the automatic whisker attacher machines (4), the coating of plating solution which remains on plated whiskers withdrawn from the bath serves as a satisfactory flux during a subsequent soldering operation.

[1] Present Address: Amchem Products, Inc., Ambler, Pa.

Experimental Results

Glycerol solvent.—In the electrodeposition of molten metals, a solvent is required which has a boiling point above the liquidus temperature of the metal or alloy electrodeposited. While it was found possible to electrodeposit molten In metal from solutions of anhydrous indium trichloride in a wide variety of polar organic compounds including ethylene glycol, 1, 2-propanediol, 1, 2, 4-butanetriol, N, N, N′, N′-tetrakis (2-hydroxypropyl) ethylenediamine, phenol, d-sorbitol, acetamide, ethylene glycol monobutyl ether, benzoic acid, phthalic anhydride, diethylene glycol, triethanolamine and ammonium formate, glycerol was the most suitable solvent. Glycerol, which has a boiling point of 290°C, is relatively nonvolatile at the usual operating temperatures of the plating baths, and its thermal decomposition rate at these temperatures is comparatively low. Glycerol fumes are nontoxic.

Materials.—Materials used in the preparation of In and In-Cd alloy plating baths are: glycerol (assay 95%, sp. gr. 1.25), A.C.S. reagent; cadmium chloride, anhydrous, powder, minimum assay 99%, A.C.S. reagent; indium trichloride, powder, anhydrous, minimum assay 96%, 0.02% maximum metallic impurities;[2] ammonium chloride, granular, A.C.S. reagent; ethylenediaminetetraacetic acid (EDTA), powder, reagent grade.[3]

Preparation of solutions.—Formulations of the glycerol solutions for electrodeposition of molten

[2] From Consolidated Mining and Smelting Co. of Canada, Trail, B.C., or Indium Corp. of America, Utica, N.Y.

[3] J. T. Baker Chemical Co., Phillipsburg, N.J., or Fisher Scientific Co., Fair Lawn, N.J.

Table I. Formulations, properties and typical operating conditions of glycerol solutions for electrodeposition of molten indium or indium-cadmium alloy

Description	Solution I		Solution II			Solution III		
	Solution for electrodeposition of In metal		Solution for Electrodeposition of In-Cd alloy			Complexed solution for electrodeposition of In-Cd alloy		
Formulation, % by weight								
$InCl_3$	12.0		6.0			5.2		
$CdCl_2$	—		1.7			1.5		
EDTA	—		—			12.6		
NH_4Cl	8.0		10.6			9.3		
Glycerol	80.0		81.7			71.4		
Electrolytic conductivity								
Specific conductance at 140°C, mho/cm	0.035		0.040			0.035		
Typical operating conditions								
Operating temperature, °C	140	165	140	140	140	140	140	140
Bath life, hr	8	4	8	8	8	8	8	8
Applied potential, v	15-24	3-24	10	18	24	12	18	24
Composition of the electrodeposited alloy, % In by weight	100	100	75-80	75-80	67-75	66-70	66-70	70-75
Approximate plating time to obtain a 15-μg deposit, sec	—	—	—	—	2	—	—	5
Approximate current density, amp/cm^2	—	—	—	—	50	—	—	25
Approximate cathode current efficiency, %	—	—	—	—	20	—	—	15

In or In-Cd alloy are given in Table I. Solutions are prepared by stirring a mixture of the constituents for 30 min, breaking up any lumps, and then heating the resulting slurry with continuous stirring at 140°C for 10 min, or at 160°C for 10 min in the case of Solution III, to form a clear solution. The solution is allowed to cool to 100°-120°C and vacuum filtered through a coarse-porosity sintered glass filtering funnel.

While it is possible to dissolve all of the indium trichloride, cadmium chloride, and ammonium chloride in the glycerol at 25°C, the EDTA is only slightly soluble. Rapid dissolution of the solids is not possible below 135°C.

The glycerol baths are clear, light amber solutions which are somewhat more viscous than glycerol. Densities average roughly 1.35 g/ml at 25°C. The baths, which are prepared, stored, and operated in Pyrex or Kimax glass vessels, are stable for years at room temperature.

The reproducibility of numerous batches of plating solutions made by several different operators was quite satisfactory in terms of specific conductance at 140°C and in terms of plating rate (with 18 or 24 v applied) at 140°C, both initially and after 5 hr at 140°C.

Glycerol baths for Electrodeposition of Molten In *and* In-Cd *Alloy*

Properties and typical operating conditions of the various solutions are given in Table I.

Ammonium chloride increases the electrical conductivity of the plating solutions considerably and improves wetting by making the solutions more effective fluxes for the base metal to be plated (for example, nickel) as well as for the molten metal being deposited. (The specific conductivity at 140°C of a solution consisting of 13% $InCl_3$ and 87% glycerol was roughly 0.001 mho/cm, compared to 0.035 mho/cm for Solution I.) Cadmium chloride and indium trichloride are present in Solutions II and III in the ratio of 1:3.54 by weight, so that the ratio of Cd to In (as metal) in the baths is 1:3 by weight. Sufficient EDTA is present in Solution III to complex all In and Cd (assuming one mole of either metal per mole of EDTA) with 35% EDTA in excess.

Inert anodes of carbon (spectroscopic graphite) were used in all experiments. During electrolysis bubbles of oxygen and/or chlorine are evolved at the anode. The carbon anode should have sufficient area so that there is no appreciable polarization or local heating at the anode during electrolysis. One or more carbon rods 1/8 in. in diameter are used as anodes. The distance between cathode and anode is generally on the order of 1 cm.

In all of the experiments described, nickel wire 2 mils (0.05 mm) in diameter was used as a cathode. Under typical operating conditions the wire was immersed 1 to 2 mils (0.025 to 0.05 mm) below the plane of the surface of the plating solution. The hot plating baths normally wet the whisker wires far above the level of immersion. For example, a 2-mil nickel whisker wire immersed 1 to 2 mils below the plane of the surface of a glycerol plating solution at 140°C is wetted and plated along approximately a 10-mil length at the tip.

Under normal electrodeposition operating conditions, some hydrogen gas is evolved at the cathode during electrolysis of the solution.

The cathode area of immersed wires increases rapidly with the growth of the electrodeposited ellipsoidal beads of molten metal. For example, under typical operating conditions an ellipsoidal bead of molten In-Cd alloy 5 mils in diameter and 10 mils long is deposited on a 2-mil wire in about 2 sec. At the end of the 2-sec plating period, the surface area of the molten In-Cd alloy is several times

as great as the original immersed area of the wire. As the surface area of the molten solder increases during electrolysis, the current drawn at constant applied voltage also increases. For this reason, operating conditions are specified in terms of applied voltage rather than current density. Approximate current densities are given in Table I for several operating conditions.

Operating temperature and voltage of the baths are not particularly critical. Samples plated from Solution II at 120°C with 6 to 36 v applied, and at 160°C with 12 to 36 v applied, flowed at 130°C or less. The flow temperature of In-Cd alloys plated from Solution III at 140°C using 1.5 to 30 v was 130°C or less.

Bath life.—The average amount of In-Cd alloy deposited on the 2-mil nickel wires used in the fabrication of surface-barrier transistors is of the order of 10 to 20 μg. Under ordinary operating conditions, bath life is limited by decomposition reactions which occur in the bath at the operating temperature, usually 140°C; depletion of Cd and of In is negligible.

Since the ratio of Cd to In both in the plating baths and in the eutectic alloy is 1:3 by weight, the ratio of Cd to In in the bath remains essentially unchanged even when large amounts of alloy are electroplated from the bath.

Although thousands of whiskers can be plated from a 25-ml sample of plating bath without any evidence of decomposition of the plating solution due to anodic oxidation, prolonged electrolysis of these baths at high currents can accelerate decomposition reactions considerably.

Normally the principal limitation of bath life arises as a result of increase in viscosity with time at operating temperature. Increased viscosity results in lower electrolytic conductance and thus lower plating rates (with a constant plating voltage applied). Eventually, baths operated at 140°C become sufficiently viscous that plating rates are significantly lower than they had been initially, and the plated deposit tends to be somewhat erratic in size or location.

Tests have shown that these solutions frequently lose several per cent of their weight during 3 hr at 140°C due to volatilization.

No changes have been observed in flow temperatures of In-Cd alloys plated from solutions held at operating temperature for various periods of time up to 16 hr.

Effects of Bath Composition and Plating Conditions on Plating Rate and Bath Life

In a series of experiments to determine the effect of variations in bath composition, the relative amounts of $CdCl_2$, $InCl_3$, and EDTA were kept constant and were in the mole ratio of 1:2.94:5.36, respectively. The independent solution composition variables were thus per cent by weight ($CdCl_2$+$InCl_3$+EDTA) as a constant mole ratio group, and per cent by weight ammonium chloride, the remainder of the bath being glycerol. Specific conductance measurements at 100°C indicated that solutions consisting of the group ($CdCl_2$+$InCl_3$+EDTA) and glycerol in the weight ratio of 1 to 3 or 4 had a maximum specific conductivity. Decrease in the concentration of such solutions resulted in less ions available for electrolytic conductance and thus lower specific conductivity. Increase in the concentration of such solutions decreased the specific conductivity because the viscosity of these solutions increased considerably with concentration. [Generally, dissolved electrolytes increase the viscosity of glycerol solutions (5).] The viscosity of the glycerol solutions increased considerably with increase in concentration of the group ($CdCl_2$+$InCl_3$+EDTA); change in the concentration of the ammonium chloride had little effect on the viscosity of the solution.

Baths which were more concentrated than Solution III had a rather sharp decrease in specific conductivity with evaporation of glycerol and thus had a limited bath life. Solution III, which has approximately the concentration at which maximum specific conductivity is obtained, is relatively insensitive to changes in specific conductivity resulting from evaporation of glycerol. Solution III has an operating life at 140°C of approximately 8 hr whereas a more concentrated bath, consisting of 2.5% $CdCl_2$, 8.9% $InCl_3$, 21.4% EDTA, 6.1% NH_4Cl, and 61.1% glycerol, by weight, had an operating life of 2-3 hr at 140°C.

Increase in the ammonium chloride content of the bath increased the specific conductance and thus increased the plating rate at a given applied voltage. However, the solubility limit of ammonium chloride in the bath at about 20°C cannot be exceeded if the bath is to be stored at room temperature.

In some cases a small amount of surface-active agent is added to glycerol baths for plating molten metals and alloys. This addition lowers the surface tension of the solution, causing the bubbles formed at the cathode during electrolysis to be smaller. For example, 0.05% by weight of decyl benzene sodium sulfonate is effective in considerably reducing the surface tension of the Solution II at 140°C. The presence of a surface-active agent, by making the bubbles smaller, results in steadier plating currents and thus more reproducible plating rates.

Composition of Electrodeposited In-Cd *Alloys*

Flow temperatures were determined by immersing whiskers, on which the beads of In-Cd alloy had been flattened, into a flux such as 9% ammonium chloride in glycerol at 130°C. If the alloy flowed at 130°C or less, the bead returned to an ellipsoidal shape.

The composition of electrodeposited In-Cd alloys was determined by quantitative spectrographic analysis. Weighed samples of clean, dry, plated whiskers were treated with about 0.6 ml of 4*N* HCl to dissolve the In-Cd alloy. The stripped whiskers were rinsed, dried, and reweighed. The solution was diluted to a concentration of 0.50 mg of In-Cd alloy/ml and analyzed spectrographically by comparison with solution standards. About 50 plated

whiskers were used to prepare each sample solution for analysis. Generally duplicate determinations were made.

Local Heating at the Cathode during Electrolysis

In some cases considerable local heating occurs at the cathode during electrolysis. For example, molten In-Cd alloy was plated on a 2-mil nickel wire immersed in Solution III, operated at a temperature of 70°C, using 18 v for electrolysis. In this case, the temperature at the cathode rose more than 50°C above the operating temperature of the bath. In one experiment, with 90 v applied to a 2-mil wire immersed about 5 mm, molten In-Cd alloy was electroplated from Solution III at room temperature (25°C), indicating a temperature rise of approximately 100°C at the cathode.

Molten In metal can be deposited on 2-mil nickel wire from Solution I operated at 140°C with 18 v applied or at 120°C with 24 v applied. Molten In-Cd alloy can be plated on 2-mil nickel wire from Solution II operated at 100°C with 24 v applied.

The principle of employing local heating at the cathode to plate molten metals or alloys from a solution operated at a temperature considerably below the liquidus temperature of the metal or alloy is of interest in applications where long bath life or minimum fuming is desired.

Chemical Plating

Small pieces of Cd and of In metal were added to both Solution II and Solution III at 140°C. With both solutions the Cd became coated with a molten alloy, indicating that chemical plating of In had occurred. The In metal was etched by both solutions but no visible deposition of Cd occurred.

Conclusions

The chemical plating experiments indicate that In is more noble than Cd at 140°C in both the complexed and the uncomplexed solutions for plating molten In-Cd alloy. Such a result might be expected from a comparison of the single electrode potentials of In and of Cd in the acid electromotive series of the elements (in aqueous solution), where $E^\circ = -0.34$ v for In and $E^\circ = -0.40$ v for Cd (6).

Increase in plating solution viscosity with time at operating temperature is believed to be due to evaporation of glycerol and/or water and to condensation polymerization of glycerol to form polyglycerides, which are more viscous than glycerol (7). Since formation of polyglycerides appears to be catalyzed by anhydrous indium trichloride, the solutions listed in Table I are less susceptable to this type of degradation than more concentrated solutions.

Both Solution II and Solution III are used in the production of semiconductor devices. Solution II deposits In-Cd alloy more than twice as fast as Solution III, but the latter is less volatile at 140°C and electrodeposits In-Cd alloys of suitable solder composition over a wider range of operating conditions than the uncomplexed solution (8).

Acknowledgment

The authors wish to express their thanks to M. Sadowsky for his interest and encouragement, to E. Murt, who performed the spectrographic analyses, and to W. Hillegas, Jr., for excellent assistance in the experimental work on the uncomplexed In-Cd plating solution.

Manuscript received July 9, 1958. This paper was prepared for delivery before the Buffalo Meeting, Oct. 6-10, 1957.

Any discussion of this paper will appear in a Discussion Section to be published in the June 1960 JOURNAL.

REFERENCES

1. E. A. Peretti, "Constitution of Indium Alloy Systems," p. 15, Indium Corp. of America, Utica, N. Y. (1956).
2. G. L. Schnable and J. G. Javes, *This Journal*, **105**, 84 (1958).
3. G. L. Schnable (to Philco Corporation), U. S. Pat. 2,818,375, Dec. 31, 1957.
4. "Soldering Whiskers on Transistor Pellets," in "Production Techniques," J. Markus, Editor, Electronics, **29**, 270 (1956).
5. "Physical Properties of Glycerol and its Solutions," by J. B. Segur in "Glycerol," C. S. Miner and N. N. Dalton, Editors, p. 285, Reinhold Publishing Corp., New York (1953).
6. W. M. Latimer, "The Oxidation States of the Elements and Their Potentials in Aqueous Solutions," 2nd Ed., Prentice-Hall, Inc., New York (1952).
7. "Chemical Properties and Derivatives of Glycerol" by J. B. Segur in "Glycerol," C. S. Miner and N. N. Dalton, Editors, pp. 366-8, Reinhold Publishing Corp., New York (1953).
8. T. J. Manns and A. J. Certa (to Philco Corporation), U. S. Pat. 2,818,374, Dec. 31, 1957.

Potential Measurements during Jet Etching of P-Type Ge and P-Type Si

Paul F. Schmidt and Maire Blomgren

Research Division, Philco Corporation, Philadelphia, Pennsylvania

ABSTRACT

Potential measurements have been made during jet etching, and the feasibility of the method has been established. Potentials during jet etching have been compared with those obtained in bath operations by other authors.

Jet etching and plating have become increasingly important for the fabrication of semiconductor devices. The current densities employed are well beyond the usual range of bath operation. Thus it appeared very desirable to investigate jet etching and plating by potential measurements. Development of special techniques was required for the peculiar geometry of the jet method. The method has been applied to p-Ge and p-Si so far, but should be applicable also to other systems.

Experimental

Jet-etching apparatus.—The apparatus consisted of a transparent plastic enclosure with removable lid; the jet and anode were inserted into the plastic chamber from opposite sides, both making an angle of 45° with the perpendicular (Fig. 1). The jet was rigidly fixed in its position. The anode consisted of a Ge or Si wafer mounted on a nickel or stainless steel disk, which in turn was screwed into a holder. Three micrometer screws permitted the movement of the holder perpendicular and parallel to the jet axis. In the direction parallel to the jet axis the accuracy was 0.2 mil, in the two perpendicular directions the accuracy was about 1 mil.

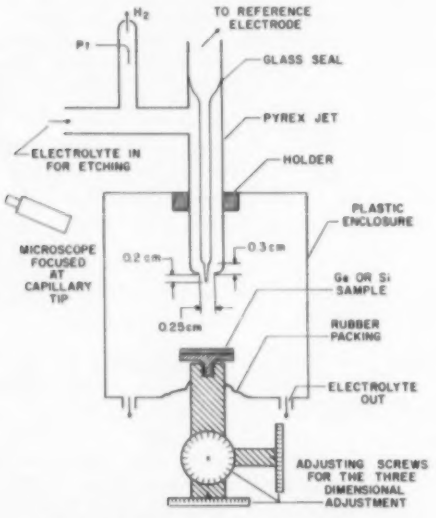

Fig. 1. Schematic of jet etching apparatus

A pocket microscope was mounted in such a fashion that it could always be brought to exactly the same position and could be focused simultaneously on the jet nozzle and on its mirror image at the shiny Ge or Si surface. Magnification by the microscope was 60X. Two drainage tubes at the bottom of the plastic chamber permitted the withdrawal of the electrolyte during etching. A lid was placed on the plastic chamber when large jet sizes were used.

The jet.—Two sizes of jet nozzles were employed: 30 and 100 mil diameter (7.6×10^{-2} and 2.5×10^{-1} cm). Inserted in the center of the jet, by means of a glass seal, is a smaller tube which tapers off to a capillary, about 0.5 cm long, 2.5 mil (6×10^{-3} cm) OD, and 1.5 mil (3.7×10^{-3} cm) ID. The capillary is located accurately in the center of the jet nozzle and extends 0.15 to 0.2 cm beyond it. The inner tube is connected to a saturated calomel electrode. The electrolyte in the outer tube was used for jet etching. The electrolyte in the inner tube, connected to the reference electrode, was usually the same as that in the outer tube except for those experiments which involved the use of free HF for jet etching. In this case the pH of the electrolyte in the inner tube was kept neutral in order to avoid excessive attack on the capillary. Only capillaries without any faults could be used; if the tip of the capillary was damaged in any way, the electrolyte from the inside would form droplets at the tip thus making it impossible to position the Ge or Si sample accurately (compare below). Also the potential values would be quite erratic with faulty capillaries.

The electrolyte for jet etching was introduced into the outer tube of the jet through a side arm. The latter in turn was connected to a small tube partially open at the tip. Inserted in this small tube was a Pt wire which served as the auxilliary electrode. Any hydrogen bubbles forming at the wire were swept out at the tip and thus did not enter the main jet stream.

Anode set up.—The anode, as already mentioned, consisted of a Ge or Si wafer mounted on a nickel or stainless steel disk which in turn could be screwed into the sample holder. When positioning the sample, the anode was moved toward the jet nozzle by means of the micrometer screws until

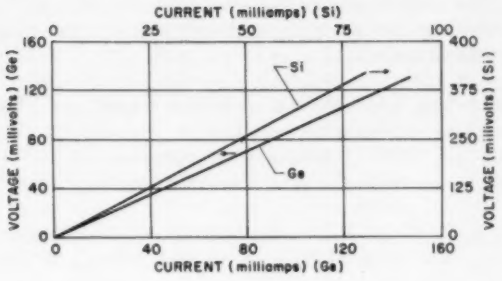

$R_{bulk\ Ge}$	: 0.5 ohms	$R_{bulk\ Si}$	: 0.6 ohms
$R_{measured}$	: 0.9 ohms	$R_{measured}$	: 5.2 ohms
$R_{each\ contact}$	: 0.2 ohms	$R_{each\ contact}$	: 2.3 ohms

Fig. 2. I-V of ohmic base contacts to Ge and Si

both the tip of the capillary and its mirror image were simultaneously in the focus of the microscope. In this fashion it was possible to make the distance between the tip of the capillary and the semiconductor surface less than 1.2×10^{-3} cm.

Preparation of Ge *and* Si *samples.*—Ohmic base contacts to the p-Ge wafers (resistivity 1 ohm-cm, lifetime about 100 μsec, thickness 0.05 cm) was obtained by sand blasting the whole back surface of the wafer and soldering pure tin to the sand blasted area. The stainless steel disk was then pressed against the tin while heating. This resulted in a good electrical and mechanical contact. In the case of p-Si (ρ about 1 ohm-cm, τ about 20 μsec, thickness = 0.05 cm), Al was evaporated onto the back surface of the chemically polished wafer and was then alloyed by heating at 850°C for 30 sec. The Al was then painted with silver paste, which again resulted in a good contact when mechanically pressed against the metal disk.

In order to check that the contact was truly ohmic, the front surface of some wafers was given the same treatment as the back surface and I.V. curves were taken. Figure 2 shows that completely ohmic contacts were obtained both on p-Ge and on p-Si. The contact resistance for each contact is about 0.2 ohm on p-Ge, and 2.3 ohm on p-Si.

In order to obtain a homogeneous current density during jet etching it was necessary to mask the Ge or Si surface except for a hole of the same size or smaller than the jet employed. The hole had to be a perfect circle without fuzzy edges; otherwise, the resulting etch pit would be of very poor quality. The masking material must also meet the requirements of being quite inert to the electrolytes employed, and of being so thin that it would not obstruct the view of the mirror image of the capillary tip when the sample is brought into position. For measurements of current efficiency it was also essential that the masking material should be easily removable without changing the weight of the Ge or Si wafer. All these requirements were met by a Teflon tape with pressure sensitive silicone adhesive.[1] The tape was applied to the chemically polished surface of the semiconductor.

[1] Produced by the Minnesota Mining and Manufacturing Co. (pressure sensitive tape No. 549).

Potential measurements.—A voltage regulator supply, model 3-150 L, of the Dressen-Barnes Corporation served as a power source. The voltage was applied between the auxilliary electrode in the side arm of the jet and the ohmic base contact of the Ge or Si wafer. A standard resistor was inserted in the circuit and the voltage across this resistor applied to one axis of a Moseley X-Y recorder. The voltage between the reference electrode and the ohmic base contact was applied to the input of a Keithley electrometer, model 210, and from there to the other axis of the X-Y recorder. Use of the Keithley electrometer was necessary because of the high resistance in the capillary (about 10^6 ohm). The response time of the recorder is 1 sec full scale on either axis.

It was found that the potential values did not depend on the speed with which the curves were taken, i.e., for times of the order of a few seconds, except, of course, for the additional *RI* drop introduced if the etching process at high current densities increased the distance between capillary and Ge surface by an appreciable amount. Usually the current was increased to its maximum value in 10 sec and decreased to zero in the same time.

Owing to the small distance between the tip of the capillary and the semiconductor surface, the *RI* drop in the electrolyte up to current densities of about 0.1 amp/cm^2 is negligible ($\leqq$ 10 mv). This was checked by experiments in which the distance between capillary and Ge surface was increased successively in steps of 0.5 mil (1.3×10^{-4} cm).

At high current densities, however, this *RI* drop must be taken into account. It is then necessary to consider the distance by which the Ge or Si surface has receded from the capillary due to the etching action. Knowledge of the current efficiency over the current range investigated, of changes in the resistivity of the solution due to heating effects, and of the total amount of charge passed at each point of the curve would be required in order to apply an accurate correction. The amount of charge passed could be determined if the current had been increased linearly with time. The current in our experiments was increased manually and therefore not quite linearly with time. Therefore it is not justified to apply a correction in this manner.

No corrections have been applied to any of the curves shown in this paper, except those applied to Fig. 3; they are stated below in the text. However, from the known resistivities of the electrolytes employed it can be calculated that the additional *RI* drop introduced by recession of the semiconductor surface during etching is less than 1 v (at 10 amp/cm^2) if the etching current is raised linearly with time over a period of 10 sec from 0 to 10 amp/cm^2. When comparing this value to the potentials obtained at 10 amp/cm^2, roughly 10 v, it can be seen that the error even at the largest current densities is less than 10%. It can be shown that the additional *RI* drop under the above conditions increases with i^2; the error at lower current densities is therefore much smaller. The *RI* drop due to the original distance between the tip of the capillary

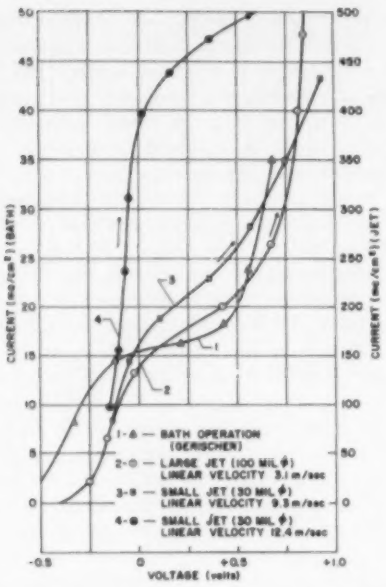
CURRENT (ma/cm²) (BATH)
CURRENT (ma/cm²) (JET)
VOLTAGE (volts)
1-Δ — BATH OPERATION (GERISCHER)
2-○ — LARGE JET (100 MIL ϕ) LINEAR VELOCITY 3.1 m/sec
3-■ — SMALL JET (30 MIL ϕ) LINEAR VELOCITY 9.3 m/sec
4-● — SMALL JET (30 MIL ϕ) LINEAR VELOCITY 12.4 m/sec

Fig. 3. Current-potential curves on p-Ge for bath operation (Gerischer and Beck) and for jet-operation using the same electrolyte. 1 ohm-cm p-Ge, 0.1M $NaClO_4$ + 0.02 M NaOH; flow rate: 3.1 m/sec.

and the semiconductor surface is about 0.5 v at 10 amp/cm^2.

The curves shown are typical of a very large number of experiments; the reproducibility was quite good. The potentials always refer to the saturated calomel electrode, except in Fig. 3 where they have been referred to the N-calomel electrode. All measurements were done at room temperature.

Since the experiments were performed on p-type material only, saturation effects inside the semiconductor are not expected to occur, and except for their appreciable resistivity Ge and Si can be treated in this respect much like metals.

Measurements of current efficiency.—These measurements were done in parallel to the potential measurements. The weight of the Ge or Si sample before and after etching was determined with a Mettler microbalance, sensitivity ± 1 μg. Before weighing, the samples were kept in a dessicator for 1 hr. It was again necessary to mask the Si or Ge wafers except for a small hole facing the jet in order to deal with a defined current density. In control runs it was found that applying the masking tape to the sample, exposing it to the electrolyte stream (without applying a bias), removing the tape and washing the sample with chloroform or CCl_4 did not change the weight of the wafer by more than ± 10 μg. The amount of charge passed during each run was chosen so as to remove 400 μg. It is believed therefore that the result of the weighings should be accurate to at least ± 5%. However, the amount of charge passed was obtained simply from the product time x constant current. This reduces the accuracy somewhat more. For accurate determinations a coulometer should be employed.

The electrolytes.—The electrolytes used had the following composition and resistivity (at room temperature):

On p-Ge: 0.1M $NaClO_4$ + 0.02M NaOH; ρ = 79.3 ohm-cm
0.2N H_2SO_4; ρ = 21 ohm-cm
0.2N H_2SO_4 + 1 cc Hyamine/1; ρ = 24.9 ohm-cm.
On p-Si: 40 g NH_4F + 8 g NaF/1; ρ = 16.4 ohm-cm
0.2N NaF + 5 cc 48% HF; ρ = 61.8 ohm-cm

The electrolyte was forced through the jet by pressure from a nitrogen tank. In separate experiments it was shown that removing dissolved oxygen from the electrolyte did not effect the potential measurements within the limit of accuracy except close to zero current.

The nitrogen pressure was 2 psig when the 100-mil jet was employed, and either 2.5 or 5 psig when the 30-mil jet was used. The corresponding linear jet velocities were 3.1 meters/sec (100-mil jet, 2 psig), 9.3 meters/sec (30-mil jet 2.5 psig), and 12.4 meters/sec (30-mil jet, 5 psig). The flow rate of the electrolyte has a very marked effect on the I.V. curves as would be expected.

Results

1. *Potentials during jet etching of p-Ge with 0.1M $NaClO_4$ + 0.02M NaOH solution, and comparison to the potential values obtained by Gerischer and Beck (1) with the same electrolyte in a stirred bath.*—Figure 3 shows the current potential curves for three different jet flow rates. For the sake of comparison the curve obtained by Gerischer and Beck is also shown. Unfortunately, the stirring rate for this curve is not given in the preliminary publication by Gerischer and Beck.

The jet curves in Fig. 3 are corrected for the total *RI* drop between base contact and tip of capillary in the following way: (*a*) From the experiments on contact resistance (Fig. 2) the resistance of the base contact is known to be about 0.2 ohm. (*b*) For the contact jet/Ge the spreading resistance inside the Ge is calculated from the formula (2): $R = \frac{1}{4a\sigma}$ (where a = radius of the contact, σ = conductivity of the Ge) to be 4.0 ohm for the large, and 6.5 ohm for the small jet. (In the experiments with the large jet the unmasked area of the Ge was 50 mils ϕ = 0.13 cm ϕ.) (*c*) From the resistivity of the solution (79.3 ohm) and an assumed distance of 1.3 x 10^{-3} cm, the resistance of the electrolyte layer between the tip of the capillary and Ge surface is calculated to be 23.1 ohm for the small jet (30 mil ϕ), and 8.1 ohm for the large jet (effectively 50 mil ϕ). (No correction has been applied for increase of the distance with etching because the curves were taken so rapidly that the additional distance is negligible compared to the original distance.)

It can be seen from Fig. 3 that the shapes of the curves are quite similar. However, the current

plateaus occur at much higher values for the jet operation, and the plateaus are not so flat.

It is evident that the vigorous stirring action of the jet causes a decrease in thickness of the Nernst diffusion layer. The fact that the position of the current plateaus depends strongly on the jet speed shows that concentration overpotentials are very pronounced in jet operation in this current density range.

The current plateaus obtained with the jet are not as horizontal as in the bath. This is due to the fact that the current density is not exactly homogeneous over the etching area, as can be seen from the slightly rounded bottom of the etch pit obtained with prolonged etching.

The current plateaus of curve 2 (100 mils ϕ jet, 50 mils ϕ etching area, 3.1 m/sec linear jet velocity) and of curve 3 (30 mils ϕ jet, 30 mils ϕ etching area, 9.3 m/sec linear jet velocity) occur at not greatly different current densities, whereas the current plateau of curve 4 (30 mils ϕ jet, 30 mils ϕ etching area, 12.4 m/sec linear jet velocity) is shifted to a much higher current density.

The thickness of the Nernst diffusion layer, which determines the position of the current plateau, is apparently smaller in the case of curve 2 than would be expected from the average flow rate of the jet (measured as volume/time). This must be due to the fact that the 50 mils ϕ etching area is exposed to the higher flow velocity in the center of the 100 mils ϕ jet. The small distance between jet nozzle and Ge surface (2 mm = 80 mils) is apparently not sufficient to suppress the velocity profile of the jet stream.

A rough calculation indicates that the thickness of the Nernst diffusion layer is about 25 times smaller for curve 4 than for curve 1.

The agreement between curve 1 (bath operation) and curves 2-4 (jet operation) is satisfactory when considering the deviations from ideal conditions mentioned above and shows that essentially the same electrode process takes place in jet etching as in bath operation.

As to the interpretation of the curves, reference is made to the publication by Gerischer and Beck (1). According to these authors the anode reaction

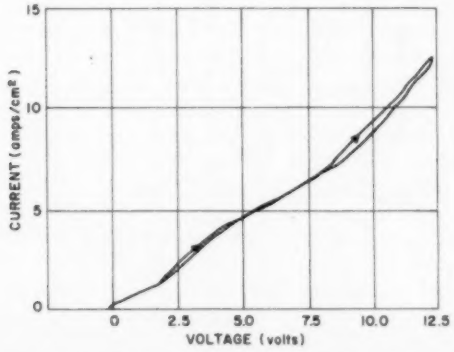

Fig. 4. Current-potential relationship at high current densities. Same electrolyte as in Fig. 3. 1 ohm-cm p-Ge, 0.1M $NaClO_4$ + 0.02M NaOH; flow rate: 12.4 m/sec.

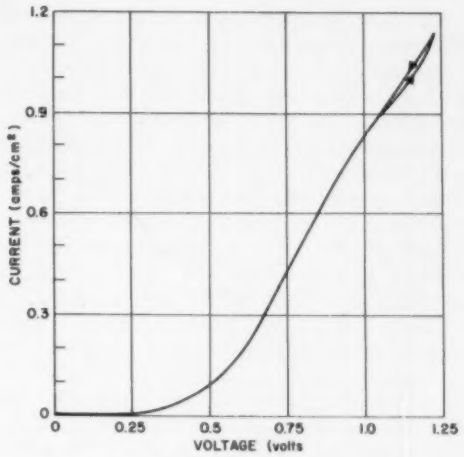

Fig. 5. Current-potential relationship in dilute H_2SO_4 at low current densities. 1 ohm-cm p-Ge, 0.2N H_2SO_4; flow rate: 9.3 m/sec.

on the first ascending branch is between Ge and OH^- ions, and on the second ascending branch between Ge and H_2O molecules. The current plateau indicates depletion of OH^- ion supply at the surface.

This solution (0.1M $NaClO_4$ + 0.02M NaOH) is not an electropolishing solution on Ge. It does not reveal crystal structure, but neither does it remove any surface structure present prior to jet etching.

Figure 4 shows an experiment (with the 30 mil ϕ jet at a flow rate of 12.4 m/sec) in which the current density was increased to 13 amp/cm². The additional *RI* drop caused by etching at high current densities is clearly seen on this graph from the difference of the potentials on the way up and down. In addition, a second levelling of the current is observed at about 5 amp/cm². This levelling marks the beginning of oxygen evolution (as indicated by current efficiency measurements), and is probably connected with the buildup of an oxide layer. At current densities much below 5 amp/cm² there is no indication of an increase in thickness of a hypothetical oxide layer with time: the current can be held constant without causing an increase of potential within a reasonable length of time. Above 5 amp/cm² an increase of potential with time at constant current is observed but cannot be distinguished easily from an additional *RI* drop caused by etching unless transient techniques were to be employed.

These remarks also apply to the current levels observed at very high current densities with the other electrolytes employed in this investigation.

2. *Current-potential curves obtained with a 0.2N solution of* H_2SO_4.—Figure 5 shows the curve obtained with 0.2*N* H_2SO_4 at low current densities, and Fig. 6 at high current densities. A second levelling of the current is again observed in Fig. 6, but it is remarkable that in the region of the levelling the current for a given potential is larger on the way down than on the way up. At higher current densities the curve taken upward coincides with

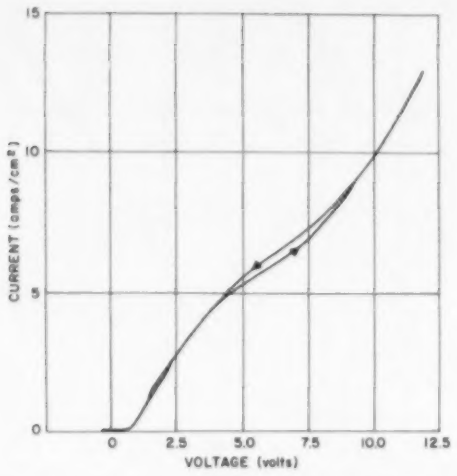

Fig. 6. Current-potential relationship in dilute H_2SO_4 at high current densities. 1 ohm-cm p-Ge, 0.2N H_2SO_4; flow rate: 9.3 m/sec.

the downward curve. This suggests that in this region the additional *RI* drop caused by etching is compensated by a decrease of potential with time at constant current. The shape of the curve in the region of low potentials is markedly different from the one obtained with the $NaClO_4$/NaOH solution and gives evidence that differences in electrode processes can be observed by potential measurements with the present jet technique.

Sulfuric acid has distinct electropolishing properties on Ge, but it still takes time for initially present surface structures to disappear.

3. *Current-potential curves obtained wth 0.2N H_2SO_4 with the addition of a wetting agent.*—Figure 7 shows the current-potential curves obtained with a 0.2 *N* H_2SO_4 + 1 cc/liter of Hyamine 2389 [Alkyl (C_9-C_{18}) tolylmethyltriethyl ammonium chloride

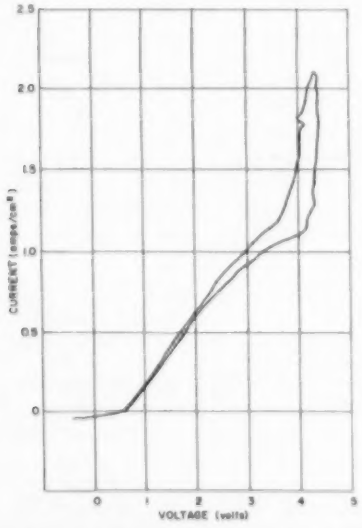

Fig. 7. Effect of addition of hyamine to dilute sulfuric acid. 1 ohm-cm p-Ge, 0.2N H_2SO_4 + 1 cc hyamine/liter; flow rate: 9.3 m/sec.

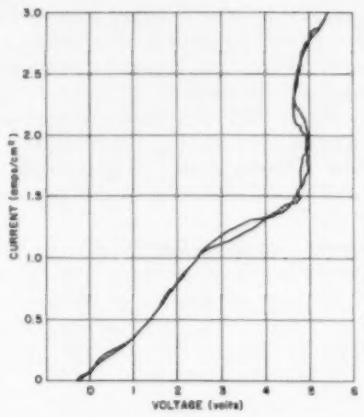

Fig. 8. Current-potential curves on p-Si in acidic fluoride solution. 1 ohm-cm p-Si, 8 g NaF + 40 g NH_4HF_2/liter; flow rate: 9.3 m/sec.

50%, H_2O 50%; Rohm & Haas Company]. The high anode potentials are remarkable. It is known that aromatic amines are adsorbed to an appreciable extent also on an anodic surface, and that they are desorbed at high anode potentials (3). The sudden jump in current at + 4.2 v suggests that the organic agent is partially desorbed at this potential, causing the current to approach the value for a clean Ge surface.

4. *Effect of crystal orientation.*—No difference in potential values was observed for the {111} and the {110} plane.

5. *Current-potential curves during jet-etching of p-Si with a solution of 40 g NH_4HF_2 + 8 g NaF/liter H_2O.*—Figure 8 shows a typical current-potential curve in the low, and Fig. 10 in the high current density range. In the region between 4 and 5 v the potential varies irregularly and rather violent fluctuations occur if the current in this region is held constant. The amplitudes of the oscillations are damped if the curves are taken with higher

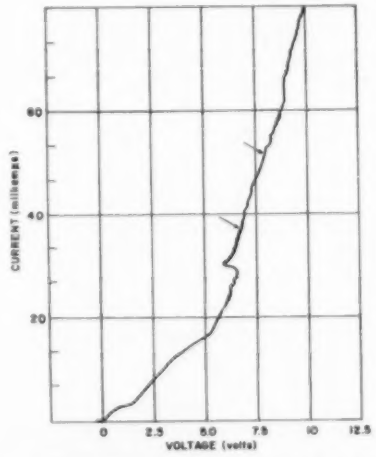

Fig. 9. Increasing size of etched area relative to jet size does not affect the general shape of the curve. 1 ohm-cm p-Si, 8 g NaF + 40 g NH_4HF_2/liter; flow rate: 12.4 m/sec; etching area 16 times jet size.

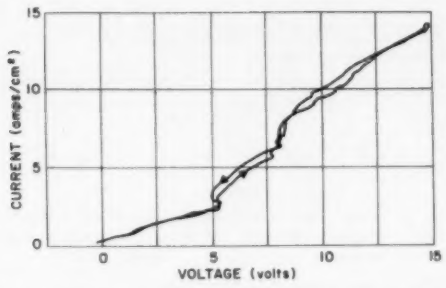

Fig 10. Current-potential curves in the same electrolyte at high current densities. 1 ohm-cm p-Si, 8 g NaF + 40 g NH_4HF_2/liter; flow rate: 12.4 m/sec.

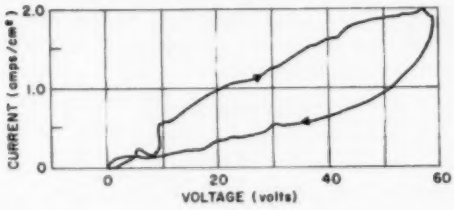

Fig. 11. Current-potential curves in an electrolyte containing less acid. 1 ohm-cm p-Si, 8 g NaF + 5 cc 48% HF/liter; flow rate: 9.3 m/sec.

speed. Also the jet flow rate has some influence. It was of interest to find out whether the fluctuations are caused by phenomena occurring at the edges of the masking tape. In Fig. 9 the diameter of the unmasked Si surface was 4 times the jet diameter; the contribution by phenomena at the periphery may therefore be expected to be less. The fluctuations nevertheless show up very clearly. Also in Fig. 9 two points are marked at which the current was held constant for 5 sec each without causing oscillations. Under the conditions of this experiment the oscillations are confined to the region between 16 and 31 ma.

A similar region of current-potential instability in the anodic oxidation of Si has been reported by Turner (5). No "run-away" region of decreasing potential with increasing current as noted by Turner was observed in our experiments presumably because the resistance of the electrolyte jet is so high (several K-ohms) that variations in electrode potential do not affect the current noticeably.

Potentials below 1 v were not very reproducible; this is probably connected with the ability of Si to form a thick oxide film in contact with air. Thus potentials in this region depend on the previous history of the sample, especially on the time elapsed since the wafer was polished chemically (with CP 4).

A thick air-formed film will not etch away rapidly before a critical potential is reached, as can be seen from the following experiment. Photodiodes on n-Si which had been exposed to air for a long time after their manufacture were biased reversely (+ 0.25 v), and light was shone through the running electrolyte jet aimed accurately at the front surface of the photodiode. (The diode area in these experiments was 30 square mils, the jet diameter was 20 mils, and the front surface of the Si had not been masked; the diode contact on the reverse side was, of course, insulated against contact with the electrolyte.) The saturation current of the photodiode increased to a value determined by the light intensity. An increasing anodic current was now applied between the Si base contact and an auxiliary electrode in the jet, so that the jet should now also act as a collector for the holes injected by the light. Until a current of 7 ma was reached, the current of the diode was quite independent of the jet current, proving that up to 7 ma the discharge of oxygen, i.e., the injection of majority carriers (electrons) was the main anodic process. Beyond 7 ma the diode current decreased abruptly to near the reverse saturation current in darkness, the jet now collecting practically all the injected holes.

If the electrolyte jet (same NH_4HF_2/NaF composition as above) is aimed at the Si surface without application of a current, a thin, semitransparent white film is formed, but the reaction is very slow and the Si is not attacked appreciably within 20 min. It is therefore more likely that the air-formed SiO_2 film rather than the formation of this whitish compound is responsible for the poor reproducibility of the potentials below 1 v. In our experiments the current density range 0-25 ma/cm² was usually traversed within 1 sec or less.

If, on the other hand, jet etching is done on purpose at a constant current density of 25 ma/cm² for a prolonged period of time, the Si is etched deeply and the surface becomes covered with a firmly adherent colorless compound, which is not soluble in water, slowly in CP 4, and dissolves slowly in strong NaOH with evolution of a gas, presumably hydrogen. The substance is thus similar to but not identical with the one described by Turner (5).

At large current densities (about 6 amp/cm²) oxygen evolution occurs as a side reaction, as shown by the current efficiency measurements (see below).

6. *Current-potential curves obtained with a solution of 8.4 g* NaF + *5 cc 48%* HF/*liter.*—This solution had been used extensively in practice but was satisfactory only at very low current densities. Figure 11 shows convincingly that at high current densities a high resistance SiO_2 film is formed which does not disappear quickly even when the current density is lowered.

7. *Measurements of current efficiency in the jet etching of p-Ge and p-Si.*—When etching p-Ge with dilute sulfuric acid the current efficiency based on a valency of +4 is usually close to 100% or just below, regardless of whether the Ge surface is masked or not. Up to moderately high current densities the current efficiency does not seem to depend much on current density; at high current densities oxygen is discharged as a side reaction and the current efficiency drops.

In solutions containing halide ions, more complex phenomena occur if the surface is not masked. Cur-

Table I

Electrolyte: 40 g NH_4HF_2 + 8 g NaF/liter; Flow rate: 3.1 m/sec

Current density range, amp/cm²	≦0.025	0.05< × <0.5	0.5< × <2	2< × <15
% Current efficiency	>>160	485-115	115-95	95-75
Remarks	Etched area covered with adherent white deposit, actual loss of Si therefore much greater, i.e., current efficiency >> 160%. Surface badly pitted under the deposit.	Shiny but not polished surface; at higher current densities transition to electropolishing.	Good electropolish at higher current densities	Electropolishing concommitant with O_2 evolution

rent efficiencies as high as 120% can be observed in HCl solution. This may well be due to the "edge-effect" described by Jirsa (4) who found that Ge goes into solution +4 valent over the whole current density range and in all electrolytes investigated by him (HCl, H_2SO_4, KOH, NH_4OH), but that at the interface solution/air/Ge divalent Ge ions are formed by the reaction: $Ge^{4+} + Ge \rightarrow 2\ Ge^{2+}$.

In contradistinction to the behavior of Ge very large deviations from a current efficiency of 100% were observed on Si. Table I summarizes the results.

It is very remarkable that apparent current efficiencies > 400% are obtained at low current densities. This rules out any explanation based on dissolution of Si as ions of lower valency. It seems in fact that an explanation must be sought along the lines of the negative difference effect investigated by Straumanis (6). A corresponding effect is not found on Ge which is more noble than hydrogen. This lends support to the assumption that current efficiencies > 200% are caused by current flow between local anodes and cathodes. The local cathodes are evidently created by an impressed anodic current in the manner described by Straumanis (6). The effect disappears at larger anodic potentials because the hydrogen evolution reaction is then suppressed on the Si surface.

At very large current densities oxygen evolution occurs but in the given electrolyte Si does not passivate, at least not below 20 amp/cm², the highest current density investigated.

Acknowledgments

The authors are greatly indebted to Dr. E. Blomgren of the University of Pennsylvania for valuable discussions and advice, and to Professor J. O'M. Bockris of the University of Pennsylvania for valuable discussions of semiconductor electrode kinetics. Our thanks are also due Mr. Larson at the University of Pennsylvania for solving the difficult task of preparing the Haber-Luggin capillaries and inserting them in the jets.

Manuscript received Sept. 24, 1958.

Any discussion of this paper will appear in a Discussion Section to be published in the June 1960 JOURNAL.

REFERENCES

1. H. Gerischer and F. Beck, *Z. Phys. Chem., N. F.*, **13**, 389 (1957).
2. H. C. Torrey and C. A. Whitmer, "Crystal Rectifiers," p. 24, McGraw-Hill Book Co. (1948).
3. E. Blomgren and J. O'M. Bockris, *J. Phys. Chem.*, in press.
4. F. Jirsa, *Z. anorg. u. allgem. Chem.* **268**, 84 (1952).
5. D. R. Turner, *This Journal*, **105**, 402 (1958).
6. M. E. Straumanis, *ibid.*, **105**, 284 (1958); M. E. Straumanis and Y. N. Wang, *ibid.*, **102**, 304 (1955).

Junction Delineation on Silicon in Electrochemical Displacement Plating Solutions

D. R. Turner

Bell Telephone Laboratories, Incorporated, Murray Hill, New Jersey

ABSTRACT

Antimony, copper, silver, platinum, and gold can be deposited on silicon by electrochemical displacement. The displacement plating process induces potential differences between abraded and polished n- and p-type silicon. This results in metal being deposited at different rates on the four types of silicon surfaces which in turn produces p-n junction delineation. The process also shows up abrupt changes in the impurity concentration at the surface. The maximum resolution between junctions in a multiple junction crystal is about 2 microns.

A number of chemical treatments have been developed to show up p- and n-regions on the surface of silicon single crystals. The first was devised by Fuller (1) and consisted of treating the Si in HF solutions containing a small amount of HNO_3. This solution stains p-type regions darker than the n-type. Silverman and Benn (2) were able to portray junctions on Si with Au deposited by electrochemical displacement from a gold cyanide plating solution in the presence of light. Recently Whoriskey (3) has improved on the reproducibility of the HF stain method by eliminating the HNO_3 and illuminating the junction with white light. He also reports good junction delineation using white light and a copper nitrate solution containing a small amount of HF. Iles and Coppen (4) obtained junction delineation on Si in a dilute silver-fluoride solution. They reported that Ag deposited preferentially on the lower conductivity material regardless of conductivity type in the dark or with room light.

The purpose of this paper is to describe a method of obtaining very sharp p-n junction delineation on Si in acid fluoride displacement plating solutions without the aid of light. Waltz (5) and Wang (6) have deposited metals on Si by electrochemical displacement from acid fluoride solutions for the purpose of making ohmic contacts. Their solutions are not suitable for junction delineation.

Electrochemical displacement plating on Si.—One metal plates on another by electrochemical displacement when the depositing metal is more noble (electropositive) than the metal receiving the deposit. Plating is literally by displacement, for each milligram-equivalent of metal depositing on Si at cathodic sites, 1 mg-equivalent of Si dissolves at anodic sites. The total anode current, therefore, equals the total cathode current. The rate of metal deposition by displacement can be controlled by regulating the rate of the anode reaction. Silicon dissolves anodically by first forming an oxide. Unless the electrolyte is capable of dissolving the oxide, the anode reaction will stop after the oxide becomes a few atom layers thick. Displacement plating also will stop under these conditions. Silverman and Benn (2) were able to deposit Au on Si by displacement from a gold cyanide plating solution because hot strongly alkaline solutions dissolve silicon dioxide forming a soluble silicate complex:

$$SiO_2 + 2KOH \rightarrow K_2SiO_3 + H_2O$$

For the same reason, Cu can be deposited on Si by displacement in a hot alkaline Cu plating solution.

Hydrofluoric acid dissolves SiO_2 by forming a soluble silicofluoride complex:

$$SiO_2 + 6HF \rightarrow H_2SiF_6 + 2H_2O$$

The rate of Si dissolution at anodic sites, and therefore the metal deposition rate at cathode sites, in acid fluoride displacement plating solutions can be regulated by controlling the rate of mass transfer of HF from the solution bulk to the anode sites. This is done easily by adjusting the bulk HF concentration in the plating solution.

Experimental Methods and Results

Five different metals were deposited on Si by electrochemical displacement: Sb, Cu, Ag, Pt, and Au. The aqueous solutions contain simple metal salts plus different amounts of HF as shown in Table I. They are all used at room temperature. The metals in Table I are arranged according to the electromotive series. Antimony is the most electronegative of the group while Au is the most electropositive. The amount of HF used in each solution is believed to be optimum for the sharpest junction delineation. A 2-min treatment is usually sufficient to portray p-n junctions in the solutions of Table I. At lower HF concentrations, the time required for delineation increases, and the deposit often is not uniform. Higher HF concentrations result in rapid metal deposition on both sides of the p-n junction so that delineation is poor or impossible. At a given HF concentration, the rate of metal deposition by displacement on Si increases the more electropositive the metal. Therefore, Au will deposit faster than the other metals. Rates of metal deposition may be equalized, however, by decreasing the HF concentration as the metal becomes more electropositive as shown in Table I.

Table I. Solutions for junction delineation on Si

Metal deposited	Metal salt	g/l	cc 48% HF/l
Sb	SbF_3	400	500
Cu	$CuSO_4 \cdot 5H_2O$	200	10
Ag	$AgNO_3$	40	4
Pt	$H_2PtCl_6 \cdot 6H_2O$	3	2
Au	$AuCl_3$	10	0.3

Experiments were carried out with single crystal bars of n- and p-type Si, half-sections of crystals with pn junctions, and bars with either single or multiple rate-grown junctions. The surface was prepared by either lapping with No. 600 SiC on glass or bright etching in an acid mixture containing HNO_3, HF, and acetic acids.[1] Silicon samples are used immediately after lapping or etching.

Adhesion of metals deposited by electrochemical displacement is relatively poor as compared to electroplated deposits. This is due, at least in part, to the undermining action of the anodic reaction which tends to dissolve Si from under the metal deposited by displacement. As expected, the adhesion of displacement plated metals is better on abraded than on polished Si surfaces. The most adherent deposits were obtained with Sb and Cu on abraded surfaces. The relative adhesion of displacement plated metals on Si is lower the more noble the metal. Gold deposits have the poorest adhesion and on polished surfaces the deposit is usually pulled off by the surface tension of the solution as the sample is removed. Adhesion of the other metals deposited on chemically polished silicon was adequate for the purpose of portraying junctions.

The best resolution of pn junctions was obtained with Cu and Ag. Most of the experimental work was done with the aqueous solution containing 200 g/l $CuSO_4 \cdot 5H_2O$ and 10 cc 48% HF/l. For the remainder of the paper, it will simply be called the Cu solution.

The solutions in Table I will deposit metal uniformly on n- or p-type Si specimens with either abraded or polished surfaces.[2] If the Si contains a p-n junction and the surface is either all abraded or all chemically polished, metal again deposits fairly uniformly, and junction delineation is poor if discernible at all. This can be improved if the p-n junction area is illuminated with white light (2-4).

In order to obtain sharp p-n junction delineation on Si in the displacement plating solution without using light, it is necessary that the surface be partly polished[2] and partly abraded. An example of the results obtained is shown in Fig. 1. The photograph at the left shows a slice of a single crystal of Si about 2 x 2 x 0.2 cm thick, containing a grown p-n junction. The junction is visible as an inverted U with p-type on top. First, the entire slice was chemically polished and then the left half was abraded by rubbing with No. 400 Aloxite paper. The sample was immersed in the Cu solution for 2 min after which it

[1] The exact composition of the chemical polishing solution is: 5 parts by vol. conc. HNO_3, 3 parts by vol. 48% HF, and 3 parts by vol. glacial acetic acid. This is identical with the etching solution known as C.P.-4 except no bromine is added.

[2] Either a chemically or a mechanically polished surface is satisfactory. A chemically polished surface was used in most of the work to be described here.

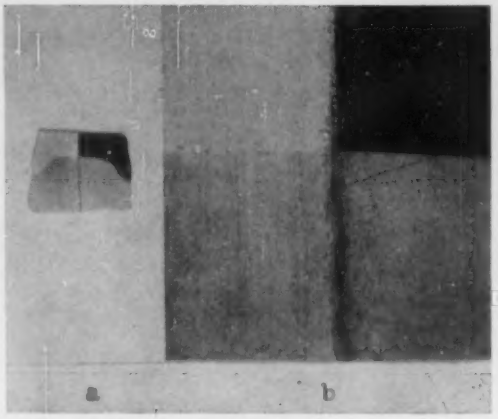

Fig. 1. P-N junction delineation on Si in the $CuSO_4$-HF solution with partly abraded and partly polished surfaces; p-region is the top half of crystal; left side is abraded while the right side is chemically polished. (a) View of large slice 2 cm x 2 cm; (b) magnified view of central region of (a).

was rinsed in water and air dried. The heaviest Cu deposit appeared at the top left on abraded p-Si while the least amount was on polished p-Si. An intermediate amount of Cu deposited on both abraded and polished n-Si. An enlarged view of the center of the specimen is shown in Fig. 1b. Good junction delineation is evident on both abraded and polished surfaces, but the greatest contrast is on polished Si.

If the junction area is illuminated with a strong light in the displacement plating solution, the results on abraded surfaces are about the same as without light. On the polished side of the crystal, however, the pattern is reversed and more Cu deposits on p-Si than on n-Si but only where the surface is illuminated. Polished areas that are not strongly illuminated behave as shown in Fig. 1. Whoriskey (3) and Iles and Coppen (4) reported that, under strong illumination, metal deposits more rapidly on n- than p-type Si. These results are obtained only when the Si is covered with a thin layer of plating solution. If the Si is immersed in a large volume of solution, a heavier deposit appears on p- than on n-Si with illumination as described previously. The reason for this reversal is not understood at present.

There is another way of obtaining sharp junction delineation on polished Si without using light or abrading part of the surface. This method requires a metal electrode connected to the p-type Si by means of an ohmic contact. The metal electrode should be the same as the metal deposited by displacement and is immersed in the plating solution along with the Si. An example of junction delineation obtained by this process in the Cu solution is shown in Fig. 2. This is a highly magnified view of the surface of a Si bar containing multiple rate-grown p-n junctions. Copper has deposited on the n-regions but not on p-type Si. This example also demonstrates the high resolution of junction delineation which is possible in displacement plating solutions. The narrow n-region in the center of the photograph is about 10 μ wide at the extreme left and is clearly visible down

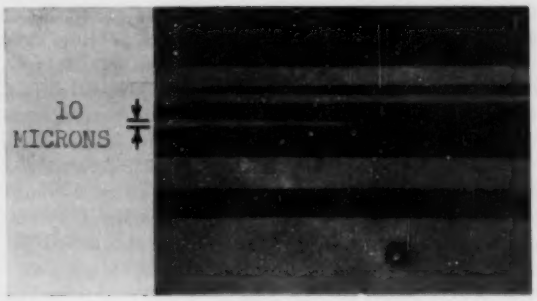

Fig. 2. An example of the high resolution of junction delineation on polished Si in the $CuSO_4$-HF solution. Surface of sample contains multiple rate-grown pn junctions. Copper deposit appears only on n-Si (light areas).

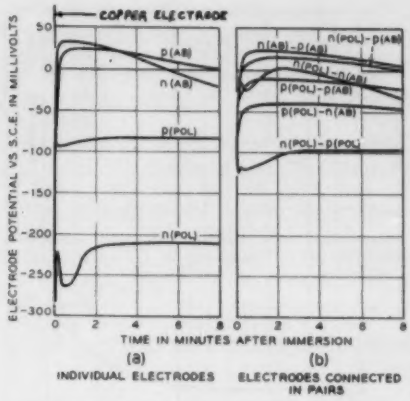

Fig. 3. Electrode potential-time curves of abraded and polished n- and p-type Si in the $CuSO_4$-HF solution.

to about 2 μ as it tapers to the right. The process also shows up abrupt changes in the impurity concentration at the surface of a Si crystal.

Junction Delineation on Germanium

Attempts were made to produce sharp pn junction delineation on Ge in the same displacement plating solutions used for Si. The results on Ge were not good as the junction was poorly defined if detectable at all. Some improvement was obtained with higher HF concentrations. The inherent differences in the electrochemical and semiconductor properties of Ge and Si probably make it impossible to obtain as sharp junction delineation on Ge as is obtained on Si in displacement plating solutions.

Mechanism of Junction Delineation

Electrochemical displacement plating on Si involves Si dissolution as well as metal deposition. It has been found that, if Si is attacked by an electrolyte, a large excess of holes and electrons is produced at the surface (7). These excess holes and electrons diffuse into the Si and change the concentration gradient of the minority current carrier between the surface and the Si bulk. The net result is to shift the measured potential of p-type Si toward more positive values while n-type Si changes in the negative direction. A similar effect is observed if excess holes and electrons are produced at the Si with illumination. The magnitude of the potential change is a function of the resistivity of the Si and the minority carrier lifetime.

The potentials of individual electrodes of n- and p-type Si with abraded and polished surfaces were measured against a saturated KCl calomel reference electrode (SCE) in an unstirred Cu solution. The electrodes were single crystal 0.7 ohm-cm n-type and 1.5 ohm-cm p-type Si. Number 400 Aloxite paper was used to prepare abraded surfaces while the polished electrodes were obtained by etching in the modified C.P.-4 solution previously described.

The recorded potentials vary with time as shown in Fig. 3a. The results show that there are considerable potential differences between abraded and polished Si and also between polished n- and p-type Si in the Cu solution. The potential of a Cu electrode in the Cu solution vs. SCE is also included in Fig. 3a for the purpose of comparison. A Cu electrode was used instead of abraded Si to bring out the junction in the experiment illustrated in Fig. 2.

All four Si electrodes exhibit large initial transients in potential. The two polished electrodes appear to reach steady potentials about 130 mv apart after 3 min immersion in the Cu solution. After the initial maximum, the potential of the abraded electrodes gradually became more negative and approached the steady potential values of polished Si electrodes. The reversal in potential between abraded n- and p-type Si after about 3 min is reproducible and is consistent with experimental results. On abraded Si, metal begins to deposit more rapidly on the n-side of a pn junction but later the rate of metal deposition becomes greater on p-Si than on n-Si.

In a voltaic cell, the negative electrode is the anode. Then according to the results of Fig. 3a, polished n-type Si is anodic to all the other electrodes. If all four types of Si electrodes are connected together in a single crystal, one would expect the least amount of Cu deposited on polished n-type Si. In actual practice, as demonstrated in Fig. 1, the least amount of metal is deposited on polished p-Si. The reason for this apparent anomaly is indicated by the results of connecting the electrodes of abraded and polished n- and p-type Si together in pairs as shown in Fig. 3b. The mixed potentials obtained are recorded as a function of time after immersion in the Cu solution. The three voltaic cells involving polished n-Si as the anode have mixed potentials very near the individual potentials of the cathode. This means that the current flowing between the electrode pairs is controlled by a polarizing effect at the polished n-Si. The effect is illustrated more clearly in Fig. 4 which shows the potential-current density relation of polished n-Si as the anode and polished p-Si as the cathode of a voltaic cell in the Cu solution. These curves were obtained by connecting the two electrodes together through a variable known resistance. The current between the electrodes was determined by measuring the *IR* drop across the shunting resistor while the electrode potentials were measured against the saturated calomel reference electrode. Initially a large resistance was placed be-

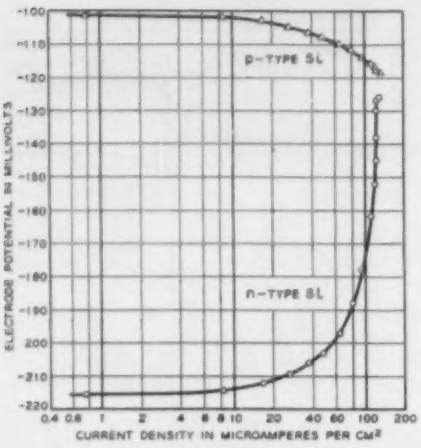

Fig. 4. Electrode potential-current density curves of polished n-Si anode and polished p-Si cathode of a voltaic cell in the $CuSO_4$-HF solution.

tween the two electrodes so the current flowing between them was small and the potentials were essentially those at open circuit. As the current between the electrodes was increased, by decreasing the shunting resistance, the potential of n-type Si acting as an anode changed more rapidly than p-type Si acting as a cathode. The maximum current flowing between the two electrodes therefore is determined primarily by the anodic polarizing effect on n-type Si.

Brattain and Garrett (8) and others have shown that holes are required to carry out anode processes on semiconductors. There is also evidence that cathodic processes on semiconductor electrodes require electrons (8-10). If the only source of holes and electrons at the surface of n- and p-type Si, respectively, is by diffusion from the bulk, then the saturation current of n-Si made anode and p-Si made cathode should be only a few microamperes per square centimeter. The results shown in Fig. 4 indicate that there must be another source for holes and electrons at the surface. As described earlier, holes and electrons are produced as a result of displacement plating. The additional holes available at the surface of the polished n-type Si electrode studied in the Cu solution allowed a maximum anode current density of about 130 $\mu a/cm^2$ when connected with a suitable cathode such as: polished p-Si, abraded Si, or a Cu wire. The maximum or saturation anode current density in the dark is a function of the equilibrium hole density and the diffusion length for holes in the surface region of the n-type Si electrode (9). This current flowing between n- and p-type Si should tend to deposit more Cu on p-Si than on n-Si. There are two electrolytic currents involved, however; one is between n- and p-type regions as just described and the other is between local anode and cathode areas that result in displacement plating. The reason that junction delineation is not obtained on an all polished Si crystal in the absence of strong light is that the rate of Cu deposition over all surfaces by electrochemical displacement is much greater than the deposition of Cu at different rates on n- and p-Si as a result of the potential difference. The displacement plating current density can be estimated from the total weight of Cu deposited in a given time. The amount of Cu deposited in 2 min from the Cu solution corresponds to an average current density of about 1.5 ma/cm^2, assuming equal anode and cathode areas and a Si dissolution valence of 4. This current density is about ten times the maximum current density between polished n-Si and polished p-Si when connected together as shown in Fig. 4. Shining light on the junction provides more holes on n-Si which increases the current flowing between n- and p-areas. This results in more Cu being deposited on p and less on n, thereby increasing the sharpness of junction delineation.

Polished p-type Si is cathodic to polished n-Si but is anodic to both abraded n- and p-Si and Cu as shown in Fig. 3a. Since holes are the majority current carrier in a p-type Si electrode, it can function as an anode up to relatively high current densities without the surface becoming depleted in holes. The current between polished and abraded p-type Si, therefore, can be about the same as the displacement plating current which results in a heavier Cu deposit on abraded p-Si and a corresponding lighter amount on polished p-Si. A Cu electrode, connected to polished p-type Si by means of an ohmic contact, behaves in the same manner as abraded p-Si in contact with polished p-Si in the Cu solution.

On the basis of the individual electrode potential measurements, abraded n-type Si should be as good a cathode in the Cu solution as abraded p-Si with respect to polished p-Si. However, current must flow between abraded n-Si and polished p-Si in the Si across the pn junction in the blocking direction to complete the electrical circuit. This limits the current between the two regions to a few microamperes and explains why the amount of Cu deposited on abraded n-Si is not as heavy as that obtained on abraded p-Si.

Summary and Conclusions

Electrochemical displacement of metals such as Cu and Ag and to a lesser extent, Sb, Au, and Pt can be used to delineate Si p-n junctions. Junction delineation is possible because of potential differences that are established between abraded and polished n- and p-type Si in displacement plating solutions. On the basis of these potential differences alone, the least amount of metal should deposit on polished n-type Si. This is not confirmed experimentally. Instead, polished p-type Si receives the least amount of metal. This is because polished n-Si cannot function as an anode at a high enough current density in the voltaic cell between n- and p-areas relative to the displacement plating current density. Shining light on the junction improves the junction portrayal because additional holes are produced by the light in n-type Si which increases the current in the voltaic cell between n- and p-surfaces.

Polished p-Si is capable of sustaining an anode reaction at relatively high rates without the aid of light. If connected to a suitable cathode, such as abraded p-Si or a Cu electrode in the Cu solution,

very little if any Cu deposits on polished p-Si while a substantial amount deposits on n-Si due to displacement plating. This produces a sharp junction delineation between n- and p-type Si.

Acknowledgment

The author wishes to acknowledge the assistance of George Peranteau in the experimental phase of the work and to U. B. Thomas for his helpful comments and discussion.

Manuscript received Feb. 2, 1959. This paper was prepared for delivery before the Ottawa Meeting, Sept. 28-Oct. 1, 1958.

Any discussion of this paper will appear in a Discussion Section to be published in the June 1960 JOURNAL.

REFERENCES

1. C. S. Fuller and J. A. Ditzenberger, *J. Appl. Phys.*, **27**, 550 (1956); C. S. Fuller, U.S. Pat. No. 2,740,-700, April 3, 1956.
2. S. J. Silverman and D. R. Benn, *This Journal*, **105**, 170 (1958).
3. P. J. Whoriskey, *J. Appl. Phys.*, **29**, 867 (1958).
4. P. A. Iles and P. J. Coppen, *ibid.*, **29**, 1514 (1958).
5. M. C. Waltz, U.S. Pat. No. 2,814,589, Nov. 26, 1957.
6. P. Wang, Recent News Paper, Electrochem. Soc. Meeting, New York (1958).
7. D. R. Turner and J. F. Dewald, To be published.
8. W. H. Brattain and C. G. B. Garrett, *Bell System Tech. J.*, **34**, 129 (1955).
9. J. B. Flynn, *This Journal*, **105**, 715 (1958).
10. D. R. Turner, Paper submitted to *This Journal*.

Diffusion of Radioactive Antimony in Silicon

J. J. Rohan, N. E. Pickering, and J. Kennedy

Radiochemistry Section, Electronic Material Sciences Laboratory, Electronics Research Directorate, Air Force Cambridge Research Center, Air Research and Development Command, Bedford, Massachusetts

ABSTRACT

The diffusion coefficient of radioactive Sb-124 in Si has been investigated in the temperature range 1190° to 1398°C, with use of a technique involving measurement of the residual integrated activity of the 0.602 Mev gamma before and after removing successive 2- to 4-μ layers perpendicular to the diffusion path. Results are compared to literature data obtained via p-n junction measurements. The diffusion coefficients are on the average about 85% higher than the literature values, while the activation energies are essentially the same. The temperature dependence of the diffusion coefficient is given by $D = 12.9 \exp(-91{,}700/RT)$ cm^2 sec^{-1} with an average error of $\pm 12\%$. Surface concentrations of Sb were in the range of 10^{19} to 10^{20} atoms cm^{-3}.

Studies of the diffusivities of donor and acceptor elements in semiconductors by means of radiotracers have been supplanted largely in recent years by methods involving the measurement of p-n junction distances. These methods (1, 2) which depend on the formation and location of p-n junctions within the crystals are faster and far less tedious than methods employing radiotracers. Up to the present, no comparison of results obtained by the two techniques appears to exist for diffusion in silicon. In germanium a radiotracer method gave diffusion coefficients for Sb which were 20 to 40% higher than those given by a p-n junction method (1, 3). Some indication that this might be the case for Sb in Si was noted in this laboratory in a study of the effect of various pressures of Sb_2O_3 vapor on the surface concentration of Sb on Si during diffusion anneals. With use of the data and techniques of Fuller and Ditzenberger (4), it was found in all cases that p-n junction measurements gave much larger values for the surface concentration, C_s, of Sb than radioactivity measurements when similar amounts of diffusant were heated in evacuated quartz tubes containing p-type single-crystal Si slabs. In these and the following experiments, boundary conditions were such that diffusion proceeded according to the error function complement equation. From p-n junction measurements then, the surface concentration, C_s, in atoms cm^{-3}, was calculated from:

$$C_s = C_o \operatorname{erfc} \frac{x}{2\sqrt{Dt}} \qquad [1]$$

where C_s is the concentration in atoms cm^{-3} of Sb at a junction located x cm from the surface of Si; D is the diffusion coefficient in cm^2 sec^{-1}, and t is the time in seconds at constant temperature. The diffusion coefficient, D, was presumed to be only temperature dependent and the surface concentration, C_s, presumed to be constant. Radioactivity measurements, described more fully later, gave C_o in terms of the total number of atoms N_T of Sb which diffused through one face of the Si slab. This is given by integration of Eq. [1] so that

$$N_T = GR_T = A\,C_o \int_0^\infty \operatorname{erfc} \frac{x}{2\sqrt{Dt}}\,dx = 1.13\,AC_o\sqrt{Dt} \qquad [2]$$

where R_T is the total activity, A is the area of the diffusion plane introduced here to account for the total number of diffused atoms, and G is a factor which relates activity to the number of atoms of Sb.

An example of the large discrepancies noted for values of C_o as found by both methods is given for a

diffusion anneal at 1380°C. From radioactivity measurements a value of $C_s = 4.3 \times 10^{19}$ atoms cm^{-3} was obtained while p-n junction measurements gave $C_s = 3.4 \times 10^{18}$ atoms cm^{-3}. The latter is consistent with a mean value obtained by Fuller and Ditzenberger (4) at the same temperature with similar amounts of Sb_2O_3, but is inconsistent with the expected solid solubility of Sb in Si even if saturation had been reached. The binary alloy system Sb-Si belongs to a class whose liquid phases are "regular" solutions and whose solid phases exhibit the phenomenon of retrograde solubility, as has been shown by Thurmond and Struthers (5). They have also shown that the logarithm of the distribution coefficient k of the solute (Sb in this case) between the solid and liquid phases of such systems is a linear function of the reciprocal of absolute temperature near the melting point of the solvent. Extrapolation of this line to the k corresponding to the melting point of the solvent (Si) gives the maximum value or segregation coefficient. The latter has been found by direct measurement to be 0.04 for Sb in the Sb-Si system (6). However, a value of 1.4 is calculated for the distribution coefficient of Sb in Sb-Si at 1380° from the C_s obtained by p-n junction measurement and the solubility of Sb in the liquid phase at this temperature (5, 7).

Apparently then C_s values for Sb in Si calculated from p-n junction measurements and the values of D given by Fuller and Ditzenberger can be too high by one or two orders of magnitude. One explanation for this is that too low values of D were used in the calculation. In the preliminary work and in much of Fuller's, the quantity $x/2\sqrt{Dt}$ had a numerical value of 2 or greater; relatively small changes in the value of erfc in such cases can lead to very large changes in C_s as calculated from Eq. [1], which is apparent on examination of tables of the error function. For example, a 50% increase in D at constant x and t can effect a tenfold reduction in C_s as calculated by Eq. [1] (p-n junction), whereas with Eq. [2] (radiotracer) the effect is to reduce C_s by only 20%. In view of the foregoing observations, it was decided to re-examine the diffusion of Sb in Si using radiotracer Sb-124 exclusively.

Discussion of Methods

Where the concentration of radioactive diffusant does not change appreciably over short distances (several microns) along the diffusion path, a method based on counting the activity in thin parallel segments of the matrix ground onto emery paper, or similar abrasive, has been used successfully for the determination of diffusion coefficients in highly impenetrable single crystals. Such concentration profiles require that the penetration parameter $\sqrt{Dt}$ be of the order of 10^{-5} cm, or greater, to insure any degree of precision and were accomplished in the case of Sb in Ge with anneal times of less than 10 days (3). However, in the case of Si in which Sb is one of the slowest diffusing elements, it would take up to 100 days to produce comparable penetrations; hence, a more suitable procedure was desired.

An alternate method for the radioassay of diffused Sb-124 in Si is to count the integrated gamma activity of a crystal following removal of thin layers parallel to one surface. On decay of Sb-124, beta particles and gamma rays are emitted. Of the several gamma rays emitted the principal one has an energy of 0.602 Mev and is virtually unabsorbed by the small thicknesses of Si encountered here. The count rate of the 0.602 mev gamma rays is therefore directly proportional to the total number of Sb atoms at all depths within the Si crystal. When the edges and one face of the crystal have been removed by grinding to depths below which the concentration of Sb is negligible, only unidimensional diffusion need be considered. The number of residual Sb atoms, N_x, in the crystal lapped down to a plane x cm below and parallel to the remaining original surface is

$$N_x = GR_x = A\,C_s \int_x^\infty \operatorname{erfc} \frac{x}{2\sqrt{Dt}}\,dx$$

$$= A\,C_s \sqrt{Dt} \left[\frac{2}{\sqrt{\pi}} \exp\left(-\frac{x^2}{4Dt}\right) - \frac{x}{\sqrt{Dt}} \operatorname{erfc} \frac{x}{2\sqrt{Dt}} \right] \quad [3]$$

where R_x is the residual 0.602 Mev gamma activity.

If C_s is known, D can be obtained directly from Eq. [3] by successive approximations using tables of the error function and its first derivative (8), (the first term inside the bracket). Since C_s is usually not known, the integral count rates, R_1 and R_2, at two depths, x_1 and x_2 may be combined to give:

$$\frac{N_1}{N_2} = \frac{R_1}{R_2} = \frac{\phi_1}{\phi_2} \quad [4]$$

where ϕ represents the terms inside the bracket of Eq. [3], and is a function of x only. Again, by successive approximations, a value for D is found which satisfies the ratios of Eq. [4].

Experimental

Samples of single-crystal Si, 200 ohm-cm n-type, 8 mm on a side and 1 mm thick, were prepared by hand lapping on glass through 3200-mesh abrasive suspended in water. They were then brought to a semi-mirror finish by a short final lapping with ¼-μ Diamet Hyprez on a silicon flat; in all cases the flatness of the samples, measured optically, was at least ± 0.1 μ out to the edges. After cleaning, the samples were washed successively in conc HNO_3 and conc HF. Two such specimens were sealed at 10^{-6} mm of air in quartz ampules containing 200 to 500 μg of radioactive Sb_2O_3. In the latter, obtained by neutron irradiation at Brookhaven National Laboratory, about 1 at. in every 10^6 at. of Sb was Sb-124. Before irradiation, the impurity content of the oxide was determined by spectroscopic analysis; the impurity content was low enough not to give rise to undesirable extraneous radioactivity. The samples were annealed in a graphite-resistor vacuum furnace which was maintained at constant temperature by a Minneapolis-Honeywell Radiamatic unit. This unit was calibrated against the melting points of Cu, Si,

and Ni contained in quartz ampules. Temperature measurement and control was ±4°C. Temperature rise and decay times in this furnace were such that no time correction was needed for samples diffused over 24 hr. At the highest temperature investigated (1398°C), the anneal was done in a globar-heated tube furnace where the samples could be introduced and withdrawn quickly. In nearly all cases, times were chosen so that the value of $\sqrt{Dt}$ would be at least 5 x 10^{-4} cm, in order to insure that count rates would not change by over three orders of magnitude while lapping through a depth of 15 μ or more.

After removal from the furnace, the samples were washed in 48% HF to remove possible oxides. The edges and one of the faces were ground off to a depth far below that at which no change in count rate was observed and autoradiographs of the active faces were taken. The samples were then weighed to constant weight on a microbalance and an initial count rate for each sample was determined. A layer of uniform thickness (2 to 4 μ in most cases) was then ground off each sample by hand lapping with 3200-mesh abrasive on glass. This process effects a clean separation between matrix and ground-off material; no extraneous activity on the matrix due to adhesion of ground-off layers was noted.

The process of grinding, weighing, and counting was repeated until the activity dropped to a value below which further processing would be impractical. All counting was done in a well-type gamma scintillation detector coupled to a single-channel spectrometer. All sample count rates were compared to the count rate of a standard of known total Sb content; backgrounds were determined at least twice a day. In most cases total counts were collected so as to give a counting error of 1% or less with 95% confidence.

Results

Evaluation of D.—The thickness of sample layers removed at each cut was calculated from the weight loss and the cross-sectional area of the sample using a density of 2.33 for Si[9]. All of the data from six temperature anneals are too bulky to reproduce here; however, an example of the basic data used in calculating D for the run at 1330°C is given in Table I.

The ratio of successive count rates and the corresponding values of x were substituted from Table I into Eq. [4] and D's were calculated for successive combinations as shown in Table II. The mean value of the D's thus calculated was taken as the final value for each sample.

Evaluation of C_s.—The surface concentration C_s was calculated from Eq. [2], substituting the mean value of D found for each sample and the corresponding total number of Sb atoms. This could be done in all cases where no extraneous surface activity was found on the samples as checked by autoradiography.

The results of six temperature anneals are summarized in Table III.

The temperature dependence of the diffusion coefficient of Sb in Si found in these experiments is expressed by the following equation:

$$D = 12.9 \exp(-91{,}700/RT) \text{ cm}^2 \text{ sec}^{-1} \qquad [5]$$

which is the least squares equation of the data in Table III, omitting the data from the run at 1355°C. The solid line in Fig. 1 is a plot of Eq. [5]; the experimental points represent the mean D value of the two samples at each temperature. The latter fall on or are close to the line except the point correspond-

Table I. Example of basic diffusion data*

Cut No.	Wt. loss per cut, μg		Total depth (x), μ		Count rate (R), counts min^{-1}	
	A	B	A	B	A	B
0	—	—	—	—	119,138	96,361
1	515	241	5.92	3.07	65,127	70,980
2	246	244	8.74	6.19	44,084	47,819
3	359	179	12.9	8.48	22,738	36,092
4	374	248	17.2	11.65	10,266	22,276
5	387	269	21.6	15.1	4,155	11,553
6	304	290	25.1	18.8	1,725	5,180
7	170	297	28.2	22.6	794	2,396
8	356	325	32.3	26.7	248	790
9	—	141	—	28.5	—	514

* Temperature, 1330°C; time, 49 hr;
Sample A: Area 0.373 cm², G 3.825 x 10^{11} at. count^{-1} min^{-1}
Sample B: 0.336 cm² 4.390 x 10^{11} at. count^{-1} min^{-1}.

Table II. Example of method for obtaining mean value of D*

Combination	Sample A D (cm² sec^{-1})	Sample B D (cm² sec^{-1})
1-2	4.01 × 10^{-12}	4.10 × 10^{-12}
2-3	3.80 × 10^{-12}	4.69 × 10^{-12}
3-4	3.77 × 10^{-12}	4.10 × 10^{-12}
4-5	3.93 × 10^{-12}	3.40 × 10^{-12}
5-6	3.84 × 10^{-12}	3.32 × 10^{-12}
6-7	3.85 × 10^{-12}	4.10 × 10^{-12}
7-8	3.69 × 10^{-12}	3.36 × 10^{-12}
8-9	—	4.10 × 10^{-12}
Mean	3.84 × 10^{-12}	3.90 × 10^{-12}
σ(rms)	±0.09 × 10^{-12}	±0.46 × 10^{-12}
% σ(rms)	±2.34	±11.8

* Temperature, 1330°C; time, 49 hr;
Sample A: Area 0.373 cm², G 3.825 x 10^{11} at. count^{-1} min^{-1}
Sample B: 0.336 cm² 4.390 x 10^{11} at. count^{-1} min^{-1}.

Table III. Summary of results

Sample	Temp, °C	Time, hr	D x 10^{12} cm² sec^{-1}	C_s x 10^{-19} at. cm^{-3}
A	1190	144	2.46 ± 0.25	2.4
B	1190	144	2.83 ± 0.48	1.9
A	1230	144	5.81 ± 0.91	—[c]
B	1230	144	5.82 ± 0.82	—[c]
A	1280	93	16.2 ± 3.8	4.5
B	1280	93	16.2 ± 1.0	5.0
A	1330	49	38.4 ± 0.9	4.9
B	1330	49	39.0 ± 4.6	4.5
A	1355	24	104 ± 7	3.5
B	1355	24	103 ± 8	3.5
A	1398	2	135 ± 18	3.1
B	1398	2	—[b]	3.2[c]

[a] Surface contamination; [b] sample destroyed in processing; [c] calculated from the N_T of B and the D of A.

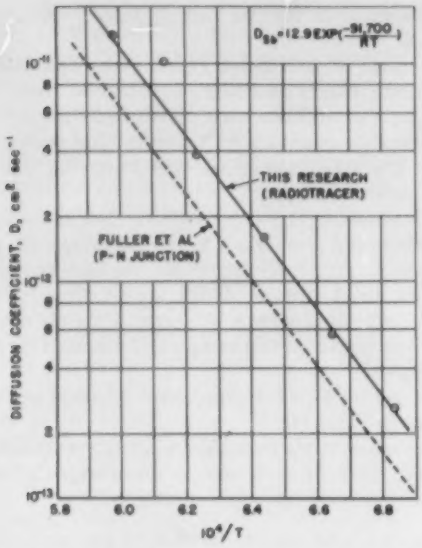

Fig. 1. Diffusion coefficients of Sb in Si plotted against reciprocal of absolute temperature.

ing to the 1355°C run. It is probable that this deviation was caused by the temperature being much higher than recorded, since some difficulties were experienced with the temperature controller during that run. For comparison a plot of the temperature dependence of the diffusion coefficient of Sb in Si as given by Fuller and Ditzenberger's equation (4),

$$D = 5.6 \exp(-91{,}000/RT) \text{ cm}^2 \text{ sec}^{-1} \qquad [6]$$

is shown (dashed line). It can be seen that, whereas both tracer and p-n junction methods gave ΔH values which are in essential agreement, the values of D obtained by the tracer method averaged about 85% higher than those by the p-n junction method in the temperature range studied.

Discussion of Results

It is difficult to analyze quantitatively the effect of all possible errors on the values of D, C_s, and ΔH reported here. The error in counting has been mentioned previously; however, this error is based on the statistics of random process. A more practical error to consider here is that of reproducibility. In our counting assembly, count rates were reproducible to ±2% which leads to errors of ±4% in the ratio of Eq. [4]. Cumulative weighing errors of ±2 μg lead to errors in the estimation of lapping depths of ±0.02 μ; such precision, however, means little in view of the fact that parallel lapping was assumed but not proved.

The most serious errors in the value of D could be due to nonparallel lapping; the effect of misalignment of the plane of lapping with respect to the plane of the original crystal face can result in a value for D which is high compared to the true value in all cases. By assuming various geometries of misalignment it is possible to estimate the error in D due to this source. This was done for various geometries and degrees of misalignment, and it was found that the worst conceivable situation would produce an error in D of about +25%. However, toward the end of this work it was possible to check the geometry and degree of misalignment by means of a Zeiss optimeter capable of measuring thicknesses with an accuracy of ±0.2 μ. These measurements indicated that the degree of misalignment was indeed small and that confidence in the inherent simplicity of hand lapping was justified. Experiments with various machines and jigs led to the conclusion that these could introduce systematic errors which would be more serious than the random errors produced by hand lapping.

Errors might also accrue due to loss of sample surface by evaporation. It was felt that such losses would be small in a closed system; this was confirmed both by micrometric measurements and by the fact that the original semi-mirror finish of the samples was preserved (although some pitting was noticed). The question of whether the diffusion coefficients obtained are truly representative of bulk diffusion has not been fully resolved. This question arises from the fact that the samples were not etched after grinding flat. It is possible that the worked surfaces and the layers immediately below might provide an easier path for diffusant penetration than would the bulk material. Indeed it was found that values of D calculated from the data of cut combinations 0-1, 0-2, etc., were much higher than the mean value in all cases. Such values for D, therefore, were not included in calculating the mean; however, it will be noted from the representative data of Tables I and II that this effect was not noticeable beyond a depth of a few microns. Samples were left in the ground state because even the most rigorously controlled etching always produced uneven surfaces that would be very poor planes of reference for such relatively shallow diffusion penetrations.

The over-all effect of all the possible errors, as well as the assumptions made in carrying out these experiments, may be illustrated by comparing the experimental diffusion of Sb into Si with that predicted by Eqs. [2] and [3]. These equations may be combined to express the fraction of total diffused atoms remaining in the crystal, i.e., after grinding down to a plane x cm below the surface, as follows:

$$\frac{N_x}{N_T} = \frac{R_x}{R_T} = \frac{\phi}{1.13} \qquad [7]$$

Figure 2 is a plot of theoretical residual atom fractions at various depths calculated from Eq. [7], substituting for $\sqrt{Dt}$ the value 8.26×10^{-4} cm corresponding to the mean value found from the diffusion anneal at 1330°C (Table II). The points are the experimentally determined count rate ratios; it is apparent that these follow the theoretical curve within experimental error. For the sake of clarity only one such curve is shown in Fig. 2, viz., that which may be verified by the data given; however, for other temperature anneals the fit of the experimental penetration with the theoretical was even more striking. Despite the fact that the rms deviations in the value of D's of the two samples in any temperature run varied considerably between samples, it

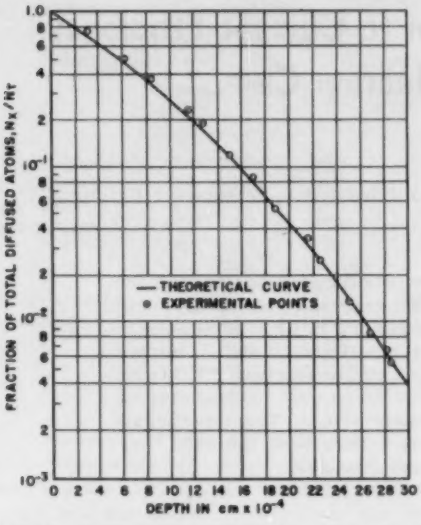

Fig. 2. Plot comparing experimental with theoretical diffusion of Sb in Si at 1330°C.

should be noted that the mean D values of both samples were in very close agreement (Table III). Such agreement, coupled with the good fit of the experimental penetration with the theoretical, seems to indicate that all of the assumptions made were vindicated and that the D's represent true bulk diffusion with an average error of ±12% which represents the mean of all the individual sample errors. From this and the closeness of the experimental points to the log D vs. $1/T$ line in Fig. 1, the estimated error in ΔH is about 1%.

Errors in C_s reflect the errors in D and the conversion factor G. The latter, from a series of calibrations, is estimated to be about ±5%. Thus, the error in C_s is about 12%.

Conclusion

Diffusion coefficients of Sb in Si measured by a radiotracer technique were found to be considerably higher than those reported in the literature where a p-n junction technique was used. The results confirmed the belief that p-n junction measurements gave too low values for D, since abnormally high values for the surface concentration of Sb on Si are calculated when p-n junction values of D are used. Surface concentrations calculated from the diffusion coefficients found in this investigation were found to be within the range expected for unsaturated Si surfaces. No explanation is offered at this time for the disagreement between the results as obtained by the two methods pending the completion of further studies using tracer acceptor elements as diffusants.

Since this work was completed, it has come to the attention of the authors that the diffusion of Sb in Si has been investigated using Sb-124 (10). Details of these experiments are insufficiently explicit to warrant comment; however the results of the work, expressed by the equation $D = 0.112 \exp(-66{,}000/RT)$ $cm^2\ sec^{-1}$ is in complete disagreement with both the authors' results and those of Fuller and Ditzenberger.

Acknowledgments

The authors are indebted to Mrs. Thelma B. Salmas for assistance in sample preparation and checking calculations; to Henry M. DeAngelis for stimulating discussions; and to Joseph R. O'Connor for furnishing the single-crystal silicon.

Manuscript received Feb. 2, 1959. This paper was prepared for delivery before the New York Meeting, April 27-May 1, 1958.

Any discussion of this paper will appear in a Discussion Section to be published in the June 1960 JOURNAL.

REFERENCES

1. W. C. Dunlap, Jr., *Phys. Rev.*, **86**, 615 (1952); D. E. Brown and W. C. Dunlap, Jr., *ibid.*, **86**, 616 (1952); W. C. Dunlap, Jr. and D. E. Brown, *ibid.*, **86**, 417 (1952).
2. C. S. Fuller, H. C. Theuerer, and W. VanRoosbroeck, *ibid.*, **85**, 678 (1952); C. S. Fuller, J. D. Struthers, J. A. Ditzenberger, and K. B. Wolfstirn, *ibid.*, **93**, 1182 (1954).
3. W. C. Dunlap, Jr., *ibid.*, **94**, 1531 (1954).
4. C. S. Fuller and J. A. Ditzenberger, *J. Appl. Phys.*, **27**, 544 (1956).
5. C. D. Thurmond, *J. Phys. Chem.*, **57**, 827 (1953); C. D. Thurmond and J. D. Struthers, *ibid.*, **57**, 831 (1953).
6. R. N. Hall, *ibid.*, **57**, 836 (1953); J. A. Burton, *Physica*, **20**, 845 (1954).
7. M. Hansen, "Aufbau der Zweistofflegierungen," Springer, Berlin (1936).
8. "Tables of the Error Function and Its Derivative," National Bureau of Standards Applied Mathematics Series 41, 1954.
9. W. C. Dunlap, Jr., "An Introduction to Semiconductors," John Wiley & Sons, Inc., New York (1957).
10. D. A. Petrov, IV. M. Shashkov, and I. P. Akimchenho, Transactions of the Second Conference on Semiconductors (Questions of the Metallurgy and Physics of Semiconductors. Akademiia Nauk Press, Moscow, 1957, ed. D. A. Petrov) Needham Heights, Mass: M. D. Friedman, Inc.

The Relation of Gas Composition to Current Efficiency in an Aluminum Reduction Cell

T. R. Beck

Metals Division Research, Kaiser Aluminum & Chemical Corporation, Permanente, California

ABSTRACT

Experience with a 10,000-amp aluminum reduction cell indicates that the previously accepted equation relating current efficiency and cell gas CO_2 concentration is an oversimplification. A modified equation, $\%\ CE = g[50 + \frac{1}{2}(\%\ CO_2)] - Z$, fits the data more satisfactorily. The new terms, g and Z, respectively, account for: (*a*) less than 100% initial CO_2 and/or reaction of CO_2 with carbon, and (*b*) a certain percentage of current inefficiency by oxidation or loss of some cathode products without involvement of CO_2. The experiments showed g to be somewhat larger than unity and to vary with the bake temperature of the anodes and Z to be somewhat larger than 3.5%.

This paper describes work done on a 10,000-amp experimental aluminum reduction cell. The cell was established for studying process variables that could not be studied satisfactorily in any other way. It was of such a size that results could be scaled up to apply directly to the present commercial cells. Although it was only 1/6 to 1/10 the size of present commercial cells, it was comparable in size to the commercial cells of three decades ago (1). Because it was operated as an independent unit with its own power supply and was not tied to a production schedule, experiments and measurements could be made and an accuracy obtained that would be virtually impossible to attain under plant conditions. Significantly smaller self-sustaining cells operating at commercial current densities are difficult to operate because of proportionately higher heat losses for their greater surface-to-volume ratio. Scale-up from still smaller externally heated bench scale cells to full scale plant cells is open to question.

In construction and dimensions it was equivalent to placing the two ends of a commercial prebaked-anode cell together after removing the center section. Dimensions of the cavity were approximately 43 in. x 65 in. cross section by 14 in. deep. Plant anodes and superstructure hardware were used. Anode dimensions were 15½ in. x 19½ in. cross section by 12 in. high.

Early in the program a test was made to evaluate the effect of anode-bake temperature on carbon consumption. Routine cell gas analyses for CO_2 and CO were made in order to determine what fraction of the carbon consumption could be attributed to the electrochemical reaction. Correlation of these gas analysis data with current efficiency was the basis for this paper.

Experimental

Anodes for use in this study were pressed and baked at the Corporation's Mead Works near Spokane, Washington. Thermocouples were installed in the baking pits to determine the maximum temperatures reached during the bake. From these data maximum-temperature-isotherms were drawn for the pits, and anodes were segregated into suitable bake temperature ranges for use in the 10,000-amp cell tests.

Each test lasted four weeks and consumed approximately 19 anodes. Each of the four anodes in the cell was changed every six days on a regular schedule. A one-week transition period between tests was used to install a new complement of anodes.

Cell conditions were held as constant as possible during the test series. Anode-cathode distance was maintained at 2 in. for all but the last three runs at which it was 1½ in. Bath composition was 89% cryolite at 1.5 NaF: AlF_3 ratio, 8% calcium fluoride, and 3% alumina. Bath temperature was maintained at 975°-985°C. Current varied from 9500 to about 11,000 amp during the course of the experiments because the power input was increased to compensate for increased heat losses as bath penetrated the insulation and because the last three runs were made at a lower anode-cathode distance.

Gas composition was measured with an Orsat gas analyzer at 2-hr intervals half way between hourly feedings of alumina. The cell gas was collected through a steel bell placed on the crust of the cell as shown in Fig. 1. The gas was drawn through Inconel and rubber tubing to the gas analyzer. The

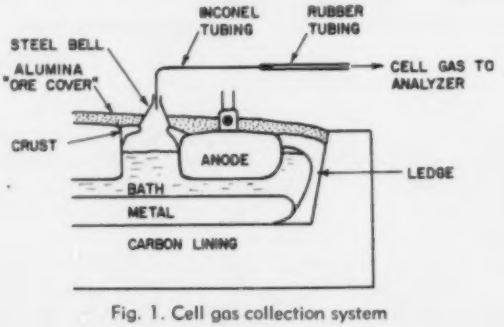

Fig. 1. Cell gas collection system

Table I. Experimental data for various bake temperature anodes. Each point represents one four-week test

	Current eff.	% CO_2	Avg. est. anode bake temp, °C	
Low-bake-temperature anodes	85.5	69.3	946	959
	86.9	71.8	972	
Medium-bake-temperature anodes	86.7	77.4	1071	1070
	88.9	79.7	1070	
High-bake-temperature anodes	86.8	80.7	1142	Approx. 1150
	85.5	78.5	1110-1190	
	86.4	79.0	1110-1190	
	88.2	81.1	1110-1190	
	86.5	78.7	1110-1190	
	84.4	77.4	1110-1190	
	84.1	75.9	1110-1190	

crust, composed of frozen cryolite, was continuous except for the single vent which was used for feeding and gas collection so there was a negligible leakage of air into the system. Reaction of the cell gas within the Inconel sample tube appears unlikely because the measured gas composition did not vary with the rate that the gas was sampled. The gas was cool before it entered the rubber tubing.

Results

The experimental data are presented in Table I and Fig. 2. Current efficiency did not vary significantly with anode-bake temperature, but per cent of CO_2 in the cell gas increased with increasing bake temperature. The low-bake-temperature-anode data are above the previously accepted Pearson and Waddington correlation (1, 2), and the high-bake-temperature-anode data are below it. There is a certain scattering of the data, but there is an unmistakable trend with anode bake temperature. For a given bake temperature, the data roughly parallel the Pearson and Waddington correlation although the slope appears to be slightly steeper.

The first four groups of anodes were run in random order to cancel the effect of cell aging. The remaining seven groups were run in the order listed.

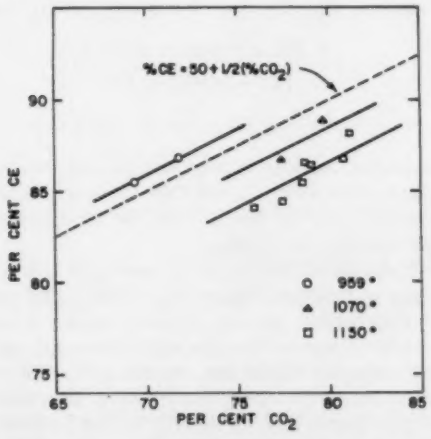

Fig. 2. Experimental data for various bake temperature anodes. Each point represents one 4-week test.

The range of current efficiency from 85.5 to 88.9% can be attributed to small changes in the operating conditions, unavoidable in an aluminum reduction cell. The 84% current efficiency in the last two runs was the result of the lower anode-cathode distance. Despite some variations in cell conditions the data for each bake temperature fell on its characteristic line. The regular deviation suggested that there were some factors ignored in the original derivation of the Pearson and Waddington equation so a more comprehensive equation was derived.

Discussion

The Pearson and Waddington equation

$$\% \text{ CE} = 50 + \tfrac{1}{2}(\% \text{ CO}_2)$$

is based on the following assumptions: (*a*) initial anode product is 100% carbon dioxide, and (*b*) carbon monoxide is produced by reduction of carbon dioxide by cathode products, i.e.,

$$CO_2 + \begin{Bmatrix} 2Na, \\ Al, \\ 2/3Al, \\ \text{etc.} \end{Bmatrix} \rightarrow CO + \begin{Bmatrix} 2Na^{+}, \\ Al^{+++}, \\ 2/3Al^{+++} \\ \text{etc.} \end{Bmatrix} + O^{=}$$

A plot of the Pearson and Waddington equation is shown in Fig. 3 with the directions of the deviations due to errors in the assumptions.

Case I is a decrease in per cent CO_2 without a change in current efficiency. This can result from primary and/or secondary formation of CO. These are inseparable in the data presented here but could perhaps be separated using a radio-carbon technique. It must be borne in mind that there is always the possibility of introduction of air during sampling which will give a low apparent CO_2, especially with plant cells which often do not have a continuous solid crust. It is felt that this error is not significant in the work with the Permanente cell because of the continuous solid crust. The nitrogen content of the samples was usually less than 1%. Small amounts of other gases have been found in reduction cell gas but not in sufficient amount to affect the results presented here significantly. Hydrogen, hydrogen sulfide, and carbonyl sulfide have been found in concentrations of a few tenths of a per cent or less (3). Formation of fluorocarbons appears to be limited to periods of anode effect (3).

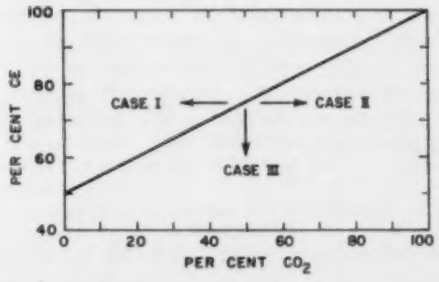

Fig. 3. Deviations due to errors in derivation assumptions for Pearson and Waddington equation.

Case II is an increase in per cent CO_2 without a change in current efficiency. A possible reaction is the formation of free carbon and CO_2 by disproportionation of CO as the pot gas temperature is reduced. No measurable amount of this free carbon formation was found with the Permanente cell.

Case III is a decrease in current efficiency without a change in the gas composition. There are a number of mechanisms that can lead to this condition. The more important possibilities are as follows. (*a*) escape of sodium from the cell or oxidation of sodium by air (Pockets of sodium metal are frequently found in the crust of the Permanente cell, substantiating this mechanism.); (*b*) direct oxidation of sodium, monovalent aluminum, or "metal fog" at the anode without the intervention of CO_2; (*c*) electronic conduction through the bath or through short circuits between anode and cathode by metal splashing or accumulated carbon "dust;" (*d*) formation of sodium and/or aluminum carbides with the lining; and (*e*) oxidation of aluminum during tapping.

Case IV, an increase in current efficiency without a change in gas composition, is not possible because it would require more than Faraday's equivalent of metal formed at the cathode.

The deviations of the experimental data in Fig. 2 can be explained by these reactions. For all three sets of data, the deviation below the Pearson and Waddington line due to Case III would be expected to be about the same. Anode quality would hardly be expected to affect significantly the factors that make up Case III. The shift in the lines to the left with lower-bake-temperature anodes can be explained by Case I.

The more general relation between current efficiency and gas composition is derived as follows:

Initial cell reaction

$$2Al_2O_3 + (6-n)\,C \rightarrow 4Al + nCO_2 + (6-2n)\,CO \quad [1]$$
$$0 \leqq n \leqq 3$$

Equivalent inefficiency reaction

$$2/3Al + CO_2 \rightarrow 2/3Al^{+++} + CO + O^{=} \quad [2]$$

Reaction of CO_2 with carbon

$$CO_2 + C \underset{y_2}{\overset{y_1}{\rightleftarrows}} 2CO \quad [3]$$

$$\% \text{ CE} = \frac{A - C - D}{A + B} \times 100 \quad [4a]$$

where A = equivalents of Al (or Na, etc.) initially formed; B = equivalents of electrons carried by electronic conduction; C = equivalents of Al reoxidized by CO_2; and D = equivalents of Al lost or reoxidized without CO_2.

To simplify the derivation the following transformation is made

$$A' = A + B$$
$$E = D + B$$
$$\therefore \% \text{ CE} = \frac{A' - C - E}{A'} \times 100 \quad [4b]$$

$$\% \text{ CO}_2 = \frac{CO_{2(p,1)} - CO_{2(r,2)} - CO_{2(r,3)}}{CO_{2(p,1)} + CO_{(p,1)} - CO_{2(r,2)} + CO_{(p,2)} - CO_{2(r,3)} + CO_{(p,3)}} \times 100 \quad [5]^*$$

Per each Eq. [1], assume x Eq. [2] and y Eq. [3]. (Note: y is the net number of CO_2's lost, i.e., $y = y_1 - y_2$ since the reaction is reversible.) $\therefore A' = 4$, $C = (2/3)\,x$, and $E = 4Z/100$, where Z is percentage of current lost by Case III.

$$\therefore \% \text{ CE} = 100\left(\frac{4 - (2/3)x - 4Z/100}{4}\right) \quad [6a]$$

and

$$\% \text{ CO}_2 = 100\left(\frac{n - x - y}{n + 6 - 2n - x + x - y + 2y}\right) = 100\left(\frac{n - x - y}{6 - n + y}\right) \quad [6b]$$

Eliminating x from [6*a*] and [6*b*] gives

$$\% \text{ CE} = \frac{6 - n + y}{3}\,[50 + \tfrac{1}{2}(\% \text{ CO}_2)] - Z \quad [6c]$$

The fraction of the initial CO_2 reacting by Eq. [3] is $f = y/n$

$$\therefore \% \text{ CE} = \frac{6 - n + nf}{3}\,[50 + \tfrac{1}{2}(\% \text{ CO}_2)] - Z \quad [7]$$

$$\% \text{ CO}_2 \text{ in primary gas} = 100\left(\frac{n}{6 - n}\right) \quad [8]$$

Substituting the value for n [Eq. 8] in Eq. [7]

$$\% \text{ CE} = 2\left[\frac{1 + f\left(\frac{\text{initial \% CO}_2}{100}\right)}{1 + \frac{\text{initial \% CO}_2}{100}}\right][50 + \tfrac{1}{2}(\% \text{ CO}_2)] - Z \quad [9]$$

Because it is difficult to separate the effect of initial anode gas composition and the reaction of CO_2 with carbon, Eq. [9] may be simplified by letting

$$g = 2\left[\frac{100 + f(\text{initial \% CO}_2)}{100 + \text{initial \% CO}_2}\right]$$
$$\therefore \% \text{ CE} = g[50 + \tfrac{1}{2}(\% \text{ CO}_2)] - Z \quad [10]$$

This equation reduces to the Pearson and Waddington equation for 100% initial CO_2, no reaction of CO_2 with carbon, and no loss of cathode products other than by reaction with CO_2.

The theoretical limits for g are $g = 1$ to 2. A value of $g = 1$ means initial $CO_2 = 100\%$ and no reaction of CO_2 with carbon. A value of $g = 2$ means that undiluted gas leaving the cell is pure CO and no CO_2 reduction by metal has occurred. Except when the cell is on anode effect, the value of g appears to be closer to unity. The value of g would be less than 1 for Case II in Fig. 3, but Case II appears to be negligible for the Permanente experimental cell.

* The subscript *p* represents material produced, subscript *r* indicates material reduced, and the numerical subscripts refer to Eqs. [1], [2], and [3].

The theoretical limits for Z are Z = 0 to 100.

The preceding sections show that (*a*) less than 100% initial CO_2 or reaction of CO_2 with carbon, and (*b*) loss of metal without reacting with CO_2 tend to shift actual pot data to opposite sides of the Pearson and Waddington line. It appears that the relation of per cent CO_2 to current efficiency found by prior investigations (2, 4) was due to a fortuitous combination of these two effects.

In Fig. 2 it is seen that the line for the highest bake-temperature anodes is about 3.5% below the Pearson and Waddington line within the range of the experimental data. Since even the highest bake-temperature anodes used probably gave a *g* value greater than one, Z must have been greater than 3.5%. The lines through the data in Fig. 2 were drawn as an example with a value of Z = 5.0. The corresponding values of *g* are as follows:

Anode bake temp, °C	*g*
959	1.070
1070	1.040
1150	1.020

In future tests it is hoped that Z can be evaluated, or at least its variation with cell variables determined. While the value of Z was probably relatively constant in these tests, there are indications from later tests that it varies significantly with bath NaF/AlF_3 ratio.

Measurement of the per cent CO_2 in cell gas has been advocated as a means of determining instantaneous values of current efficiency (4). Results in this work indicate that this is a very questionable practice.

Summary and Conclusions

Current efficiency and cell gas composition were measured on a 10,000-amp experimental aluminum reduction cell for operation with groups of anodes baked at temperatures from 950° to 1190°C. The following are the conclusions from this work:

1. Current efficiency did not vary significantly with anode bake temperature.

2. The percentage of CO_2 in the cell gas varied with anode bake temperature, increasing with increasing bake temperature.

3. This produced deviations from the previously accepted equation:

$$\% \text{ CE} = 50 + \tfrac{1}{2}(\% \text{ CO}_2)$$

4. The data could be correlated by a new equation:

$$\% \text{ CE} = g\,[50 + \tfrac{1}{2}(\% \text{ CO}_2)] - Z$$

5. Some oxidation or loss of cathode products by other than reaction with CO_2 is indicated by a value of Z that is at least 3.5%.

6. The value of *g* was greater than unity and increased for low-bake-temperature anodes, which indicates less than 100% initial CO_2 and/or reaction of initially formed CO_2 with carbon in cell.

7. Use of the oversimplified equation, $\% \text{ CE} = 50 + \tfrac{1}{2}(\% \text{ CO}_2)$, to calculate current efficiency from gas analyses is a questionable practice.

Acknowledgment

The author wishes to thank Bernard Porter and other members of the Research staff for helpful criticisms and Kaiser Aluminum & Chemical Corporation for permission to publish this work.

Manuscript received Dec. 22, 1958. This paper was prepared for delivery before the San Francisco Meeting, April 29-May 3, 1956.

Any discussion of this paper will appear in a Discussion Section to be published in the June 1960 JOURNAL.

REFERENCES

1. T. G. Pearson, Royal Institute of Chemistry, Lectures, Monographs and Reports, No. 3, pp. 36-63 (1955).
2. T. G. Pearson and J. Waddington, *Discussions Faraday Soc.*, No. 2, 307 (1947).
3. J. L. Henry and R. D. Holliday, *J. Metals*, **9**, 1384 (1957).
4. E. Pruvot, *Alluminio*, **22**, No. 6, 721 (1953).

December 1959 Discussion Section

A Discussion Section, covering papers published in the January-June 1959 JOURNALS, is scheduled for publication in the December 1959 issue. Any discussion which did not reach the Editor in time for inclusion in the June 1959 Discussion Section will be included in the December 1959 issue.

Those who plan to contribute remarks for this Discussion Section should submit their comments or questions in triplicate to the Managing Editor of the JOURNAL, 1860 Broadway, New York 23, N. Y. *not later than September 1, 1959.* All discussions will be forwarded to the author(s) for reply before being printed in the JOURNAL.

Electromotive Force Series of Metals in Fused Salts and Activities of Metal Chlorides in 1:1 Molar KCl-NaCl Solutions

S. N. Flengas and T. R. Ingraham

Mines Branch, Department of Mines and Technical Surveys, Ottawa, Ontario, Canada

ABSTRACT

The potentials of a series of metal-metal chloride systems in an equimolar mixture of molten potassium and sodium chlorides have been measured against a silver-silver chloride reference electrode. An electromotive force series of metals at different temperatures has been established for this particular solvent. Experiments with a chlorine electrode have shown that the solutions of silver chloride in the KCl-NaCl solvent are ideal, and hence, deviations from ideality of the other chlorides in this solvent can be attributed directly to the formation of complexes in the melts. Three types of behavior have been observed for the salts studied in this solvent: ideality, and positive and negative deviations from ideality. The theoretical aspects of complex formation in melts are discussed.

The work reported in this paper is the culmination of experiments begun in 1956 for the purpose of establishing electromotive force series of metal-metal chloride systems in a solvent consisting of 1:1M KCl-NaCl, at temperatures between 650° and 900°C. In the initial experimental work, a thermodynamically reversible, diffusion-free, silver-silver chloride reference electrode (1) was developed. This electrode was used to obtain the standard potentials of several systems (2-5). In this paper, the data have been used to establish emf series of metals at various temperatures.

A theoretical interpretation of these data required the definition of an "ideal" reference standard state. By choosing the pure metal chlorides at the temperatures of experiment as the standard state, it was observed that the experimental standard cell potentials showed pronounced deviations from ideality. To resolve the differences, a chlorine-chloride ion electrode was constructed, and the properties of the silver-silver chloride electrode were investigated in detail. Having established the properties and thermodynamic functions of the silver chloride solutions, the activity coefficients and other related thermodynamic properties of the remaining chlorides were calculated.

Standard Electrode Potentials in Fused Salts

Experimental

The preparation of materials and the detailed experimental procedure for electrode potential measurements in fused salts has been described in detail in previous publications (1-5). The potentials of the systems Mn-$MnCl_2$, Zn-$ZnCl_2$, Cr-$CrCl_2$, Tl-TlCl, Cd-$CdCl_2$, Fe-$FeCl_2$, Pb-$PbCl_2$, Sn-$SnCl_2$, Co-$CoCl_2$, Ni-$NiCl_2$, and Cu-CuCl were investigated with cells of the type

	M	$MCl_n(x_2)$		
	(-)	KCl-NaCl (1/1 Mole)		
		(Indicator electrode)		
Asbestos		$AgCl(x_1)$		Ag
fiber		KCl-NaCl (1/1 mole)		(+)
		(Reference electrode)		

[*A*]

A typical design of the all-silica cell is given in Fig. 1. In this cell the reference electrode solution is

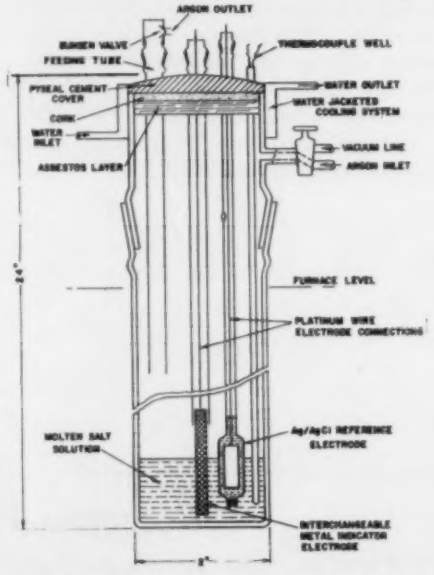

Fig. 1. Cell design for metal electrode potential measurements: Cell [A]

M	$MCl_n(x_2)$		Asbestos	$AgCl(x_1)$		Ag
(—)	KCl-NaCl		fiber	KCl-NaCl		(+)
	(1/1 mole)			(1/1 mole)		

separated from the solution in the indicator electrode by a small asbestos fiber sealed into the end of the silica tubing of the reference electrode. The fiber absorbs the salts and makes a good electrical contact between the two solutions while hindering diffusion. Analysis of the solutions from both electrode compartments indicated that this method of separation was effective. For dilute salt solutions, the presence of a large excess of the same ionic melt on both sides of the junction effectively eliminated junction potentials.

The reaction for a cell of the type shown above is:

$$\mathrm{M\ (s)} + n\ \mathrm{Ag^+(AgCl\ in\ KCl\text{-}NaCl)} = \mathrm{M^{n+}(MCl_n\ in\ KCl\text{-}NaCl)} + n\mathrm{Ag(s)} \qquad [A']$$

The relationship between the cell potential and salt concentrations in the melt is given by the Nernst equation in the expanded form

$$E(\text{cell A}) = E^\circ(\mathrm{Ag/Ag^+}) - E^\circ(\mathrm{M/M^{n+}}) + (RT/n\mathbf{F})\ln\frac{x_2}{x_1^n} - (RT/n\mathbf{F})\ln\frac{\gamma_2}{\gamma_2^n} \qquad [1]$$

where $E^\circ(\mathrm{M/M^{n+}})$ is the *standard electrode potential* [with the IUPAC Stockholm sign convention (16)] of M in the metal chloride MCl_n and $E^\circ(\mathrm{Ag/Ag^+})$ is the *standard electrode potential* of Ag in AgCl. The γ and x are, respectively, the mean activity coefficients and mole fractions of the metal chlorides taking part in the cell reaction. If the E° are referred to the standard chlorine-chloride electrode at the same temperature (see below), they become equal to *minus the formation potentials* of MCl_n and AgCl, respectively, in their standard states (pure salt at the temperature of the experiment) as defined by Hamer, Malmberg, and Rubin (6). Mole fractions are defined in the usual way, which is

$$x_i = n_i/\Sigma n_j \qquad [2]$$

where n_i is the number of moles of the i^{th} constituent.

From Eq. [1], assuming that the activity coefficients for dilute solutions are constant, it is possible to calculate a cell potential which proved to be independent of concentration. This is done simply by subtracting the term $(RT/n\mathbf{F})\ln(x_1^n/x_2)$ from the experimentally obtained potential, E (cell A). The potential thus derived is constant over the range of concentrations for which the activity coefficients are constant and will be called the "apparent standard cell potential," $E^{\circ\prime}$ (cell A). From Eq. [1], the apparent standard cell potentials are given by

$$E^{\circ\prime}(\text{cell A}) = E^\circ(\mathrm{Ag/Ag^+}) - E^\circ(\mathrm{M/M^{n+}}) + (RT/n\mathbf{F})\ln(\gamma_1^n/\gamma_2) \qquad [3]$$

The standard cell potential E°(cell A) would be given by Eq. [3] without the activity coefficient term.

Apparent standard cell potentials can be obtained in either of two ways: by the graphical method, which involves the interpolation (or extrapolation) of the log x_2/x_1^n vs. E(cell A) curve to zero log-value (Fig. 2), or by calculation from the Nernst equation. In the latter method the Nernst curves must be linear, and the slopes of the straight lines must be identical with the theoretical values of $(2.303\ RT/n\mathbf{F})$. From Eq. [3] it is seen that the experimentally derived apparent standard cell potential $E^{\circ\prime}$(cell A) includes, in addition to the standard electrode potentials, the dilution effect as an activity coefficient term. Since standard electrode potentials are known (6), Eq. [3] can be used to calculate activity coefficients in melts.

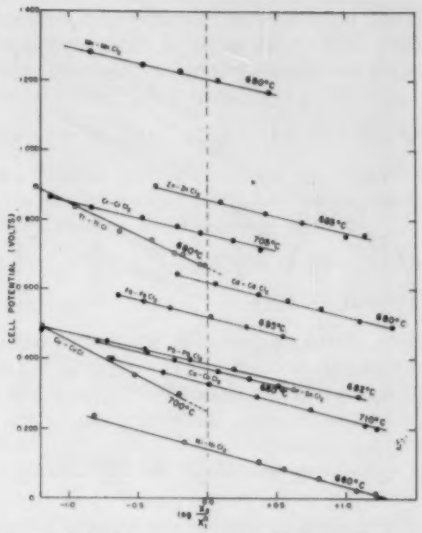

Fig. 2. Electromotive force of Cell [A] for different metals as a function of log (x_2/x_1^n) at constant temperature. (x_1 = 6.235×10^{-5}).

Results

The results of potential measurements with these cells at different salt concentrations are given in Fig. 2. In this graph the experimentally obtained cell potentials E(cell A) are plotted vs. the logarithm of the mole fraction ratio in the two half-cells, following the Nernst equation [1]. It will be observed that the relationship is linear, which justifies the assumption made for the definition of the apparent standard cell potential $E^{\circ\prime}$(cell A) of Eq. [3]. This linearity indicates that the activity coefficients of the metal chlorides are either unity or constant for the concentration range of the experiments. The apparent standard cell potentials for each system, obtained by graphical interpolation or extrapolation at zero log-term, are indicated by the intercepts with the dotted line in the center of Fig. 2.

The slopes of the straight lines are in most cases in good agreement with the Nernst equation, with the exception of the Ni-$NiCl_2$ system in which a slope of 0.107 is obtained instead of 0.096. Cell potentials in Fig. 2 are corrected for small thermoelectric forces. These were measured separately on the bimetallic systems of the electrodes (with their connections) and are given in Fig. 3.[1]

[1] Potentials given in some of our previous publications (1-4) have not been corrected for thermoelectric effects. For such corrections, reference should be made to Fig. 3.

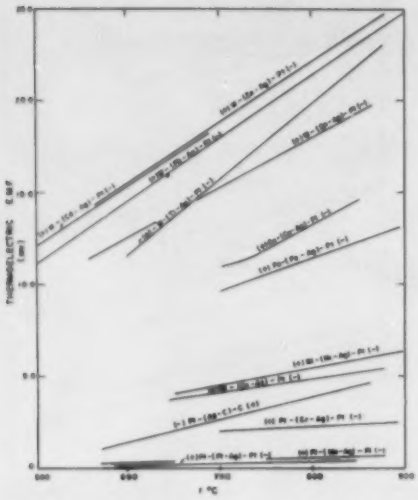

Fig. 3. Thermoelectric electromotive forces of the bimetallic systems of the various types of electrodes used in this study.

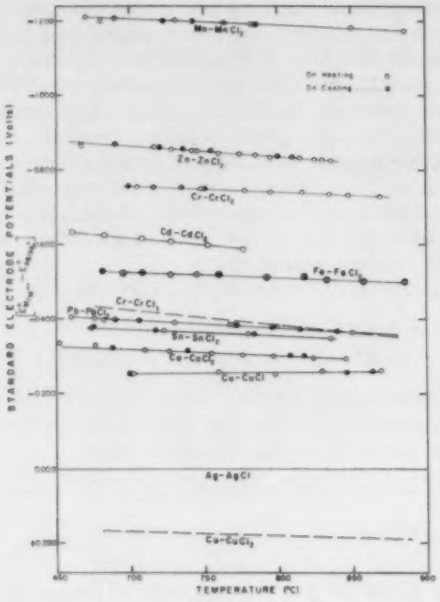

Fig. 4. Variation of standard electrode potentials with temperature.

The effect of temperature change on the apparent standard cell potentials $E^{\circ\prime}$ (cell A) was also measured; the results are summarized in Fig. 4. It is seen that between 650° to 900°C the relationship of temperature and apparent standard cell potential is linear and the temperature coefficient is small. Standard cell potentials for the systems Cu-$CuCl_2$ and Cr-$CrCl_2$ are shown in the graph by dotted lines to indicate that these values were not obtained experimentally but were calculated using a process described previously (4). In fact, neither of these potentials could be measured directly because of a spontaneous reduction of the higher valency chlorides by the corresponding metal electrodes.

The emf series derived in the present investigation at temperatures of 700°, 800°, and 900°C are given in the first three columns of Table I from our observed values of $E^{\circ\prime}$ (cell A). In the same tabulation are also included the standard potentials, calculated from E° (cell A) values derived from thermal data by Hamer, Malmberg, and Rubin (6). A third set of data is included to demonstrate the agreement between the standard electrode potentials obtained in this study in the presence of 1/1M KCl-NaCl solvent and those published recently by Laitinen and Liu (7) in the KCl-LiCl eutectic solvent. Since the latter were determined at 450°C, it was necessary to extrapolate our values to this temperature.

Table I. Standard electrode potentials[a] of metals in fused 1:1 KCl-NaCl

	$E^{\circ}(M/M^{n+}) - E^{\circ}(Ag/Ag^{+})$, v							
	This study			Hamer, *et al.*[b]			At 450°C	
Electrode	700°C	800°C	900°C	700°C	800°C	900°C	This study[c]	Laitinen and Liu[d]
Mn, $MnCl_2$	−1.206	−1.190	−1.172	−1.010	−0.981	−0.955	−1.230	−1.212
Zn, $ZnCl_2$	−0.860	−0.835	−0.810	−0.665	−0.650	−0.630	−0.930	−0.929
Cr, $CrCl_2$	−0.758	−0.740	−0.728	−0.565	−0.526	−0.505	−0.810	−0.788
Tl, TlCl	−0.665	—	—	−0.665	—	—	—	—
Cd, $CdCl_2$	−0.620	−0.580	—	−0.415	−0.367	—	−0.630	−0.679
Fe, $FeCl_2$	−0.520	−0.510	−0.498	−0.305	−0.292	−0.270	−0.560	−0.534
Cr, $CrCl_3$	−0.425	−0.385	−0.345	−0.385	−0.380	−0.375	−0.525	−0.523
Pb, $PbCl_2$	−0.390	−0.376	−0.355	−0.315	−0.286	−0.270	−0.447	−0.464
Sn, $SnCl_2$	−0.370	−0.354	−0.340	−0.405	−0.435	−0.450	−0.410	−0.445
Co, $CoCl_2$	−0.324	−0.300	−0.275	−0.195	−0.155	−0.135	−0.372	−0.354
Cu, CuCl	−0.260	−0.256	−0.260	−0.140	−0.145	−0.152	−0.240	−0.214
Ni, $NiCl_2$	−0.140	—	—	−0.095	—	—	—	−0.158
Ag, AgCl	0.0	0.0	0.0	0.0	0.0	0.0	0.0	0.0
Cu, $CuCl_2$	+0.170	+0.180	+0.192	+0.410	+0.430	+0.450	+0.200	+0.189
Cl_2, Cl^-	+0.845	+0.820	+0.795	+0.850	+0.826	+0.794	+0.905	+0.853

[a] It will be noted that the sign of the electrode potentials is in accord with the recommendations of the IUPAC Stockholm Convention [See Licht and deBethune (16)]. The potentials are referred to Ag/AgCl.
[b] Standard potentials calculated from thermal data.
[c] Extrapolated values from our experimental data obtained at temperatures between 650° to 900°C in 1:1 KCl-NaCl.
[d] Values obtained by Laitinen and Liu (7) in KCl-LiCl at 450°C.

From Table I, it is readily seen that both the sequence and the magnitude of the potentials in the experimentally derived emf series of metals are different from those calculated by Hamer, Malmberg, and Rubin (6). These differences are due to the effects of solvent on the salts, as expressed by the γ term in Eq. [3]. On the other hand, standard potentials obtained experimentally in this study and by Laitinen and Liu (7) are in substantial agreement. The small differences in the magnitude of the potentials should be attributed to the difference in solvents and to the error in extrapolating our data to 450°C. It should also be noted that standard potentials determined by Laitinen and Liu are given without thermoelectric force corrections. The corrections are probably a few millivolts only and should be added to the measured potentials. The agreement should therefore be, in most cases, even better than that shown in Table I.

Thermodynamic Properties of Solutions of Silver Chloride in 1/1M KCl-NaCl

The standard cell potentials obtained in cell [A] represent the difference between the individual standard electrode potentials of the reference and indicator electrode systems. Consequently, it is not possible to calculate individual activities of the metal chlorides in solution unless the thermodynamic properties of one species are known. Although preliminary results (1) indicated ideality of the AgCl (KCl-NaCl) system, it was necessary to confirm this by determining the activities of silver chloride in solution. The thermodynamic properties of pure silver chloride have been studied by several investigators (8-10, 17), using silver-chlorine cells of various designs. The agreement between the different data is quite good. On the other hand, there is little information on the properties of solutions of silver chloride in fused salt solvents. Stern (11, 12) investigated the systems AgCl-KCl and AgCl-NaCl, at 800°C and showed that, whereas the former deviates from ideality positively, the latter deviates negatively. Takahashi (13) investigated the system AgCl(KCl-LiCl) and found a small deviation from ideality. In these studies the pure silver chloride state was also chosen as the standard state for reference.

In the present investigation, a cell consisting of silver-silver ion and chlorine-chloride ion electrodes was developed and used to measure the thermodynamic properties of solutions of silver chloride in the 1/1M KCl-NaCl solvent at temperatures varying between 650°-900°C.

Experimental

The cell used to measure the potentials of silver chloride in the molten salt solution was of the following type:

Ag (-)	AgCl (x) KCl-NaCl (1/1 mole)	‖		
Asbestos fiber	KCl-NaCl 1/1 mole	‖	Cl_2 (1 atm) C (graphite)	(+) [B]

The cell consisted of a chlorine-chloride ion reference electrode and a silver-silver ion indicator electrode. The cell reaction is simply the formation of silver chloride in solution, i.e.:

$$Ag(s) + \tfrac{1}{2}Cl_2(g) = Ag^+Cl^-(\text{in KCl-NaCl}) \quad [C]$$

The relationship between the cell potential and the mole fraction of silver chloride (x), is given by the Nernst equation in the expanded form:

$$E(\text{cell } B) = E^\circ(Cl^-/Cl_2) - E^\circ(Ag/Ag^+) - (RT/F)\ \ln(x\gamma) \quad [4]$$

where the E° are the *standard electrode potentials* in pure silver chloride (which is the standard state), and x and γ are, respectively, the mole fraction and mean activity coefficient of silver chloride in solution in the potassium-sodium chloride solvent.

The actual cell design is shown in Fig. 5. The lower part of this cell was constructed from silica tubing and the upper part from Pyrex tubing. The two parts were joined by a graded seal. The over-all dimensions of the cell were 2 in. x 20 in. The silver electrode was a rod of pure silver wire (99.99%) connected to the potentiometer by platinum wire.

The inert electrode for the chlorine-chloride ion system was a ¼ in. diameter rod of spectrographically pure graphite. A 20,000-ohm resistance in series with the electrodes was used as an additional precaution to reduce the potentiometric current and prevent any polarization phenomena. One of the features of this cell is the activation of the graphite electrode before use. The end of the rod was coated with a concentrated sucrose solution and then carbonized in a chlorine atmosphere at 800°C for 24 hr. The result was a thin, porous, and highly absorbent carbon deposit. This cell, like all the others used in this investigation, was fitted with a small asbestos fiber to separate the two solutions. It will be noted

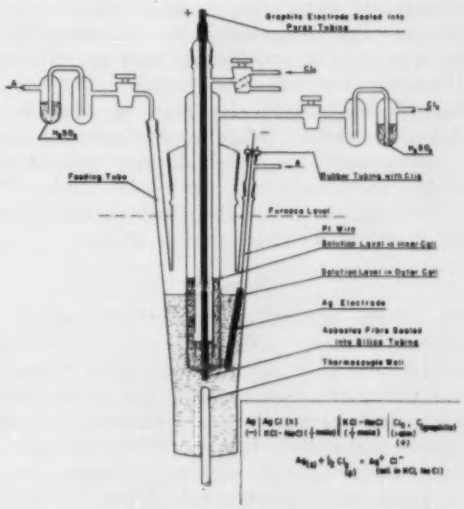

Fig. 5. Design of the silver-chlorine cell: Cell [B]

Ag (—)	AgCl (x) KCl-NaCl (1/1 mole)	‖ Asbestos fiber	KCl-NaCl (1/1 mole)	Cl_2 (1 atm) (+) C (graphite)

that the main significant differences between this cell and those used by other investigators (8, 9) are (*a*) the effective separation between the two half-cells by the asbestos fiber, and (*b*) the simple method of activating the carbon electrode.

Prior to a run, the dry potassium-sodium chloride mixture was added to both the inner and outer half-cells, the amounts being arranged so that when the contents were molten the height in the inner cell would be greater than that in the outer cell. After the salts had melted, the graphite electrode was placed in position, and dry pure chlorine gas was introduced into the cell and permitted to escape after bubbling through the melt. To obtain steady and reproducible potential measurements, it was necessary to leave the cell in operation for about 24 hr before taking potential readings. A sulfuric acid outlet trap prevented air from leaking into the cell and also provided a means of estimating the chlorine gas flow. It was found that the cell potential was independent of the rate of chlorine gas flow, and the cell was operated normally under a very slow flow (about 30 cc/min).

Solutions of silver chloride were prepared *in situ* by adding weighed amounts of silver chloride to the molten salt solvent and mixing well with a small electrically-operated platinum stirrer. To insure that true equilibrium had been attained after each addition of solute, the cell was allowed to stand for about 24 hr during which the potentials were checked several times. It was observed that with vigorous stirring, equilibrium was attained in a short time and that afterward the potentials remained practically unchanged. Small fluctuations of the potentials, of the order of ±0.4 mv, did actually occur and were attributed to local temperature changes in the cell. Thus, a complete run lasted several days, during which the chlorine electrode was in continuous use. The silver electrode was immersed in the solution only while potential measurements were being made. It was then withdrawn into the space above the solution. Purified argon was used to provide an inert gas protection for the silver electrode compartment.

The chlorine-chloride ion electrode may be regarded as a standard reference electrode for potential measurements in fused chloride salts. Unfortunately, in comparison with the silver-silver chloride electrode, it has the disadvantage of being rather fragile and complicated in design.

Results

The results of the experiments in which the electromotive forces of the silver-chlorine cell were measured as a function of temperature at various mole fractions of silver chloride, are shown in Fig. 6. All potentials have been corrected for small thermoelectric effects. It is apparent that the cell potential varies linearly with temperature over the temperature range between 650° to 900°C.

The variation of E(cell B) with log x, according to the Nernst equation [4], is shown in Fig. 7, for 700°, 800°, and 900°C. The relationship over most of the curves is linear, and the slopes of the straight

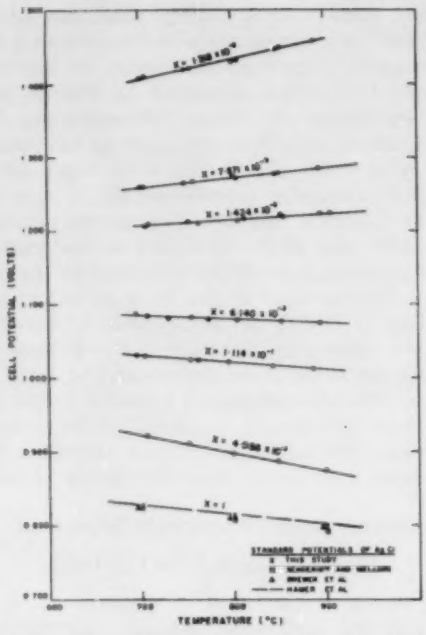

Fig. 6. Variation of emf with temperature for Cell [B]

lines agree very well with the calculated slopes from the Nernst equation at these temperatures for a one-electron electrode reaction. The standard cell [B] potential is obtained by graphical extrapolation of the straight lines in Fig. 7, to zero log x. These potentials, according to Eq. [4], would include the activity coefficient term of the Nernst equation, if any. It will be observed, in Fig. 7, that one of the experiments was continued to higher concentrations of silver chloride than the others. At a mole fraction of about 0.5, which corresponds to a log x term of about −0.2, the curve deviates from linearity. This is attributed mainly to the generation

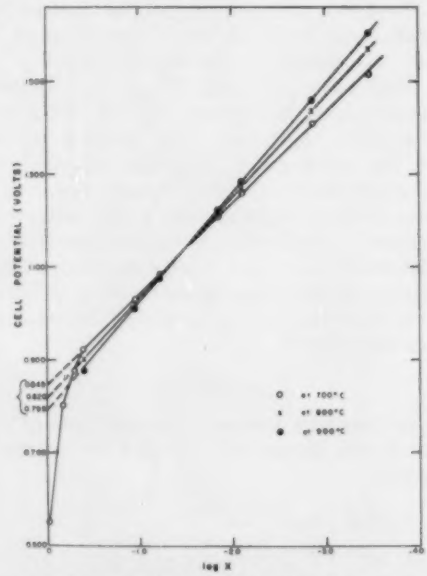

Fig. 7. EMF of Cell [B] as a function of log x at constant temperature.

of a junction potential at high silver chloride concentration. On this basis, it can be calculated that the junction potential between pure silver chloride and the potassium-sodium chlorides is about 300 mv. This junction potential decreases rapidly as soon as some of the potassium-sodium chloride mixture has been added to the silver chloride side, and at a mole fraction of about 0.5 it disappears completely.

However, it should be pointed out that part of this potential, which is termed a junction potential, could be due to a difference in the chloride ion activities in the two half-cell solutions. The activity of chloride ion in the potassium-sodium chloride half-cell, is equal to the activity of chloride ion in the silver chloride half-cell only for dilute silver choride solutions.

To investigate the combined effects of chloride ion activity and junction potential, a silver-chlorine cell without transference was operated. This was done by simply removing the asbestos fiber that separated the two half-cells and thus permitting free mixing of the solutions. The observed electromotive force initially was only 2 mv less than in the corresponding cell of the closed type, for the same chloride ion concentration (0.32*M*). After a short time, however, the potential of the open cell became erratic and this was attributed to the chemical depolarization of the silver electrode caused by small amounts of chlorine gas dissolving and migrating in the molten mixture. Hence, further experiments with this type of cell were discontinued. However, the initially observed difference of 2 mv, which is almost within the area of experimental error for the method, indicates that the effects of chloride ion activity coefficient had almost disappeared even in this rather concentrated silver chloride solution.

In Fig. 6 the dashed line at a mole fraction $x = 1$ indicates the formation potential of pure silver chloride at different temperatures, as calculated from thermal data by Hamer, Malmberg, and Rubin(6). The triangular and square points along this line represent the experimental results obtained by Senderoff and Mellors (9), and the potentials calculated from the free energy functions as tabulated by Brewer, *et al.* (10) for the Ag-AgCl system. It is evident from Fig. 6 that the potentials calculated by Hamer and co-workers are a little larger than the experimental ones, although the agreement with the calculations of Brewer is good. Deviations between the potential data are probably due to the uncertainty of the thermal data. The crosses along this line represent standard formation potentials derived experimentally in the present study, in the presence of solvent, and the agreement between the experimental data by the different methods is striking.

From the data in Fig. 6, using the well-known equations,

$$\Delta F^\circ = -E^\circ \mathbf{F} = -RT \ln K \qquad [5]$$

$$d \ln K/dT = \Delta H/RT^2 \qquad [6]$$

$$\Delta F = \Delta H - T\Delta S \qquad [7]$$

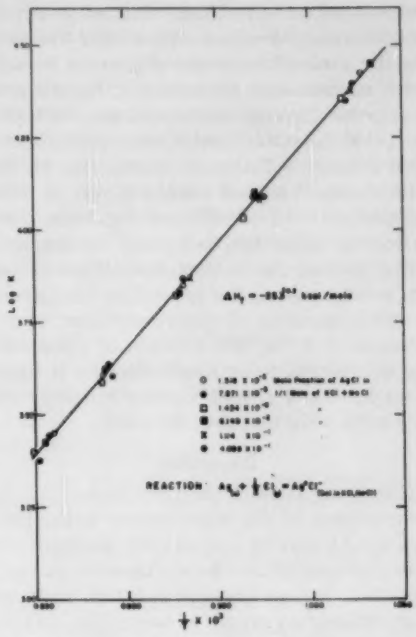

Fig. 8. Variation of log K with the reciprocal of absolute temperature of the reaction:

$$Ag(s) + \tfrac{1}{2}Cl_2(g) = Ag^+Cl^- \text{ (in KCl-NaCl)}$$

it is possible to calculate the enthalpies and entropies of formation of silver chloride in the presence of solvent. The results of the calculations are shown in Fig. 8, in which the logarithm of the equilibrium constant for the formation reaction of silver chloride is plotted against the reciprocal of absolute temperature. It will be noted that the agreement between the different sets of data from which these points were calculated is very good. The relationship is linear for the range of temperature, i.e., between 650°-900°C. From the slope of the straight line the heat of formation of silver chloride is calculated as: $\Delta H_f = -26.3 \pm 0.2$ kcal mole^{-1}. The summary of all thermal data for silver chloride is given in Table II.

From Table II it can be readily derived that the standard partial molal free energy of mixing of silver chloride with the potassium-sodium chloride

Table II. Thermal data for silver chloride

Temp, °C	Standard free energy of formation, kcal mole^{-1}	Standard enthalpy of formation, kcal mole^{-1}	Standard entropy of formation, cal. deg^{-1} mole^{-1}
700	−19.48[a]	−26.3[a]	−7.1[a]
	−19.42[b]	−25.3[b]	−6.1[b]
	−19.35[c]	−26.0[c]	−6.8[c]
800	−18.91[a]	−26.3[a]	−7.0[a]
	−18.79[b]	−25.3[b]	−6.1[b]
	−18.84[c]	−26.0[c]	−6.7[c]
900	−18.33[a]	−26.3[a]	−6.9[a]
	−18.19[b]	−25.3[b]	−6.1[b]
	−18.31[c]	−26.0[c]	−6.6[c]

[a] This study. Data obtained from solutions of silver chloride in KCl-NaCl solvent.
[b] Senderoff and Mellors (9). Data obtained on pure silver chloride.
[c] Brewer, *et al.* (10). Data obtained on pure silver chloride.

molten salt solvent is of the order of only −0.05 to −0.15 kcal mole^{-1}, a value surprisingly low and well within the area of experimental error of the data used for comparison. Accordingly, for all practical purposes, the activity coefficient of silver chloride in the 1/1M KCl-NaCl solution is unity ($\gamma = 1.0$). From the data in Table II, it can also be derived that the standard partial molal entropy of mixing is of the order of −0.9 to −0.3 cal/deg mole, the value again depending on the data used for the comparison. The indication is that the standard entropy change accompanying the process of solution is very small and in the area of experimental error of these measurements. Thus, the solution of silver chloride will be considered to be ideal over the temperature range of 650°-900°C and for the range of concentrations from very dilute up to 0.5*M*.

Discussion

By taking the state of the pure metal chlorides at the temperature of the experiments as the standard state, Eq. [3] can be applied to measure the activity coefficients of the metal chlorides in the fused salt solution. By setting the activity coefficient of silver chloride (γ_1) equal to unity, Eq. [3] can be rearranged to read

$$\log \gamma\,(MCl_n) = ({}_nF/2.303RT)\,[E^\circ - E^{\circ\prime}] \quad [8]$$

where $E^{\circ\prime}$ is the apparent standard cell [A] potential experimentally obtained in this study, and E° is the calculated standard cell [A] potential from tabulated formation potentials given by Hamer, Malmberg, and Rubin (6) (cf. Table I).

Hence, the activity coefficients can be readily calculated by using Eq. [8] and the data given in Tables I and II. The accuracy of the values thus obtained depends on the accuracy of our observed potentials and on the accuracy of the thermal data from which Hamer's standard potentials have been calculated. The results of these calculations are given in Table III. Also shown in Table III are the range of concentration, for which the activity coefficients were found to be constant and the variation of activity coefficient with temperature. It is obvious from the table that only the solutions of silver chloride and thallous choride in this solvent behave ideally. For all the other metal chloride solutions studied, a marked deviation from ideality is observed.

For metal chloride solutions such as $MnCl_2$, $ZnCl_2$, and all the others for which the activity coefficients are less than unity, the formation of complexes can be postulated. It would appear that these salts in solution are complexed to the extent that only about 1/100 to 1/1000 of the amount present is free to contribute to the electrode potential. For these chlorides the activity coefficients show the expected behavior, i.e., they increase with increasing temperature. The constancy of the activity coefficients in dilute solutions, for the range of concentrations investigated, indicates that in these solutions the complex species remain unchanged.

Two notable exceptions to the general pattern of complex formation are represented by chromic and stannous chloride. For these salts the activity coefficients are larger than unity. On the assumption that no phase changes are involved, this behavior would indicate that the solvent has a bond-loosening effect on the solute.

In Table III, the standard partial molal free energies of mixing are calculated from the data, using the equation:

$$\overline{\Delta F^\circ}_{mix.} = RT \ln \gamma = + n\mathbf{F}\,[E^\circ(\text{cell A}) - E^{\circ\prime}(\text{cell A})] \quad [9]$$

The quantity defined by Eq. [9] represents the difference between the free energy of the salt in its hypothetical standard state as a solute [i.e., a solution containing unit mole fraction of the salt but having in all other respects the thermodynamic properties of the state of infinite attenuation of the solute, as defined by Lewis and Randall (18)] minus the free energy of the salt in its actual standard state as the pure salt. It is of interest to note that the effect of temperature on the standard partial molal free energies of mixing is, in most cases, very small. Only in the cases of stannous chloride and chromic chloride is the change significant. For chromic chloride the "ideality" of the solutions is closely

Table III. Activity coefficients, standard partial molal free energies and entropies of mixing of metal chlorides in 1:1M KCl-NaCl

Salts	Range of mole fractions, $10^4\,x$	Activity coefficients γ_2			$\overline{\Delta F^\circ}$ (mixing), cal mole^{-1}			$\overline{\Delta S^\circ}$ (mixing), cal deg^{-1} mole^{-1}		
		700°C	800°C	900°C	700°C	800°C	900°C	700°C	800°C	900°C
$MnCl_2$	5.87-107.0	0.0093	0.011	0.014	−9,040	−9,640	−10,000	3.6	3.7	3.5
$ZnCl_2$	22.20-717.0	0.0091	0.018	0.028	−8,990	−8,530	−8,300	−2.0	−2.3	−2.0
$CrCl_2$	2.84-93.5	0.010	0.010	0.013	−8,900	−9,820	−10,280	8.9	8.9	8.8
TlCl	36.10-603.0	1.0	—	—	0.0	—	—	—	—	—
$CdCl_2$	23.40-835.0	0.0075	0.010	—	−9,460	−9,820	—	6.1	5.8	—
$FeCl_2$	8.85-138.0	0.0059	0.0089	0.011	−9,920	−10,050	−10,520	4.4	4.1	4.4
$CrCl_3$	4.00-90.0	0.24	1.18	2.4	−2,770	+350	+2,070	−22.0	−22.2	−22.0
$PbCl_2$	3.25-628.0	0.17	0.14	0.19	−3,460	−4,150	−3,920	3.7	3.8	3.9
$SnCl_2$	6.32-125.0	2.3	5.7	8.9	+1,610	+3,730	+5,070	−15.1	−11.7	−9.8
$CoCl_2$	7.60-612.0	0.046	0.043	0.063	−5,950	−6,690	−6,460	3.9	4.2	3.9
CuCl	10.80-391.0	0.24	0.30	0.34	−2,770	−2,570	−2,560	−0.7	−0.8	−0.8
$NiCl_2$	5.94-666.0	0.34	—	—	−2,080	—	—	—	—	—
AgCl	3.37-6850.0	1.0	1.0	1.0	0.0	0.0	0.0	(−0.5)	(−0.5)	(−0.5)
$CuCl_2$	10.0 -390.0	0.0033	0.0045	0.0061	−11,070	−11,530	−11,900	5.5	5.4	5.5

related to temperature. At about 800°C the solutions are almost "ideal," but with increasing temperature a positive deviation from ideality is evident.

From the dependence of the standard partial molal free energies of mixing on temperature, the standard partial molal enthalpies and entropies of mixing can be calculated for the systems shown in Table III. The latter are also given in this table.

The standard partial molal entropies of mixing, as shown in the last three columns of Table III, also suggest that complex ions are present in all of these systems. It is necessary here to define the term "complex" as used throughout this study. In a very broad sense a "complex" in an ionic melt should be defined as a group of atoms for which the binding forces are stronger than the forces tending to separate them. The latter type of forces obviously includes the interactions between similar groups of atomic aggregates and also the interactions with the solvent. In terms of structure, a "complex" in solution should be a group of atoms in which the immediate neighbors of any atom are arranged in some orderly way, but the arrangement becomes more random gradually with increasing distance from the center of the complex. The definition is almost that on a liquid, with the difference that there is a distinction between the random distribution of atoms or ions in the solvent, and the locally more ordered distribution of atoms in a complex.

Although the presence of finite complexes in melts has been demonstrated both by potentiometric (14) and by spectrophotometric measurements (15), it seems reasonable that in ionic metals there should exist several intermediate states of aggregation between the so-called "noncomplexed" ionic state and the type of finite complexes found in aqueous solutions.

The actual values of the activity coefficients, and of other thermodynamic functions which characterize these complexes in solution will depend entirely on the definition of a noncomplexed state. A completely different set of data would be obtained if, instead of choosing the pure metal salt as the standard state, the state of infinite dilution were chosen. In fact, only the existing differences between any two states are measured directly, and a thermodynamic definition of a noncomplexed state is quite arbitrary. Even the "ideal solution" appears to arise from cancelling out of opposing effects in the binding forces within the complex itself.

In support of this view is the behavior of the solutions of silver chloride in alkali chlorides. Stern (11,12) found that the partial molal free energy of mixing of silver chloride in potassium chloride is negative, and that of silver chloride in sodium chloride is positive. In the present investigation it was found that in a solution of silver chloride in 1/1M mixture of potassium and sodium chlorides, the standard partial free energy of mixing is zero and the solutions are "ideal." It is apparent that by regulating the composition of the solvent and temperature it is possible to obtain solutions with positive, negative, or zero deviation from ideality. Thus, one may conclude that what is theromdynamically an "ideal" state is not necessarily a noncomplexed state.

Acknowledgment

The authors wish to acknowledge the help of Mr. P. Hernandez, Mines Branch glassblower, in constructing the silica apparatus used in the foregoing experiments.

Manuscript received Nov. 28, 1958. This paper was prepared for delivery before the Ottawa Meeting, Sept. 28-Oct. 2, 1958.

Any discussion of this paper will appear in a Discussion Section to be published in the June 1960 JOURNAL.

REFERENCES

1. S. N. Flengas and T. R. Ingraham, *Can. J. Chem.*, **35**, 1139 (1957).
2. S. N. Flengas and T. R. Ingraham, *ibid.*, **35**, 1254 (1957).
3. S. N. Flengas and T. R. Ingraham, *ibid.*, **36**, 780 (1958).
4. S. N. Flengas and T. R. Ingraham, *ibid.*, **36**, 1103 (1958).
5. S. N. Flengas and T. R. Ingraham, *ibid.*, **36**, 1063 (1958).
6. W. Hamer, M. Malmberg, and B. Rubin, *This Journal*, **103**, 8 (1956).
7. H. A. Laitinen and C. H. Liu, *J. Am. Chem. Soc.*, **80**, 1015 (1958).
8. E. J. Salstrom, *ibid.*, **55**, 2426 (1933).
9. S. Senderoff and G. W. Mellors, *Rev. Sc. Instr.*, **29**, 151 (1958).
10. L. Brewer, *et al.*, as reported by L. L. Quill in "Chemistry and Metallurgy of Miscellaneous Materials," Paper 6, McGraw Hill Book Co., New York (1950).
11. K. H. Stern, *J. Phys. Chem.*, **60**, 679, (1956).
12. K. H. Stern, *ibid.*, **62**, 385 (1958).
13. M. Takahashi, *J. Electrochem. Soc., Japan*, **25**, 432 (1957).
14. S. N. Flengas and Sir E. K. Rideal, *Proc. Roy. Soc., London*, **A233**, 443 (1956).
15. D. M. Gruen, "Spectrophotometry Applied to the Analysis of Fused Salts," Paper presented at the 11th Annual Summer Symposium, Division of Anal. Chem., Amer. Chem. Soc., June 19, 1958.
16. T. S. Licht and A. J. deBéthune, *J. Chem. Ed.*, **34**, 443 (1957).
17. J. H. Hildebrand and E. G. Salstrom, *J. Am. Chem. Soc.*, **52**, 4650 (1930); **54**, 4257 (1932).
18. G. N. Lewis and M. Randall, "Thermodynamics," Ch. XXII, McGraw-Hill Book Co., New York (1923).

The Oxygen-Evolution Reaction at Gold Anodes

I. Accuracy of Overpotential Measurements

Sidney Barnartt

Research Laboratories, Westinghouse Electric Corporation, Pittsburgh, Pennsylvania

ABSTRACT

The oxygen-evolution reaction at gold anodes was studied in 0.1M H_2SO_4 at 25°C. The factors affecting the accuracy of overpotential measurements and a new cell design for improved accuracy with a Luggin-Haber capillary are described. Current distribution in the cell, limitations imposed by competing reactions and by the *IR* drop included in the measurement, overpotential-time curves at constant current density, and the accuracy with which Tafel's equation is obeyed are presented. The current density range for accurate measurements was found to be 3×10^{-6} to 10^{-2} amp cm^{-2}. Overpotential measurements taken with decreasing and increasing currents were reproducible to ±1 mv, and deviations from the Tafel line were within this variation. At constant current density the gold anodes oxidized to hydrated Au_2O_3 following the linear law, and the current density dependence of the oxidation rate indicated a blister mechanism.

The steady-state overpotential measurements necessary for distinguishing possible rate-determining steps in anodic oxygen evolution have been compiled by Bockris (1). Data reported to date, however, have shown little consistency. Inherent experimental difficulties are probably greater than, and certainly have not been as intensively investigated as, those for the hydrogen evolution reaction (2, 3).

Platinum anodes have been studied in greatest detail (2). For this electrode there is general agreement that anodic oxygen evolution follows Tafel's equation (4):

$$\eta = a + b \log i \qquad [1]$$

where η is the steady-state overpotential at the applied current density (c.d.) i. The Tafel constants a and b reported by various authors are discrepant. Recently Bockris and Huq (5) investigated platinum in sulfuric acid solutions under conditions of extreme purification. Greater consistency in the Tafel plots was reported; the slope b was reproducible to ±12% or better. In the absence of applied current, a reversible oxygen electrode was apparently obtained for the first time.

This paper reports a detailed study of the accuracy attainable for oxygen overpotential measurements at gold anodes in 0.1M H_2SO_4 at 25.0°C. The various sources of error in overpotential measurements are evaluated, a new cell design for uniform current distribution described, and the c.d. limits determined for measuring η to ±1 mv. It will be seen that Tafel's equation is obeyed within this deviation.

Sources of Error

The following is a general outline of the sources of error involved in the experimental measurement of steady-state overpotential.

Current distribution.—When measurements are made by the direct method (while current is flowing) with a Luggin-Haber capillary (6), the current distribution over the test electrode should be uniform (7). With cell geometries having nonuniform distribution, the c.d. at the point of measurement generally will not be a constant and known fraction of the average c.d. at all values of overpotential (8-10). Even when interrupted currents are used and the potential is measured very rapidly after the interruption, it is desirable to use a cell having uniform current distribution (11).

It is recognized that a mechanically polished electrode surface will contain fine scratches and a large number of sharp micro peaks. In the primary current distribution (that in the absence of electrode polarization) the current density approaches infinity at sharp peaks. When the electrode is polarized, however, the distribution (secondary) is more uniform. The greater the ratio of Wagner's characteristic length parameter $\kappa \left| \partial\eta/\partial i \right|$, where κ is the solution conductivity, to the average scratch depth λ, the more uniform the current distribution (10). If Tafel's equation applies, $\left| \partial\eta/\partial i \right|$ decreases and the distribution becomes less uniform as the c.d. is increased, since

$$\partial\eta/\partial i = \pm 0.4343\ b/i \qquad [2]$$

where the plus sign refers to anodic and the negative sign to cathodic reactions. For even roughly polished electrodes in most electrolytes, the ratio of Wagner's characteristic length to average scratch depth is expected to be sufficiently large that the current distribution over the surface will be essentially uniform. The surface roughness, however, must be taken into consideration in calculating the true current density.

Shielding by the capillary.—It has been shown that large errors in overpotential can result from shielding of the electrode at the point of measurement, unless the capillary tip is either sufficiently far removed from the electrode surface (12, 13) or is

against the electrode and has a properly designed opening (14-16). For an open tip capillary of diameter d, negligible shielding will occur if the distance between the tip and electrode surface is $2d$ or greater.

IR-drop corrections.—Where a Luggin-Haber capillary with open tip is used, correction must be made for the *IR* voltage drop (V_{IR}) in the electrolyte between the tip and the electrode. These corrections can be appreciable, even in solutions of moderately high conductivity. For example, at 10^{-2} amp cm^{-2}, the following values of V_{IR} in 0.1M H_2SO_4 ($\kappa = 0.046$) were calculated for a capillary tip of diameter d positioned a distance $3d$ from a plane electrode:

d(cm):	0.5	0.1	0.02
V_{IR}(v):	0.290	0.058	0.012

These values were obtained from the equation:

$$V_{IR} = (3d - d/3)\, i/\kappa \qquad [3]$$

which is based on the observation (12, 13) that the potential inside the capillary is equal to that at a distance $d/3$ closer to the electrode in the undistorted field.[1] The above example illustrates the general requirement of positioning the capillary very close to the electrode and, hence, for using a capillary with small outer diameter in order to avoid shielding errors.

Where a coating forms on the electrode surface, as often occurs during anodic overpotential measurements, the resistance of the coating must be evaluated. This is done by actual measurement of the total *IR* drop included in the overpotential measurement, from which the *IR* drop in the electrolyte, calculated as above, is subtracted to obtain the *IR* drop within the coating.

Roughness factor.—For an electrode surface with roughness factor q (ratio of true area to apparent area), Tafel's equation may be written in the form

$$\eta = a + b \log(i'/q) = a' + b \log i' \qquad [4]$$

where i' is the apparent c.d. and $a' = a - b \log q$. If q remains constant throughout the measurements, the correct slope b is obtained when η is plotted against $\log i'$. The apparent a-value from this plot, however, is the value a'; this is too small, as compared with the true a, by the amount $b \log q$.

For systems in which the roughness factor changes with changing c.d., the measurements may appear to follow a Tafel line, but both the slope and the a-value will be in error. This type of error should be revealed by a drift of the apparent Tafel line when determined with decreasing, then with increasing, current densities.

There is evidence that the roughness factor of a polished metal may vary by an order of magnitude, depending on subsequent treatments (17, 18). Therefore, where the electrode surface undergoes change, e.g., by oxidation during anodic oxygen evolution, prepolarization to a stable surface should precede the overpotential measurements.

[1] This observation refers (12) to a capillary tip with ID = 2/3 OD; the capillaries used in the apparatus to be described conformed to this geometry.

Impurities.—Trace impurities, present in the electrolyte or adsorbed on the electrode surface, may produce large errors in overpotential (5, 19-21). The observable effects of impurities on η-measurements include: (*a*) prolonged potential drift with time, (*b*) irreproducibility of steady-state potentials, and (*c*) depolarization accompanying increased agitation, particularly at low c.d., resulting from competing reactions involving impurities.

Competing reactions.—Any competing reaction depolarizes the electrode reaction under study, i.e., the measured overpotential corresponds to a current smaller than the observed total current. Competing reactions may occur even in highly purified systems; during anodic oxygen evolution, for example, metal dissolution and oxide formation often proceed simultaneously. Soluble products of the cathode reaction can diffuse to the anolyte and depolarize the anode reaction, and vice versa.

Potential-time variations.—The use of arbitrary polarization times has often resulted in failure to attain the steady-state η-values, as has been emphasized for anodic oxygen evolution by the work of Hickling and Hill (22). In general it is preferable to approach the steady state from two directions, e.g., with increasing and with decreasing current density, in order to avoid errors resulting from slow drifts or temporary potential arrests.

Concentration polarization.—Concentration changes at the electrode surface impose an upper limit to the c.d. range over which accurate overpotentials can be measured. The maximum permissible c.d. will generally be considerably lower than the so-called limiting current (at which the current efficiency begins to fall). An appreciable concentration change of any dissolved substance which affects the electrode potential will contribute to concentration polarization. In most cases the accompanying potential changes will be complex and not amenable to accurate calculation. Therefore, the fractional concentration change at the electrode should be maintained small by the use of increased agitation, a more concentrated solution, or a lower c.d. range.

From the mathematical theory of diffusion, the concentration at the electrode, C_e (mole cc^{-1}), of any solution constituent under steady-state conditions is given by the relation (23-25):

$$C_e - C_s = f\, l/D \qquad [5]$$

where C_s is its bulk concentration, l the thickness of the diffusion layer (cm), D its diffusion coefficient (cm^2 sec^{-1}), and f its flux at the electrode boundary (mole cm^{-2} sec^{-1}). The flux is equal to the rate at which the constituent is added at the electrode surface by the electrode reaction and by electrical transference.

In most practical systems involving forced convection of a complex nature, Eq. [5] is applied as a first approximation, with the assumption that the only effect of convection is a decrease in the parameter l. Quantitative theoretical predictions for convective effects in several simplified systems have been reviewed (26).

Experimental Procedure

Materials.—Reagent-grade sulfuric acid was distilled in an all-Pyrex still. Distilled water was treated with small amounts of KOH and $KMnO_4$ and redistilled in an all-Pyrex still. In each case the first portion of the distillate was rejected and the middle fraction used.

Oxygen gas was purified by passage through a column of cupric oxide heated to 700°C in a Vycor tube, then into an all-Pyrex system through bubblers containing 1M NaOH and 1M H_2SO_4, and finally through a fritted Pyrex tube to trap droplets. The purified gas was led into the cell through a short length of flexible, unplasticized polytrifluorochloroethylene (Kel-F) tubing.

Anodes of solid gold and of gold-plated copper were used. The solid electrode was machined from pure gold rod (99.98% Au, principal impurities Ag and Pt metals). The plated electrode was prepared by electroplating gold at 2 ma/cm^2 and 70°C from the following solution (reagent-grade chemicals): 0.05M K $Au(CN)_2$, 0.2M, KCN, and 0.1M K_2CO_3. The surface was alternately plated and polished until a gold layer 75 μ thick was achieved. Diamond polishing compound with a particle size of 3 μ was used for the final polish on each electrode.

The following surface treatments of the gold electrodes, prior to insertion in the cell, were standardized. Precleaning involved degreasing in solvents, treatment cathodically in hot 3M NaOH, then immersion in 10M HNO_3. The final treatment of the plated electrode consisted in electroplating an additional 3 μ thickness of gold to produce a smooth, matte surface. The solid gold electrode was made anodic in 1M H_2SO_4 at 5×10^{-3} amp cm^{-2} for 5 min to produce a very thin brown oxide, then the latter was dissolved in 5M HCl; the final surface remained almost mirror bright.

Two saturated calomel electrodes (SCE), of the type having a Pyrex salt-bridge junction tube containing a controlled diffusion crack (27), were used to follow potential changes. These were checked periodically with each other and with a third electrode; the voltage between any two never exceeded 0.1 mv.

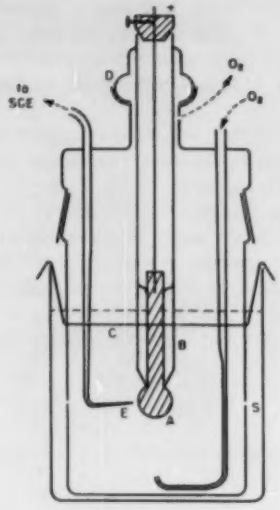

Fig. 2. Cell I

Cell design.—Two cells were used, both designed for uniform current distribution and based on concentric spherical geometry with conical sectioning (7), as indicated in Fig. 1. The following two distortions were introduced in the actual cells. (*A*) The insulator was shortened, as shown in Fig. 1 by the broken vertical lines, so that the 60° angle was maintained only for a distance r_a, where r_a is the radius of the inner electrode. In the cells used the inner electrode was the anode with $r_a = 0.50$ cm. (*B*) It was assumed that, provided the cell diameter exceeded 10 r_a, the outer spherical electrode (cathode) could be highly distorted with little effect on current distribution at the anode. For this reason the cathode was removed to an external compartment, and the diameter of the anode compartment was made 12 r_a in cell I (Fig. 2) and 16 r_a in cell II (Fig. 3). These distortions were expected to produce relatively small non-uniformities of current distribution at the anode A.

The cells were constructed of Pyrex glass. The 60° conical insulator was ground from precision-bore tubing B, and the rod portion of the anode was machined to fit snugly into the bore. The ball joint D

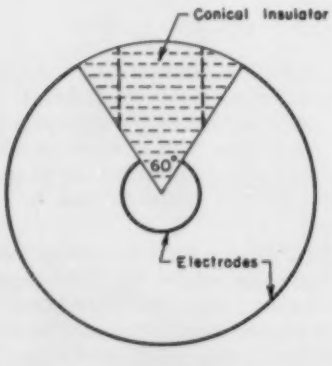

Fig. 1. Conical sectioning of concentric spheres

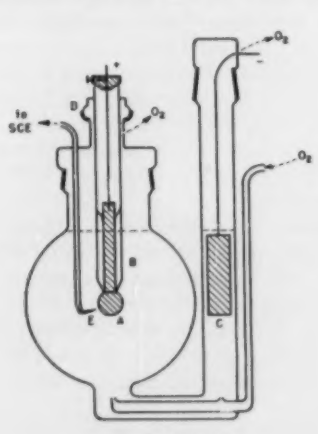

Fig. 3. Cell II

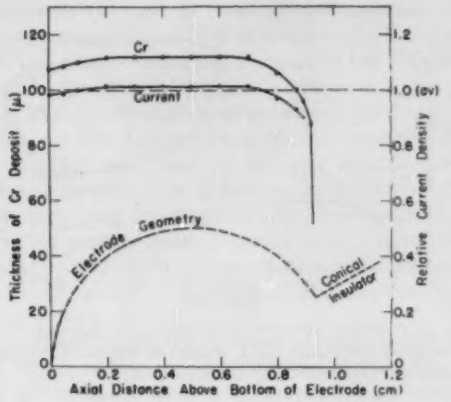

Fig. 4. Current distribution over the anode determined by electrodeposition of chromium.

permitted accurate positioning of the anode with respect to the fixed capillary tip E. A tip of diameter $d = 0.20$ mm was used and was positioned at a distance of about $3d$ from the anode.

In cell I the anolyte boundaries were cylindrical, 12 r_a in diameter and 12 r_a in height. Contact with the catholyte was made through a slot S, 0.5 mm wide, which was concentric with the anode. The cathode C was a platinum wire ring situated near the top of the catholyte. The primary current distribution over the electrode surface in this cell was obtained by measuring the distribution of chromium, electroplated under conditions shown previously (28) to yield good agreement with the primary distribution as measured by the potential-mapping method. Figure 4 shows the measured distribution of chromium over a copper electrode, and the current distribution calculated from it using the current efficiency data of Dubpernell (29). It may be concluded that the current distribution in this cell is sufficiently uniform for overpotential measurements, and that negligible error is incurred when one uses the average c.d. instead of that directly opposite the capillary tip.

In cell II the anolyte was approximately spherical in shape, of diameter 16 r_a. This cell incorporated the following improvements over cell I. (*A*) Both compartments were covered, with only a small hole for escape of oxygen. (*B*) The cathode, a platinized-platinum cylindrical gauze, had much larger surface area. (*C*) Oxygen was bubbled around the cathode as well as the anode, thus tending to sweep out any hydrogen formed at high c.d. The uniformity of current distribution was not measured in cell II, but was assumed to be just as satisfactory as in cell I. Cell II with the solid gold anode was used for measurements reported below except where otherwise stated. The reference compartment of each cell was, of course, filled with the solution under study. Traces of KCl entering this compartment from the reference electrode had a long diffusion path to the capillary tip.

Measurement of overpotential.—Polarizing current was drawn from a 30-v lead-acid battery source, through a resistance box designed to allow a sudden change in current to a preselected value without breaking the circuit. The anode-SCE voltage, E_{obs}, was measured with a shielded potentiometer (L&N Co. model K3) and a current-sensitive galvanometer having sensitivity of 1.3×10^{-9} amp/mm. The sensitivity-selecting switches of the potentiometer were replaced by four push-button switches in an external shielded circuit, by means of which a resistance of 10^5, 10^6, 10^7, or 10^8 ohms was inserted in series with the voltage being measured. With this circuit it was possible to prevent the out-of-balance current drain from exceeding 10^{-9} amp during a voltage measurement.

The reversible voltage E_1 between the SCE and a hydrogen electrode of the Hildebrand type was measured in the solutions used in the present study and the overpotential for the oxygen-evolution reaction was then given by:

$$\eta = E_{obs} + E_1 - 1.229 \qquad [6]$$

where 1.229 v represents the reversible emf between the oxygen and hydrogen electrodes in a given solution at 25°C (30).

Results and Discussion

Oxide formation.—In dilute sulfuric acid, gold anodes become covered with hydrated Au_2O_3 (31, 45). At very low c.d. Au_2O first forms, then converts through AuO to Au_2O_3 before oxygen evolution commences (32). The color of the oxide changes from yellowish brown to reddish brown as it thickens.

A coating was prepared at 10^{-3} amp cm^{-2} for 23 hr and was carefully flaked off the electrode. Chemical analysis for Au and H_2O (and oxygen by difference) indicated $Au(OH)_3$; some change in hydration could have occurred, however, during removal of the coating. X-ray diffraction patterns of the oxide were attempted with a Guinier focusing camera (33); no diffraction lines were obtained, although the instrument had high sensitivity and gave good patterns for evaporated gold films 100Å thick.

The kinetics of oxide growth at constant c.d was investigated at 10^{-3} and 10^{-4} amp cm^{-2} apparent anodic c.d. It was found that the amount of oxide on the spherical anode could be determined by dissolving it in 10 ml of 5M HCl, then analyzing the solution for Au spectrophotometrically (absorption peaks in the ultraviolet at 226 and 314 mμ). Oxide layers 1Å in average thickness are detectable by this method.

Figure 5 presents the oxidation rate measurements. Linear oxidation curves were obtained, corresponding to constant current efficiency for oxide formation. In 0.1M H_2SO_4, the oxidation rates at 10^{-3} and 10^{-4} amp cm^{-2} are 143 and 6.8 Å/hr, respectively, corresponding to current efficiencies for oxide formation of 1.13% at 10^{-3} amp cm^{-2} and 0.53% at 10^{-4} amp cm^{-2}. Such low current efficiencies would have negligible depolarizing effects. Measurements were made also in 0.05M H_2SO_4 at 10^{-4} amp cm^{-2}; as seen in Fig. 5, the change in acid concentration had no appreciable effect on the oxidation curve.[9]

[9] Armstrong, Himsworth, and Butler (44) found linear oxidation curves for gold in 0.1M H_2SO_4, as determined by cathodic reduction of the oxide, with a current efficiency of 0.9% independent of c.d.

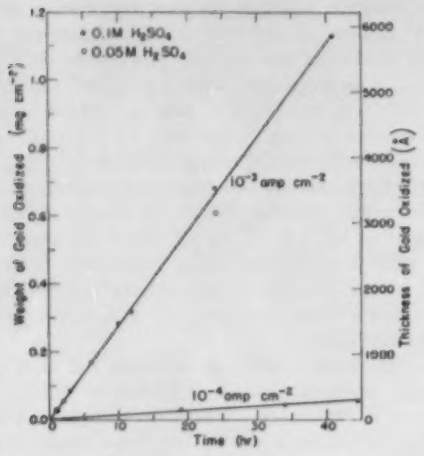

Fig. 5. Anodic formation of gold oxide in sulfuric acid solutions, 25°C.

Linear oxidation curves may be interpreted as resulting from a blister mechanism, in which local separation occurs at the oxide-metal interface in a manner similar to that postulated for gas-metal reactions (34). In support of this mechanism, it was noted that the oxide exhibited poor adhesion, and the thicker coatings could be readily flaked away from the gold substrate.

The blister mechanism may be used to explain the increase in current efficiency for oxide formation with increasing c.d. According to this mechanism, localized interfacial separation occurs when the oxide layer has grown to a critical thickness, such that the local adhesive force is exceeded by the compressive force in the oxide at that point. A blister forms, the distorted oxide cracks, the electrolyte then contacts the exposed metal surface, and rapid oxidation begins there again. In the absence of gas evolution, the oxidation rate should increase with c.d.; it would tend to be roughly proportional to c.d. if the critical oxide thickness for blistering is very small, as appears to be the case for gold anodes where linear oxidation occurs even at low film thicknesses (Fig. 5). The effect of simultaneous gas evolution, however, is to increase the oxidation rate by causing increased rate of blistering. Gas pressure can build up within the blisters, because the surface tension of the liquid tends to prevent the escape of gas through the small cracks in the blistered oxide layer. The gas pressure within a local blister helps to overcome the adhesive force at adjacent areas, thus increasing the rate of blistering and decreasing the critical oxide thickness. Since the rate of gas evolution is proportional to c.d., the higher the c.d. the greater the increase in oxidation rate resulting from this gas-evolution effect. Thus the blister mechanism is qualitatively consistent with the observed fact that the current efficiency for oxidation increased with c.d.

Potential-time variations.—In 0.1M H_2SO_4, oxygen-saturated but before any electrolysis, a clean gold electrode assumes a potential of 0.83 v vs. RHE,[a] which is 0.4 v less than the reversible oxygen potential. After prolonged electrolysis of the solution (roughly 0.2 coulomb/ml), however, the typical behavior of a clean gold electrode is that shown in Fig. 6. Upon immersion (zero time) the potential rises quickly to a value higher than the reversible oxygen potential and approaches the reversible Au/Au_2O_3 (hydrated) potential, 1.363 v (35, 36), indicating that gold tends to oxidize in the electrolyzed solution. After the electrode is made anode for a short time at very low c.d., the potential decay curve tends to arrest at the same value.

[a] Single electrode potentials refer to the reversible hydrogen electrode in the same solution.

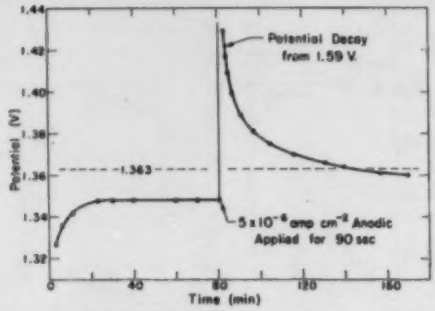

Fig. 6. Potential behavior of a fresh gold electrode in preelectrolyzed 0.1M H_2SO_4, 25°C. Potential referred to reversible hydrogen electrode (RHE) in same solution.

When a clean gold surface was made anode at 10^{-5} or 10^{-4} amp cm^{-2}, the potential increased to a value 3 to 5 mv higher than the steady-state value, then decreased to the steady value after passage of about 1 coulomb cm^{-2}. The potential was followed for an additional 40 hr, and remained constant to ±0.5 mv as the oxide layer thickened. It was concluded that no deleterious impurities were diffusing into the cell from the reference compartment.

In the procedure that was adopted for determining the η-i relationship, a relatively heavy oxide coating was first formed at a c.d. near the upper end

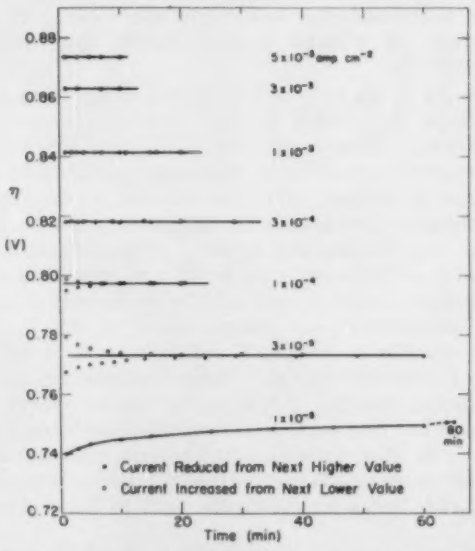

Fig. 7. Overpotential vs. time for oxygen evolution at gold anode in 0.10M H_2SO_4, 25°C.

of the range (at least 40 coulomb cm^{-2} passed). Then the current was decreased in steps to the minimum value and finally increased in steps to the maximum value. A typical set of η vs. time curves are shown in Fig. 7. The steady-state overpotentials obtained with decreasing or with increasing current were the same within ±0.5 mv. One experiment was continued through a second cycle of decreasing followed by increasing current densities, and the steady-state overpotentials remained the same within ±1 mv. Preliminary electrolysis of the solution with an auxiliary anode produced no appreciable change in the steady-state η-i curve.

The constant current curves of Fig. 7 exhibit a time effect at low current densities. When the current is decreased from a higher value the overpotential is initially lower than the steady-state value, and when the current is increased from a lower value η exceeds the steady-state value initially. This is a reproducible effect.

At 10^{-5} amp cm^{-2} the potential drift with time was prolonged (Fig. 7). The value of η after 1 hr was still 3 mv below the extrapolated η-log i curve. This behavior was characteristic of all runs, hence $i = 3 \times 10^{-5}$ was chosen as the lower limit for steady-state overpotential measurements. The interpretation of this time effect is considered in the next section from the standpoint of competing reactions.

Competing reactions.—The reversible single electrode potentials, referred to the standard hydrogen electrode (SHE), at 25°C for possible reactions at gold anodes, and for possible cathodic reactions, in dilute sulfuric acid solids are given in Table I.

Table I. Reversible electrode potentials at 25°C referred to SHE*

(a) $O_2 + H^+ + e^- = HO_2$; $E = -0.13 - 0.0592\ pH + 0.0592 \log [O_2]/[HO_2]$

(b) $2H^+ + 2e^- = H_2$; $E = -0.0592\ pH - 0.02\% \log [H_2]$

(c) $O_2 + 2H^+ + 2e^- = H_2O_2$; $E = 0.682 - 0.0592\ pH - 0.0296 \log [O_2]/[H_2O_2]$

(d) $O_2 + 4H^+ + 4e^- = 2H_2O$; $E = 1.229 - 0.0592\ pH + 0.0148 \log [O_2]$

(e) $Au(OH)_3 + 3H^+ + 3e^- = Au + 3H_2O$; $E = 1.363 - 0.0592\ pH$

(f) $Au^{+3} + 3e^- = Au$; $E = 1.50 + 0.0197 \log [Au^{+3}]$

(g) $Au^+ + e^- = Au$; $E = 1.7 + 0.0592 \log [Au^+]$

(h) $HO_2 + 3H^+ + 3e^- = 2H_2O$; $E = 1.7 - 0.0592\ pH + 0.0197 \log [HO_2]$

(i) $H_2O_2 + 2H^+ + 2e^- = 2H_2O$; $E = 1.77 - 0.0592\ pH + 0.0296 \log [H_2O_2]$

(j) $S_2O_8^{-2} + 2e^- = 2SO_4^{-2}$; $E = 2.01 + 0.0296 \log [S_2O_8^{-2}] - 0.0592 \log [SO_4^{-2}]$

(k) $O_3 + 2H^+ + 2e^- = O_2 + H_2O$; $E = 2.07 - 0.0592\ pH + 0.0296 \log [O_3]/[O_2]$

(l) $OH + H^+ + e^- = H_2O$; $E = 2.8 - 0.0592\ pH + 0.0592 \log [OH]$

* Standard electrode potentials are from Latimer (36), except for reaction (e) (35, 36). Potentials follow the IUPAC-Stockholm sign convention. [ ] denotes activity.

Reactions (a) to (c) are possible cathodic processes which yield products that would depolarize the oxygen evolution reaction at the anode. Of these, H_2O_2 is expected to be the primary depolarizer produced at low currents, hydrogen gas at high currents. The latter tends to be swept out of the solution by oxygen bubbling and has been shown to have no appreciable depolarizing effect at moderate current densities (37). Hydrogen peroxide was detected in the solution, at the end of an η vs. i run, with titanium sulfate reagent; spectrophotometric analysis indicated a concentration of 5×10^{-6}M. The maximum c.d. for H_2O_2 oxidation at the anode, corresponding to this concentration, can be computed from Eq. [5]; thus with $l = 5 \times 10^{-3}$ cm for gas-bubbling conditions (38), $D \sim 10^{-5}$ cm^2 sec^{-1}, and $C_s = 0$, one obtains $f = 1 \times 10^{-11}$ mole cm^{-2} sec^{-1}. This corresponds to a diffusion current density, $i_d = 2Ff$, of 2×10^{-4} amp cm^{-2}, which would result in measurable depolarization at an applied c.d. of 3×10^{-4} amp cm^{-2} or less. Actually the measured H_2O_2 concentration was determined soon after electrolysis at high c.d.; after prolonged electrolysis with gradually decreasing currents the H_2O_2 concentration would be less than the measured value, and the c.d. for observable depolarization would be less than 3×10^{-4} amp cm^{-2}. The typical potential-time curves in Fig. 7 indicated depolarization beginning at 1×10^{-5} amp cm^{-2}, hence this may be attributed to the presence of cathodically produced H_2O_2.

Of the possible simultaneous anodic reactions which could lower the current efficiency, (e) to (l) in Table I, oxide formation (e) and metal dissolution (f) tend to occur at low overpotentials. The rate of the former reaction has already been shown to be insignificant. The metal dissolution rate is expected to be small because of the relatively low solubility of the oxide in dilute acids (30):

$$Au(OH)_3 = Au^{+3} + 3OH^- \quad K = 8.5 \times 10^{-46} \quad [7]$$

This was confirmed in 0.1M H_2SO_4; the average current efficiency for gold dissolution at 10^{-5} amp cm^{-2} over a 24-hr period was found to be 0.007%.

At high values of η water tends to oxidize anodically to H_2O_2 and HO_2 by reactions (i) and (h), but these substances are very unstable with respect to further anodic oxidation, i.e., reactions (a) and (c). Peroxidisulfuric acid can be produced by reaction (j) and ozone by reaction (k); these products have greater stability in the anolyte, as shown by the fact that they can be generated at the anode in large quantities in more concentrated H_2SO_4 solutions (39, 40).

Thermodynamically, either of the latter two products is capable of oxidizing a fresh gold electrode, as indicated by the reactions:

$$2Au + 3H_2S_2O_8 + 6H_2O = 2Au(OH)_3 + 6H_2SO_4, \quad \Delta G^\circ = -90 \text{ kcal} \quad [8]$$

$$2Au + 3O_3 + 3H_2O = 2Au(OH)_3 + 3O_2, \quad \Delta G^\circ = -98 \text{ kcal} \quad [9]$$

where the values of ΔG°, the standard free energy change at 25°C, were calculated from the standard electrode potentials of Table I. Hence one of these substances might have produced the effect shown in Fig. 6, in which a fresh gold electrode in a used solution assumes a potential higher than the reversible oxygen potential and approaching that of the Au/Au(OH)$_3$ electrode. It may be noted that H_2O_2, which accumulated in the solution as found above, would not produce such high potentials (41). Attempts to detect $H_2S_2O_8$ in the solution after prolonged electrolysis, by the use of Ni(OH)$_2$ reagent (sensitivity approximately 5 ppm), were negative. More significantly, it was found that the potential of a clean gold surface in un-electrolyzed 0.1M H_2SO_4 remained constant at about 0.83 v when $K_2S_2O_8$ was added to the solution, even in concentrations as high as 0.002M.

The effect of ozone was determined qualitatively in the following manner. A platinum wire was placed inside a small Pyrex tube through which the purified oxygen gas passed before entering the cell. An induction coil (laboratory leak tester) was used to produce sparking to the platinum wire for a period of 9 min, thus introducing a little ozone into the oxygen gas bubbling around the electrode. At the end of this period the potential of the gold electrode had risen to 1.30 v, which is above the reversible oxygen potential but below the Au/Au(OH)$_3$ potential. Thus oxidation of an appreciable fraction of the gold surface was indicated.

From the above evidence it was concluded that ozone is an anodic by-product at the higher current densities, and is responsible for the marked change in potential behavior of a fresh gold electrode produced by pre-electrolysis of the solution.

IR-drop measurements.—An upper limit to the c.d. range may be imposed by the accuracy with which the *IR* drop included in the overpotential measurement is determined. To calculate the *IR* drop within the solution for a capillary of diameter d positioned at a distance $3d$ from the electrode, Ohm's law in the form $i = -\kappa dV/dn$ was integrated for concentric spheres, from $n = r_o$ to $n = r_o + 3d - d/3$, to give the equation:

$$V_{IR} = (ir_o^2/\kappa)\,[1/r_o - 1/(r_o + 3d - d/3)] \quad [10]$$

This assumes that the potential inside the capillary is equal to that at a distance $d/3$ closer to the electrode in the undistorted field, as was observed for parallel planes (12), a good approximation for concentric spheres with $3d << r_o$. The maximum allowable magnitude of V_{IR} was taken to be 10 mv for experimental error ±1 mv. Substitution of this value into Eq. [10] yields i_{max}, the highest c.d. at which accurate correction can be made for the *IR* drop in the electrolyte. For 0.1M H_2SO_4 ($\kappa = 0.046$) in the cells used ($d = 0.02$, $r_o = 0.50$), one obtains $i_{max} = 1 \times 10^{-2}$ amp cm^{-2}.

In order to determine *IR* drops within the oxide coating, the total *IR* drop included in the measured overpotential was evaluated directly at 10^{-5} amp cm^{-2} in 1.0M H_2SO_4, with an oxide of typical thickness preformed over the anode. The interrupted-current method was used: the electrode was polarized to the steady-state potential, the applied current was switched off by means of a rapid electronic switch, and the anode vs. SCE voltage-decay curve displayed on an oscilloscope.[4] The "instantaneous" voltage decay agreed with that calculated from Eq. [10] within 1 mv. Thus the *IR* drop within the oxide was negligible at 10^{-2} amp cm^{-2}, or at any lower c.d. Similar measurements were not made in 0.1M H_2SO_4, but the same conclusion was drawn from the absence of appreciable deviations from Tafel's equation as described below.

Table II. Overpotential-current density relationship for oxygen evolution at gold anodes in 0.100M H_2SO_4, 25.0°C

Electrode	Cell	Tafel constants a'	b
Plated	I	0.977	0.0461
Plated	II	0.977	0.0450
Solid	II	0.976	0.0445
Solid	II	0.976	0.0447
Mean Tafel line		0.977	0.0450

Concentration changes at the anode surface.—The increase in acid concentration at the anode surface may be estimated from Eq. [5]. At any current density i, $f = (1 - t_+)i/2\mathbf{F}$, where t_+ is the cation transference number. For 0.1M H_2SO_4, $t_+ = 0.82$ (42), $D = 1.9 \times 10^{-5}$ cm^2 sec^{-1} (43), $l = 0.005$ cm (38), and the calculated concentration change at $i_{max} = 0.010$ amp cm^{-2} is $C_o - C_o = 0.002$, mole l^{-1}, a change of only 2.4%. Therefore concentration polarization effects were expected to be negligible in these experiments.

Overpotential-current density relationship.—Over the c.d. range for precise measurements as defined above, 3×10^{-5} to 10^{-2} amp cm^{-2}, Tafel's equation was accurately obeyed. The Tafel constants for various runs are given in Table II, and Fig. 8 shows a typical Tafel line. In each run the points obtained with decreasing and then increasing current densities all fell on the line within ±1 mv. Essentially the same Tafel constants were obtained in all runs; substitu-

[4] Tektronix, Inc., Portland, Oreg., type 545 oscilloscope with type 53/54D amplifier.

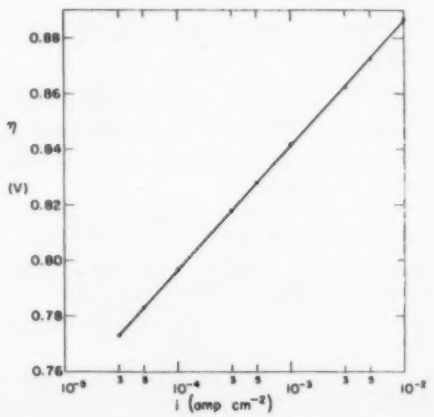

Fig. 8. Typical Tafel plot for oxygen evolution at gold anode in 0.1M H_2SO_4, 25°C.

tion of the slot cell for cell II or of the plated gold electrode for the solid one had no appreciable effect.

The Tafel constants in Table II are based on the apparent surface area; roughness factors were not measured. It was anticipated that the roughness factor for the dull oxide surface on the plated electrode (q_p) would be greater than that (q_s) for the solid electrode (bright oxide surface which reflected clear images). If $q_p = 2q_s$, for example, the effect on the Tafel a constant would be 0.015 v. The fact that no appreciable effect was found indicated that oxide growth on these two surfaces produced the same roughness factor, in spite of the large difference in surface brightness.

The mean value, $b = 0.045$ at 25°C, does not coincide with the predicted value for any mechanism of anodic oxygen evolution given in the compilation of Bockris (1). The exchange current density:

$$i_o = 10^{-(a/b)} = (1/q)\ 10^{-(a'/b)} \qquad [11]$$

has the unusually low value $2 \times 10^{-29}/q$. In addition to the Tafel constants, the measurements required to fix the mechanism of anodic oxygen evolution include the effects of pH and neutral salts on the overpotential. Conclusions concerning the mechanism, therefore, must be deferred to a future paper in which such measurements will be presented.

Manuscript received Oct. 13, 1958. This paper was prepared for delivery before the Ottawa Meeting, Sept. 28-Oct. 2, 1958.

Any discussion of this paper will appear in a Discussion Section to be published in the June 1960 JOURNAL.

REFERENCES

1. J. O'M. Bockris, *J. Chem. Phys.*, **24**, 817 (1956).
2. J. O'M. Bockris, Editor, "Modern Aspects of Electrochemistry," p. 226, Butterworths Publications, Ltd., London (1954).
3. J. O'M. Bockris in "Electrochemical Constants," p. 243, National Bureau Stds. Circular 524 (1953).
4. J. Tafel, *Z. physik. Chem.*, **50**, 641 (1905).
5. J. O'M. Bockris and A. K. M. S. Huq, *Proc. Roy. Soc.*, **A237**, 227 (1956).
6. F. Haber, *Z. physik. Chem.*, **32**, 208 (1900).
7. C. Kasper, *Trans. Electrochem. Soc.*, **77**, 353 (1940).
8. C. Kasper, *ibid.*, **78**, 131 (1940).
9. C. Kasper, *ibid.*, **78**, 147 (1940).
10. C. Wagner, *This Journal*, **98**, 116 (1951).
11. S. Barnartt, *J. Chem. Phys.*, **21**, 2090 (1953).
12. S. Barnartt, *This Journal*, **99**, 549 (1952).
13. R. Piontelli, G. Bianchi, U. Bertocci, C. Guerci, and B. Rivolta, *Z. Elektrochem.*, **58**, 54 (1954).
14. R. Piontelli and G. Bianchi, *Gazz. chim. ital.*, **80**, 581 (1950).
15. R. Aletti, U. Bertocci, G. Bianchi, C. Guerci, R. Piontelli, G. Poli, and G. Serravalle, "Proceedings of the Third Meeting of the International Committee of Electrochemical Thermodynamics and Kinetics," p. 30, Bern (1951).
16. R. Piontelli, G. Bianchi, and R. Aletti, *Z. Elektrochem.*, **56**, 86 (1952).
17. F. P. Bowden and E. K. Rideal, *Proc. Roy. Soc.*, **A120**, 59, 80 (1928).
18. F. P. Bowden and E. A. O'Connor, *ibid.*, **A128**, 317 (1930).
19. J. O'M. Bockris and B. E. Conway, *Trans. Faraday Soc.*, **45**, 989 (1949).
20. A. M. Azzam, J. O'M. Bockris, B. E. Conway, and H. Rosenberg, *ibid.*, **46**, 918 (1950).
21. A. Hickling and W. H. Wilson, *Nature*, **164**, 673 (1949).
22. A. Hickling and S. Hill, *Disc. Faraday Soc.*, **1**, 236 (1947).
23. H. J. S. Sand, *Z. physik. Chem.*, **35**, 641 (1900).
24. H. J. S. Sand, *Phil. Mag.*, **1**, 45 (1901).
25. T. R. Rosebrugh and W. L. Miller, *J. Phys. Chem.*, **14**, 816 (1910).
26. C. W. Tobias, M. Eisenberg, and C. R. Wilke, *This Journal*, **99**, 359C (1952).
27. G. A. Perley, *Trans. Electrochem. Soc.*, **92**, 497 (1947).
28. S. Barnartt, *This Journal*, **98**, 311 (1951).
29. G. Dubpernell in "Modern Electroplating," A. G. Gray, Editor, 2nd ed., p. 145, John Wiley & Sons, Inc., New York (1953).
30. W. M. Latimer, "Oxidation Potentials," 2nd ed., Prentice Hall, New York (1952).
31. J. W. Mellor, "A Comprehensive Treatise on Inorganic and Theoretical Chemistry," Vol. 3, p. 580 (1923).
32. S.E.S. El Wakkad and A. M. Shams El Din, *J. Chem. Soc.*, **1954**, 3098.
33. A. Guinier, "X-ray Crystallographic Technology," Hilger and Watts, London (1952).
34. U. R. Evans, *Trans. Electrochem. Soc.*, **91**, 547 (1947).
35. R. H. Gerke and M. D. Rourke, *J. Am. Chem. Soc.*, **49**, 1855 (1927).
36. T. F. Buehrer and W. E. Roseveare, *ibid.*, **49**, 1989 (1927).
37. A. Rius, J. Llopis, and P. Gandia, *Annales Real Soc. Esp. Fis. Quim.*, **B46**, 225 (1950).
38. C. V. King, *This Journal*, **102**, 193 (1955).
39. J. W. Mellor, "A Comprehensive Treatise on Inorganic and Theoretical Chemistry," **10**, p. 418 (1930).
40. F. Fischer and K. Bendixsohn, *Z. anorg. Chem.*, **61**, 13, 183 (1909).
41. J. O'M. Bockris and L. F. Oldfield, *Trans. Faraday Soc.*, **51**, 249 (1955).
42. W. J. Hamer, *J. Am. Chem. Soc.*, **57**, 662 (1935).
43. E. A. Hollingshead and A. R. Gordon, *J. Chem. Phys.*, **8**, 423 (1940).
44. G. Armstrong, F. R. Himsworth, and J. A. V. Butler, *Proc. Roy. Soc.*, **A143**, 89 (1933).
45. F. Jirsa and O. Buryànek, *Z. Elektrochem.*, **29**, 126 (1923).

Electrokinetic Measurements on Stainless Steel Capillaries

B. Levy and A. R. Fritsch

Radiation & Nucleonics Laboratory, Materials Engineering Departments, Westinghouse Electric Corporation, East Pittsburgh, Pennsylvania

ABSTRACT

Electrokinetic potentials of stainless steel in HCl, H_2SO_4, and $K_2Cr_2O_7$ solutions have been measured by the streaming current technique. Negative zeta potentials are obtained in H_2O and in low acid concentrations. Isoelectric acid concentrations occur between 10^{-4} and $10^{-3}N$. At higher concentrations positive potentials are obtained. $K_2Cr_2O_7$ adsorbs irreversibly at its isoelectric concentration of 10^{-5}M as evidenced by the inability of water washing to return the sample to its original negative zeta potential.

A technique has been developed recently by Hurd and Hackerman (1, 2) making it possible to measure the electrokinetic potentials of bulk metals. Prior to this all quantitative measurements have been made on metal sols (3). The experiments performed by Hurd and Hackerman involved platinum, silver, and gold capillaries and water solutions of KCl and KOH in the concentration range from 10^{-4} to 10^{-2}M. In all cases the electrokinetic potential was found to be negative. The magnitudes of the potentials were explained on the basis of the relative strengths of the metal oxide and the oxide-counter ion bonds, the larger negative potentials being obtained with the metals forming the stronger oxide bonds. In the present study, electrokinetic potentials of types 304 and 347 stainless steel were measured in HCl, H_2SO_4, and $K_2Cr_2O_7$ solutions. The purpose of the work is to determine if changes in the electrical double layer of adsorbed ions, as determined by electrokinetic measurements, can be correlated with such factors as corrosion, corrosion inhibition, and formation of deposits on metal surfaces. This paper is in the nature of a report on the progress that has been made thus far.

Experimental

The technique developed by Hurd and Hackerman was employed in making the measurements. It consists of measuring the streaming current due to liquid flow through a metal capillary. Unless special precautions are taken, part of this streaming current will flow through the walls of the capillary, thus obscuring the results. In order to eliminate this difficulty an external shunting resistor is placed in series with a pair of Pt electrodes located close to, but not touching, the ends of the metal capillary. It has been shown by Hurd and Hackerman that, if the outside walls of the capillary are isolated from the solution, then the "apparent" resistance of the Pt, Au, and Ag capillaries is large compared to an external resistor ranging from 10^4 to 10^5 or 10^6 ohms. This effect has been verified for the stainless steel capillaries in the present study and is probably due to polarization at the ends of the capillary (Table I, sample 4).

A L&N No. 9835 D-C microvolt amplifier and Varian G-10 recorder are used to measure the voltage drop across this resistor, thus making it possible to calculate the streaming current and thereby the zeta potential from the following equation:

$$I = \frac{\Delta P r^2 D \zeta}{4 \eta l}$$

where I is streaming current, statamp; ΔP the pressure drop across the capillary, dynes/cm^2; ζ the zeta potential, statvolts; η the viscosity, poises; D the dielectric constant of the solution; r the radius of the capillary, cm; and l the length of the capillary, cm.

A check on the operation of the equipment is shown in Fig. 1, where the voltage drop across a 40-k external resistor is plotted against the pressure drop (ΔP).

All of the solutions used in the experiments were prepared from reagent grade chemicals using singly distilled water. The steel capillaries were used as received or treated with acetone, boiling NaOH, and HNO_3. The results were similar qualitatively regardless of pretreatment as is seen in Table I, samples 1-4.

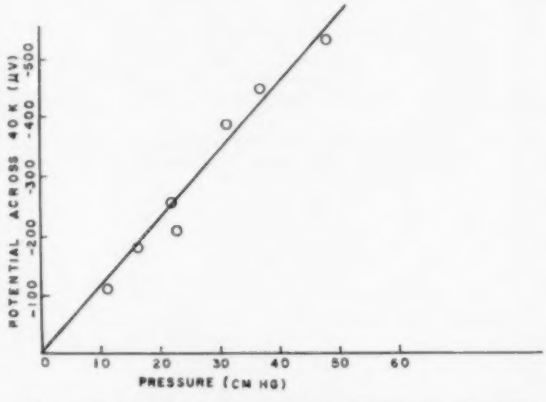

Fig. 1. Potential vs. pressure across 40 K external resistor, sample 2; type 304 stainless steel; $r = 1.46 \times 10^{-3}$ cm; $l = 2.54$ cm, solution H_2O.

Table I. Zeta potential of type 304 stainless steel in H_2SO_4 solutions

Sample 1. $l = 2.22$ cm, $r = 1.40 \times 10^{-3}$ cm, external resistor = 40 K

Solution		Zeta potential, mv
H_2O		−12.8
$10^{-4}N$ H_2SO_4		−4.32
$10^{-4}N$ H_2SO_4		−2.27
$10^{-4}N$ H_2SO_4		−0.27
$10^{-3}N$ H_2SO_4		+13.2
$10^{-2}N$ H_2SO_4		+84.0

Sample 2. $l = 2.54$ cm, $r = 1.46 \times 10^{-3}$ cm, external resistor = 40 K

Solution		Zeta potential, mv
H_2O		−88.0
$10^{-4}N$ H_2SO_4		−28.1
		−25.8
	Avg	−27.0
$10^{-4}N$ H_2SO_4		−0
$10^{-3}N$ H_2SO_4		+31.7
		+54.5
	Avg	+43.1
$10^{-2}N$ H_2SO_4		+37.2
$10^{-1}N$ H_2SO_4		+24.9

Sample 3. $l = 3.60$ cm, $r = 1.60 \times 10^{-3}$ cm, external resistor = 20 K

Pretreatment: acetone, NaOH, HNO_3 (each reagent was followed by ½-hr refluxing with H_2O in a Soxhelet extractor)

Solution		Zeta potential, mv
H_2O		−64.1
		−64.4
		−69.2
		−65.3
		−56.5
		−63.8
	Avg	−63.9
$10^{-5}N$ H_2SO_4		−32.5
		−29.6
		−34.0
		−35.4
		−33.9
	Avg	−33.1
$10^{-4}N$ H_2SO_4		−17.3
		−11.1
		−7.58
		−9.61
	Avg	−11.4
$10^{-3}N$ H_2SO_4		+38.0
		+41.4
	Avg	+39.7
$10^{-2}N$ H_2SO_4		+128
		+143
		+140
	Avg	+137

Sample 4. $l = 3.54$ cm, $r = 1.64 \times 10^{-3}$ cm

Pretreatment: ½-hr acetone followed by ½-hr H_2O

Concentration	Zeta potential, mv external resistor = 10^4 Ω	Zeta potential, mv external resistor = 10^6 Ω	Zeta potential, mv external resistor = 10^8 Ω
H_2O	−75.3	−71.8	−70.1
	−61.9	−67.1	−67.1
	−64.5	−62.1	−61.9
	−56.5	−46.4	−46.4
	−49.7	−50.8	−47.6
	−42.6	−46.9	−46.0
Avg	−58.4	Avg −57.5	Avg −56.5
$10^{-4}N$ H_2SO_4	−42.3	−42.8	−43.1
	−35.3	−30.2	−30.8
	−43.1	−29.8	−48.1
	−42.8	−46.0	−45.7
	−55.4	−42.8	−30.1
	−46.6	−28.4	−57.2
	−42.3	−43.8	−38.3
		−43.8	−42.4
		−42.3	−42.6
			−31.7
Avg	−44.0	Avg −38.9	Avg −41.0
$10^{-3}N$ H_2SO_4	−30.0	−22.6	−28.4
	−27.0	−20.9	−24.6
		−25.9	−23.2
		−28.3	−26.5
		−25.1	−28.2
		−26.7	−25.8
Avg	−28.5	Avg −24.9	Avg −26.1
$10^{-4}N$ H_2SO_4	Both positive and negative values		
$10^{-3}N$ H_2SO_4	Both positive and negative values		
H_2O	−44.8	−45.6	−46.0
	−54.8	−49.1	−47.7
	−16.5	−25.6	−23.6
Avg	−38.7	Avg −40.1	Avg −39.1
$10^{-2}N$ H_2SO_4	+393	+401	
	+394	+394	
Avg	+394	Avg +398	

Results and Discussion

Table I lists the results, in the order performed, on type 304 stainless steel capillaries as a function of H_2SO_4 concentration. As is seen, the agreement between the samples is not too good except insofar as the isoelectric point is concerned. This occurs at a concentration close to $10^{-4}N$ H_2SO_4. The lack of quantitative agreement is probably not too surprising. Since the zeta potential of the metal is apparently that of an oxide layer, differences in the nature and extent of oxide film buildup will affect the magnitude of the zeta potential but may not affect the isoelectric point.[1] The transformation from a negative to a positive zeta potential may provide a sensitive indication of the first signs of metal corrosion.

If Grahame's model (4) for the electrical double layer is assumed, the situation at the metal-H_2O interface may be pictured schematically as in Fig. 2. The zeta potential is, by definition, the potential at the surface of shear of the double layer as compared to that of the solution. This surface of shear is generally assumed to coincide with the boundary between the outer Helmholtz layer and the diffuse layer. The sign of the zeta potential is determined by the excess charge in the combined inner and outer Helmholtz layer. Experimentally, type 304 stainless steel has a negative zeta potential in H_2O. Therefore, Fig. 1 shows an excess of OH^- ions in the Helmholtz layer located at sites adjacent to metal atoms. The oxygen atoms would appear to be ideal sites for the adsorption of protons. Perhaps the reason that stainless steel does not have a positive

[1] Suggested by one of the reviewers of this paper.

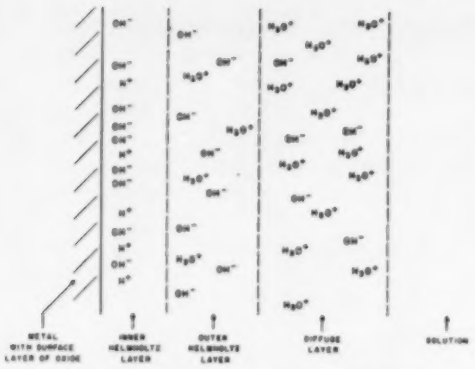

Fig. 2. Structure of the electrical double layer

zeta potential in water is the relatively high dehydration energy that must be supplied in order for the protons to enter the inner Helmholtz layer as compared to the similar process with OH^- ions. As H_2SO_4 is added to the solution there are fewer OH^- ions in the solution and correspondingly more H_3O^+ ions. This leads to a decrease in negative potential due to: (*a*) a decrease in the number of OH^- ions available for adsorption in the inner Helmholtz layer, (*b*) adsorption of protons at oxygen sites, and (*c*) partial decomposition of the oxide by protons accompanied by the formation and adsorption of positively charged metal ions.

These processes proceed with continued increase in acid concentration until a point is reached where there are an equal number of positive and negative ions in the Helmholtz layer. Further addition of acid causes the zeta potential to become positive.

In Table II the results are given for type 304 stainless steel in HCl solutions. Once again the zeta potential changes from negative to positive with increased HCl concentration. The isoelectric point occurs between 10^{-4} and $10^{-3}N$ HCl. Potentials with HCl were found to be more erratic than with H_2SO_4 solutions, possibly due to the ability of the Cl^- ions to penetrate the surface film which in turn may

Table II. Zeta potential of type 304 stainless steel in HCl solutions

Sample 5. l = 3.19 cm, r = 2.56 x 10^{-2} cm, external resistor = 40 K

Solution	Zeta potential, mv
H_2O	−15.2
	−13.2
	−18.6
	−6.98
	−14.0
	Avg −13.6
$10^{-5}N$ HCl	−9.79
	−11.2
	−12.2
	Avg −11.1
$10^{-4}N$ HCl	+8.93
	+7.64
	+12.6
	Avg +9.72
H_2O	−24.0
	−21.1
	Avg −22.6
$10^{-3}N$ HCl	+48.8
	+58.4
	+55.3
	Avg +54.2
H_2O	−37.0
	−45.5
	Avg −41.3
$10^{-2}N$ HCl	Values ranged from +4.9 to +146
H_2O	−30.0
	−29.5
	Avg −29.8
$10^{-1}N$ HCl	Avg +239
	Values ranged from +166 to +392
H_2O	−35.0

Table III. Zeta potential of type 347 stainless steel in H_2SO_4 solutions

Sample 6. l = 3.30 cm, r = 3.94 x 10^{-2} cm, external resistor = 10 K

Solution	Zeta potential, mv		
H_2O	−102		
	−98.0		
	−96.8		
	Avg −98.9		
$10^{-5}N$ H_2SO_4	−58.1		
	−63.8		
	−68.9		
	−68.9		
	−69.4		
	Avg −65.8		
$10^{-4}N$ H_2SO_4	−41.3		
	−40.2		
	−41.3		
	−44.9		
	−45.2		
	Avg −42.6		
$10^{-3}N$ H_2SO_4	+15.7		
	+16.6		
	+16.6		
	+14.1		
	+15.6		
	+19.8		
	+15.2		
	+19.5		
	Avg +16.6		
H_2O	−54.3		−89.6
	−49.7		−77.8
	−53.0		−87.3
	−53.0	after standing over	−71.5
	−51.3	weekend	−61.0
	Avg −51.5		−82.2
			−83.6
			−82.4
		Avg	−79.4
$10^{-3}N$ H_2SO_4	+6.2		
$10^{-2}N$ H_2SO_4	Very slightly positive, same result after standing overnight		
H_2O	−133		
	−149		
	−148		
	−186		
	−151		
	−108		
	Avg −146		
$10^{-1}N$	Erratic		

give rise to active corrosion. These special properties of Cl^- ions are evidenced by their ability to cause stress corrosion cracking (5).

Tables III and IV give the results for type 347 stainless steel in H_2SO_4 and HCl solutions, respectively. In H_2SO_4 the isoelectric point occurs between 10^{-4} and $10^{-5}N$. In HCl it is probably closer to $10^{-5}N$. For both solutions the results are somewhat more erratic than with the type 304 stainless steel.

The effects of the acid on the metal surface do not appear to be permanent since the shift to positive potentials with high acid concentration can be reversed easily to negative values by flowing H_2O through the capillary in most instances. This offers support to the generally accepted view that an oxide layer is formed quickly on clean metal surfaces (6), if it is assumed that the acid treatment completely dissolved the oxide layer.

Table V gives the results of a series of experiments that have been run with type 304 stainless steel in $K_2Cr_2O_7$ solutions. The zeta potential was found to be negative in concentrations from 10^{-5} to 10^{-4}M. At 10^{-3}M $K_2Cr_2O_7$ and above, the potentials obtained appear to become insensitive to pressure changes and alternate erratically between low positive and low negative values. Powers and Hackerman (7) have demonstrated by tracer techniques that S.A.E. 1020 steel forms distinct anodic and cathodic areas, accompanied by the deposition of a nonadherent film, in 10^{-4}M Na_2CrO_4. They find that at concentrations of 10^{-3}M Na_2CrO_4 the steel is passivated, and chromate is deposited uniformly on the steel surface and cannot be removed by any physically nondestructive means. King, Goldschmidt, and Mayer (8) have demonstrated a significant decrease in the corrosion rate of iron in 10^{-3}M $K_2Cr_2O_7$ as compared to that found at lower concentrations. The results of the zeta potential determinations in $K_2Cr_2O_7$ at concentrations greater than 10^{-4}M may be the result of the masking, by polarization, of anodic and cathodic areas. Measurements were made with a fresh sample of type 304 stainless steel at successively higher concentrations of $K_2Cr_2O_7$. At 10^{-3}M $K_2Cr_2O_7$ the zeta potential becomes zero. The apparatus was then rinsed with distilled water and a determination made using the same capillary in H_2O. The sample remained at the isoelectric point. Previous measurements showed that there was no apparent permanent change in the behavior of the metal when treated with HCl and H_2SO_4 solutions. Evidently there is a very strong irreversible attachment of the Cr_2O_7 equal to the steel surface, in agreement with the data of Powers and Hackerman. To test this point still further, a new sample of type 304 stainless steel was treated first with H_2O, then 10^{-3}M $K_2Cr_2O_7$, and finally with H_2O. Once again the 10^{-3}M solution caused the zeta potential to go to zero and remain there after treatment with H_2O. Still another series of experiments were performed with a new sample of stainless steel. The order of the experiments consisted of runs with H_2O, 10^{-4}M $K_2Cr_2O_7$, and H_2O. The zeta potential remained negative in the 10^{-4}M $K_2Cr_2O_7$ solution.

Table IV. Zeta potential of type 347 stainless steel in HCl solutions

Sample 7. $l = 3.32$ cm, $r = 1.20 \times 10^{-2}$ cm, external resistor = 10 K

Solution	Zeta potential, mv
H_2O	−86.6
	−86.6
	−95.5
	−116
	−92.0
	Avg −95.3
$10^{-4}N$ HCl	−131
	−115
	−169
	Avg −138
$10^{-5}N$ HCl	Erratic results
H_2O	−84.4
	−94.7
	−82.9
	−105
	−105
	Avg −94.4
$10^{-6}N$ HCl	−69.2
	−81.9
	−71.9
	−67.8
	Avg −72.7
$10^{-4}N$ HCl	−11.7
	−12.5
	Avg −12.1
$10^{-3}N$ HCl	+0.42
$10^{-2}N$ HCl	+106 followed by erratic results
H_2O	−106
	−104
	−76.1
	−139
	−109
	−73.4
	Avg −101
$10^{-1}N$ HCl	+2060 then erratic, no change in potential with change in direction or flow rate
H_2O	No response to direction or rate of flow

Gatos (9) has measured the supression of the polarographic maxima by corrosion inhibitors in systems containing either dissolved O_2, Ni^{++}, or Pb^{++}. At cathodic potentials lower than those at which the polarographic maxima occur, the dropping mercury electrode is assumed to be nonpolarized. When the potential of the polarographic maxima is reached and at higher potentials where the diffusion current is the controlling factor, the dropping mercury electrode is generally considered to be polarized. Enhanced corrosion inhibition is often considered to be due to polarization of the metal by the inhibitor. Gatos has shown a distinct correlation between the supression of the polarographic maxima and corrosion inhibition, and thereby has given strong support to the theory of corrosion inhibition by adsorption of polarizing substances. He has pointed out that,". . . capillary active anions and negative colloids in general preferentially suppress (polarographic) maxima appearing on the positive side of the electrocapillary zero (positive maximum)

Table V. Zeta potential of type 304 stainless steel in $K_2Cr_2O_7$ solutions

Sample 8. $l = 3.20$ cm, $r = 1.48 \times 10^{-2}$ cm, external resistor = 20 K

Solution	Zeta potential, mv
H_2O	−38.6
	−38.1
	−36.6
	Avg −37.8
	After standing over weekend
	−13.5
	−4.33
	−9.81
	−14.1
	−13.4
	−12.6
	−13.8
	−15.0
	−16.0
	−16.5
	Avg −12.9
10^{-6}M $K_2Cr_2O_7$	−19.3
	−16.5
	−19.3
	−17.8
	−17.5
	−16.0
	−16.4
	Avg −17.5
10^{-4}M $K_2Cr_2O_7$	−12.5
	−11.9
	−13.0
	−12.0
	−13.0
	Avg −12.5
10^{-3}M $K_2Cr_2O_7$	+ and − values finally zero
10^{-2}M $K_2Cr_2O_7$	+ and − values finally zero
10^{-1}M $K_2Cr_2O_7$	+ and − values finally zero

Sample 9. $l = 3.54$ cm, $r = 1.59 \times 10^{-2}$ cm, external resistor = 20 K

Solution	Zeta potential, mv
H_2O	−46.9
	−48.0
	−42.3
	−45.9
	−49.2
	−45.9
	Avg −46.4
10^{-5}M $K_2Cr_2O_7$	−47.3
	−47.3
	−42.6
	Avg −45.7
10^{-4}M $K_2Cr_2O_7$	−33.8
	−37.7
	−31.6
	−24.7
	Avg −32.0
10^{-3}M $K_2Cr_2O_7$	+ and − values finally zero
H_2O	+ and − values finally zero

Sample 10. $l = 3.69$ cm, $r = 1.64 \times 10^{-2}$ cm, external resistor = 20 K

Solution	Zeta potential, mv
H_2O	−24.6
	−20.6
	−22.2
	Avg −22.5
10^{-3}M $K_2Cr_2O_7$	First — finally zero
H_2O	Zero

Sample 11. $l = 3.68$ cm, $r = 1.57 \times 10^{-2}$ cm, external resistor = 20 K

Solution	Zeta potential, mv
H_2O	−47.3
	−40.6
	Avg −44.0
10^{-4}M $K_2Cr_2O_7$	−24.8
	−22.7
	Avg −23.8
H_2O	−61.6

whereas capillary-active cations and positive colloids are effective with the negative (electrocapillary) maxima."

The electrokinetic data with $K_2Cr_2O_7$ solutions bear a certain similarity with that of Gatos in that both are concerned with the electrical double layer of adsorbed material at the metal-solution interface. When a concentration is reached at which the isoelectric point is observed in the streaming current experiments, the nature of the metal-solution interface must be similar to that which occurs at the electrocapillary maxima with the dropping Hg electrode, since both correspond to a net zero charge of adsorbed ions at the surface. It may therefore be assumed in the electrokinetic studies that the metal is polarized at the isoelectric point and thereby passivated. As Gatos has pointed out, the polarographic technique for screening corrosion inhibitors is nonspecific in that a substance which is effective in suppressing the polarographic maxima may prove to be a good inhibitor for one substance and be a poor one for another. The electrokinetic technique makes it possible to run tests on the material of immediate interest and to correlate the results with corrosion data on systems containing the identical type of metal, corrosion solution and inhibitor.

Summary

1. The zeta potentials of type 304 and type 347 stainless steel were measured in H_2SO_4 and HCl solutions in the concentration range of from 10^{-6} to $10^{-1}N$. Steel samples go through the isoelectric point at concentrations between 10^{-4} and $10^{-3}N$.

2. The irreversible adsorption of 10^{-3}M $K_2Cr_2O_7$ was demonstrated by electrokinetic measurements and found to be in agreement with the data in the literature.

Acknowledgment

The authors wish to express their sincere appreciation to Drs. W. E. Wallace, K. H. Sun, G. R. Taylor, and D. G. Gardner for their many helpful discussions and suggestions, and also to the Pennsylvania Advanced Reactor Project jointly sponsored by Westinghouse Electric Corp. and Pennsylvania Power and Light Co. for supporting the work.

Manuscript received Aug. 1, 1958. This paper was prepared for delivery before the New York Meeting, April 27-May 1, 1958.

Any discussion of this paper will appear in a Discussion Section to be published in the June 1960 JOURNAL.

REFERENCES

1. R. M. Hurd and N. Hackerman, *This Journal*, **102**, 594 (1955).
2. R. M. Hurd and N. Hackerman, *ibid.*, **103**, 316 (1956).
3. H. R. Kruyt, "Colloid Science," Vol. 1 pp. 168-170, 208-209, 233, Elsevier Publishing Co., New York (1952).
4. D. C. Grahame, *Chem. Rev.*, **41**, 441 (1947).
5. See, for example T. P. Hoar and J. G. Hines, *J. Iron Steel Inst.*, **182**, 124 (1956).
6. H. A. Smith and K. A. Allen, *J. Phys. Chem.*, **58**, 449 (1954).
7. R. A. Powers and N. Hackerman, *This Journal*, **100**, 314 (1953).
8. C. V. King, E. Goldschmidt, and N. Mayer, *ibid.*, **99**, 423 (1952).
9. H. C. Gatos, *ibid.*, **101**, 433 (1954).

Brief Communications

Electron Diffraction of Zinc Silicate Phosphor

S. Yamaguchi

The Institute of Physical & Chemical Research, 31 Kamifuji (Hongo), Tokyo, Japan

A commercial sample of zinc silicate phosphor (Zn_2SiO_4:Mn), in powder form and of unknown history, was studied by electron diffraction using two different wave lengths (0.029 and 0.0455Å) (1). Electrons accelerated to 150 kv or more can penetrate thick grains to a depth of about 3000Å, whereas soft electrons at about 50 kv can only graze their surfaces. The thickness of the surface layer which can be penetrated by the latter electrons is about 200Å. The diffraction patterns observed at the same spot of the sample with the soft and hard electrons are shown in Fig. 1 and 2, respectively. For convenience in comparing these two figures, the negatives were enlarged 2.3 and 3.7 times, respectively. This is the approximate ratio of ring diameter at the two wave lengths.

Estimation of grain size.—A phosphor of practical use is as a rule granular, and it is of significance to estimate the grain size. A discontinuous diffraction ring [for the interplanar spacing 4.04Å, the (300) diffraction from the hexagonal pseudocell of Zn_2SiO_4 (2)] found in Fig. 2 was utilized for a rough estimation of the grain size. In this ring we can count about 80 spots diffracted from individual crystallites. The cross section of the incident beam used was about 0.05 mm. If we assume that the diffraction spots (4.04Å) correspond to sixfold symmetry of each crystal, we obtain the grain size of the sample

$$S = \frac{50}{80/6} = 4\mu$$

Diffraction intensity.—In comparing the figures we recognize that the intensity of certain diffraction spots found in Fig. 1 is distinctly stronger than that of the corresponding spots in Fig. 2. This implies that on the surfaces of the phosphor grains there

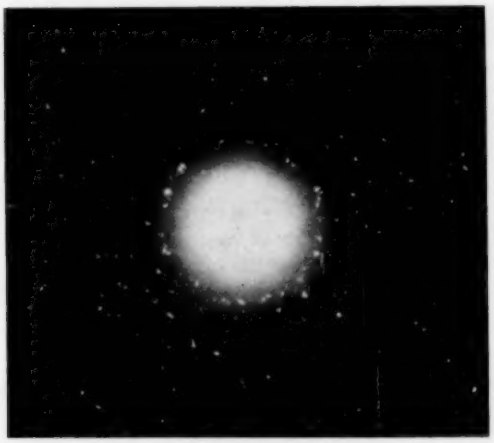

Fig. 1. Diffraction pattern with soft electrons. Wave length, 0.0455Å; camera length, 495 mm; positive enlarged 2.3X.

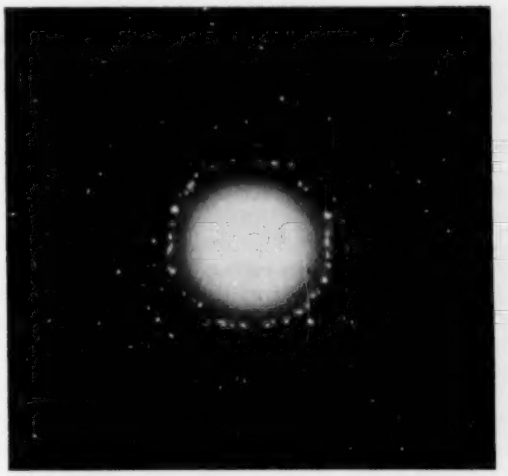

Fig. 2. Diffraction pattern with hard electrons. Wave length, 0.0290Å; positive enlarged 3.7X.

are lattices which are not only distinguishable from those of the substrate, but also are suitable for diffracting soft electrons. The number of diffraction spots found in Fig. 1 is roughly proportional to the number of crystallites able to diffract the soft electrons. Since the electrons used for a television screen are rather slow (about 10 kv), the diffraction phenomenon taking place on this screen is quite similar to that in Fig. 1. An important problem to be studied in the future, is whether electroluminescence depends on the coherent scattering of the incident electrons or not.

Manuscript received March 2, 1959.

Any discussion of this paper will appear in a Discussion Section to be published in the June 1960 JOURNAL.

REFERENCES

1. S. Yamaguchi, *J. Chem. Phys.*, **27**, 1114 (1957).
2. R. W. G. Wyckoff, "Crystal Structures," Vol. II, Chap. VIII, p. 57, Interscience Publishers, Inc., New York (1951).

Influence of Crystallographic Orientation on the Pitting of Iron in Distilled Water

Jerome Kruger

National Bureau of Standards, Washington, D. C.

A review paper by Greene and Fontana (1) indicates that pitting is random with respect to surface structure. Recent work in our laboratory indicates, however, that this is not true for pit formation on iron in distilled water. Initially this work was carried out with an Armco iron single-crystal sphere ⅜-in. in diameter which had flat surfaces cut parallel to the {111}, {110}, and {100} planes. These surfaces were prepared by mechanical polishing prior to chemical polishing using MirroFe[1] solution. When the crystal thus prepared was immersed for 3 hr in distilled water at room temperature, it was observed that the {110} plane had the greatest number of pits per unit area. The {100} had approximately one-half as many pits as the {110}, and the {111} had only around one-quarter as many as the {110}. The number and location of pits was not always the same for a given time interval of immersion. The order of pitting activity, {110}> {100}>{111}, however, remained the same in every one of the seven runs carried out. Figure 1 illustrates this order of activity on the three different planes cut on the same iron crystal.

In order to see if the use of MirroFe for polishing was responsible for the effect observed, the surfaces after mechanical polishing were etched with a dilute solution of HCl prior to carrying out a run. The results were the same as for the surfaces polished with MirroFe. The effect of orientation of the corroding surface, horizontal or vertical, was also checked, and again the same order of pitting activity was observed for the crystallographic planes studied.

[1] Manufactured by MacDermid Inc., Waterbury, Conn.

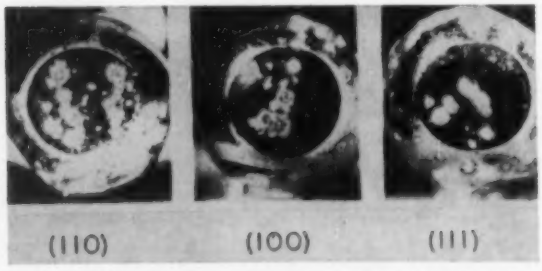

Fig. 1. Three different crystallographic planes of an iron single crystal corroded in distilled water for 3 hr at 25°C. 2.5X.

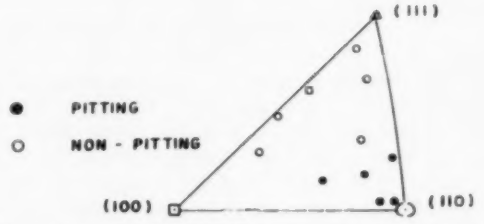

Fig. 2. Stereographic triangle showing pitting on grains of iron having different crystallographic orientations.

Other studies were carried out using a purer iron than Armco (235 ppm of impurities to 2460 ppm for Armco). Here a specimen containing large grains of many different surface orientations were used. As Fig. 2 shows, all those grains whose orientations were near that of the {110} crystallographic plane pitted every time or every time but one, while those which were nearer the {111} or {100} orientations pitted only once or not at all during the course of five runs.

As with the Armco iron, those surfaces having an orientation nearer the {110} exhibited the greatest amount of pitting. Irrespective of crystallographic orientation, the general level of pitting attack was lower for the purer iron.

Acknowledgment

The author is indebted to R. S. Smethurst, Jr., who carried out some of the experimental work and to the Corrosion Research Council who supported this work in part.

Manuscript received April 22, 1959.

Any discussion of this paper will appear in a Discussion Section to be published in the June 1960 JOURNAL.

REFERENCE

1. N. D. Greene and M. G. Fontana, *Corrosion*, **15**, 41 (1959).

Columbus Program

THE ELECTROCHEMICAL SOCIETY

One Hundred and Sixteenth Meeting

October 18, 19, 20, 21, and 22, 1959

Sunday through Thursday

CONDENSED TECHNICAL PROGRAM

Monday, October 19, 1959

Battery (Abstracts 1-10) 9:30 A.M.-12:00 M; 2:00-4:30 P.M. (Hall of Mirrors, Deshler Hilton Hotel)
Corrosion—Electronics (Abstracts 42-48) 9:00 A.M.-12:00 M.; 2:00-5:15 P.M. (Ballroom, Deshler Hilton Hotel)
Electro-Organic (Abstracts 123-128) 9:30 A.M.-12:00 M.; 2:30-3:30 P.M. (Yellow Room, Deshler Hilton Hotel)
Electrothermics and Metallurgy (Abstracts 137-144) 9:30-11:30 A.M.; 2:00-4:00 P.M. (Parlor B, Neil House)

Tuesday, October 20, 1959

Battery (Abstracts 11-20) 9:00-11:30 A.M.; 2:30-5:00 P.M. (Hall of Mirrors, Deshler Hilton Hotel)
Corrosion—Electronics (Abstracts 49-54) 9:00-11:30 A.M.; 2:00-4:30 P.M. (Ballroom, Deshler Hilton Hotel)
Electro-Organic (Abstracts 129-136A) 9:00-11:30 A.M;. 2:00-4:00 P.M. (Yellow Room, Deshler Hilton Hotel)
Electrothermics and Metallurgy (Abstracts 145-151) 9:30-11:30 A.M.; 2:00-3:30 P.M. (Parlor B, Neil House)

Wednesday, October 21, 1959

Battery (Abstracts 21-28) 9:30 A.M.-12:00 M.; 2:00-3:30 P.M. (Hall of Mirrors, Deshler Hilton Hotel)
Corrosion—Electronics (Abstracts 55-62) 9:00 A.M.-12:15 P.M.; 2:00-5:15 P.M. (Grand Ballroom, Neil House)
Electrodeposition (Abstracts 63-74) 9:00 A.M.-12:00 M.; 2:00-4:50 P.M. (Yellow Room, Deshler Hilton Hotel)
Electronics—Semiconductors (Abstracts 85-102) 9:00 A.M.-12:15 P.M.; 2:00-5:30 P.M. (Ballroom, Deshler Hilton Hotel)

Thursday, October 22, 1959

Corrosion (Abstracts 29-41) 9:00 A.M.-12:00 M.; 2:00-4:30 P.M. (Grand Ballroom, Neil House)
Electrodeposition (Abstracts 75-84) 9:00-11:30 A.M.; 2:00-4:30 P.M. (Yellow Room, Deshler Hilton Hotel)
Electronics—Semiconductors (Abstracts 103-122A) 9:00 A.M.-12:45 P.M.; 2:00-5:45 P.M. (Ballroom, Deshler Hilton Hotel)

GENERAL INFORMATION

Convention Headquarters will be the Deshler Hilton Hotel, Broad and High Streets, Columbus, Ohio.

Rates per day for rooms at the Deshler Hilton Hotel are: single, $7.50, 9-11, 12-14; double-bed room, $12, 13, 15; twin-bed room, $12-14, 15-18, 18-20; suite, parlor, 1 bedroom, $24-40; parlor, 2 bedrooms, $44.50 and 58.50.

Rates per day for rooms at the Neil House are: single room, $6, 7, 7.50, 8, 9, 10; double-bed rooms, $9.50, 10, 10.50, 11.50, 12.50; twin-bed rooms, $12, 13, 14, 15; suite—parlor, bed room, $16 and up.

Requests for room reservations should be mailed to the hotel. BE SURE to state your intention to attend The Electrochemical Society meeting. Early reservations are advised. If your wife will be attending, be sure to indicate this on your request for reservation.

The Office of the Secretary is in Parlor 216, Ballroom Floor.

Ladies' Headquarters is in Parlor 212, Ballroom Floor.

The Local Committee Office is in Parlor 218, Ballroom Floor.

All technical sessions will be held in the Deshler Hilton Hotel and in the Neil House.

REGISTRATION

The registration desk will be in the East Section of the Ballroom Foyer, Deshler Hilton Hotel. Following is the registration schedule:

Sunday, Oct. 18—3:00 to 9:00 P.M.
Monday, Oct. 19—8:00 A.M. to 6:00 P.M.
Tuesday, Oct. 20—8:30 A.M. to 5:00 P.M.
Wednesday, Oct. 21—8:30 A.M. to 4:00 P.M.
Thursday, Oct. 22—8:30 A.M. to 12:00 M.

Registration fees are:

Members	$ 7.00
Nonmembers	13.00*
Ladies	5.00
Students	2.00
Thursday only	5.00

*If a nonmember fills out a membership application blank and is subsequently elected to membership in the Society, the difference between the nonmember and member registration fee will be applied to his first year's dues.

INFORMATION ABOUT COLUMBUS

Columbus is best known for its industrial diversification and rapid postwar growth. It is strategically located in the industrial heart of the nation so that raw materials and finished products flow freely to and from other industrial centers. Large manufacturing establishments include branches of: North American Aviation, Inc., Ternstedt Division of General Motors, Westinghouse (Appliance Division), Western Electric, American Brake Shoe, American Blower Company, and Surface Combustion Company. A number of large firms such as Jeffrey Manufacturing Company (mining equipment), Lennox Furnace Company, Seagrave Corporation (firefighting equipment), and Columbus Coated Fabrics Corporation maintain their headquarters and major manufacturing facilities in Columbus. Many smaller industrial firms such as Industrial Nucleonics, Jaeger Machine Company, and Ohio Semiconductors contribute to the diversification and technologic orientation of the industrial community.

Battelle Memorial Institute, the world's largest contract research laboratory, is located in Columbus. The Ohio State University and the Ohio State Research Foundation are well known for scientific and technologic achievements. Capital University is well known for its outstanding liberal arts college, conservatory of music and theological seminary.

As the State Capital, Columbus offers the usual attractions of a metropolitan center in terms of fine restaurants and shopping facilities.

SYMPOSIA

The Battery Division has scheduled symposia on The Leclanché Cell, The Silver-Silver Oxide Electrode, The Lead-Acid Cell, The Nickel Cadmium Cell, and a General Session, all in the Hall of Mirrors, Deshler Hilton Hotel.

The Corrosion Division has scheduled two general sessions, both in the Grand Ballroom Neil House.

The Corrosion and **Electronics Divisions** have scheduled a three-day Joint Symposium on The Surface Chemistry of Metals and Semiconductors, sponsored

jointly by the Office of Naval Research and The ECS, on Monday and Tuesday in the Ballroom of the Deshler Hilton Hotel, and on Wednesday in the Grand Ballroom, Neil House.

The Electrodeposition Division has scheduled symposia on Electrode Reactions in Nonaqueous Solutions, Electro- and Chemical-Polishing, and two general sessions, all in the Yellow Room, Deshler Hilton Hotel.

The Electronics Division—Semiconductor Group has scheduled symposia on Elemental Semiconductors, Bulk Properties; Semiconducting Compounds; Process Technology; and Surface Phenomena, Diffusion, all in the Ballroom, Deshler Hilton Hotel.

The Electro-Organic Division has scheduled four sessions, all in the Yellow Room, Deshler Hilton Hotel.

The Electrothermics and Metallurgy Division has scheduled symposia on Refractory Coatings and Less Common Metals, in Parlor B, Neil House.

GENERAL FUNCTIONS

Symposia Chairmen Breakfasts

On **Monday, Tuesday, Wednesday,** and **Thursday,** October 19, 20, 21 and 22, special breakfasts will be held for symposia chairmen. On the day at which he presides at a session, each chairman should be in the Victorian Room, Deshler Hilton Hotel, at 7:45 A.M.

Monday Buffet Supper and Entertainment

On Monday evening, October 19, an informal buffet supper will be held at the Valley Dale Country Ballroom. Cocktails will be served before supper, and music and entertainment will be provided for the balance of the evening. Special buses will leave the Deshler Hilton Hotel at 5:45 P.M. and will return to the hotel after the entertainment.

Tuesday Palladium Medal Lecture

On Tuesday, October 20, at 5:00 P.M. Professor A.N. Frumkin will deliver the Palladium Medal Lecture in the Ballroom of the Deshler Hilton Hotel.

Tuesday Palladium Medal Reception and Banquet

On Tuesday, October 20, a reception and banquet will be held for the Palladium Medalist, Professor A. N. Frumkin. Cocktails will be served from 6:30 to 7:30 P.M. in the Ballroom Foyer, Deshler Hilton Hotel. Professor Frumkin will receive the Palladium Medal at the banquet. An outstanding speaker will talk on a subject of general interest.

Wednesday Buffet Supper and Get-together

This affair, to be held on Wednesday, October 21, is planned as a gay evening of fun and light entertainment. It will begin at 6:30 P.M. in the Ballroom Deshler Hilton, with cocktails, followed by a buffet supper, music, and an audience participation program. Come and have fun.

PLANT TRIPS

A number of plant trips are being arranged, including a trip to Battelle Memorial Institute's Nuclear Reactor. Final information on the trips will be available later.

LADIES PROGRAM

All the ladies are cordially invited to make Room 212 off the Ballroom Foyer, Deshler Hilton Hotel, their headquarters. Coffee hour will be a daily event from 10 to 11 o'clock except on Wednesday when a special event is scheduled. Members of the Ladies' Committee will be on hand to assist and acquaint guests with the program and to held make the visit to Columbus enjoyable in every way possible.

Sunday, Oct. 18—Registration from 3:00 to 9:00 P.M.

Monday, Oct. 19—Coffee Hour and Get Acquainted Meeting in Room 212 from 10:00 to 11:00 A.M. Buses will leave the Hotel at 12:30 P.M. to take the ladies to the Ohio Union on the Ohio State University campus, where lunch will be served. After the luncheon there will be a talk on flower arrangements, followed by optional tours of the Ohio Union, Ohio State Museum, and the Department of Horticulture. Walking shoes are recommended.

Monday evening, Oct. 19, the ladies are invited to attend a Buffet Supper at the Valley Dale Country Ballroom (see General Functions).

Tuesday, Oct. 20—Coffee Hour in Room 212 from 10:00 to 11:00 A.M.

Tuesday afternoon, the ladies are invited to attend a luncheon at 1:00 P.M. at the Columbus Athletic Club, followed by a program of folk lore songs by Mrs. Anne Laylin Grimes.

Tuesday evening, the ladies are invited to attend the reception and banquet at 6:30 P.M. in the Ballroom (see General Functions).

Wednesday, Oct. 21—At 10:00 A.M., buses will leave the Deshler Hilton Hotel to take the ladies to Ilonka's Provincial House, where they will be served a complimentary brunch. A bus tour to the Ericson Glass Works at Bremen, Ohio, will start from there and occupy most of the afternoon.

Wednesday evening, the ladies are invited to attend the Buffet Supper and Informal Get-Together beginning at 6:30 P.M. in the Ballroom (see General Functions).

Thursday, Oct. 22—Coffee Hour in Room 212 from 10 to 11:00 A.M. All ladies are cordially invited to attend an informal sherry party at 11:30 A.M. at the home of Mrs. F. W. Fink, 1900 North Devon Road, Columbus, Ohio. Mrs. Fink is the Chairman of the Ladies Committee.

BOARD AND COMMITTEE MEETINGS

Sunday, Oct. 18, 2:00 P.M.—Meeting of the **Board of Directors** in Room 307, Deshler Hilton Hotel.

Sunday, Oct. 18, 7:30 P.M.—Meeting of the **Investment Advisory Panel** in Private Dining Room 10.

Monday, Oct. 19, 4:30 P.M.—Meeting of the **Council of Local Sections** in Room 307.

Monday, Oct. 19, 5:00 P.M.—Meeting of the **Sustaining Membership Committee** in Private Dining Room 10.

Monday, Oct. 19, 5:00 P.M.—Meeting of the **Editorial Staff of the Journal** in Private Dining Room 12.

Wednesday, Oct. 21, 5:00 P. M.—Meeting of the **Membership Committee,** in Private Dining Room 10.

LUNCHEONS AND BUSINESS MEETINGS OF DIVISIONS

Electro-Organic Division Luncheon and Business Meeting, Tuesday, Oct. 20, 12:15 P.M. in Room 307, Deshler Hilton Hotel.

Battery Division Luncheon and Business Meeting, Tuesday, Oct. 20, 12:15 P. M. in Private Dining Rooms 10, 11, and 12, Deshler Hilton Hotel.

Electrodeposition Division Luncheon and Business Meeting, Wednesday, Oct. 21, 12:15 P.M. in Spanish Room, Deshler Hilton Hotel.

Corrosion Division News Luncheon and Business Meeting, Thursday, Oct. 22, 12:15 P.M. in Mezzanine Parlor 4, at the Neil House.

COST OF VARIOUS FUNCTIONS

(other than registration)

Please buy tickets as early as possible.

Symposia Chairmen Breakfasts-Standard menu prices	
Monday Buffet Supper and Entertainment	$5.25
Tuesday Palladium Medal Reception and Banquet, men	7.50
ladies	6.00
Wednesday Buffet Supper	4.50
Division Luncheons	3.50
Transportation for plant visits	1.00
Ladies' Program	
Monday luncheon	2.00
Tuesday luncheon	2.00
Wednesday transportation to Bremen	1.00

JOURNALS

Copies of the July, August, September, and October issues of the "Journal of The Electrochemcial Society" will be available at the registration desk. The price of a single copy of the Journal is $1.25 to members and $1.75 to nonmembers.

EXTENDED ABSTRACTS

The Battery Division is making available an extended abstract booklet containing 1000-word abstracts of most of the papers presented at the Division's Columbus Meeting. Copies of the booklet may be obtained from C. H. Clark, 34 Pleasant Place, Deal, N. J., after Sept. 15 for $2.00 each.

DISCUSSION

No recordings will be made of oral discussions. Those contributing to the discussion of a paper and desiring their remarks to be published will be supplied by the symposium chairman with a printed form on which any discussion may be written. These forms should be given to the Secretary-Treasurer of the Division or to the Managing Editor of the *Journal* after the session; they can be mailed to the Managing Editor of the *Journal*, 1860 Broadway, New York 23, N. Y. The discussion will then be referred to the author for reply. Publication of the discussion and the comments of the author depends on publication of the article in the Journal.

Written discussion should be submitted within two months following publication of the article in the *Journal*. A Discussion Section is published semiannually in the *Journal*.

EMPLOYMENT POSTERS

Companies which desire to recruit employees at the Columbus Meeting will have posters to this effect on a board near the registration desk. Companies are requested to confine their announcements to this board.

NOTE

In the Index to Authors, the abstract number is used. Address of each author is included with the abstract.

SPRING MEETING
at the
La Salle Hotel
CHICAGO, ILLINOIS
May 1, 2, 3, 4, and 5, 1960

Sessions probably will be scheduled on:

Electric Insulation
Electronics (including Luminescence and Semiconductors)
Electrothermics and Metallurgy
Industrial Electrolytics
Theoretical Electrochemistry

Abstracts for the Chicago Meeting (*not exceeding 75 words in length*) must reach Society Headquarters, 1860 Broadway, New York 23, N.Y., *not later than January 4, 1960* to be included in the Program.

Please indicate on the abstract for which Division's symposium the paper is to be scheduled and underline the name of the author who will present the paper at the Chicago Meeting.

Technical Program

BATTERY

Monday, October 19, 1959
The Leclanché Cell
with J. C. White presiding

(HALL OF MIRRORS, Deshler Hilton Hotel)

9:30 A.M.—"Study of the Recuperation Reaction in the Leclanché Dry Cell" by M. P. Korver, R. S. Johnson, and N. C. Cahoon (Abstract No. 1)
10:00 A.M.—"A Method of Increasing the Service Life of Leclanché Dry Cells" by H. J. DeWane (Abstract No. 2)
10:30 A.M.—"A Method for Evaluating Battery Grade Manganese Dioxide" by Friedrich Kornfeil (Abstract No. 3)
11:00 A.M.—"An Improved Iodide Method for the Analysis of Manganese Dioxide" by F. J. Krivanek and N. C. Cahoon (Abstract No. 4)
11:30 A.M.—"Impedance of Leclanché Cells" by R. J. Brodd and H. J. DeWane (Abstract No. 5)

Battery (cont'd)
Monday, October 19, 1959
The Leclanché Cell (cont'd)
with W. S. Herbert presiding

(HALL OF MIRRORS, Deshler Hilton Hotel)

2:00 P.M.—"The Overpotentials of Some Oxide Electrodes and the Discharge Mechanism" by W. C. Vosburgh, J. H. DeLap, and H. B. Mark, Jr. (Abstract No. 6)
2:30 P.M.—"Gravity Field Effects on Zinc Anode Discharge in Alkaline Media" by M. Eisenberg and H. F. Bauman (Abstract No. 7)
3:00 P.M.—"Magnesium Primary Cells with Perchlorate Electrolytes" by G. S. Lozier and C. K. Morehouse (Abstract No. 8)
3:30 P.M.—"A Synchronized Square Wave Generator and Switching Unit for Electrochemical Studies" by N. C. Cahoon and H. F. Schaefer (Abstract No. 9)
4:00 P.M.—"Sine Wave Pulse Current Tester for Batteries" by K. Kordesch and A. Marko (Abstract No. 10)

Battery (cont'd)
Tuesday, October 20, 1959
The Silver-Silver Oxide Electrode
with Walter Hamer presiding

(HALL OF MIRRORS, Deshler Hilton Hotel)

9:00 A.M.—"The Silver/Silver-Oxide Electrode System" by B. D. Cahan, J. B. Ockerman, R. Amlie, and P. Rüetschi (Abstract No. 11)
9:30 A.M.—"Oxides on the Silver Electrode" by C. P. Wales and Jeanne Burbank (Abstract No. 12)
10:00 A.M.—"The Stability and Solubility of AgO in Alkaline Solutions" by T. P. Dirkse and Brandon Wiers (Abstract No. 13)
10:30 A.M.—"The Oxidation of the Silver Electrode in Alkaline Solutions" by T. P. Dirkse (Abstract No. 14)
11:00 A.M.—"The Effect of Cycling on the Silver Electrode" by T. P. Dirkse and J. De Vries (Abstract No. 15)

MEETING ROOM SCHEDULES

Meeting	Monday		Tuesday		Wednesday		Thursday	
	A.M	P.M.	A.M	P.M.	A.M	P.M.	A.M	P.M.
Battery	B	B	B	B	B	B		
Corrosion							D	D
Corrosion—Electronics	A	A	A	A	D	D		
Electrodeposition					C	C	C	C
Electronics—Semiconductors					A	A	A	A
Electro-Organic	C	C	C	C				
Electrothermics and Metallurgy	E	E	E	E				

Deshler Hilton Hotel: A = Ballroom; B = Hall of Mirrors; C = Yellow Room.
Neil House: D = Grand Ballroom; E = Parlor B.

12:15 P.M.—Battery Division Luncheon and Business Meeting in Private Dining Rooms 10-12, Deshler Hilton Hotel.

Battery (cont'd)
Tuesday, October 20, 1959
General Session
with C. H. Clark presiding

(HALL OF MIRRORS, Deshler Hilton Hotel)

2:30 P.M.—"Factors Affecting the Photogalvanic Behavior of Silver-Silver Halide Electrodes" by S. Zaromb, M. Lasser, and F. Kalhammer (Abstract No. 16)
3:00 P.M.—"Silver Halide Photogalvanic Batteries" by S. Zaromb, M. Lasser, and L. Bockstie (Abstract No. 17)
3:30 P.M.—"Burgess Mercury Cells" by T. H. Loverude (Abstract No. 18)
4:00 P.M.—"Investigation of the Electrochemical Characteristics of Organic Compounds, V. Heterocyclic Nitro Compounds" by R. Glicksman and C. K. Morehouse (Abstract No. 19)
4:30 P.M.—"Investigation of the Electrochemical Characteristics of Organic Compounds, VI. Aromatic Hydroxy, Aromatic Amine, and Aminophenol Compounds" by R. Glicksman (Abstract No. 20)
5:00 P.M.—Palladium Medal Address by A. N. Frumkin in the Ballroom, Deshler Hilton.

Battery (cont'd)
Wednesday, October 21, 1959
The Lead-Acid Cell
with E. J. Ritchie presiding

(HALL OF MIRRORS, Deshler Hilton Hotel)

9:30 A.M.—"The Principal Source of α-PbO_2 in the Positive Plate Material of the Lead-Acid Battery" by V. H. Dodson (Abstract No. 21)
10:00 A.M.—"The PbO_2 Electrode" by R. T. Angstadt, B. D. Cahan, and P. Rüetschi (Abstract No. 22)
10:30 A.M.—"The Microscopy of the Effect of Environmental Changes on the Forming Process" by A. C. Simon and E. L. Jones (Abstract No. 23)
11:00 A.M.—"The Microscopy of the Forming Process in the Positive and Negative Plate" by A. C. Simon and E. L. Jones. (Abstract No. 24)
11:30 A.M.—"Internal Resistance of Lead-Acid Cells; Submarine Battery Size" by J. J. Lander and E. E. Nelson (Abstract No. 25)

Battery (cont'd)
Wednesday, October 21, 1959
The Nickel Cadmium Cell
with A. Fleischer presiding

(HALL OF MIRRORS, Deshler Hilton Hotel)

2:00 P.M.—"Nickel-Cadmium Cell Electrodes" by A. J. Salkind and P. F. Bruins (Abstract No. 26)
2:30 P.M.—"Investigations on the Reaction Mechanism of the Nickel-Cadmium Cell" by S. Uno Falk (Abstract No. 27)
3:00 P.M.—"Sealed Nickel-Cadmium Cells Containing Palladium" by H. N. Seiger (Abstract No. 28)

CORROSION

Thursday, October 22, 1959
with R. T. Foley presiding

(GRAND BALLROOM, Neil House)

9:00 A.M.—"The Attack of Copper-Gold, Silver-Gold, Copper-Nickel, and Silver-Copper Alloys by Sulfur at Elevated Temperatures" by B. D. Lichter and Carl Wagner (Abstract No. 29)
9:25 A.M.—"Anodic Oxidation of High-Purity Aluminum in Water" by W. E. Tragert and J. R. Rairden (Abstract No. 30)
9:50 A.M.—"The High-Temperature Aqueous Corrosion Resistance of the Uranium-5% Zirconium-1½% Niobium Alloy" by J. E. Draley, Sherman Greenberg, and W. E. Ruther (Abstract No. 31)
10:15 A.M.—"Evidence for a Logarithmic Oxidation Process for Stainless Steel in Aqueous Systems" by Milton Stern (Abstract No. 32)
10:40 A.M.—"Passivating Inhibitors" by A. C. Makrides and Milton Stern (Abstract No. 33)
11:05 A.M.—"Dissolution of Metals in Aqueous Acid Solutions" by A. C. Makrides (Abstract No. 34)
11:30 A.M.—"Potential Behavior of a Uranium Electrode as a Function of Partial Pressure of Oxygen" by J. W. Ward and J. T. Waber (Abstract No. 34A)
12:15 P.M.—Corrosion Division News Luncheon and Business Meeting in the Mezzanine Parlors, Neil House.

Corrosion (cont'd)
Thursday, October 22, 1959
with M. A. Streicher presiding

(GRAND BALLROOM, Neil House)

2:00 P.M.—"An Electrochemical Study of Passive Films on Fe-Cr Alloys" by D. Caplan, A. Harvey, and M. Cohen (Abstract No. 35)
2:20 P.M.—"Effect of Surface Preparation on Air-formed Films on Iron" by C. D. Stockbridge, P. B. Sewell, and M. Cohen (Abstract No. 36)
2:40 P.M.—"Nitric-Hydrofluoric Acid Pickling of Zirconium Alloys" by M. A. DeCrescente, P. F. Santoro, A. S. Powell, and R. H. Gale (Abstract No. 37)
3:00 P.M.—"An Investigation of Chemical Variables Affecting the Formation of Films on Copper in Aqueous Solutions" by W. H. Davenport, V. F. Nole, and W. D. Robertson (Abstract No. 38)
3:20 P.M.—Ten-minute intermission
3:30 P.M.—"Dissolution of Single Crystals of Copper in Aqueous Ethylenediamine" by L. H. Jenkins (Abstract No. 39)
3:50 P.M.—"The Electrochemical Behavior and Passivity of Titanium" by Milton Stern and Herman Wissenberg (Abstract No. 40)
4:10 P.M.—"The Influence of Noble Metal Alloy Additions on the Electrochemical and Corrosion Behavior of Titanium" by Milton Stern and Herman Wissenberg (Abstract No. 41)

CORROSION—ELECTRONICS

Joint Symposium
Monday, October 19, 1959
The Surface Chemistry of Metals and Semiconductors
General Aspects of the Chemistry and Physics of Surfaces
Sponsored Jointly by the Office of Naval Research and The ECS
with H. C. Gatos presiding

(BALLROOM, Deshler Hilton Hotel)

9:00 A.M.—Introductory Remarks by H. C. Gatos
9:15 A.M.—"Introduction to the Physics and Chemistry of Surfaces" by W. H. Brattain (Abstract No. 42)
10:15 A.M.—"Metal Surfaces" by H. J. Juretschke (Abstract No. 43)
11:00 A.M.—Fifteen-minute intermission
11:15 A.M.—"Semiconductor Surfaces" by Paul Handler (Abstract No. 44)

Corrosion—Electronics

Joint Symposium (cont'd)
Monday, October 19, 1959
The Surface Chemistry of Metals and Semiconductors (Cont'd)
General Aspects of the Chemistry and Physics of Surfaces (cont'd)
Sponsored Jointly by the Office of Naval Research and The ECS
with J. W. Faust, Jr., presiding

(BALLROOM, Deshler Hilton Hotel)

2:00 P.M.—"Clean Surfaces" by H. E. Farnsworth (Abstract No. 45)

Nature and Behavior of Imperfect Surfaces

2:45 P.M.—"The Role of Imperfections in Surface Reactions" by N. Cabrera (Abstract No. 46)
3:30 P.M.—Fifteen-minute intermission
3:45 P.M.—"Damaged Surface Layers—Semiconductors" by T. M. Buck (Abstract No. 47)
"Damaged Surface Layers—Metals" by L. E. Samuels will be included in the published Proceedings but will not be presented at this symposium.
4:30 P.M.—"Effect of Imperfections on Dissolution" by J. J. Gilman (Abstract No. 48)

Corrosion—Electronics

Joint Symposium (cont'd)
Tuesday, October 20, 1959
The Surface Chemistry of Metals and Semiconductors (cont'd)

Electrode Behavior of Metals and Semiconductors

Sponsored Jointly by the Office of Naval Research and The ECS
with Milton Stern presiding

(BALLROOM, Deshler Hilton Hotel)

9:00 A.M.—"Metal and Semiconductor Electrode Processes" by H. Gerischer (Abstract No. 49)
9:45 A.M.—"Experimental Techniques for the Study of Semiconductor Electrodes" by J. F. Dewald (Abstract No. 50)
10:30 A.M.—Fifteen-minute intermission
10:45 A.M.—"Electrode-Solution Interfaces" by H. J. Engell (Abstract No. 51)

Corrosion—Electronics

Joint Symposium (cont'd)
Tuesday, October 20, 1959
The Surface Chemistry of Metals and Semiconductors (cont'd)

Etching Processes

Sponsored Jointly by the Office of Naval Research and The ECS
with C. V. King presiding

(BALLROOM, Deshler Hilton Hotel)

2:00 P.M.—"Electrolytic Attack of Metals" by Paul Lacombe (Abstract No. 52)
2:45 P.M.—"Electrolytic Etching of Semiconductors" by D. R. Turner (Abstract No. 53)
3:30 P.M.—Fifteen-minute intermission
3:45 P.M.—"The Etching of Metals and Semiconductors" by J. W. Faust, Jr. (Abstract No. 54)
5:00 P.M.—The Palladium Medal Address by A. N. Frumkin in the Ballroom, Deshler Hilton Hotel.

Corrosion—Electronics

Joint Symposium (cont'd)
Wednesday, October 21, 1959
The Surface Chemistry of Metals and Semiconductors (cont'd)

Surface Reactions in Liquid Media

Sponsored Jointly by the Office of Naval Research and The ECS
with M. A. Streicher presiding

(GRAND BALLROOM, Nell House)

9:00 A.M.—"Kinetics of Dissolution Processes" by Norman Hackerman (Abstract No. 55)
9:45 A.M.—"Electrochemistry of Dissolution Processes" by J. V. Petrocelli (Abstract No. 56)
10:30 A.M.—Fifteen-minute intermission
10:45 A.M.—"Dissolution of Metals" by C. V. King (Abstract No. 57)
11:30 A.M.—"Dissolution of Semiconductors" by H. C. Gatos (Abstract No. 58)

Corrosion—Electronics

Joint Symposium (cont'd)
Wednesday, October 21, 1959
The Surface Chemistry of Metals and Semiconductors (cont'd)

Surface Reactions in Gaseous Media

Sponsored Jointly by the Office of Naval Research and The ECS
with E. A. Gulbransen presiding

(GRAND BALLROOM, Nell House

2:00 P.M.—"Adsorption and Chemisorption" by M. Boudart (Abstract No. 59)
2:45 P.M.—"Chemisorption and Catalysis" by R. P. Eischens (Abstract No. 60)
3:30 P.M.—Fifteen-minute intermission
3:45 P.M.—"On the Mechanism of the Oxidation of Metals" by K. Hauffe (Abstract No. 61)
4:30 P.M.—"The Influence of Crystal Orientation on Oxidation of Metals" by A. T. Gwathmey and K. R. Lawless (Abstract No. 62)

ELECTRODEPOSITION

Wednesday, October 21, 1959
Electrode Reactions in Nonaqueous Solutions
with Abner Brenner presiding

(YELLOW ROOM, Deshler Hilton Hotel)

9:00 A.M.—"Anodic Methoxylation" by K. E. Kolb, T. W. Lippincott, and C. L. Wilson (Abstract No. 63)
9:30 A. M.—"The Electrolysis of Dibasic Acids and Their Mono-Acid Esters in Nonaqueous Solution" by W. E. Garrison, Jr., A. M. Hartley, Sherlock Swann, Jr., and C. S. Marvel (Abstract No. 64)
10:00 A.M.—"Electrolysis of Organic Solvents, I. Electrolysis of Simple Amides" by D. E. Couch and Abner Brenner (Abstract No. 65)
10:30 A.M.—"Studies of Germanium Electrodes in a Ziegler Electrolyte" by R. J. Flannery, D. Trivich, and J. E. Thomas, Jr. (Abstract No. 66)
11:00 A.M.—"Electrolysis in Anhydrous Ether" by I. E. Gillet (Abstract No. 67)
11:30 A.M.—"Electrolyte for Deposition at −60°C" by H. B. Maier (Abstract No. 68)
12:15 P.M.—Electrodeposition Division Luncheon and Business Meeting in the Yellow Room, Deshler Hilton Hotel.

Electrodeposition (cont'd)
Wednesday, October 21, 1959
Electro- and Chemical-Polishing
with D. G. Foulke presiding

(YELLOW ROOM, Deshler Hilton Hotel)

2:00 P.M.—"Electropolishing in Chloride Solutions" by E. B. Saubestre (Abstract No. 69)
2:30 P.M.—"Anodic Films on Copper in Phosphoric Acid" by J. H. Bartlett and F. H. Giles, Jr. (Abstract No. 70)
3:00 P.M.—"Polishing Regions for Copper in Phosphoric Acid" by J. H. Bartlett and F. H. Giles, Jr. (Abstract No. 71)
3:20 P.M.—"Application of Electropolishing and Chemical Polishing to Heat Sink Material" by P. T. Woodberry (Abstract No. 72)
3:50 P.M.—"Electropolishing in Cyanide Electrolytes" by F. Sullivan and E. H. Newton (Abstract No. 73)
4:20 P.M.—"Some Electrode Processes on Copper Anodes in Orthophosphoric Acid Solution" by K. F. Lorking (Abstract No. 74)

Electrodeposition (cont'd)
Thursday, October 22, 1959
General Session
with D. R. Turner presiding

(YELLOW ROOM, Deshler Hilton Hotel)

9:00 A.M.—"Electrical Migration in the Absence of Electrolysis" by Abner Brenner (Abstract No. 75)
9:30 A.M.—"Relationship between Brightness and Structure in Electroplated Nickel" by Rolf Weil and R. A. Paquin (Abstract No. 76)
10:00 A.M.—"Measurement of Elastic Modulus and Internal Friction in Electrodeposits" by H. J. Read and A. H. Graham (Abstract No. 77)
10:30 A.M.—"Electrodeposition of Amorphous Selenium" by A. K. Graham, H. L. Pinkerton, and H. J. Boyd (Abstract No. 78)
11:00 A.M.—"Zinc Plating of Carbonitrided Steel" by H. T. Francis and L. R. Kohan (Abstract No. 79)

Electrodeposition (cont'd)
Thursday, October 22, 1959
General Session
with Fielding Ogburn presiding

(YELLOW ROOM, Deshler Hilton Hotel)

2:00 P.M.—"Adherence of Thick Chromium Deposits as Affected by Surface Preparation" by H. Chessin and C. L. Alderuccio (Abstract No. 80)
2:30 P.M.—"Deposition of New Chromium-Iron Alloy Plate of Banded Structure" by L. D. McGraw, J. A. Gurklis, C. L. Faust, and J. E. Bride (Abstract No. 81)
3:00 P.M.—"Electrodeposition of Chromium from Low Valence Compounds, I. Investigation of Bath Types

and Operating Conditions" by G. R. Sherwood, M. R. Holmes, and Finn Bergishagen (Abstract No. 82)

3:30 P.M.—"Studies of Hydrogen Embittlement by the Use of Deuterium" by G. B. Wood (Abstract No. 83)

4:00 P.M.—"The Source of the Nitrogen Impurity in Electrodeposited Chromium" by N. Ryan and E. J. Lumley (Abstract No. 84)

ELECTRONICS—SEMICONDUCTORS

Wednesday, October 21, 1959
Elemental Semiconductors, Bulk Properties
with H. H. Kedesdy presiding

(BALLROOM, Deshler Hilton Hotel)

9:00 A.M.—"Determination and Identification of Impurities in Silicon from Low-Temperature Hall Data" by R. T. Bate, I. R. Weingarten, and D. J. Shombert (Abstract No. 85)

9:15 A.M.—"Use of Hall Measurements in Evaluating Polycrystalline Silicon" by P. J. Olshefski, D. J. Shombert, and I. R. Weingarten (Abstract No. 86)

9:35 A.M.—"Radio Frequency Carrier and Capacitive Coupling Procedures for Resistivity and Lifetime Measurements on Silicon" by I. R. Weingarten and M. Rothberg (Abstract No. 87)

9:55 A.M.—"Steady-State Diffusion of Charge Carriers in High-Purity Single-Crystal Silicon" by Milton Green and I. N. Greenberg (Abstract No. 88)

10:20 A.M.—"Lifetime in Germanium as a Function of Gas Adsorption" by M. S. Fink and M. J. Katz (Abstract No. 89)

10:40 A.M.—Fifteen-minute intermission

10:55 A.M.—"Analysis of de Haas-van Alphen Type Oscillations in Graphite" by D. E. Soule (Abstract No. 90)

11:20 A.M.—"Some Optical and Electrical Properties of Crystalline Boron" by G. K. Gaulé, J. T. Breslin, J. R. Pastore, C. G. Pochop, and R. A. Shuttleworth (Abstract No. 91)

11:40 A.M.—"Diffusion of Injected Carriers in Silicon" by C. H. Champness (Abstract No. 92)

12:00 M.—Recent News Papers. Titles and short abstracts will be available at the meeting.

Electronics—Semiconductors (cont'd)
Wednesday, October 21, 1959
Semiconducting Compounds
with G. A. Silvey presiding

(BALLROOM, Deshler Hilton Hotel)

2:00 P.M.—"Preparation and Electrical Properties of Alloyed P-N Junctions of InSb" by C. A. Lee and George Kaminsky (Abstract No. 93)

2:20 P.M.—"Properties of Ternary Alloys in the System In-Sb-Te" by A. J. Rosenberg (Abstract No. 94)

2:40 P.M.—"Determination and Properties of Some Elements in GaAs" by E. Arnold, J. Black, and S. Weissberger (Abstract No. 95)

3:00 P.M.—"Mechanism of Preferential Etching of A^{III} B^{V} Compounds" by H. C. Gatos, M. C. Lavine, and M. J. Button (Abstract No. 96)

3:20 P.M.—Fifteen-minute intermission

3:35 P.M.—"Preparation and Electrical Properties of Mercury Selenide" by T. C. Harman (Abstract No. 97)

3:55 P.M.—"Mechanical and Infrared Excitation of Luminescence in CdS Crystals" by D. M. Warschauer and D. C. Reynolds (Abstract No. 98)

4:15 P.M.—"Properties of CdSb and CdSb-ZnSb Alloys" by A. J. Strauss (Abstract No. 99)

4:35 P.M.—"Physical Chemistry of the II-V Semiconductors CdSb and $CdAs_2$" by V. J. Lyons, V. J. Silvestri, and G. A. Silvey (Abstract No. 100)

4:50 P.M.—"Optical and Electrical Properties of CdSb and $CdAs_2$" by W. J. Turner, A. S. Fischler, and W. E. Reese (Abstract No. 101)

5:05 P.M.—"Phase Diagram for the Pseudo-Binary System CdTe-In_2Te_3" by Lars Thomassen and D. R. Mason (Abstract No. 102)

Electronics—Semiconductors (cont'd)
Thursday, October 22, 1959
Process Technology
with A. W. Postlethwaite presiding

(BALLROOM, Deshler Hilton Hotel)

9:00 A.M.—"Purification of Arsenic" by J. M. Whelan, J. D. Struthers, and J. A. Ditzenberger (Abstract No. 103)

9:20 A.M.—"Preparation of High-Purity Gallium" by Pierre de la Bretèque (Abstract No. 104)

9:45 A.M.—"Impurity Distribution of Various Doping Techniques in Floating Zone Crystal Growing" by A. L. MacDonald and E. Y. Wang (Abstract No. 105)

10:05 A.M.—"Vibratory Polishing and Lapping of Semiconductor Materials" by J. E. Cline and S. J. Solomon (Abstract No. 106)

10:25 A.M.—"Chemical Etching of Silicon, III. A Temperature Study in the Acid System" by Harry Robbins and Bertram Schwartz (Abstract No. 107)

10:40 A.M.—Fifteen-minute intermission

10:55 A.M.—"A Low Resistance Ohmic Contact for Silicon Semiconductor Devices" by S. L. Matlow and E. L. Ralph (Abstract No. 108)

11:15 A.M.—"A Chemical Treatment for Rendering Silicon-Doped Aluminum Solderable" by S. L. Matlow and H. J. Gould (Abstract No. 109)

11:35 A.M.—"Depletion Layer Calculations for the Design of Diffused Semiconductor Devices" by H. Lawrence and R. M. Warner, Jr. (Abstract No. 110)

11:55 A.M.—"Development of Damage-Nucleated Structures in Silicon by Highly Preferential Etching" by P. R. Pennington and J. D. Turner (Abstract No. 111)

12:05 P.M.—"Silicon Transistors and Device Fabrication Using Damage-Nucleated Etched Structures" by W. P. Waters and P. Walker (Abstract No. 112)

12:25 P.M.—"A New Technique for Controlling Germanium Meltback Transistor Characteristics" by R. Jones and R. H. Zimmerli (Abstract No. 113)

Electronics—Semiconductors (cont'd)
Thursday, October 22, 1959
Surface Phenomena, Diffusion
with E. I. Doucette presiding

(BALLROOM, Deshler Hilton Hotel)

2:00 P.M.—"A New Approach to Semiconductor Surface Reactivity" by G. A. Wolff (Abstract No. 114)

2:25 P.M.—"Theory of Surface Conductance in Semiconductors" by D. R. Frankl (Abstract No. 115)

2:45 P.M.—"P-Layers on Vacuum Heated Silicon" by J. T. Law, T. M. Buck, and F. G. Allen (Abstract No. 116)

3:05 P.M.—"Surface Channel Studies on Silicon P-N Junctions" by Raymond Solomon and P. O. Johnson (Abstract No. 117)

3:25 P.M.—Fifteen-minute intermission

3:40 P.M.—"Diffusion in Silicon Carbide" by Hung-Chi Chang and L. F. Wallace (Abstract No. 118)

4:00 P.M.—"Surface Concentration of Indium in Germanium from Gaseous Diffusion" by K. M. Busen, E. L. Meeks, and G. A. Shirn (Abstract No. 119)

4:20 P.M.—"Capillary Alloying: An Improved Alloying Method" by K. M. Busen, J. J. Casey, Kurt Lehovec, and A. C. Webb (Abstract No. 120)

4:45 P.M.—"Impurity Redistribution and Junction Formation in Silicon by Thermal Oxidation" by M. M. Atalla and E. Tannenbaum (Abstract No. 121)

5:05 P.M.—"Metallurgical Analysis of the Bulk Diffusion Phenomenon in Silicon Power Transistors" by P. X. Flaherty (Abstract No. 122)

5:25 P.M.—"Diffusion of Phosphorus into Silicon through an Oxide Layer" by D. Kahng and M. O. Thurston (Abstract No. 122A)

ELECTRO-ORGANIC

Monday, October 19, 1959
with Garrett Thiessen presiding

(YELLOW ROOM, Deshler Hilton Hotel)

9:30 A.M.—"Application of Constant Potential Electrolysis to the Process for Electrolytic Formation of Hydrazobenzene in Alkaline Emulsion. Mechanism

for the Processes at Soluble and Insoluble Cathodes" by Taro Sekine, Tadashi Seki, and Kiichiro Sugino (Abstract No. 123)

10:30 A.M.—"Preparation of Crossed-Pinacols by Cathodic Reduction" by M. J. Allen and W. Pierson (Abstract No. 124)

11:00 A.M.—"Kolbe Decomposition Potentials by Condenser and Ballistic Galvanometer" by G. W. Thiessen and F. F. Rawlings (Abstract No. 125)

11:30 A.M.—"Electrolytic Formation of Oximes" by Tadao Hayashi and C. L. Wilson (Abstract No. 126)

Electro-Organic (cont'd)
Monday, October 19, 1959
with C. L. Wilson presiding

(YELLOW ROOM, Deshler Hilton Hotel)

2.00 P.M.—"The Stereo Selective Electrochemical Reduction of Nonconjugated Steroidal Ketones and Alpha Ketols" by Peter Kabasakalian, Alvin Basch, James McGlotten, and Milton Yudis (Abstract No. 127)

2:30 P.M.—"Electrochemical Research in India and Japan" by M. J. Allen (Abstract No. 128)

Electro-Organic (cont'd)
Tuesday, October 20, 1959
with R. A. Day, Jr., presiding

(YELLOW ROOM, Deshler Hilton Hotel)

9:00 A.M.—"Polarographic Reduction of Some Acetylenic Linkages" by A. H. Gropp and J. C. Ramsey, Jr. (Abstract No. 129)

9:30 A.M.—"Polarographic Reductions of Benzyl Halides" by L. W. Marple, L. E. I. Hummelstedt, and L. B. Rogers (Abstract No. 130)

10:00 A.M.—"Polarography in Formamide, I. Some Transition Metal Ions, Zinc and Cadmium Ions" by G. H. Brown and Hsiao-shu-Hsiung (Abstract No. 131)

10:30 A.M.—"Polarographic Studies in Dimethylformamide, VI. Reduction of Polyhalogenated Hydrocarbons" by Stanley Wawzonek and R. C. Duty (Abstract No. 132)

11:00 A.M.—"Millicoulometric Determination of Polarographic n-Values" by Thos. De Vries and J. L. Kroon (Abstract No. 133)

12:15 P.M.—Electro-Organic Luncheon and Business Meeting in the Yellow Room, Deshler Hilton Hotel.

Electro-Organic (cont'd)
Tuesday, October 20, 1959
with Stanley Wawzonek presiding

(YELLOW ROOM, Deshler Hilton Hotel)

2:00 P.M.—"Polarographic Reduction of Some Diketones" by R. L. Flurry and R. A. Day, Jr. (Abstract No. 134)

2:30 P.M.—"Polarographic Reduction of Nonconjugated Steroidal Ketones" by Peter Kabasakalian and James McGlotten (Abstract No. 135)

3:00 P.M.—"Electrolytic Reduction of Some Alkylnitrosamines" by G. C. Whitnack, R. D. Weaver, and H. W. Kruse (Abstract No. 136)

3:30 P.M.—"Rotating Cathode-Type Cell for the Preparation of Benzidine" by K. S. Udupa, G. S. Subramanian, and H. V. K. Udupa (Abstract No. 136A)

5:00 P.M.—Palladium Medal Address by A. N. Frumkin in the Ballroom, Deshler Hilton Hotel.

ELECTROTHERMICS AND METALLURGY

Monday, October 19, 1959
Refractory Coatings
with J. M. Blocher, Jr., presiding

(PARLOR B, Neil House)

9:30 A.M.—"Refractory Ceramic Coatings Today and Tomorrow" by F. D. Shaw (Abstract No. 137)

10:00 A.M.—"The Adhesion of Vitreous Oxide Coatings to Metals" by B. W. King and W. H. Duckworth (Abstract No. 138)

10:30 A.M.—"A Liquid Phase Coating for Refractory Metals" by G. D. Oxx, Jr., and L. F. Coffin, Jr. (Abstract No. 139)

11:00 A.M.—"Testing Procedures for Evaluation of Coated Materials" J. L. Harp and J. M. Allen (Abstract No. 140)

Electrothermics and Metallurgy (cont'd)
Monday, October 19, 1959
Refractory Coatings (Cont'd)
with David Roller presiding

(PARLOR B, Neil House)

2:00 P.M.—"Problems of Applying Metallic Coatings to Nonmetallic Bases" by S. W. Bradstreet (Abstract No. 141)

2:30 P.M.—"Coating Uranium Dioxide Powders with Metallic Films" by J. H. Oxley, J. F. Hannah, J. M. Blocher, Jr., and I. E. Campbell (Abstract No. 142)

3:00 P. M.—"Silicon Carbide Coatings on Graphite Paper" by J. G. Kemp (Abstract No. 143)

3:30 P.M.—"Metal-Ceramic Coatings for Protection of Graphite" by W. L. Aves (Abstract No. 144)

Electrothermics and Metallurgy (cont'd)
Tuesday, October 20, 1959
Refractory Coatings (cont'd)
with M. A. Steinberg presiding

(PARLOR B, Neil House)

9:30 A.M.—"Inorganic Coatings for Leading Edges of Boost-Glide Vehicles" by H. A. Pearl (Abstract No. 145)

10:00 A.M.—"Coatings for Structural Aircraft Materials" by D. H. Leeds (Abstract No. 146)

10:30 A.M.—"Refractory Coatings for Ramjet and Supersonic Aircraft Applications" by S. Sklarew (Abstract No. 147)

11:00 A.M.—"Protective Coatings for Medium Temperature Ranges" by A. R. Stetson (Abstract No. 148)

Electrothermics and Metallurgy (cont'd)
Tuesday, October 20, 1959
Less Common Metals
with A. C. Loonam presiding

(PARLOR B, Neil House)

2:00 P.M.—"Reactions in the Niobium-Hydrogen System" by W. M. Albrecht, W. D. Goode, and M. W. Mallett (Abstract No. 149)

2:30 P.M.—"A Study of the Iodide Niobium Process" by R. F. Rolsten (Abstract No. 150)

3:00 P.M.—"The Behavior of Rhenium in Electron Tube Environments" by G. B. Gaines, C. T. Sims, and R. I. Jaffee (Abstract No. 151)

5:00 P.M.—Palladium Medal Address by A. N. Frumkin in the Ballroom, Deshler Hilton Hotel.

Abstracts

In the Index to Authors, the Abstract Number is the number listed in the right-hand column.

BATTERY

Abstract No. 1

Study of the Recuperation Reaction in the Leclanché Dry Cell

M. P. Korver, Research Labs., National Carbon Co., Division of Union Carbide Corp., Cleveland, Ohio, **R. S. Johnson,** Riegel Textile Corp., Ware Shoals, S. C., and **N. C. Cahoon,** Edgewater Development Lab., National Carbon Co., Cleveland, Ohio

The cathodic reaction in the Leclanché dry cell has been described previously as consisting of two steps. The first is the reduction of Mn^{IV} to Mn^{II} and the second is the reaction of Mn^{II} produced in the first step with unreacted Mn^{IV} to form an insoluble Mn^{III} by-product. Two reactions can occur producing MnOOOH and $ZnO \cdot Mn_2O_3$, manganite and hetaerolite, respectively. The latter reactions, termed recuperation reactions, have been subjected to analysis and rate studies to determine the effects of factors such as pH, concentration, and temperature. The basic concepts of heterogeneous chemical kinetics have been applied and a simple mathematical equation was found which was applicable to all the data. These findings support the cathodic reaction mechanism theory presented previously.

Abstract No. 2

A Method of Increasing the Service Life of Leclanché Dry Cells

H. J. DeWane, National Bureau of Standards, Washington 25, D. C.

A simple, inexpensive rectifying system for "charging or rejuvenating" dry cells has been investigated. The circuit consists of a filament transformer, a Ge diode in parallel with a resistor, a current limiting lamp, and three batteries in series. D-size cells were charged for a number of cycles after completion of standard ASA performance tests, and the electrical output or increased service was calculated. Some cells were also cycled continuously. The latter procedure results in a greater gain in service.

Abstract No. 3

A Method for Evaluating Battery Grade Manganese Dioxide

Friedrich Kornfeil, Energy Conversion Research Branch, U. S. Army Signal Research and Development Lab., Fort Monmouth, N. J.

A method is described for evaluating manganese dioxide as a cathode material. The principle of this method is to discharge a mixture of MnO_2 and acetylene black at a constant effective current density in a simply constructed test cell. The circuitry used eliminates the potential drop due to the internal resistance of the test cell, thereby adding substantially to the simplicity of the preparation of the sample for the test. Data are presented which show the correlation of the results of this technique with those of industrial high drain (16-2/3 ohm) capacity tests of dry cells containing the same oxides.

Abstract No. 4

An Improved Iodide Method for the Analysis of Manganese Dioxide

F. J. Krivanek and **N. C. Cahoon,** Development Div., National Carbon Co., P. O. Box 6056, Cleveland 1, Ohio

The accurate determination of the available oxygen content of manganese dioxide samples is of considerable importance to the battery industry, since this value is often used to indicate the suitability of the sample for use. A study of a recently proposed method based on the liberation of iodine in an acid solution has resulted in significant improvements in accuracy and reliability. The revised method gives excellent results with synthetic samples. However, the lack of satisfactory results using the improved method with ore samples suggests that interfering substances are present.

Abstract No. 5

Impedance of Leclanché Cells

R. J. Brodd and **H. J. DeWane,** National Bureau of Standards, Washington 25, D. C.

Cells with various MnO_2: acetylene black ratios were constructed and discharged on standard tests. The impedance of the cells was measured over the frequency range 50-50 kc/s by a substitution method. Results are interpreted from an analysis of Cole-Cole impedance plots.

Abstract No. 6

The Overpotentials of Some Oxide Electrodes and the Discharge Mechanism

W. C. Vosburgh, J. H. DeLap, and **H. B. Mark, Jr.,** Dept. of Chemistry, Duke University, Durham, N. C.

Discharge of electrodeposited MnO_2 electrodes for short periods at pH8, with time for reattainment of equilibrium, shows that the potential of partially discharged MnO_2 is a linear function of the amount of lower oxide formed, for part of the discharge. With this relationship, some previous data on the overpotential of MnO_2 in acid electrolytes are interpreted more simply than before, and a similar relationship and mechanism can be applied to PbO_2 and other oxide electrodes.

Abstract No. 7

Gravity Field Effects on Zinc Anode Discharge in Alkaline Media

M. Eisenberg and **H. F. Bauman,** Electrochemistry Lab., Lockheed Missiles and Space Division, Sunnyvale, Calif.

This study was undertaken as a follow-up to theoretical predictions relating to the behavior of batteries with soluble anodes in gravity-free fields, such as are encountered in space flight. Since weightlessness conditions cannot be obtained under ordinary circumstances in the laboratory, an indirect experimental approach was selected. Concentration gradients and interfacial concentration of dissolved zinc were determined at 3 different orientations to the direction of the gravitational field at the zinc anode surface by means of slow boundary sampling methods. Through a correlation of these results with mass transfer theory of free convection, predictions for the behavior of zinc anodes in gravity-free fields are made.

Abstract No. 8

Magnesium Primary Cells with Perchlorate Electrolytes

G. S. Lozier and **C. K. Morehouse,** RCA Semiconductor and Materials Div., Radio Corp. of America, Somerville, N. J.

The desirable properties of an aqueous perchlorate electrolyte in magnesium primary cells are: high anode efficiency, low tendency to complex, and stability in presence of strong oxidizing agents. These properties have led to the development of magnesium primary cells with HgO, AgO, NiO, CuO, and MnO_2 cathodes. Magnesium dry cells containing CuO and MnO_2 cathodes have a favorable shelf life and give greater watt-hour capacities on a weight and volume basis than Leclanché dry cells.

Abstract No. 9

A Synchronized Square Wave Generator and Switching Unit for Electrochemical Studies

N. C. Cahoon and **H. F. Schaefer,** National Carbon Battery Development Labs., National Carbon Research Labs., Cleveland, Ohio

An interrupter for producing a repetitive square wave pulse of direct current is combined with a synchronized switching relay for electrochemical studies. This unit provides a means of obtaining semi-instantaneous readings of either the open or closed cell voltage or electrode potential of an electrochemical system when in operation. The change in shape of the voltage-time pulse, displayed on an oscilloscope screen, shows the extent to which the square wave is modified by the electrode system and provides a useful tool for studying electrodes.

Abstract No. 10

Sine Wave Pulse Current Tester for Batteries

K. Kordesch, Research Labs., National Carbon Co., 12900 Snow Rd., Parma, Ohio, and **A. Marko,** Wright Air Development Center, Fairborn, Ohio

The separation of the polarization and resistance component of the voltage drop occurring in a battery under load conditions is measured with a 60-cycle, a-c operated instrument which is portable, allows direct readings without an oscilloscope, and is especially suited for development and production control tasks. Results of measurements on Leclanché cells, alkaline primary and secondary batteries, lead acid batteries, and fuel cells are presented. The relation to cell performance is discussed.

Abstract No. 11

The Silver/Silver-Oxide Electrode System

B. D. Cahan, J. B. Ockerman, R. Amlie, and **Paul Rüetschi,** Research Center, The Electric Storage Battery Co., Yardley, Pa.

Constant current anodization of silver in KOH was studied using a high-speed recorder with an electrometer input. Growth of anodic films was measured with

a superimposed square-wave technique whereby interface resistance and capacitance were followed continuously. The mechanisms for the conversion of Ag to Ag_2O, of Ag_2O to AgO, and of the evolution of oxygen are discussed in detail. Decay of oxygen overvoltage on AgO has been studied and correlated with BET areas. Discharge and self-discharge reactions and efficiency of discharge of each species have been studied similarly.

Abstract No. 12

Oxides on the Silver Electrode

C. P. Wales and **Jeanne Burbank,** U. S. Naval Research Lab., Washington 25, D. C.

Silver electrodes were studied by potential and x-ray diffraction patterns. Silver was charged anodically in 35% KOH by either constant current or constant potentential and discharged at a low or high rate. Attempts were made to form anodically an oxide higher than AgO. The anodic products of silver in 2N H_2SO_4 were determined. The basis for the theory that silver oxides are formed by introducing oxygen into the octants of the face-centered cubic silver lattice was examined.

Abstract No. 13

The Stability and Solubility of AgO in Alkaline Solutions

T. P. Dirkse and **Brandon Wiers,** Dept. of Chemistry, Calvin College, Grand Rapids, Mich.

AgO is stable in boiling water and decomposes but very little at room temperature in strongly alkaline solutions. The presence of Ag_2O does not affect this stability, but the presence of unoxidized silver does increase the rate of decomposition. AgO decomposes at temperatures above 100°C. When AgO dissolves in strongly alkaline solutions the dissolved form is primarily AgO and $AgO(OH)_2^-$. The standard free energy of formation of the latter is −85,380 cal/mole.

Abstract No. 14

The Oxidation of the Silver Electrode in Alkaline Solutions

T. P. Dirkse, Dept. of Chemistry, Calvin College, Grand Rapids 6, Mich.

The formation of Ag_2O and AgO was studied by means of constant current and constant potential processes. The efficiency of these oxide formations was determined by measuring the gain in weight of Ag electrodes under various conditions of charge, and the extent of the polarization of these processes was measured by using an interrupted current technique.

Abstract No. 15

The Effect of Cycling on the Silver Electrode

T. P. Dirkse and **J. De Vries,** Dept. of Chemistry, Calvin College, Grand Rapids, Mich.

Sintered silver electrodes have been cycled at various current rates and temperatures. An attempt is made to determine whether this treatment alters the capacity or physical characteristics of the silver electrode.

Abstract No. 16

Factors Affecting the Photogalvanic Behavior of Silver-Silver Halide Electrodes

S. Zaromb, M. Lasser, and **F. Kalhammer**, Research Dept., Philco Corp., Philadelphia, Pa.

The quantum yields of photochemically formed Ag available for electrolytic discharge in Ag-AgCl and Ag-AgBr cells depended mainly on method of electrode preparation, electrolyte composition, and light wavelength, but did not vary with the intensity of illumination for average solar radiation. Direct recombination of the photochemical reaction products and corrosion of Ag by an oxidant in the electrolyte are the main yield limiting factors.

Abstract No. 17

Silver Halide Photogalvanic Batteries

S. Zaromb, M. Lasser, and **L. Bockstie,** Research Dept., Philco Corp., Philadelphia, Pa.

Batteries rechargeable by the photolysis of silver halides are obtained by effecting spontaneous separation and storage of the photochemical reaction products utilizing selectively permeable membrane arrangements. Initial and continuous quantum yields vary with electrolyte compositions and electrode and membrane compositions and structure. The results are interpreted in terms of reaction rates, carrier mobilities, local energy potentials, and rectifying interfaces.

Abstract No. 18

Burgess Mercury Cells

T. H. Loverude, Burgess Battery Co., Division of Servel, Inc., Freeport, Ill.

A brief description is made of the general operating principles of the mercury cell. Several unique features of the Burgess mercury cells are outlined, and a description of the Burgess Hg-3 cell is made showing how they have controlled venting, simplified electrical contact between the cathode and the cathode can, and other construction features.

Abstract No. 19

Investigation of the Electrochemical Characteristics of Organic Compounds, V. Heterocyclic Nitro Compounds

R. Glicksman and **C. K. Morehouse,** RCA Semiconductor and Materials Div., Radio Corp. of America, Somerville, N. J.

A study of the electrochemical characteristics of nitropyridine and other heterocyclic nitro compounds shows that the cathode potential of these compounds during current flow is dependent on the aromaticity of the compound, as well as the type and position of substituent groups on the aromatic ring. The effect of these factors on the cathode potential is interpreted in terms of the electron density distribution in the molecule. Performance characteristics of magnesium dry cells containing 2,5-dinitrofuran and various nitropyridine compounds as cathodes are also presented.

Abstract No. 20

Investigation of the Electrochemical Characteristics of Organic Compounds, VI. Aromatic Hydroxy, Aromatic Amine, and Aminophenol Compounds

R. Glicksman, RCA Semiconductor and Materials Div., Radio Corp. of America, Somerville, N. J.

A study of the electrochemical characteristics of aromatic hydroxy, aromatic amine, and aminophenol compounds in basic electrolyte shows that the anode potential of these compounds is dependent on the aromaticity of the compound, as well as the type and position of substituted groups on the aromatic ring. The effect of these factors on the anode potential is interpreted in terms of the electron density distribution in the molecule. The use of these compounds as anode materials in primary cells is also considered

Abstract No. 21

The Principal Source of αPbO_2 in the Positive Plate Material of the Lead-Acid Battery

V. H. Dodson, Electric Auto-Lite Co., Toledo Ohio

An examination of positive plate material (*a*) formed from positive pastes of various densities (cube weights), (*b*) formed in aqueous sulfuric acid solutions of various specific gravities, and (*c*) at various stages of development indicates that the major source of α-PbO_2 in the positive material is unsulfated lead oxide. A method for estimating α- and β-PbO_2 in a mixture of the two is also described.

Abstract No. 22

The PbO_2 Electrode

R. T. Angstadt, B. D. Cahan, and **P. Rüetschi,** Research Center, The Electric Storage Battery Co., Yardley, Pa.

Electrode potentials of α-PbO_2 and β-PbO_2 were measured in solutions of sulfuric acid and perchloric acid with controlled concentration of Pb^{++} ion, as a function of pH and temperature. The double layer capacity of PbO_2 electrodes has been studied over a wide range of potentials under steady-state and transient

conditions with the use of a square wave technique. The range of thermal stability and transition points of α-PbO_2 and β-PbO_2 have been determined.

Abstract No. 23

The Microscopy of the Effect of Environmental Changes on the Forming Process

A. C. Simon and **E. L. Jones,** U. S. Naval Research Lab., Washington 25, D. C.

The effect of varying temperature, acid concentration, and current density were studied in relation to the microstructure produced. To determine the effective limits of the process, temperature was varied from 4° to 80°C, current density from 0.23 to 2.3 amp/dm² and acid from 1.050 to 1.450 sp gr. While the actual efficiency of the forming process was not determined under these varying environmental conditions, it was found that the microstructure and extent of formation varied widely.

Abstract No. 24

The Microscopy of the Forming Process in the Positive and Negative Plate

A. C. Simon and **E. L. Jones,** U. S. Naval Research Lab., Washington 25, D. C.

To determine the suitability of microscopy for such a purpose an exploratory study was made of the microscopic changes in structure that occur during the forming process. Samples taken at spaced intervals during the forming operation were prepared for microscopic examination by means of plastic impregnation. The examination more or less confirmed the generally held views on the subject, but emphasized the need for further investigation as to the effect of environment.

Abstract No. 25

Internal Resistance of Lead-Acid Cells; Submarine Battery Size

J. J. Lander and **E. E. Nelson,** Naval Research Lab., Washington, D. C.

Lead-acid cells of submarine battery size were discharged through resistance-inductance circuits. The data are analyzed to show no contribution to voltage loss other than *IR* losses in the cells during the initial voltage transient; consequently, a method is provided for the unequivocal determination of the internal resistance. Circuit geometry is an important factor determining the types of discharge curves which can be obtained.

Abstract No. 26

Nickel-Cadmium Cell Electrodes

A. J. Salkind and **P. F. Bruins,** Research Center, The Electric Storage Battery Co., Yardley, Pa.

Voltage decays of electrodes in nickel-cadmium cells were measured in cells stored at temperatures between −18° and 52°C. The heat of reaction of the cell was calculated from the slope of a plot of E/T vs. the logarithm of the vapor pressure of water and was found to be −62 kcal/g mole. The solid reaction products of the cell were studied by x-ray techniques.

Abstract No. 27

Investigations on the Reaction Mechanism of the Nickel-Cadmium Cell

S. Uno Falk, Svenska Ackumulator AB Jungner, Stockholm, Sweden

X-ray diffraction patterns from electrodes submerged in electrolyte have been obtained during charge and discharge by means of a special test cell, and the composition of the active materials has been determined. The question whether CdO or $Cd(OH)_2$ is formed during discharge has been subject to special attention. The low potential reaction of the positive plate has been studied. The emf and the dE/dT have been determined between −40° and +50°C at various states of charge.

Abstract No. 28

Sealed Nickel-Cadmium Cells Containing Palladium

H. N. Seiger, AVCO, RAD, Wilmington, Mass.

An investigation of the charge and discharge characteristics of cells containing palladium as a H_2-O_2 recombination catalyst was carried out. Preliminary measurements of the internal pressure indicate the catalytic coefficient for Pd:Ni is 1.4. The charge and discharge characteristics of the cells are unaffected by the pressure of the palladium catalyst.

CORROSION

Abstract No. 29

The Attack of Copper-Gold, Silver-Gold, Copper-Nickel, and Silver-Copper Alloys by Sulfur at Elevated Temperatures

B. D. Lichter (present address: Air Force Cambridge Research Center, Bedford, Mass.) and **Carl Wagner** (present address: Max-Planck Institut fur Physikalische Chemie, Gottingen, Germany), Dept. of Metallurgy, Massachusetts Institute of Technology, Cambridge, Mass.

Cu-Au alloys involving 10 and 33 mole % Au and Ag-Au alloys involving 12 mole % Au are attacked by liquid or gaseous sulfur above 400°C very rapidly with formation of a composite scale consisting of an outer homogeneous sulfide layer and an inner two-phase layer involving Au-rich alloy and sulfide in accord with theoretical considerations regarding the instability of a plane alloy-sulfide interface. The tendency to form a rugged alloy-sulfide interface decreases with higher Au contents especially at lower temperatures, and the rate of attack by sulfur decreases accordingly. Ag-Cu alloys involving 40 mole % Cu are also rapidly sulfidized at 400°C and yield a single sulfide layer of uniform thickness. Cu-Ni alloys sulfidized at 400°C yield a scale consisting of an outer layer which is supposedly digenite $Cu_{1.8}S$, and an inner layer which is supposedly a solid solution of Cu_2S in nickel sulfide.

Abstract No. 30

Anodic Oxidation of High-Purity Aluminum in Water

W. E. Tragert and **J. R. Rairden,** Research Lab., General Electric Co., P. O. Box 1088, Schenectady, N.Y.

The effect of applying an anodic potential during the oxidation of high-purity aluminum in double-distilled water has been studied with particular reference to the influence of an electric field on the crystal structure and composition of the oxide formed. The films can be characterized by nearly cubic close-packing of anions and by a temperature dependence of composition. Results are reported at several anodizing temperatures and over a range of anodizing currents.

Abstract No. 31

The High-Temperature Aqueous Corrosion Resistance of the Uranium-5% Zirconium-1½% Niobium Alloy*

J. E. Draley, Sherman Greenberg, and **W. E. Ruther,** Argonne National Laboratory, Lemont, Ill.

Uranium-5% zirconium-1½% niobium shows good corrosion resistance, as gamma quenched, in water to about 315°C. Optimum heat treatment results in a rate of about 6 mg/cm²/day at 260°C. Moderate aging, e.g., 400°C for 2 hr, results in reduced corrosion rates in the initial stages of corrosion, but corrosion resistance can be destroyed by over-aging. The alloy is also sensitive to hydrogen content. Ultimate failure is believed due to absorption of corrosion product hydrogen.

* Work performed under auspices of USAEC.

Abstract No. 32

Evidence for a Logarithmic Oxidation Process for Stainless Steel in Aqueous Systems

Milton Stern, Metals Research Labs., Union Carbide Metals Co., Division of Union Carbide Corp., Niagara Falls, N.Y.

Upon immersion of stainless steel into ferrous-ferris solution, the potential gradually approaches the reversible potential of the solution. During this period,

an oxidation process occurs, the rate of which decreases with time. The observed kinetics are consistent with equations which describe ion current through thin oxides as a function of the field across the oxide and are similar to kinetics reported for anodic oxidation of metals which form thin amorphous oxides. Therefore, it is believed that evidence has been obtained for growth of a similar type of oxide on passive stainless steel.

Abstract No. 33

Passivating Inhibitors

A. C. Makrides and **Milton Stern,** Technology Dept., Union Carbide Metals Co., P. O. Box 580, Niagara Falls, N.Y.

Results of an experimental study of the mechanism of passivation of Ti, Ni, and various steels by oxidizing inhibitors are presented. In particular, experiments were designed to differentiate between adsorption and reduction of inhibitor. It is suggested that for the cases examined inhibitor adsorption, if any, is of minor importance. Passivity is obtained only if the reduction rate of the oxidizing inhibitor exceeds a certain critical value characteristic of the metal. For a number of systems, the reduction rate is limited only by the rate of transport of inhibitor to the metal-solution interface. Thus, whether passivity or acceleration (of dissolution) is observed depends on mass transport rates which are, in turn, dependent on hydrodynamic flow conditions.

Abstract No. 34

Dissolution of Metals in Aqueous Acid Solutions

A. C. Makrides, Technology Dept., Union Carbide Metals Co., P. O. Box 580, Niagara Falls, N.Y.

A previously proposed interpretation of potential-current density curves obtained in dissolution of metals in aqueous acid solutions is examined in detail. It is shown that the dissolution rate-electrode potential curve for iron, nickel, and chromium-iron alloys, in solutions containing other redox couples besides H^+/H_2, closely approximates the anodic polarization curve of the metal. The bearing of these findings on the mechanism of passivating inhibitors proposed by Stern is discussed briefly.

Abstract No. 34A

Potential Behavior of a Uranium Electrode as a Function of Partial Pressure of Oxygen*

J. W. Ward and **J. T. Waber,** University of California, Los Alamos Scientific Lab., P. O. Box 1663, Los Alamos, N. Mex.

The potential of a uranium electrode coated with oxide was measured as a function of the partial pressure of oxygen. Although the equilibria involved are established slowly, the potential values were reproducible. The behavior with only traces of oxygen present was considered. An explanation is offered for the observed behavior.

* Work done under the auspices of the A.E.C.

Abstract No. 35

An Electrochemical Study of Passive Films on Fe-Cr Alloys

D. Caplan, A. Harvey, and **M. Cohen,** Division of Applied Chemistry, National Research Council, Ottawa, Canada

An attempt to deduce the nature of films left on Fe-Cr alloys by various surface preparations was made using electrochemical measurements. Electron microscopy and diffraction and parallel experiments with Cr and Fe were carried out for purposes of clarification. Cathodic reduction after certain preparations such as electropolishing yields an anomalous transient high negative potential suggesting an outer film of high hydrogen overvoltage which is slowly cathodically reduced to expose a surface of lower hydrogen overvoltage. With highly passive films it was found necessary to follow the potential during etching in order to remove the passive film without overetching.

Abstract No. 36

Effect of Surface Preparation on Air-formed Films on Iron

C. D. Stockbridge, P. B. Sewell, and **M. Cohen,** National Research Council of Canada, Ottawa, Canada

Surfaces of pure iron single and polycrystals have been prepared by electropolishing and electropolishing with subsequent etching or cathodic reduction. The nature of the surfaces has been investigated electrochemically and by electron diffraction. Electropolishing in the perchloric-acetic bath leaves a thin oxide on the surface which changes its thickness and structure with time of exposure to air. This film is different from that formed after either cathodic reduction or light acid treatment of the electropolished surface. In all cases the oxides are cubic and are either Fe_3O_4 or γFe_2O_3 depending on the orientation and surface treatment.

Abstract No. 37

Nitric-Hydrofluoric Acid Pickling of Zirconium Alloys

M. A. DeCrescente (present address: CANEL, Middletown, Conn.) **P. F. Santoro, A. S. Powell,** and **R. H. Gale,** Materials Development Lab., Nuclear Div., Combustion Engineering, Inc., Windsor, Conn.

The dissolution of Zircaloy-2 has been studied in the temperature range of 60°-100°F in unagitated and agitated hydrofluoric-nitric acid solutions. The dissolution rate was found to increase with HF concentration and agitation. The energy of activation for the Zircaloy-2 pickling process compares very well to the value for the unalloyed zirconium pickling process, 3.3 kcal/mole. The energy of activation does not depend on agitation.

Abstract No. 38

An Investigation of Chemical Variables Affecting the Formation of Films on Copper in Aqueous Solutions

W. H. Davenport, V. F. Nole, and **W. D. Robertson** (present address: Yale University, New Haven, Conn.)
Chase Brass and Copper Co., Waterbury, Conn.

The growth of copper oxide films in aqueous solutions has been studied by an electrometric method. Quantitative data have been obtained on the growth of films as a function of the solution variables, anion type and concentration, pH, and oxygen concentration. In air-stirred chloride solutions, film thickness increases with increasing chloride concentration, passes through a maximum in solutions approximately 0.01 molar, and then decreases. A maximum is also obtained for pH dependence in the range pH 5.9-9.0. Cuprous oxide is formed below about pH 10.5, and cupric oxide predominates at higher values.

Abstract No. 39

Dissolution of Single Crystals of Copper in Aqueous Ethylenediamine

L. H. Jenkins, Solid State Div., Oak Ridge National Lab., Oak Ridge, Tenn.

Single crystal plates of 99.999% copper were exposed to aqueous solutions of ethylenediamine saturated with air. Rates of dissolution of low index faces at fixed stirring rates between 7° and 60°C were determined and the activation energy for the process was calculated. Observations of the metal surfaces with optical and electron microscopes at different stages of the reaction revealed the effects of crystal orientations and imperfections on facet formation and pitting of the surfaces.

Abstract No. 40

The Electrochemical Behavior and Passivity of Titanium

Milton Stern and **Herman Wissenberg,** Metals Research Labs., Union Carbide Metals Co., Division of Union Carbide Corp., Niagara Falls, N.Y.

In the active condition, corrosion of titanium is controlled by activation polarization. The metal presents a surface with a low exchange current for a variety of electrochemical reactions. Low exchange currents are not conducive to establishment of passivity. However, this is overcome by unusually active critical potentials

for passivity. This accounts for the ease with which titanium is passivated by many substances which are only slightly oxidizing. It also explains the ease with which the metal can be protected anodically by galvanic coupling to other metals and alloys. Anodic deposition of thick titanium oxide films is observed under some experimental conditions.

Abstract No. 41

The Influence of Noble Metal Alloy Additions on the Electrochemical and Corrosion Behavior of Titanium

Milton Stern and **Herman Wissenberg**, Metals Research Labs., Union Carbide Metals Co., Division of Union Carbide Corp., Niagara Falls, N.Y.

Alloying of titanium with small amounts of noble metals markedly improves its corrosion resistance in reducing-type acids without any impairment of its high resistance to oxidizing media. The mixed potentials of titanium noble metal alloys are more noble than the critical potential for passivity of titanium in the same environment. Passivity is observed in hydrogen-saturated systems without the presence of a redox system more oxidizing than the hydrogen electrode. The mixed potential of titanium noble metal alloys is much more sensitive to traces of oxidizing agents than unalloyed metal.

CORROSION—ELECTRONICS

Abstract No. 42

Introduction to the Physics and Chemistry of Surfaces

W. H. Brattain, Bell Telephone Labs., Murray Hill, N.J.

The fundamental concepts of the physics and chemistry of surfaces will be considered starting with Langmuir's work on thermionic emission and adsorption on metal surfaces and ending with the simple surface or phase boundary that occurs at a p-n junction in a semiconductor. The semiconductor surface seems to be the better model for most catalytic surfaces. Future progress depends on measuring both physical and chemical changes on the same surface at the same time.

Abstract No. 43

Metal Surfaces

H. J. Juretschke, Dept. of Physics, Polytechnic Institute of Brooklyn, 333 Jay St., Brooklyn 1, N.Y.

The paper reviews the concepts which have been found useful in the discussion of various properties of metal surfaces. It includes a summary of theoretical work done in this area, predictions made by theory, and a discussion of experimental results and what they tell about the relation of the theory to actual surfaces.

Abstract No. 44

Semiconductor Surfaces

Paul Handler, University of Illinois, Urbana, Ill.

A brief history of the research in semiconductor surface physics is presented. Emphasis is placed on the limits of present theory and the importance of knowing the composition and structure of the surface of interest. The feasibility of new experimental approaches to the study of surfaces, such as nuclear magnetic resonance and quadropole resonance, is discussed. A review of recent developments in understanding the energy level diagram of the cleaned germanium surface is reviewed.

Abstract No. 45

Clean Surfaces

H. E. Farnsworth, Dept. of Physics, Brown University, Providence, R.I.

The method of obtaining atomically clean surfaces of refractory materials by prolonged heating at high temperatures in ultra-high vacua cannot be applied to most materials. Two alternative methods have been used in ultra-high vacua: (*a*) cleaving of crystals, and (*b*) argon-ion bombardment followed by annealing. The first method is limited to materials and conditions which permit cleaving. The second method has been applied more generally and has been found effective for a compound with low melting point as well as for more refractory elements and compounds.

Abstract No. 46

The Role of Imperfections in Surface Reactions

N. Cabrera, University of Virginia, Charlottesville, Va.

(No abstract received)

Abstract No. 47

Damaged Surface Layers—Semiconductors

T. M. Buck, Bell Telephone Labs., Inc., Murray Hill, N.J.

Preparation of semiconductor surfaces usually involves cutting and lapping or polishing. The damage produced by abrasion of this sort causes marked changes in surface recombination velocity, field effect mobility, conductivity, etching rate, and other properties. The type of abrasive material and the manner of treatment strongly influence the depth of the damaged layer. Estimates of these depths by various methods of detection will be presented along with discussion of the nature of the damage.

Abstract No. 48

Effect of Imperfections on Dissolution

J. J. Gilman, Research Lab., General Electric Co., Schenectady, N.Y.

At high rates of dissolution, the process is controlled by the rate of diffusion in the solvent, but surface imperfections play an important and often dominant role when dissolution is slow. Adsorbed species, dislocations, and point-defect clusters are the imperfections involved. They interact in highly specific ways. This is revealed by the sensitivity of the shapes of etch-pits to adsorbed species in the solvent and impurities in the solid for the case of LiF crystals; to whether an In or an Sb atom is at the center of a dislocation in the case of InSb crystals; and to optical activity in the solvent in the case of calcite crystals.

Abstract No. 49

Metal and Semiconductor Electrode Processes

H. Gerischer, Max Planck Institute, Stuttgart. Germany

The rate of surface reactions as electrode processes combined with transfer of electrically charged particles between the neighboring phases depends on the strength of electrical fields in the interface and on electron reactivity. The different order of magnitude of mobile electrons in a metal and in a semiconductor as well as the different distribution of states cause important differences in the distribution of charges near the interface and in the surface reactivity of electrons. The influence of these phenomena on electrode reaction kinetics with ion transfer or electron transfer at the interface will be discussed and compared with some examples.

Abstract No. 50

Experimental Techniques for the Study of Semiconductor Electrodes

J. F. Dewald, Bell Telephone Labs., Murray Hill, N.J.

Experimental techniques for the study of semiconductor electrodes are reviewed, and the theory involved in the treatment of the resulting data is discussed for several specific cases. A new transient technique, which is particularly useful with large-energy-gap semiconductors, is described.

Abstract No. 51

Electrode-Solution Interfaces

H. J. Engell, Max Planck Institut fur Eisenforschung, Düsseldorf, Germany

The differences of the distribution of charges at the surfaces of a metal electrode and a semiconductor electrode are considered. Using a simplified model the

densities of the charge carriers in a semiconductor electrode can be calculated. The result of the calculation is in agreement with measurements of the differential capacity of germanium electrodes. The influence of the current passing through the electrode surface and of the formation of traps is considered.

Abstract No. 52

Electrolytic Attack of Metals

Paul Lacombe, Case Institute of Technology, Cleveland, Ohio

Electrolytic etching of metals produces various results: intergranular attack, attack of crystalline surfaces which is orientation dependent, formation of etch pits, and anodic oxide films. The behavior of a metal or alloy depends on composition, temperature of the electrolyte, and above all on the electrode potential which varies with the metal. The method involving variation of the potential permits the establishment of the best conditions for the specific attack of each phase in an alloy. Applications to Al, Fe, stainless steel, Ti, Zr, U, and their alloys will be discussed.

Abstract No. 53

Electrolytic Etching of Semiconductors

D. R. Turner, Bell Telephone Labs., Inc.. Murray Hill, N.J.

Anodic reactions at semiconductor electrodes require electron holes. If the hole concentration in the semiconductor is relatively low, as in low resistivity n-type Ge or Si, the available holes in the surface region are used up at low current densities, and the etch rate is slow. The anodic current under these conditions can be increased by providing additional holes at the surface. Holes produced as a result of illuminating the semiconductor give uniform electrolytic etching on n-type semiconductors. Germanium is electrolytically etched in several electrolytes while silicon can only be dissolved anodically in fluoride solutions.

Abstract No. 54

The Etching of Metals and Semiconductors

J. W. Faust, Jr., Research Labs., Westinghouse Electric Corp., Pittsburgh, Pa.

Etching may be defined as the controlled removal of surface atoms. Various physical and chemical changes that can be used for etching are reviewed briefly. Studies on those aspects of dissolution of metals and semiconductors that relate to etching are discussed in more detail. Similarities and differences in the etching of metals and semiconductors are taken up, using specific systems for illustration.

Abstract No. 55

Kinetics of Dissolution Processes

Norman Hackerman, Dept. of Chemistry, University of Texas, Austin 12, Texas

The kinetics of dissolution of solids is governed in general by transport phenomena, or by whatever process is required to disrupt the primary aggregating forces in the solid, or by some combination of both. In principle the steps can be separated experimentally and studied individually. For processes which are controlled by transport the problems, both theoretical and experimental, are those of fluid dynamics and of the diffusion layer in nonturbulent systems. For processes in which the rate depends on bond disruption the principal step may be one of solvation or it may involve an oxidation-reduction system. The latter is predominant in most cases involving metals, and then it becomes necessary to determine which, if either, of the electron transfer processes is limiting. Most attention is given to problems in the last area.

Abstract No. 56

Electrochemistry of Dissolution Processes

J. V. Petrocelli, Research Labs., The International Nickel Co., Inc., Bayonne, N.J.

The basic electrochemical concepts and ideas underlying the phenomena of metal dissolution are reviewed. The emphasis is on the electrochemistry of metallic corrosion in aqueous solutions. The role of oxidation potentials as a measure of the "driving force" is discussed and the energetic factors which determine the relative electrode potential are described. It is shown that a consideration of electrochemical kinetics, in terms of current-voltage characteristics, allows an electrochemical classification of metals and leads to the modern views of the electrochemical mechanism of corrosion and passivity.

Abstract No. 57

Dissolution of Metals

C. V. King, Dept. of Chemistry, New York University, New York, N.Y.

In solutions of reagents which form soluble products and in regions of nonpassivating electrical potentials, metals often dissolve at rates controlled by convective-diffusive transport of reagent. The characteristics of such rates and some empirical and theoretical aspects of the "diffusion layer" will be discussed. Conditions under which transport control is replaced by other types of control will be discussed and examples will be presented. Adsorption of a reaction product may inhibit dissolution, or complete surface coverage by a necessary intermediate may limit the dissolution rate, for example.

Abstract No. 58

Dissolution of Semiconductors*

H. C. Gatos, Lincoln Lab., Massachusetts Institute of Technology, Lexington, Mass.

There are many similarities between semiconductors and metals regarding their dissolution kinetics, passivity, and electrochemistry in aqueous solutions. These similarities will be discussed particularly with reference to germanium. On the other hand, semiconductivity and structure are responsible for certain unique features associated with the dissolution behavior of semiconductors. Specific adsorption of ions, for instance, plays a prominent role in the dissolution kinetics of germanium. In addition to the behavior of elementary semiconductors that of certain intermetallic compound semiconductors will be discussed.

* The work reported in this paper was performed by Lincoln Laboratory, a center for research operated by Massachusetts Institute of Technology with the joint support of the U.S. Army, Navy, and Air Force.

Abstract No. 59

Adsorption and Chemisorption

M. Boudart, Princeton University, Princeton, N.J.

(No abstract received)

Abstract No. 60

Chemisorption and Catalysis

R. P. Eischens, Texaco Research Center, Beacon, N.Y.

The most direct evidence concerning chemisorbed molecules is obtained from their infrared spectra. These spectra show the structure of the chemisorbed molecules, effect of interactions between these molecules, and effect of modifying the adsorbent metal by other components. Infrared results show that the chemistry of the surface metal atoms is similar to that of metal atoms in coordination compounds. This tends to restore catalysis to the domain of the chemist and suggests that factors inherent in the physical structure of metals, such as lattice defects or surface geometry, are not essential to the basic catalytic process.

Abstract No. 61

On the Mechanism of the Oxidation of Metals

K. Hauffe, Farbwerk Hoechst AG, Frankfurt (Main), Germany

After a short introduction on the relationship between diffusion process and field transport phenomena in tarnishing layers on metals and alloys, the mechanism of oxidation of iron is discussed. Epitaxy plays an important role on the gradient of the concentration of

lattice defects and, therefore, on the validity of the parabolic rate law. Classical examples of metal oxidation with a parabolic rate law are presented and the various reasons for the deviation observed are elucidated on the systems iron in CO/CO_2 and Cu_2O in O_2. In addition, the oxidation of alloys with interrupted oxide-metal interfaces is treated. Finally, attention is focussed on the difficulties in explaining the low temperature-oxidation mechanism.

Abstract No. 62

The Influence of Crystal Orientation on Oxidation of Metals

A. T. Gwathmey and **K. R. Lawless,** Dept. of Chemistry, University of Virginia, Charlottesville, Va.

The influence of crystal orientation on the rate of formation and on the epitaxy of oxide films formed on large metal crystals will be discussed. Past studies will be reviewed, new results will be presented, and emphasis will be placed on important questions which must yet be answered in order to understand oxidation. Primary consideration will be given to crystals of copper.

ELECTRODEPOSITION

Abstract No. 63

Anodic Methoxylation

K. E. Kolb, and **T. W. Lippincott,** Ohio State University, Columbus, Ohio, and **C. L. Wilson,** Cranberry Lake, Sloatsburg, N.Y.

Electrolysis of sodium methoxide in methanol at a graphite or platinum anode in an undivided cell gives formaldehyde, sodium formate, and sodium methyl carbonate. If furan or thiophene is also present, two methoxyl groups are added to the molecules to give 2,5-dimethoxy-2,5-dihydrofuran (or thiophene). The yield is as high as 50%. If, instead of direct, alternating current is used, no methoxylation reaction is observed until the frequency is lowered to three cycles or less per second. This suggests that an intermediate radical is formed on the anode with an unexpectedly long lifetime of about 20 sec.

Abstract No. 64

The Electrolysis of Dibasic Acids and Their Mono-Acid Esters in Nonaqueous Solution

W. E. Garrison, Jr., A. M. Hartley, Sherlock Swann, Jr., and **C. S. Marvel,** Dept. of Chemistry and Chemical Engineering, University of Illinois, Urbana, Ill.

The electrolysis of a series of ammonium salts of aliphatic dicarboxylic acids, in methanol, has been carried out. Polymers were formed at the anode from adipic, azelaic, sebacic, and hexadecane-1,16-dicarboxylic acids. These polymers could be separated into soluble and insoluble fractions. The soluble fractions were found to be of low molecular weight and linear, with some ester linkages. The dimethyl ester of dotriacontane-1,32-dicarboxylic acid was synthesized in 57% yield by electrolysis of the ammonium salt of monomethyl hexadecane-1,16-dicarboxylate.

Abstract No. 65

Electrolysis of Organic Solvents, I. Electrolysis of Simple Amides

D. E. Couch and **Abner Brenner,** National Bureau of Standards, Washington 25, D.C.

Except for water and ammonia, the electrolysis of few solvents has been investigated. A general project on the electrolysis of organic solvents has been initiated to study the products and the development of a mechanism of the electrode reactions. This first report deals with the electrolysis of several simple amides.

Crystalline compounds have been produced by the electrolysis of N,N'dimethylformamide, N-methylformamide and N,N'dimethylacetamide with bright platinum electrodes. These materials were formed by the electrolysis of anhydrous solvent and by the electrolysis of the solvent containing 5-10% by volume of 1M H_2SO_4. However, if water is present in large amounts, 50% by volume, the yield of product is reduced and impurities which make separation of the product difficult are formed. Little or no gas is formed at the anode but at the cathode hydrogen is produced with 95-100% efficiency.

Abstract No. 66

Studies of Germanium Electrodes in a Ziegler Electrolyte

R. J. Flannery (present address: Research Labs., Standard Oil Co. (Indiana), 2500 New York Ave., Whiting, Ind.) **D. Trivich,** and **J. E. Thomas, Jr.,** Wayne State University, Detroit, Mich.

The behavior of n- and p-type germanium electrodes, particularly under anodic conditions, was studied in a Ziegler electrolyte composed of triethyl aluminum and sodium fluoride. D-C anodic and A-C current-voltage curves indicate current saturation effects in n-type but not in p-type germanium. Germanium does not dissolve anodically, and the anode products are characteristic of a reaction of ethylide ions with holes. The cathode product, aluminum, forms a rectifying junction on n-Ge or p-Si.

Abstract No. 67

Electrolysis in Anhydrous Ether

I. E. Gillet, Chef de Travaux d'Electrochimie et de Chimie Organique Appliquee, Universite de Liege, 2, rue A. Stevart, Liege, Belgium

Electrolyses have been carried out on anhydrous ethyl ether made conductive by dissolution of inorganic salts or Grignard reagents ($AlCl_3$ or $AlCl_3 + LiCl$ or $MgBr_2$ or RMgBr). Polarization curves have been determined and products analyzed. Results and conclusions are presented, the main conclusion being that ether itself reacts easily at both electrodes and is sometimes the only reacting substance, the dissolved salt being used only to conduct the current in solution.

Abstract No. 68

Electrolyte for Deposition at −60°C

H. B. Maier, Bergen Labs. Inc., Clinton, N.J.

An electrolyte which is liquid and conductive at −60°C consists of ethanol, water, sodium sulfate, nickel sulfate, and additional inorganic and organic materials. The salts are dissolved in the water, and a large amount of ethanol (approximately 80% by volume) is added to form an electrolyte solution having a low freezing point. Conduction at −60°C, after running overnight, is 1.5 ma at 13 v for electrodes 1 $in.^2$ in area, ⅞ in. apart. The anode consisted of a strip of nickel, the cathode of a strip of copper. During removal of the electrolysis cell from the freezing unit, no gassing was observed. A small amount of black powder was seen on the cathode. Further tests are being conducted to obtain a uniform metallic coating at −60°C.

Abstract No. 69

Electropolishing in Chloride Solutions

E. B. Saubestre, Enthone, Inc., A Subsidiary of American Smelting and Refining Co., 442 Elm St., New Haven, Conn.

Solution formulas and operating conditions are presented which permit electropolishing of a wide number of metals and alloys in solutions containing chlorides. These solutions resemble the perchloric acid type of electropolishing solution in many respects. Outstanding feature of these solutions is the very wide range of current densities over which electropolishing occurs. These solutions are most useful for treating small parts.

Abstract No. 70

Anodic Films on Copper in Phosphoric Acid

J. H. Bartlett, University of Illinois, Dept. of Physics, Urbana, Ill., and **F. H. Giles, Jr.,** University of South Carolina, Columbia, S.C.

If initially a copper anode in phosphoric acid is in the steady state and if the current is then interrupted, break curves of the variation of voltage with time may

be recorded. At the lower voltages, such curves decay in a manner resembling an exponential, and the convection layer disappears at the same time. If the voltage is just above the point corresponding to the knee of the current-voltage curve, there is superimposed on the above break curve a similar one with a much smaller time constant. This is what would be observed if concentration gradients in a much thinner layer were being ironed out. This time constant increases with voltage, indicating that the thickness does, also.

Abstract No. 71

Polishing Regions for Copper in Phosphoric Acid

J. H. Bartlett, University of Illinios, Dept. of Physics, Urbana, Ill., and **F. H. Giles, Jr.,** University of South Carolina, Columbia, S.C.

By microscopic observations of a vertical copper anode during electrolysis in phosphoric acid, the dependence of electropolishing on voltage and current density has been recorded. In 50% H_3PO_4, two regions of applied voltage were found in which polishing occurred: a lower region just at and above the knee of the steady-state current-voltage curves (between 0.1 and 0.26 v with respect to 0.1*N* calomel) and an upper region which extended from a steady-state voltage of approximately 0.8 v with respect to 0.1 calomel up into the region of oxygen evolution.

The sensitivity of the polishing surface to electrical and mechanical changes in each of these regions of polishing has been observed, as well as the variation with acid concentration of the extent of the polishing regions themselves. These data are discussed in terms of our knowledge of the Cu-H_3PO_4 anodic system, and the significance to the theory of the mechanism of electropolishing is considered.

Abstract No. 72

Application of Electropolishing and Chemical Polishing to Heat Sink Material

P. T. Woodberry, Avco, RAD, 201 Lowell St., Wilmington, Mass.

Electropolishing and chemical polishing techniques were used to prevent the occurrence of defective zones of copper-copper interfaces in the electrodeposition of thick copper. Electropolishing could be substituted for grinding and machining of nodules prior to subsequent layer deposition. Copper was polished, electropolished, or chemically polished before deposition of thick nickel; the effect of surface preparation and type of copper on the elevated temperature properties of this system are discussed.

Abstract No. 73

Electropolishing in Cyanide Electrolytes

F. Sullivan and **E. H. Newton,** Arthur D. Little, Inc., Cambridge, Mass.

The theory and practice of electropolishing silver, sterling silver, gold alloys, and brass in cyanide electrolytes are described. Commercial electropolishing of silver plate, pilot plant experience in electropolishing sterling silver, and laboratory investigations into gold alloys and brass electropolishing are covered. Compositional and operational variables in each process are reviewed.

Abstract No. 74

Some Electrode Processes on Copper Anodes in Orthophosphoric Acid Solution

K. F. Lorking, Aeronautical Research Labs., Box 4331, G. O. P., Melbourne, Australia

Theories on the structure of the electrical double layer formed at polarizable anode surfaces and on electrode processes at reacting anodes are used to indicate the processes to be expected on copper anodes in orthophosphoric acid solutions. A description and discussion are given of experiments showing the influence of increasing anode potential on surface finish and film formation on copper anodes in orthophosphoric acid. Theories of the mechanism of electropolishing are discussed and it is shown that modifications of these theories are indicated by experimental observations.

Abstract No. 75

Electrical Migration in the Absence of Electrolysis

Abner Brenner, National Bureau of Standards, Washington 25, D.C.

Electrical migration of ions has always been observed in experiments involving electrolysis. J. W. Richards believed that electrical migration was a secondary effect of current flow and was due to stresses set up by the electrolytic decomposition at the electrodes. He considered that the mechanism of the flow of current in electrolytes was the same as that in metals.

An experiment was devised for examining electrical migration in the absence of electrolysis. By means of a magnetic field and a liquid commutator, a direct current was induced into a closed circuit consisting of electrolyte. No electrolysis was involved. Electrical migration was determined by the movement of Erythrosin B into a capillary. The experiment showed that electrical migration occurred in the absence of electrolysis and was qualitatively of about the same magnitude as that observed in the presence of electrolysis.

Abstract No. 76

Relationship between Brightness and Structure in Electroplated Nickel

Rolf Weil and **R. A. Paquin,** Dept. of Metallurgy, Stevens Institute of Technology, Hoboken, N.J.

The as-plated surface microstructure of deposits of varying brightnesses was examined by electron microscopy. A linear relationship was found between the fraction of the surface area with roughness less than 0.15 μ and the logarithm of the quantity of light reflected. No direct relationship between the degree of preferred orientation and brightness was found, but the fiber axis is related to the structural type and the addition agents in the bath.

Abstract No. 77

Measurement of Elastic Modulus and Internal Friction in Electrodeposits

H. J. Read and **A. H. Graham,** Dept. of Metallurgy, The Pennsylvania State University, University Park, Pa.

Experimental techniques and calculations for the determination of elastic modulus and internal friction from sonic measurements on thin-walled tubes prepared by electrodeposition are described. A method of making the tubes with the necessary precision is presented. Data on the effects of some plating variables are given, but special attention is devoted to relationships between the structures of the deposits and the elastic properties under study.

Abstract No. 78

Electrodeposition of Amorphous Selenium

A. K. Graham, H. L. Pinkerton, and **H. J. Boyd,** Graham, Savage and Associates, Inc., Jenkintown, Pa.

Amorphous selenium coatings have been electroplated in thicknesses up to (and thicker coatings can be prepared) 30 μ (1.2 mils) on bright nickel cathodes. Data are given for studies leading to the selection of the optimum bath and operating conditions for the formation of reproducible, uniform, and adherent deposits. It is shown that the plating baths employed and the amorphous deposits obtained are extremely sensitive to a variety of conditions, thus emphasizing the need for further study of the electrodeposition of selenium in the amorphous form.

Abstract No. 79

Zinc Plating of Carbonitrided Steel*

H. T. Francis and **L. R. Kohan,** Armour Research Foundation, 10 West 35th St., Chicago 16, Ill.

A fundamental study was made of the difficulty sometimes encountered in barrel zinc plating of carbonitrided steel parts. A very successful laboratory technique was devised for simulation of barrel plating in a still plating bath. Results suggest that the difficulty in achieving zinc coverage on the hardened parts is caused by a "plate and dissolve" mechanism.

* This work was supported by the Shakeproof Division of Illinois Tool Works.

Abstract No. 80

Adherence of Thick Chromium Deposits as Affected by Surface Preparation

H. Chessin and **C. L. Alderuccio,** Van der Horst Corp. of America, Olean, N.Y.

Photomicrographs show that honing, a mild and slow-speed operation as compared to either grinding or machining, may cause extensive damage to the surface of cast iron. Chromium electrodeposited on these damaged surfaces will exhibit poor adherence not because the adherence of the chromium to the iron is poor but because the surface layer of iron is weak.

Abstract No. 81

Deposition of New Chromium-Iron Alloy Plate of Banded Structure

L. D. McGraw, J. A. Gurklis, and **C. L. Faust,** Electrochemical Engineering Div., Battelle Memorial Institute, Columbus 1, Ohio, and **J. E. Bride,** Diamond Alkali Co., Cleveland, Ohio

A new bath composition and its operating conditions are described for electrodeposition of hard, bright, chromium-iron alloy plate having banded microstructure. A precipitation mechanism is proposed to account for the microstructure of the plate.

Abstract No. 82

Electrodeposition of Chromium from Low Valence Compounds, I. Investigation of Bath Types and Operating Conditions

G. R. Sherwood, M. R. Holmes, and **Finn Bergishagen,** Dept. of Chemistry, Wayne State University, Detroit 2, Mich.

Excellent quality chromium metal can be deposited at comparatively good efficiency from baths in which the chromium is chiefly trivalent. Presence of divalent chromium in such baths does not seem essential but does seem beneficial. A mixed bath, containing chiefly chloride-formate-fluoborate, is recommended rather than a bath containing one salt only.

Abstract No. 83

Studies of Hydrogen Embrittlement by the Use of Deuterium

G. B. Wood, National Bureau of Standards, Washington 25, D.C.

Fundamental studies dealing with the passage of the hydrogen isotopes through SAE 4130 steel are discussed. The rate of passage of hydrogen through steel, the amount of hydrogen causing embrittlement, and the resulting severity of embrittlement are correlated. The use of deuterium as the embrittling isotope permits a differentiation between hydrogen electrolytically introduced into steel and that introduced due to metallurgical procedures. Hydrogen embrittlement of steel accompanying cadmium and chromium plating and alkaline and acid electrolytic treatment in the presence and absence of poisons are discussed.

Abstract No. 84

The Source of the Nitrogen Impurity in Electrodeposited Chromium

N. Ryan and **E. J. Lumley,** Aeronautical Research Labs., Dept. of Supply, Box No. 4331, G. P. O., Melbourne, C. 1, Vic., Australia

High-purity chromium deposited from chromic acid electrolytes containing either sulfate or fluoride catalysts invariably contains small amounts of nitrogen as an undesirable impurity. The amount of this nitrogen impurity is shown to be increased by increased nitrate ion concentration in the electrolyte but not affected by dissolved atmospheric nitrogen or ammonium compounds. It is demonstrated that the nitrate impurity is decomposed at the cathode by reduction with hydrogen to form ammonia as the major product. Some of the atomic nitrogen which is possibly formed at a stage during this reduction is probably adsorbed continuously into the electrodeposited metal.

ELECTRONICS—SEMICONDUCTORS

Abstract No. 85

Determination and Identification of Impurities in Silicon from Low-Temperature Hall Data

R. T. Bate, Battelle Memorial Institute, 505 King Ave., Columbus 1, Ohio, **I. R. Weingarten,** and **D. J. Shombert,** Research Lab., Merck, Sharp and Dohme, Rahway, N.J.

Low-temperature measurements of the Hall effect have been used to determine donor and acceptor concentrations and in some cases to identify the major impurity in silicon. A simple apparatus for making these measurements with liquid helium is described. Typical results are presented and correlated with mobility data at 80° or 55°K and lifetime data at room temperature. Interpretation of the Hall coefficient measurements is discussed.

Abstract No. 86

Use of Hall Measurements in Evaluating Polycrystalline Silicon

P. J. Olshefski, Electronic Chemicals Div., Chemical Div., Merck & Co., Inc., Danville Pa., **D. J. Shombert,** and **I. R. Weingarten,** Research Labs., Merck, Sharp and Dohme, Rahway, N.J.

Hall measurements at room temperature have been used to determine the average net carrier density in polycrystalline silicon. The method does not require cutting of samples and destruction of the rod. Current contacts are made to the ends of the rod with strips of metal foil; Hall contacts are made with two titanium blades which close on the rod. Hall measurements made this way on single-crystal zone-refined rods agree with measurements on samples cut from the rods in the conventional manner. Average carrier densities measured in the polycrystalline rods have been correlated with the resistivities of the same rods after 1, 2, 3. . . floating zone passes.

Abstract No. 87

Radio Frequency Carrier and Capacitive Coupling Procedures for Resistivity and Lifetime Measurements on Silicon

I. R. Weingarten and **M. Rothberg,** Research Labs., Merck, Sharp and Dohme, Rahway, N.J.

By the use of the rf carrier and capacitive coupling it has been possible to measure the resistance and lifetime of silicon rods without making direct ohmic contact to the sample. Even with contacts, the use of an rf carrier to observe lifetime by photoconduction decay eliminates the need for insuring solid ohmic contacts as is required with the d-c carrier. With the low-loss insulation between coupling capacitors and sample, an rf bridge will measure separately both the sample resistance between the coupling capacitors and the value of the coupling capacitance.

Abstract No. 88

Steady-State Diffusion of Charge Carriers in High-Purity Single-Crystal Silicon

Milton Green and **I. N. Greenberg,** U. S. Army Signal Research and Development Lab., Fort Monmouth, N.J.

Results of irradiating high-purity silicon (ca 1900 ohm cm p-type and 590 ohm cm n-type) with light near metal-to-silicon contact junctions (all found to be rectifying at room temperature) were investigated. An expression is presented for the photocurrent at steady-state illumination (focused as a very narrow line parallel to the junction), one-dimensional geometry, and sample long compared to a diffusion length. In the preliminary experiments it was found that the diffusion phenomenon was masked by the photoeffect due to light scattered directly to the junction. Since the scattered light is most difficult to eliminate, it was minimized by using a broad line of light of variable breadth extending from the junction to a certain distance along the specimen. Expressions for the photocurrent under this condition and one-dimensional geometry are presented and compared with experiment.

Abstract No. 89

Lifetime in Germanium as a Function of Gas Adsorption

M. S. Fink and **M. J. Katz,** U. S. Army Signal Research and Development Lab., Fort Monmouth, N.J.

Changes of lifetime in germanium have been measured as a function of adsorption of various gases at different temperatures, pressures, and time. Data show an interesting dependence of the direction and magnitude of the changes on the nature of the adsorbate and its interaction with the adsorbing surface. Interpreted in terms of adsorption theory, the measurements imply a better understanding of the chemical origin of surface states and their effect on electronic properties.

Abstract No. 90

Analysis of de Haas-van Alphen Type Oscillations in Graphite

D. E. Soule, National Carbon Co., Research Labs., Cleveland, Ohio

Oscillations of the de Haas-van Alphen type have been observed in the Hall effect and magnetoresistance in graphite single crystals. They have been studied as a function of carrier type (majority electrons and holes), magnetic field orientation, temperature, and acceptor doping. Analysis of results has revealed the anisotropy and fine structures of the Fermi surface, effective masses, collision broadening, carrier concentrations, Fermi energies, and electronic band overlap.

Abstract No. 91

Some Optical and Electrical Properties of Crystalline Boron

G. K. Gaulé, J. T. Breslin, J. R. Pastore, C. G. Pochop, and **R. A. Shuttleworth,** U.S. Army Signal Research and Development Lab., Fort Monmouth, N.J.

Optical transmission measurements have been made on boron crystals obtained from a melt and from a vapor phase. Essential differences in the absorption coefficient vs. wave-length curves were observed. Most samples were chemically rather impure, p-type, of high resistivity, and had a high Seebeck coefficient. Some material, however, showed a more "metallic" character. Contacts were nearly ohmic in all cases; photoconductivity was always small. Potential technical uses of some optical and electrical properties are discussed.

Abstract No. 92

Diffusion of Injected Carriers in Silicon

C. H. Champness, Northern Electric Labs., 1401 St. Patrick St., Montreal, Que., Canada

The field-free diffusion of minority carriers injected at a point into silicon has been studied. The time from injection to the maximum due to the arriving carriers has been measured for various emitter collector distances. Results do not agree with the conventional treatment of diffusion and life time. There are indications that, due to heavy injection of carriers, there is enhanced recombination resulting in an effective life time which decreases as the emitter point is approached.

Abstract No. 93

Preparation and Electrical Properties of Alloyed P-N Junctions of InSb

C. A. Lee and **George Kaminsky,** Bell Telephone Labs., Inc., Murray Hill, N.J.

A study of p-n junction characteristics at liquid nitrogen temperatures has been made on junctions prepared by alloying cadmium to n-type InSb. Reports of junctions in InSb have been published, but, apart from sensitivity of detection of infrared radiation, no other junction characteristics were presented. Our investigations indicate that cadmium seems to be unique among the Group II and VI elements in that p-n junctions, exhibiting good rectifying properties, can be made with conventional alloying techniques.

Abstract No. 94

Properties of Ternary Alloys in the System In-Sb-Te*

A. J. Rosenberg, Lincoln Lab., Massachusetts Institute of Technology, Lexington, Mass.

Four known semiconducting binary compounds (InSb, InTe, In_2Te_3, Sb_2Te_3) exist in the system, In-Sb-Te. Together with elemental Te and (amorphous) Sb, they comprise a group of six semiconducting phases with fundamentally different crystal symmetry, chemical bonding, and electronic properties. A study of the general phase relationships and electronic characteristics of ternary compositions of In, Sb, and Te has been undertaken, and the preliminary data are discussed.

* The work reported in this paper was performed by Lincoln Laboratory, a center for research operated by Massachusetts Institute of Technology, with the joint support of the U.S. Army, Navy, and Air Force.

Abstract No. 95

Determination and Properties of Some Elements in GaAs

E. Arnold, J. Black, and **S. Weissberger,** Sylvania Electric Products Inc., Bayside, N.Y.

The concentration of residual impurities and of added donor and acceptor elements in zone melted GaAs was determined by spectroscopic, spectrophotometric, and neutron activation analyses. Approximate values of the effective segregation coefficients and solubility limits of elements from Groups II, IV, VI of the periodic table were determined from chemical analysis and metallographic examination of doped ingots. The net donor or acceptor concentrations, as determined from chemical analysis, were compared with the free carrier concentrations as determined from Hall measurements on single crystals. It was found that the two concentrations do not always agree. The agreement is discussed for a number of elements in relation to their concentration and position in the periodic table, with reference to such factors as dislocation density and heat treatment.

Abstract No. 96

Mechanism of Preferential Etching of $A^{III}B^{V}$ Compounds*

H. C. Gatos, M. C. Lavine, and **M. J. Button,** Lincoln Lab., Massachusetts Institute of Technology, Lexington, Mass.

Etching of intermetallic compounds with the zinc-blende structure has been studied in several aqueous media as a function of temperature and orientation. Examination of the etching characteristics of the{III} and {III} planes indicates that no dislocation etch-pits are revealed in one of these planes in a large number of aqueous solutions, although dislocation etch-pits are consistently revealed in the other. By introducing small amounts of various elements into the zinc-blende lattice, etch-pits are revealed in both planes. A model is proposed for explaining this phenomenon based on lattice vacancies and edge dislocations.

* The work reported in this paper was performed by Lincoln Laboratory, a center for research operated by Massachusetts Institute of Technology with the joint support of the U.S. Army, Navy, and Air Force.

Abstract No. 97

Preparation and Electrical Properties of Mercury Selenide*

T. C. Harman, Lincoln Lab., Massachusetts Institute of Technology, Lexington, Mass.

Large single-crystal ingots of mercury selenide have been prepared by the Bridgman technique. The technique used for the reaction and crystallization of the compound is described. At 77°K, most pure material possessed a carrier concentration of $2 \times 10^{17}/cm^3$ and an electron Hall mobility of 63,000 $cm^2/v\text{-}sec$. Information on the HgSe-CdSe alloys and results of selective doping experiments are also presented.

* The work reported in this paper was performed by Lincoln Laboratory, a center for research operated by Massachusetts Institute of Technology with the joint support of the U.S. Army, Navy, and Air Force.

Abstract No. 98

Mechanical and Infrared Excitation of Luminescence in CdS Crystals

D. M. Warschauer and **D. C. Reynolds,** Wright Air Development Center, Wright Air Force Base, Ohio

Mechanically excited edge and impurity emission in thermally or optically stimulated cadmium sulfide will be discussed in terms of recent band models and a necessary set of impurity levels. The potential applications of this effect in computer storage devices, infrared detectors, etc., will be covered. Unlike the polarization of edge emission and the red luminescence of silver, the orientation of the electric vector of red emission from copper in cadmium sulfide is parallel to the c-axis.

Abstract No. 99

Properties of CdSb and CdSb-ZnSb Alloys*

A. J. Strauss, Lincoln Lab., Massachusetts Institute of Technology, Lexington, Mass.

The variation in thermoelectric power of CdSb samples prepared under different conditions of crystallization is described. The thermoelectric power depends strongly on whether CdSb is formed by direct crystallization or by crystallization of metastable Cd_3Sb_2 and subsequent solid-state reaction of the latter compound with Sb. Thermal analysis data on the phase diagram of the CdSb-ZnSb pseudo-binary system, together with x-ray and thermoelectric data on the alloys, are also presented.

* The work reported in this paper was performed by Lincoln Laboratory, a center for research operated by Massachusetts Institute of Technology with the joint support of the U.S. Army, Navy, and Air Force.

Abstract No. 100

Physical Chemistry of the II-V Semiconductors CdSb and $CdAs_2$

V. J. Lyons, V. J. Silvestri, and **G. A. Silvey,** Research Center, International Business Machines Corp., Poughkeepsie, N.Y.

The thermal dissociation of CdSb and $CdAs_2$ may be represented by the following equations:

$$3CdAs_2 \rightleftharpoons Cd_3As_2 + As_4 \quad [1]$$

$$CdSb \rightleftharpoons Cd + Sb \quad [2]$$

A study of the reactions under equilibrium conditions has provided measurements of the dissociation pressures for the compounds. Crystal pulling of the compounds was carried out in sealed quartz tubes wherein magnetic suspension of the seed and crystal was employed. Several methods of purification were used during preparation of the compounds. A comparison of results indicates that the highest degree of purification was obtained through segregation of impurities during crystal pulling. Experiments are described relating to the effect of annealing on monocrystalline $CdAs_2$ under equilibrium conditions.

Abstract No. 101

Optical and Electrical Properties of CdSb and $CdAs_2$

W. J. Turner, A. S. Fischler, and **W. E. Reese,** Research Center, International Business Machines Corp., Poughkeepsie, N.Y.

CdSb has an optical gap of 0.51 ev and transmission to 32 μ. The net electron concentration in the single crystal CdSb studied was approximately 10^{16} cm^{-3} and had room temperature Hall mobility of 250 cm^2/v-sec.

$CdAs_2$ is tetragonal with a gap of 1.11 ev and optimum transmission in the c-direction from the edge to 35 μ. Pulled $CdAs_2$ crystals showed net electron concentrations of 10^{15} cm^{-3} to 10^{17} cm^{-3}. Hall mobilities over 300 cm^2/v-sec have been observed in the 10^{15} cm^{-3} material. The conductivity of the c-direction $CdAs_2$ is a factor of four larger than the a-direction over the temperature range of 77°-300°K.

Abstract No. 102

Phase Diagram for the Pseudo-Binary System CdTe-In_2Te_3*

Lars Thomassen and **D. R. Mason,** Dept. of Chemical & Metallurgical Engineering, University of Michigan, Ann Arbor, Mich.

The phase diagram for pseudo-binary system CdTe-In_2Te_3 has been investigated by correlating information from differential thermal analysis measurements, microscopic studies, and x-ray powder patterns. In checking the terminal points for this diagram, the melting point for CdTe was found to be 1098° ± 2°C, which represents a considerable deviation from the previously reported value of 1045° C. No congruently melting compounds form along this particular line in the ternary system Cd-In-Te.

* Supported by Project MICHIGAN and the National Science Foundation.

Abstract No. 103

Purification of Arsenic

J. M. Whelan, J. D. Struthers, and **J. A. Ditzenberger,** Bell Telephone Labs., Inc., Murray Hill, N.J.

Small concentrations of sulfur and selenium present in high-purity arsenic cannot be removed easily from InAs and GaAs by zone refining. Three proposed methods for reducing the concentrations of these impurities in arsenic have been re-examined using tracer techniques. These are (*a*) vacuum sublimation, (*b*) sublimation in hydrogen, and (*c*) condensation into and distillation from a lead bath. Under favorable conditions, arsenic has been prepared containing the following atom fractions of sulfur, selenium, and tellurium, respectively: 1.1. x 10^{-9}, ~2 x 10^{-9}, and 2 x 10^{-9}.

Abstract No. 104

Preparation of High-Purity Gallium

Pierre de la Bretèque, Aluminium-Industrie-Aktien-Gesellschaft, Zurich, Switzerland

The preparation of high-purity gallium has been realized by purifying the sodium gallate in combination with a treatment of metallic gallium. Purification of sodium gallate is obtained by adding Na_2S; precipitation of the impurities in form of sulfides is favored by an addition of nickel salts. The metallic gallium is subjected to the following treatment: washing in an acid solution, filtering of the metal on porous plates, finally oxidation at elevated temperature by means of oxygen, followed by renewed filtering.

Abstract No. 105

Impurity Distribution of Various Doping Techniques in Floating Zone Crystal Growing

A. L. MacDonald and **E. Y. Wang,** Semiconductor Div., Raytheon Co., Newton, Mass.

In doping single-crystal silicon grown by floating zone techniques, one must use different doping procedures than commonly associated with the conventional Czochralski method. Several techniques have been investigated such as doping in the initial molten zone, using predoped rod, and reaction between molten zone and impurity vapor. Theoretical and experimental results for these methods are presented. The advantages for particular resistivity and impurity requirements are also discussed.

Abstract No. 106

Vibratory Polishing and Lapping of Semiconductor Materials

J. E. Cline and **S. J. Solomon,** Semiconductor Div., Raytheon Co., Newton, Mass.

The Syntron* vibratory polishing machine has been adapted for use in lapping of semiconductor materials and in polishing of device structures for metallographic examination. When conventional polishing techniques are used, alloyed semiconductor device structures present difficulties because of their small size, differing degrees of hardness, and brittleness of the semiconductor chip. It was found that the vibratory polisher in routine operation produces metallographic sections without scratches, rounding, or broken edges.

* Syntron Co., Homer City, Pa.

Abstract No. 107

Chemical Etching of Silicon, III. A Temperature Study in the Acid System

Harry Robbins and **Bertram Schwartz,** Hughes Products, Semiconductor Lab., Newport Beach, Calif.

Data showing the relationship between the etch rate of silicon and the temperature of the etchant are presented for several solutions composed of HF, HNO_3, H_2O, and $HC_2H_3O_2$. The activation energy of the reaction in solutions of various compositions is discussed in relation to the mechanism of the reaction.

Abstract No. 108

A Low Resistance Ohmic Contact for Silicon Semiconductor Devices

S. L. Matlow and **E. L. Ralph,** Hoffman Electronics Corp., Evanston, Ill.

A combination chemiplated and electroplated contact has been developed for use on silicon semiconductor devices. The chemiplating is done in an HF solution of $KAu(CN)_2$. The electroplating follow up can be with either a copper or gold solution. Data are given on the relationship between plating conditions and the resistance and bonding strength of the contact. A mechanism is proposed to explain the observed relationships.

Abstract No. 109

A Chemical Treatment for Rendering Silicon-Doped Aluminum Solderable

S. L. Matlow and **H. J. Gould,** Hoffman Electronics Corp., Evanston, Ill.

The use of aluminum alloying for making ohmic and rectifying contacts to silicon is well known in the art of the fabrication of silicon semiconductor devices. After alloying the aluminum is primarily in the form of the α-phase (silicon doped). The various aluminum fluxes and solders available commercially do not work well on the α-phase. A set of chemical dip treatments is reported which render the α-phase solderable and give a strong bond to the aluminum.

Abstract No. 110

Depletion Layer Calculations for the Design of Diffused Semiconductor Devices

H. Lawrence and **R. M. Warner, Jr.,** Bell Telephone Labs., Inc., Murray Hill, N.J.

Diffused junctions in semiconductors generally exhibit linearly graded behavior at low voltage and step behavior at high voltage as far as depletion layer properties are concerned. These properties have been calculated for wide ranges of voltage and diffusion parameters for the case of a complementary error function distribution. The results delineate the ranges for which the two aproximations are valid and supply data for the extensive transition range where neither approximation is satisfactory. Results were obtained by solving Poisson's equation for the stated distribution analytically and by solving the equation specifying field continuity at the junction with the aid of the IBM 704.

Abstract No. 111

Development of Damage-Nucleated Structures in Silicon by Highly Preferential Etching

P. R. Pennington and **J. D. Turner,** Hughes Products, Semiconductor Lab., Newport Beach, Calif.

Study of the rates of etch by certain caustic etches on oriented silicon surfaces has revealed the existence of exceptionally high etch preferentiality. The rate of etch in a [111] direction is only a small fraction of the rates in directions normal to [111]. Structures with precisely controlled orientation and geometry may be etched in silicon with these preferential etches, their positions being determined by deliberately including damaged regions on the silicon surface.

Abstract No. 112

Silicon Transistors and Device Fabrication Using Damage-Nucleated Etched Structures

W. P. Waters and **P. Walker,** Hughes Products, Semiconductor Lab., Newport Beach, Calif.

Preferential caustic etching can be used to produce the crystallographically oriented structures required for fabrication of semiconductor devices. Precisely controlled damage of the surface nucleates a structure with reproducible penetration. Size and geometry is determined by etch composition, etch time, and material orientation. Hexagonal, triangular, or rectangular pit forms and mesa structures are readily obtained. Hexagonal collector and emitter pits are used to produce webs of controlled one-half mil thickness. Silicon transistors are fabricated by aluminum evaporation.

Abstract No. 113

A New Technique for Controlling Germanium Meltback Transistor Characteristics

R. Jones and **R. H. Zimmerli,** General Electric Co., Electronics Park, Syracuse, N.Y.

The electrical characteristics of meltback transistors are determined by the impurity concentration and gradient in the physical structure. A special power control was developed which controls growth rate and time of growth accurately throughout the meltback cycle. Important electrical characteristics have been considerably improved as indicated by h_{FE} and higher power gain.

Abstract No. 114

A New Approach to Semiconductor Surface Reactivity

G. A. Wolff, U. S. Army Signal Research and Development Lab., Fort Monmouth, N.J.

A surface study by combined physical, chemical, and crystallographic means leads to the following conclusions. The structure of clean surfaces of Si, Ge, SiC, and other semiconductors differs from the bulk structure because of abnormal bonding of the surface atoms. The normal bonding state is largely restored when halogens, chalcogens, or certain IIIb, Vb metals react with the surface atoms, "anion" and "cation" faces in III-V and II-VI compounds, and their bonding state are identified.

Abstract No. 115

Theory of Surface Conductance in Semiconductors

D. R. Frankl, Research Labs., Sylvania Electric Products Inc., Bayside, N. Y.

The Schrieffer theory of mobility of carriers in the space-charge layer near the surface of a semiconductor has been extended by eliminating an approximation in the form of the potential. The results are thus valid for accumulation as well as inversion layers and for carriers repelled from as well as attracted to the surface. Numerical results are presented for germanium and silicon.

Abstract No. 116

P-Layers* on Vacuum Heated Silicon

J. T. Law, T. M. Buck, and **F. G. Allen,** Bell Telephone Labs., Inc., Murray Hill, N.J.

Chemical p-layers have been found whenever etched silicon samples are heated in a Pyrex vacuum system to temperatures above 1300°K. By controlled etching these layers were found to extend 2-6 μ into the bulk. Experiments are described which show that the acceptor impurity is boron, originating from the Pyrex glass envelope. By using a quartz system, these layers have been eliminated. The electrically active residual impurities at the surface from all other sources are less than 10^9 cm^{-2}.

* See F. G. Allen, *J. Phys. Chem. Solids*, **8**, 120 (1959).

Abstract No. 117

Surface Channel Studies on Silicon P-N Junctions

Raymond Solomon and **P. O. Johnson,** Semiconductor Lab., Hughes Aircraft Co., Newport Beach, Calif.

Surface channels on silicon junctions have been investigated with a chopped light probe. The phase shift of the induced a-c photocurrent, relative to a standard signal, is measured as a function of distance of the light spot from the junction. The total phase shift along the surface may be as great as 360° and varies with surface preparation and ambient condition. It is observed that channels up to 20 mil in extent can exist even though the surface is not inverted. The properties of these anomalous channels are discussed in detail.

Abstract No. 118

Diffusion in Silicon Carbide

Hung-Chi Chang and **L. F. Wallace,** Westinghouse Electric Corp., Materials Engineering Depts., Pittsburgh, Pa.

The diffusion of acceptor and donor elements into silicon carbide has been performed in an open-tube carrier-gas system at temperatures from 1600° to above 2000°C. Techniques have been developed for measuring the diffusion constants based on the p-n junction depth and resistivity changes. Diffusion constants of aluminum in α-SiC have been investigated more quantitatively and are given by $D_{Al} = 1.8 \exp(-113{,}000/RT)$ for the [0001] direction with an average estimated error of $\pm 50\%$.

Abstract No. 119

Surface Concentration of Indium in Germanium from Gaseous Diffusion

K. M. Busen, E. L. Meeks, and **G. A. Shirn,** Sprague Electric Co., North Adams, Mass.

Impurities are indiffused into germanium from the vapor phase, using a specially designed closed system. Correlations are established between the vapor pressure of the impurity and the concentration of the impurity on the germanium surface for various temperatures and times of the indiffusion cycle.

Abstract No. 120

Capillary Alloying: An Improved Alloying Method

K. M. Busen, J. J. Casey, Kurt Lehovec, and **A. C. Webb,** Sprague Electric Co., North Adams, Mass.

The alloying is done by placing a semiconductor wafer on the end of a capillary, and allowing the wafer to be in contact with a liquid metal or alloy contained in the capillary. The application of this procedure for diode and transistor technology is discussed and relations are given for calculating the alloying depth.

Abstract No. 121

Impurity Redistribution and Junction Formation in Silicon by Thermal Oxidation

M. M. Atalla and **E. Tannenbaum,** Bell Telephone Labs., Inc., Murray Hill, N. J.

In the process of growing an oxide on doped silicon, electrically active impurities near the Si/SiO_2 interface are redistributed depending on the diffusion coefficients and the distribution coefficient of the impurity between the oxide and the semiconductor. An analysis of this phenomenon predicts that single junction or two junction material can be obtained by oxidation of the surface of a compensated silicon crystal. For parabolic growth of the oxide, the surface concentration is independent of time, and the junction depth, gradient, and sheet resistivity vary with $t^{1/2}$. This has been demonstrated experimentally by oxidation of a compensated p-type silicon crystal doped with gallium and antimony.

Abstract No. 122

Metallurgical Analysis of the Bulk Diffusion Phenomenon in Silicon Power Transistors

P. X. Flaherty, Raytheon Co., Semiconductor Div., Newton, Mass.

In the analysis of bulk diffused silicon devices, it is necessary to use metallographic techniques other than conventional to determine basewidth thickness and junction condition. A bevel and stain technique in conjunction with the interferometric measuring methods has been employed successfully. Discussion of results and slides showing various facets of the bulk diffusion phenomenon are given.

Abstract No. 122A

Diffusion of Phosphorus into Silicon through an Oxide Layer

D. Kahng and **M. O. Thurston,** Electron Device Lab., The Ohio State University, Columbus, Ohio

The diffusivity of phosphorus in an amorphous silicon dioxide layer on silicon under oxidizing conditions has been measured as a function of temperature and phosphorus concentration. The results have been used to predict quantitatively the phosphorus distribution in silicon for the case in which the sample is as free of oxide as possible initially, and the oxide grows during the diffusion. Masking effects in preoxidized silicon are also discussed theoretically and experimentally.

ELECTRO-ORGANIC

Abstract No. 123

Application of Constant Potential Electrolysis to the Process for Electrolytic Formation of Hydrazobenzene in Alkaline Emulsion. Mechanism for the Processes at Soluble and Insoluble Cathodes

Taro Sekine, Tadashi Seki, and **Kiichiro Sugino,** Lab. of Organic Electrochemistry, Dept. of Chemical Engineering, Tokyo Institute of Technology, Ookayama, Meguro-ku, Tokyo, Japan

To verify the proposed mechanism for hydrazobenzene formation at soluble cathode, constant potential electrolysis was carried out for each step of the reduction at Ni and Zn cathodes. At Ni, azoxybenzene and azobenzene could be reduced at about −1.25 v, (vs. S.C.E.) to hydrazobenzene, although the rate of the latter was very slow. At Zn, these reductions took place very smoothly at $-1.50 \sim -1.57$ v, at which the deposition of Zn^{++} ion occurs. The results in alcoholic alkaline solution are given for reference.

Abstract No. 124

Preparation of Crossed-Pinacols by Cathodic Reduction

M. J. Allen and **W. Pierson,** Research Dept., CIBA Pharmaceutical Products Inc., Summit, N.J.

The preparation of various crossed-pinacols by cathodic reduction of equimolar mixtures of two aromatic ketones is described. Also to be discussed is the apparent effect of the reference potential at the working electrode on the yield of crossed-pinacol.

Abstract No. 125

Kolbe Decomposition Potentials by Condenser and Ballistic Galvanometer

G. W. Thiessen and **F. F. Rawlings,** Monmouth College, Monmouth, Illl.

Decomposition potentials were determined for water and pyridine with Kolbe and other electrolytic solutes. Accepted values for non-Kolbe and Kolbe systems in water were obtained with no perceptible difference between uninhibited acetate and inhibited benzoate. Evidence of a preliminary solvent process was found for aqueous systems. Pyridine revealed no solvent process and a higher decomposition potential for benzoate than acetate. Benzoate can be Kolbe discharged in pyridine. Consistent mechanisms for aqueous and nonaqueous Kolbe systems are presented.

Abstract No. 126

Electrolytic Formation of Oximes

Tadao Hayashi, Dept. of Chemistry, Ohio State University, Columbus 10, Ohio, and **C. L. Wilson,** Cranberry Lake, Sloatsburg, N.Y.

Reduction of an aqueous mixture containing an aliphatic or cycloaliphatic ketone and an inorganic nitrite

or nitrate gave good yields of the ketoxime. Optimum conditions which gave yields of up to 70% are: pH 5.0, temperature, preferably below 15°, nitrite concentration of about 10%, and a rotating zinc cathode. Ketones used include acetone, methyl ethyl ketone, methyl isobutyl ketone, cyclopentanone, and cyclohexanone. Acetophenone gave no oxime and the reasons are discussed.

Abstract No. 127

The Stereo Selective Electrochemical Reduction of Nonconjugated Steroidal Ketones and Alpha Ketols

Peter Kabasakalian, Alvin Basch, James McGlotten, and **Milton Yudis,** Schering Corporation, Bloomfield, N.J.

Electrochemical reduction of a number of nonconjugated nuclear ketones at a stirred mercury cathode afforded the equatorial epimeric alcohol with a high degree of stereospecificity and in good yield comparable to reduction with sodium in alcohol. With α-hydroxy or acetoxy ketols. the hydroxyl function was cleaved reductively and the ketone reduced to an alcohol. Stereospecific reduction did not occur for the C_{20} side chain ketones but 50 to 70% of the C_{20} β-epimer was formed. The stereochemistry of electrochemical reduction of steroidal ketones is compared with chemical methods.

Abstract No. 128

Electrochemical Research in India and Japan

M. J. Allen, Research Dept., CIBA Pharmaceutical Products, Inc., Summit, N.J.

The Central Electrochemical Research Institute, in Karaikudi, India will be described together with a resumé of the basic and developmental research being done at this Institute. A discussion of the electrochemical work at Tokyo Institute of Technology and Kyoto University will also be presented. Also to be included is a description of the excellent instrumentation available in Japan for polarographic research. A film covering the trip will be shown.

Abstract No. 129

Polarographic Reduction of Some Acetylenic Linkages

A. H. Gropp and **J. C. Ramsey, Jr.,** Dept. of Chemistry, University of Florida, Gainesville, Fla.

Two series of unsaturated quaternary ammonium salts were prepared, each compound containing an acetylenic linkage. In one series the unsaturated group was held constant and the saturated groups varied; in the other series the saturated groups were held constant and the unsaturated group lengthened. It was found that increasing the size of the saturated groups lowered the polarographic reduction potential, while lengthening the unsaturated group increased the reduction potential.

Abstract No. 130

Polarographic Reductions of Benzyl Halides

L. W. Marple, L. E. I. Hummelstedt, and **L. B. Rogers,** Dept. of Chemistry and Laboratory for Nuclear Science, Massachusetts Institute of Technology, Cambridge 39, Mass.

The polarogram for benzyl chloride in a supporting electrolyte of lithium chloride has a dip in the limiting current due to electrostatic repulsion from the interface of the monovalent anion produced by electron transfer. The dip is decreased by the presence of electronegative substituents on the ring and is eliminated by a moderate concentration of surface-active tetramethylammonium ions in the solution.

Benzyl bromide and iodide each undergo two one-electron reduction steps. At concentrations greater than 10^{-4} M, adsorption phenomena arising from the reduction product, dibenzyl, are encountered.

Abstract No. 131

Polarography in Formamide, I. Some Transition Metal Ions, Zinc and Cadmium Ions

G. H. Brown and **Hsiao-shu Hsiung,** Dept. of Chemistry, University of Cincinnati, Cincinnati, Ohio

Polarographic data of certain transition metal ions, cadmium and zinc in formamide, have been obtained. The half-wave potentials (against a S. C. E.) were determined as follows: Cr −1.56, Mn −1.57, Fe −1.40, Co −1.20, Ni −0.98, Cu −0.12, Zn −1.07, Cd −0.69. All of these half-wave potentials were taken using 0.2M sodium perchlorate as the supporting electrolyte. Diffusion current constants of the ions studied in formamide were relatively small compared with other solvents; the difference is due mostly to the high viscosity of formamide.

Abstract No. 132

Polarographic Studies in Dimethylformamide VI. Reduction of Polyhalogenated Hydrocarbons

Stanley Wawzonek and **R. C. Duty,** Dept. of Chemistry, State University of Iowa, Iowa City, Iowa

The stability of carbanion intermediates in dimethylformamide suggested a study of the polarographic reduction of polyhalogenated hydrocarbons to determine whether carbenes would be formed as intermediates. Carbon tetrachloride was the only compound found to give a polarographic behavior which suggested the formation of a carbene. Three waves were obtained representing a reduction to chloroform, methylene chloride, and methyl chloride, respectively. The first wave was higher than the second and suggested the following steps.

$$CCl_4 + 2e \rightarrow :CCl_3 + Cl^-$$
$$:CCl_3 \rightarrow :CCl_2 + Cl^-$$
$$:CCl_2 + 2e \rightarrow :\ddot{C}Cl_2$$
$$:\ddot{C}Cl_2 + \text{solvent} \rightarrow CH_2Cl_2$$

Abstract No. 133

Millicoulometric Determination of Polarographic n-Values

Thos. De Vries, Dept. of Chemistry, Purdue University, Lafayette, Ind., and **J. L. Kroon,** Dow Chemical Co., Midland, Mich.

The microcoulometer, previously described, was used to determine polarographic n-values. The microcells held 0.3 - 0.7 ml of solution and the electrolysis time varied from 60 to 240 min. A dropping mercury electrode, with silver-silver chloride or silver iodide as reference electrode, was used. For aqueous solutions of 0.001M saccharin and hydrochloric acid as supporting electrolyte, an average n-value of 3.92 was obtained. The carbonyl and not the sulfanomide group of the molecule is reduced. For tetraiodophthalic anhydride in a buffered solution also containing 20% dimethylformamide, an average n-value of 8.0 was obtained, corresponding to the fission of the carbon-iodine bonds. For 2,2-dinitropropane in anhydrous ethyl alcohol, n-values of 1.4 to 2.2, instead of 4, were obtained. Apparently an intermediate compound, formed during the reduction step, is reoxidized at the anode to give the low results.

Abstract No. 134

Polarographic Reduction of Some Diketones

R. L. Flurry and **R. A. Day, Jr.,** Chemistry Dept., Emory University, Atlanta 22, Ga.

The polarographic reduction of p-diacetylbenzene, dibenzoylmethane, m-dibenzoylbenzene, 1,8-dibenzoylnaphthalene, 1,4-dibenzoylbutane has been studied in buffered ethanol-water solutions over a pH range of 2 to 13. Coulometric determinations of the number of electrons consumed under various conditions were run. Several products have been prepared by controlled potential electrolysis, and an attempt to explain the mechanism of reduction of these compounds is presented.

Abstract No. 135

Polarographic Reduction of Nonconjugated Steroidal Ketones

Peter Kabasakalian and **James McGlotten,** Schering Corp., Bloomfield, N.J.

The direct polarographic reduction of nonconjugated ketones in various positions both on the nucleus and the side chain of a steroid molecule has been carried out successfully. The polarographic reduction of hydroxyl

and acetoxyl groups alpha to a carbonyl group is reported for the first time. The reduction wave of these groups in 20-ketosteroids merged with the reduction wave of the carbonyl group. In contrast, two distinct polarographic reduction waves were obtained with 16-hydroxy (or acetoxy)-17-ketosteroids.

Abstract No. 136

Electrolytic Reduction of Some Alkylnitrosamines

G. C. Whitnack, R. D. Weaver, and **H. W. Kruse,** Chemistry Div., Research Dept., U. S. Naval Ordnance Test Station, China Lake, Calif.

Polarographic reduction studies of some alkynitrosamines have been made in acidic, neutral, and alkaline solutions. Diffusion controlled waves were obtained and the mechanism of reduction is discussed. Data indicate that the course of reduction depends on pH and is rather complex in strong mineral acid. Good yields (50-75%) of 1,1-disubstituted hydrazines were obtained by large-scale electrolyses at a mercury cathode. Ammonia, alkylamine, nitrous oxide, and nitrogen were established as additional products of the reduction.

Abstract No. 136A

Rotating Cathode-Type Cell for the Preparation of Benzidine

K. S. Udupa, G. S. Subramanian, and **H. V. K. Udupa,** Central Electrochemical Research Institute, Karaikudi 3, S. India

The paper describes the work on the reduction of nitrobenzene in alkaline medium using rotating cathode. Conditions of electrolysis are similar to those established by Day and co-workers except that the reduction has been carried out employing higher current densities of the order of 15-20 amp/dm^2 as compared to 2 amp/dm^2. The reduction proceeds quite smoothly and almost quantitative yield of hydrazobenzene is obtained. A rotating disk-type m.s. cathode has been used along with cylindrical diaphragm of asbestos cloth supported on m.s. cage as anode chamber. The best conditions are (*a*) 10-20% alkali (NaOH) as catholyte and anolyte, (*b*) a depolarizer ratio of (w/v) 1:4, (*c*) current density of the order of 15-20 amp/dm^2, (*d*) temperature between 80°-85°C, (*e*) addition of 1% (w/v) of PbO to the catholyte. The paper also deals with the method of isolation and recovery of the product and subsequent conversion to benzidine.

ELECTROTHERMICS AND METALLURGY

Abstract No. 137

Refractory Ceramic Coatings Today and Tomorrow

F. D. Shaw, Bettinger Corp., Milford, Mass.

This paper presents a review of present-day refractory coatings for protecting metals against oxidation erosion and abrasion at elevated temperatures. The more promising "super refractories" (carbides, nitrides, borides, and intermetallic cermets) are considered with respect to current developments in coating technology.

Abstract No. 138

The Adhesion of Vitreous Oxide Coatings to Metals

B. W. King and **W. H. Duckworth,** Battelle Memorial Institute, 505 King Ave., Columbus, Ohio

Results of an investigation of the fundamentals of the adherence of glasses to metals are presented. A distinction is made between the conditions essential for adherence and the phenomena related to adherence. Surface roughness was found not to be essential but to improve the apparent adherence when the bond was relatively weak. A theory is presented for the adherence of glasses to metals.

Abstract No. 139

A Liquid Phase Coating for Refractory Metals

G. D. Oxx, Jr., and **L. F. Coffin, Jr.,** Research Lab., General Electric Co., Schenectady, N.Y.

The concept of using a phase that is liquid at service temperatures as a component of coatings for refractory metals has been described. The liquid, an alloy of gold and silicon, is retained on a molybdenum surface by a capillary system made of molybdenum disilicide. The coating has the advantage of good thermal shock and has a self-healing characteristic.

Abstract No. 140

Testing Procedures for Evaluation of Coated Materials

J. L. Harp and **J. M. Allen,** Battelle Memorial Institute, 505 King Ave., Columbus 1, Ohio

Recent developments in aeronautics have focused attention on the behavior of materials under conditions of high heat flux and high temperature. Materials of interest must be protected from erosion and oxidation when exposed to a flow of high-temperature air; these materials and their coatings both must be thermal-shock resistant. Evaluation of bare and protected materials as heat sinks in rocket-motor tests indicates that electrodeposited and flame sprayed coatings appear to be the most successful.

Abstract No. 141

Problems of Applying Metallic Coatings to Nonmetallic Bases

S. W. Bradstreet, Armour Research Foundation, Technology Center, Chicago 16, Ill.

(No abstract received)

Abstract No. 142

Coating Uranium Dioxide Powders with Metallic Films

J. H. Oxley, J. F. Hannah, and **J. M. Blocher, Jr.,** Battelle Memorial Institute, 505 King Ave., Columbus Ohio, and **I. E. Campbell,** National Steel Corp., Weirton, W. Va.

Conditions for tungsten coating of uranium dioxide powders by hydrogen reduction of tungsten hexachloride in a fluidized bed of the powder product have been established. The coated material should contain approximately 20 wt % tungsten to obtain essentially complete coverage of micron-sized uranium dioxide. The use of mechanical vibration was found to be necessary to obtain a satisfactory coating. Metals other than tungsten can be deposited on uranium dioxide powder particles and a number of such coated powders are now being explored for nuclear fuel applications.

Abstract No. 143

Silicon Carbide Coatings on Graphite Paper

J. G. Kemp, National Carbon Co., Fostoria, Ohio

(No abstract received)

Abstract No. 144

Metal-Ceramic Coatings for Protection of Graphite

W. L. Aves, Chance Vought Aircraft Co., Dallas, Texas

(No abstract received)

Abstract No. 145

Inorganic Coatings for Leading Edges of Boost-Glide Vehicles

H. A. Pearl, Bell Aircraft Co., Buffalo, N.Y.

(No abstract received)

Abstract No. 146

Coatings for Structural Aircraft Materials

D. H. Leeds, Douglas Aircraft Co., Santa Monica, Calif.

(No abstract received)

Abstract No. 147

Refractory Coatings for Ramjet and Supersonic Aircraft Applications

S. Sklarew, Marquardt Aircraft Co., Van Nuys, Calif.

(No abstract received)

Abstract No. 148

Protective Coatings for Medium Temperature Ranges

A. R. Stetson, Solar Aircraft Corp., San Diego, Calif.

(No abstract received)

Abstract No. 149

Reactions in the Niobium-Hydrogen System

W. M. Albrecht, W. D. Goode, and **M. W. Mallett,** Battelle Memorial Institute, 505 King Ave., Columbus, Ohio

Equilibria and elevated-temperature x-ray studies show that a solid solution of hydrogen in niobium is produced throughout most of the system. A miscibility gap was found at low temperatures and pressures with a critical point at about 140°C, 0.01 mm of mercury hydrogen pressure, and 0.3 H/Nb. Sorption rates at 300° to 550°C were initially linear. At higher temperatures, sorption rates were controlled by diffusion in the metal matrix. Diffusion coefficients at 600° to 700°C can be expressed by:

$$D = 0.0215 \exp [\ (-9370 \pm 600)/RT]$$

Desorption rates were slower than those predicted by diffusion.

Abstract No. 150

A Study of the Iodide Niobium Process

R. F. Rolsten, Eastern Lab., E. I. du Pont de Nemours and Co., Inc., Gibbstown. N.J.

It was established that the rate of deposition of niobium by the thermal decomposition of niobium iodides can be expressed in units of moles of niobium deposited per unit length of a decomposition element per unit of time. The rate of deposition of niobium was studied for deposition temperatures from 750° to 1100°C, feed temperatures from 240° to 470°C, and with grades of crude niobium having different surface areas.

Abstract No. 151

The Behavior of Rhenium in Electron Tube Environments

G. B. Gaines, C. T. Sims, and **R. I. Jaffee,** Battelle Memorial Institute, Columbus, Ohio

Rhenium, tungsten, and rhenium-coated tungsten have been exposed to carburizing atmospheres and to water-cycle attack, rhenium and tungsten to aluminum oxide at 1750°C for 7000 hr, and rhenium to boron-containing atmospheres. It was confirmed that rhenium, unlike most other refractory metals, does not form a carbide. Rhenium forms a boride, which forms a eutectic with another boride, or with rhenium, and melts under 2250°C. Thoriated rhenium maintains microstructural and mechanical integrity after long exposure in vacuum at 1750°C in contact with alumina. Rhenium and rhenium-coated tungsten are highly resistant to water-cycle effects.

INDEX TO AUTHORS

(The number in the right hand column is the abstract number used in the Technical Program and in the Abstracts.)

	Abstract No.
Albrecht, W. M.	149
Alderuccio, C. L.	80
Allen, F. G.	116
Allen, J. M.	140
Allen, M. J.	124, 128
Amlie, R.	11
Angstadt, R. T.	22
Arnold, E.	95
Atalla, M. M.	121
Aves, W. L.	144
Bartlett, J. H.	70, 71
Basch, Alvin	127
Bate, R. T.	85
Bauman, H. F.	7
Bergishagen, Finn	82
Black, J.	95
Blocher, J. M., Jr.	142
Bockstie, L.	17
Boudart, M.	59
Boyd, H. J.	78
Bradstreet, S. W.	141
Brattain, W. H.	42
Brenner, Abner	65, 75
Breslin, J. T.	91
Bride, J. E.	81
Brodd, R. J.	5
Brown, G. H.	131
Bruins, P. F.	26
Buck, T. M.	47, 116
Burbank, Jeanne	12
Busen, K. M.	119, 120
Button, M. J.	96
Cabrera, N.	46
Cahan, B. D.	11, 22
Cahoon, N. C.	1, 4, 9
Campbell, I. E.	142
Caplan, D.	35
Casey, J. J.	120
Champness, C. H.	92
Chang, Hung-Chi	118
Chessin, H.	80
Cline, J. E.	106
Coffin, L. F., Jr.	139
Cohen, M.	35, 36
Couch, D. E.	65
Davenport, W. H.	38
Day, R. A., Jr.	134
DeCrescente, M. A.	37
de la Bretèque, Pierre	104
DeLap, J. H.	6
De Vries, J.	15
De Vries, Thos.	133
Dewald, J. F.	50
DeWane, H. J.	2, 5
Dirkse, T. P.	13, 14, 15
Ditzenberger, J. A.	103
Dodson, V. H.	21
Draley, J. E.	31
Duckworth, W. H.	138
Duty, R. C.	132
Eischens, R. P.	60
Eisenberg, M.	7
Engell, H. J.	51
Falk, S. Uno	27
Farnsworth, H. E.	45
Faust, C. L.	81
Faust, J. W., Jr.	54
Fink, M. S.	89
Fischler, A. S.	101
Flaherty, P. X.	122
Flannery, R. J.	66
Flurry, R. L.	134
Francis, H. T.	79
Frankl, D. R.	115
Gaines, G. B.	151
Gale, R. H.	37
Garrison, W. E., Jr.	64
Gatos, H. C.	58, 96
Gaule, G. K.	91
Gerischer, H.	49
Giles, F. H., Jr.	70, 71
Gillet, I. E.	67
Gilman, J. J.	48
Glicksman, R.	19, 20
Goode, W. D.	149
Gould, H. J.	109
Graham, A. H.	77
Graham, A. K.	78
Green, Milton	88
Greenberg, I. N.	88
Greenberg, Sherman	31
Gropp, A. H.	129
Gurklis, J. A.	81
Gwathmey, A. T.	62
Hackerman, Norman	55
Handler, Paul	44
Hannah, J. F.	142
Harman, T. C.	97
Harp, J. L.	140
Hartley, A. M.	64
Harvey, A.	35
Hauffe, K.	61
Hayashi, Tadao	126
Holmes, M. R.	82
Hsiung, Hsiao-shu	131
Hummelstedt, L. E. I.	130
Jaffee, R. I.	151
Jenkins, L. H.	39
Johnson, P. O.	117
Johnson, R. S.	1
Jones, E. L.	23, 24
Jones, R.	113
Juretschke, H. J.	43
Kabasakalian, Peter	127, 135
Kahng, D.	122A
Kalhammer, F.	16
Kaminsky, George	93
Katz, M. J.	89
Kemp, J. G.	143
King, B. W.	138
King, C. V.	57
Kohan, L. R.	79
Kolb, K. E.	63
Kordesch, K.	10
Kornfeil, Friedrich	3
Korver, M. P.	1
Krivanek, F. J.	4
Kroon, J. L.	133
Kruse, H. W.	136
Lacombe, Paul	52
Lander, J. J.	25
Lasser, M.	16, 17
Lavine, M. C.	96
Law, J. T.	116
Lawless, K. R.	62
Lawrence, H.	110
Lee, C. A.	93
Leeds, D. H.	146
Lehovec, Kurt	120
Lichter, B. D.	29
Lippincott, T. W.	63
Lorking, K. F.	74
Loverude, T. H.	18
Lozier, G. S.	8
Lumley, E. J.	84
Lyons, V. J.	100
MacDonald, A. L.	105
Maier, H. B.	68
Makrides, A. C.	33, 34

	Abstract No.
Mallett, M. W.	149
Mark, H. B. Jr.	6
Marko, A.	10
Marple, L. W.	130
Marvel, C. S.	64
Mason, D. R.	102
Matlow, S. L.	108, 109
McGlotten, James	127, 135
McGraw, L. D.	81
Meeks, E. L.	119
Morehouse, C. K.	8, 19
Nelson, E. E.	25
Newton, E. H.	73
Nole, V. F.	38
Ockerman, J. B.	11
Olshefski, P. J.	86
Oxley, J. H.	142
Oxx, G. D., Jr.	139
Pastore, J. R.	91
Paquin, R. A.	76
Pearl, H. A.	145
Pennington, P. R.	111
Petrocelli, J. V.	56
Pierson, W.	124
Pinkerton, H. L.	78
Pochop, C. G.	91
Powell, A. S.	37
Rairden, J. R.	30
Ralph, E. L.	108
Ramsey, J. C., Jr.	129
Rawlings, F. F.	125
Read, H. J.	77
Reese, W. E.	101
Reynolds, D. C.	98
Robbins, Harry	107
Robertson, W. D.	38
Rogers, L. B.	130
Rolsten, R. F.	150
Rothberg, M.	87
Rosenberg, A. J.	94
Rüetschi, Paul	11, 22
Ruther, W. E.	31
Ryan, N.	84
Salkind, A. J.	26
Santoro, P. F.	37
Saubestre, E. B.	69
Schaefer, H. F.	9
Schwartz, Bertram	107
Seiger, H. N.	28
Seki, Tadashi	123
Sekine, Taro	123
Sewell, P. B.	36
Shaw, F. D.	137
Sherwood, G. R.	82
Shirn, G. A.	119
Shombert, D. J.	85, 86
Shuttleworth, R. A.	91
Silvestri, V. J.	100
Silvey, G. A.	100
Simon, A. C.	23, 24
Sims, C. T.	151
Sklarew, S.	147
Solomon, Raymond	117
Solomon, S. J.	106
Soule, D. E.	90
Stern, Milton	32, 33, 40, 41
Stetson, A. R.	148
Stockbridge, C. D.	36
Strauss, A. J.	99
Struthers, J. D.	103
Subramanian, G. S.	136A
Sugino, Kiichiro	123
Sullivan, F.	73
Swann, Sherlock, Jr.	64
Tannenbaum, E.	121
Thiessen, G. W.	125
Thomas, J. E. Jr.	66
Thomassen, Lars	102
Thurston, M. O.	122A
Tragert, W. E.	30
Trivich, D.	66
Turner, D. R.	53
Turner, J. D.	111
Turner, W. J.	101
Udupa, H. V. K.	136A
Udupa, K. S.	136A
Vosburgh, W. C.	6
Waber, J. T.	34A
Wagner, Carl	29
Wales, C. P.	12
Walker, P.	112
Wallace, L. F.	118
Wang, E. Y.	105
Ward, J. W.	34A
Warner, R. M., Jr.	110
Warschauer, D. M.	98
Waters, W. P.	112
Wawzonek, Stanley	132
Weaver, R. D.	136
Webb, A. C.	120
Weil, Rolf	76
Weingarten, I. R.	85, 86, 87
Weissberger, S.	95
Whelan, J. M.	103
Whitnack, G. C.	136
Wiers, Brandon	13
Wilson, C. L.	63, 126
Wissenberg, Herman	40, 41
Wolff, G. A.	114
Wood, G. B.	83
Woodberry, P. T.	72
Yudis, Milton	127
Zaromb, S.	16, 17
Zimmerli, R. H.	113

Feature Section

A Short Survey of the Status of the Society

Presidential Address*

Sherlock Swann, Jr.

I should like first to tell you how happy I am to be back with you again after missing the last three meetings, and to express my deep appreciation to those who carried on for me, particularly to Dr. Hackerman, our Past President, and Dr. Gardiner, our new President.

We are meeting for the seventh time in Philadelphia, the city of our foundation. The preliminary meeting in 1901 and that at which the Society was founded in 1902 have been described several times in presidential addresses, but a few remarks may still be appropriate. President Hering stated in his address at the Philadelphia Meeting in 1907 that the Society was founded as a result of discussions on electrochemistry by three of the Charter Members in Philadelphia. Obviously, these three talked to three more, as the original invitation to the preliminary meeting was sent out by six of the Charter Members. Let us say that since that time the members of The Electrochemical Society have talked a lot of electrochemistry. It was thought that a society could be founded with seventy-five members, but the response was far greater than expected. Three hundred and thirty-seven pledges of membership were obtained from thirty-eight states and eight foreign countries.

At this point, I should like to extend a greeting to our foreign visitors, whom we have always welcomed as members. Until 1915, some were on the Membership Committee. Guye and Haber served for many years, others for shorter terms. At one time, Dr. Morral, when he was at Purdue University, prepared Spanish abstracts of our preprints, particularly for the South American countries. Drs. Sõllner, Jacquet, de Nora, and Simnad have held the Society's Weston Fellowship for research. Due to insufficient funds, the fellowship was discontinued but we hope to replace it as soon as possible by the Consolidated Fellowship, and may I say that the time for the granting of this fellowship has been considerably shortened by recent gifts. I have not classified our members from Canada as foreign. They have attended many meetings and have been active in the affairs of the Society since its foundation. The Society was made international in 1930 by incorporation as The Electrochemical Society.

I mentioned before that there were three hundred and thirty-seven Charter Members, about eighteen of whom were from other countries. We now have a total slightly in excess of three thousand members, about three hundred and seventy-five of whom are from other countries. Not long ago, I was talking to a colleague who pointed out to me the fact that The Electrochemical Society was the only small independent chemical society in this country. This caused me to wonder, as it has others before me, why we have been successful. I believe that there are several reasons. The first one that comes to mind is our diversity.

Electrochemistry is a very broad subject. As President Thurnauer said of the Society in 1957, we are not large but our activities are complex. In carrying out research in electrochemistry, general knowledge is of the utmost importance. My own field of electro-organic, for example, bears close resemblance to the general chemistry of the late nineteenth century. General knowledge is most easily acquired in discussions with those in related fields. Membership in our Society makes such discussion easy. I can remember that, when the Bylaws of our Division were being written, we set our symposium date for the fall to coincide with that of the Electrodeposition Division because of the close relationship between the two fields. In the past when the Society was much smaller and single instead of simultaneous sessions were held, it was possible to listen personally to papers in all fields of electrochemistry and over the years to know the speakers well. This is not true to the same extent any longer, but it is still relatively easy to find the speaker in whose work you are interested.

Electrochemistry is a broad field in another way. President Faust in 1951 called attention to the fact that when the Society was founded the educational qualifications of the American Chemical Society kept out many engineers interested in electrochemistry. Some years ago, I had found that some of our members were not members of the American Chemical Society, but had assumed the number to be small. This apparently is not the case. In comparing samples of the directories of the two societies published in 1956, I found that the number of our members who do not belong to the American Chemical Society is considerable. This may be explained by the fact that they need not be chemists or chemical engineers but they must have had training in one of the natural sciences. I also was interested in the nature of our membership. In 1907, C. F. Burgess, in discussing the Presidential Address of Carl Hering (in those days presidential addresses were open for discussion), said that it was his impression that seventy to eighty per cent of our members were in industry. President W. C. Moore said in his address in 1947 that when he attended a meeting of the Society in 1914 he found that he was among industrial men. Due to the greatly increased interest in theoretical electrochemistry, I had thought that the percentage of members in academic positions had increased markedly, but, again, I was wrong. Some figures on the registration at the Spring Meeting in New York last year give an indication of the type of our membership: about eighty-three per cent industrial, ten per cent academic, and seven per cent government. In addition, I found in a sample from our 1956 directory that our membership was predominantly industrial. The nature of our membership has, then, not changed over the years.

Although its interests are broad in scope, the Society is individual in character. Several times in its history, the possibility of becoming associated with another society has been brought up but has always been rejected. One instance of historical importance took place at the Philadelphia Meeting in 1907. President Hering in his address brought up a proposal by W. A. Noyes for the American Chemical Society, that all papers on physical and electro- chemistry read before either society be combined in one monthly publication to be in

* Delivered at the Philadelphia Meeting, May 5, 1959.

the charge of one publication board and that the *Journal of Physical Chemistry* be combined with this new publication. I might mention that at that time the *Journal of Physical Chemistry* was edited by Wilder D. Bancroft, one of our Charter Members, and Joseph E. Trevor. In the discussion that followed, which I have mentioned previously, it developed that the new journal was to be the sole publication of the Society. It was agreed that we could save money, but it was felt, particularly by C. F. Burgess and L. J. Kahlenberg, that if we accepted this proposal we would lose our individuality. Burgess said further that he was afraid that papers accepted for the new journal would be too theoretical for our membership. Since that time, as I pointed out earlier, our interests have become more theoretical, but we still maintain a balance with the applied.

I want to say something now about the structure and management of the Society. Beginning in 1938, far-reaching changes were initiated and have continued over the years. To assist in financing, Sustaining Memberships and, later, Patron Memberships were established. I might say that the idea of corporation memberships was not a new one. It was suggested by President Kruesi in his address in 1929. We now have one hundred and sixteen Sustaining Members and five Patron Members. This still is not a true representation of the support that we are receiving from the industry, as many of the companies have taken out multiple memberships. We greatly appreciate this support. At the same time, it gives us confidence that our operation is successful. Besides corporation membership, we now have an Advisory Panel to take care of our investments, which have prospered well. We have changed from the semiannual TRANSACTIONS, and the BULLETIN, to a monthly JOURNAL in which we accept advertising just as we did before 1916. The sales of the JOURNAL are considerable. As President Udy said in 1955, the Society has become a rather big business. The present management is more functional than it was. For many years, the Board of Directors was composed of the President, the immediate Past President, six Vice-Presidents, nine Managers, the Treasurer, and the Secretary. Vice-President and Manager were just titles given to members elected to the Board. No particular duties were involved. The number of Vice-Presidents has been reduced to three, with definite duties, and the office of Manager eliminated. The three Vice-Presidents are members of the Ways and Means Committee of seven. There have been Ways and Means Committees before, but there is no mention of them in the Bylaws under which the Society operated at that time. It is stated in the present Bylaws that this committee shall act as an advisory group to the President and Board of Directors on all phases of the Society's business. As the Board grows, it will become increasingly necessary to refer matters to committees for recommendation. The other officers have been replaced by two members of the Council of Local Sections and the Chairmen of the separate Divisions.

I should like to show you how the Local Sections and Divisions have grown in importance. The first Local Sections were formed in 1907 in Wisconsin, Philadelphia, and New York. I might say that a large segment of the Wisconsin Section was made up of the faculty of the University of Wisconsin. There are now eighteen Local Sections and another in formation. The first Divisions, those of Electrothermics and Electrodeposition, were formed in 1922. Before that time, the fields of interest of the Society were represented by so-called Technical Committees. There are now nine Divisions which are responsible for the technical programs at the meetings of the Society. I can remember well when symposia were arranged by the Board of Directors. The question of what we should discuss would be brought up. Somebody would say that we had not heard about a certain subject for a long time and we would then agree to have a symposium on it. It is now in the divisional bylaws that symposia are to be held at regular intervals, as I indicated earlier. As an example of the importance of the activities of the Divisions, the symposia at this meeting [Philadelphia, 1959] on Electrode Processes and on Liquid Dielectrics are being supported by agencies of the government. In this connection, I should like to mention some remarks by President Lidbury in his address in 1915. He said that it was likely that we would come more frequently into contact with agencies of a constructive nature, of which the scientific bureaus of the government are typical, that they do a great work and that our respect and admiration of it is likely to be proportional to our knowledge of it, that their primary purpose coincides with our own, the assistance of the application of knowledge to industry. President Lidbury obviously was not referring to the situation which exists today, but his statement is nonetheless prophetic.

Other changes which show the growth of the Society are in the Editorial Board and in the establishment of our New York office, now headed by an Executive Secretary, Mr. Robert K. Shannon, who very kindly supplied me with some of the data that I have given you. For a long time, the Publication Committee was made up of a Chairman and several other members. The different fields of activity of the Society were not necessarily represented. I believe that the Secretary was the only editor. Colin G. Fink acted in that capacity for many years. There was no office of the Society in the present sense. There is now an Editorial Staff, representing different departments, headed by the Chairman of the Publication Committee. The former Publication Committee has been replaced by the Technical Editor assisted by editors representing the separate Divisions. Again, the management of the Society has become more functional.

I should like to conclude by saying, as others have said before me, that the Society offers far more than science and technology. The first meeting that I attended was held in Bridgeport, Conn., in 1928. I went with Dr. W. C. Moore, who had previously persuaded me to become a member. I knew immediately that I was interested in the Society. That interest was not due to the papers that I listened to. There was nothing strictly electro-organic on the program. I believe that it was due to the enthusiasm of the group and the fact that I was made to feel that I belonged. As I continued to attend meetings, it was easy to form friendships, many of them quite by accident, such as finding myself with some kindred spirits at one of the Society's functions or sitting next to somebody on a bus to be taken on a plant trip. I recommend highly to the newer members and guests of the Society that they attend its functions.

We have grown and are growing in numbers and in fields of interest. In this growth, it is absolutely essential to have unity. President Veasey in 1947 urged that special groups be supported, encouraged, and enlarged, but that these groups get behind the Society and make sure that it enlarges its borders and remains a most healthy tree trunk from which all branches can radiate in perfect coordination. In the preliminary meeting in 1901 before the founding of the Society, a motion was made to spell the name Electrochemical with a hyphen, Electro-Chemical. This was defeated, twenty-nine to twenty-one. Let us keep things this way.

A Short Survey of the Status of the Society

Presidential Address*

Sherlock Swann, Jr.

I should like first to tell you how happy I am to be back with you again after missing the last three meetings, and to express my deep appreciation to those who carried on for me, particularly to Dr. Hackerman, our Past President, and Dr. Gardiner, our new President.

We are meeting for the seventh time in Philadelphia, the city of our foundation. The preliminary meeting in 1901 and that at which the Society was founded in 1902 have been described several times in presidential addresses, but a few remarks may still be appropriate. President Hering stated in his address at the Philadelphia Meeting in 1907 that the Society was founded as a result of discussions on electrochemistry by three of the Charter Members in Philadelphia. Obviously, these three talked to three more, as the original invitation to the preliminary meeting was sent out by six of the Charter Members. Let us say that since that time the members of The Electrochemical Society have talked a lot of electrochemistry. It was thought that a society could be founded with seventy-five members, but the response was far greater than expected. Three hundred and thirty-seven pledges of membership were obtained from thirty-eight states and eight foreign countries.

At this point, I should like to extend a greeting to our foreign visitors, whom we have always welcomed as members. Until 1915, some were on the Membership Committee. Guye and Haber served for many years, others for shorter terms. At one time, Dr. Morral, when he was at Purdue University, prepared Spanish abstracts of our preprints, particularly for the South American countries. Drs. Söllner, Jacquet, de Nora, and Simnad have held the Society's Weston Fellowship for research. Due to insufficient funds, the fellowship was discontinued but we hope to replace it as soon as possible by the Consolidated Fellowship, and may I say that the time for the granting of this fellowship has been considerably shortened by recent gifts. I have not classified our members from Canada as foreign. They have attended many meetings and have been active in the affairs of the Society since its foundation. The Society was made international in 1930 by incorporation as The Electrochemical Society.

I mentioned before that there were three hundred and thirty-seven Charter Members, about eighteen of whom were from other countries. We now have a total slightly in excess of three thousand members, about three hundred and seventy-five of whom are from other countries. Not long ago, I was talking to a colleague who pointed out to me the fact that The Electrochemical Society was the only small independent chemical society in this country. This caused me to wonder, as it has others before me, why we have been successful. I believe that there are several reasons. The first one that comes to mind is our diversity.

Electrochemistry is a very broad subject. As President Thurnauer said of the Society in 1957, we are not large but our activities are complex. In carrying out research in electrochemistry, general knowledge is of the utmost importance. My own field of electro-organic, for example, bears close resemblance to the general chemistry of the late nineteenth century. General knowledge is most easily acquired in discussions with those in related fields. Membership in our Society makes such discussion easy. I can remember that, when the Bylaws of our Division were being written, we set our symposium date for the fall to coincide with that of the Electrodeposition Division because of the close relationship between the two fields. In the past when the Society was much smaller and single instead of simultaneous sessions were held, it was possible to listen personally to papers in all fields of electrochemistry and over the years to know the speakers well. This is not true to the same extent any longer, but it is still relatively easy to find the speaker in whose work you are interested.

Electrochemistry is a broad field in another way. President Faust in 1951 called attention to the fact that when the Society was founded the educational qualifications of the American Chemical Society kept out many engineers interested in electrochemistry. Some years ago, I had found that some of our members were not members of the American Chemical Society, but had assumed the number to be small. This apparently is not the case. In comparing samples of the directories of the two societies published in 1956, I found that the number of our members who do not belong to the American Chemical Society is considerable. This may be explained by the fact that they need not be chemists or chemical engineers but they must have had training in one of the natural sciences. I also was interested in the nature of our membership. In 1907, C. F. Burgess, in discussing the Presidential Address of Carl Hering (in those days presidential addresses were open for discussion), said that it was his impression that seventy to eighty per cent of our members were in industry. President W. C. Moore said in his address in 1947 that when he attended a meeting of the Society in 1914 he found that he was among industrial men. Due to the greatly increased interest in theoretical electrochemistry, I had thought that the percentage of members in academic positions had increased markedly, but, again, I was wrong. Some figures on the registration at the Spring Meeting in New York last year give an indication of the type of our membership: about eighty-three per cent industrial, ten per cent academic, and seven per cent government. In addition, I found in a sample from our 1956 directory that our membership was predominantly industrial. The nature of our membership has, then, not changed over the years.

Although its interests are broad in scope, the Society is individual in character. Several times in its history, the possibility of becoming associated with another society has been brought up but has always been rejected. One instance of historical importance took place at the Philadelphia Meeting in 1907. President Hering in his address brought up a proposal by W. A. Noyes for the American Chemical Society, that all papers on physical and electro- chemistry read before either society be combined in one monthly publication to be in

* Delivered at the Philadelphia Meeting, May 5, 1959.

the charge of one publication board and that the *Journal of Physical Chemistry* be combined with this new publication. I might mention that at that time the *Journal of Physical Chemistry* was edited by Wilder D. Bancroft, one of our Charter Members, and Joseph E. Trevor. In the discussion that followed, which I have mentioned previously, it developed that the new journal was to be the sole publication of the Society. It was agreed that we could save money, but it was felt, particularly by C. F. Burgess and L. J. Kahlenberg, that if we accepted this proposal we would lose our individuality. Burgess said further that he was afraid that papers accepted for the new journal would be too theoretical for our membership. Since that time, as I pointed out earlier, our interests have become more theoretical, but we still maintain a balance with the applied.

I want to say something now about the structure and management of the Society. Beginning in 1938, far-reaching changes were initiated and have continued over the years. To assist in financing, Sustaining Memberships and, later, Patron Memberships were established. I might say that the idea of corporation memberships was not a new one. It was suggested by President Kruesi in his address in 1929. We now have one hundred and sixteen Sustaining Members and five Patron Members. This still is not a true representation of the support that we are receiving from the industry, as many of the companies have taken out multiple memberships. We greatly appreciate this support. At the same time, it gives us confidence that our operation is successful. Besides corporation membership, we now have an Advisory Panel to take care of our investments, which have prospered well. We have changed from the semiannual TRANSACTIONS, and the BULLETIN, to a monthly JOURNAL in which we accept advertising just as we did before 1916. The sales of the JOURNAL are considerable. As President Udy said in 1955, the Society has become a rather big business. The present management is more functional than it was. For many years, the Board of Directors was composed of the President, the immediate Past President, six Vice-Presidents, nine Managers, the Treasurer, and the Secretary. Vice-President and Manager were just titles given to members elected to the Board. No particular duties were involved. The number of Vice-Presidents has been reduced to three, with definite duties, and the office of Manager eliminated. The three Vice-Presidents are members of the Ways and Means Committee of seven. There have been Ways and Means Committees before, but there is no mention of them in the Bylaws under which the Society operated at that time. It is stated in the present Bylaws that this committee shall act as an advisory group to the President and Board of Directors on all phases of the Society's business. As the Board grows, it will become increasingly necessary to refer matters to committees for recommendation. The other officers have been replaced by two members of the Council of Local Sections and the Chairmen of the separate Divisions.

I should like to show you how the Local Sections and Divisions have grown in importance. The first Local Sections were formed in 1907 in Wisconsin, Philadelphia, and New York. I might say that a large segment of the Wisconsin Section was made up of the faculty of the University of Wisconsin. There are now eighteen Local Sections and another in formation. The first Divisions, those of Electrothermics and Electrodeposition, were formed in 1922. Before that time, the fields of interest of the Society were represented by so-called Technical Committees. There are now nine Divisions which are responsible for the technical programs at the meetings of the Society. I can remember well when symposia were arranged by the Board of Directors. The question of what we should discuss would be brought up. Somebody would say that we had not heard about a certain subject for a long time and we would then agree to have a symposium on it. It is now in the divisional bylaws that symposia are to be held at regular intervals, as I indicated earlier. As an example of the importance of the activities of the Divisions, the symposia at this meeting [Philadelphia, 1959] on Electrode Processes and on Liquid Dielectrics are being supported by agencies of the government. In this connection, I should like to mention some remarks by President Lidbury in his address in 1915. He said that it was likely that we would come more frequently into contact with agencies of a constructive nature, of which the scientific bureaus of the government are typical, that they do a great work and that our respect and admiration of it is likely to be proportional to our knowledge of it, that their primary purpose coincides with our own, the assistance of the application of knowledge to industry. President Lidbury obviously was not referring to the situation which exists today, but his statement is nonetheless prophetic.

Other changes which show the growth of the Society are in the Editorial Board and in the establishment of our New York office, now headed by an Executive Secretary, Mr. Robert K. Shannon, who very kindly supplied me with some of the data that I have given you. For a long time, the Publication Committee was made up of a Chairman and several other members. The different fields of activity of the Society were not necessarily represented. I believe that the Secretary was the only editor. Colin G. Fink acted in that capacity for many years. There was no office of the Society in the present sense. There is now an Editorial Staff, representing different departments, headed by the Chairman of the Publication Committee. The former Publication Committee has been replaced by the Technical Editor assisted by editors representing the separate Divisions. Again, the management of the Society has become more functional.

I should like to conclude by saying, as others have said before me, that the Society offers far more than science and technology. The first meeting that I attended was held in Bridgeport, Conn., in 1928. I went with Dr. W. C. Moore, who had previously persuaded me to become a member. I knew immediately that I was interested in the Society. That interest was not due to the papers that I listened to. There was nothing strictly electro-organic on the program. I believe that it was due to the enthusiasm of the group and the fact that I was made to feel that I belonged. As I continued to attend meetings, it was easy to form friendships, many of them quite by accident, such as finding myself with some kindred spirits at one of the Society's functions or sitting next to somebody on a bus to be taken on a plant trip. I recommend highly to the newer members and guests of the Society that they attend its functions.

We have grown and are growing in numbers and in fields of interest. In this growth, it is absolutely essential to have unity. President Veasey in 1947 urged that special groups be supported, encouraged, and enlarged, but that these groups get behind the Society and make sure that it enlarges its borders and remains a most healthy tree trunk from which all branches can radiate in perfect coordination. In the preliminary meeting in 1901 before the founding of the Society, a motion was made to spell the name Electrochemical with a hyphen, Electro-Chemical. This was defeated, twenty-nine to twenty-one. Let us keep things this way.

Current Affairs

Candidates for Society Offices, 1960

R. A. Schaefer

W. J. Hamer

J. R. Musgrave

A. U. Seybolt

The Board of Directors of the Society, in accordance with the provisions of our Constitution, has approved the following Report of the Nominating Committee.

Report of Nominating Committee

The Nominating Committee is pleased to inform you that the following persons are recommended as candidates for national office with terms starting in April 1960:

For President to Serve One Year (1960-1961)
Ralph A. Schaefer

For Vice-President to Serve Three Years (1960-1963)—
Walter J. Hamer
John R. Musgrave
Alan U. Seybolt

These were the only offices to be filled, because the Treasurer and the Secretary have terms continuing through the year beginning in April 1960. All candidates have been contacted, have accepted the nominations, and have agreed to serve if elected.

(Signed) C. L. Faust, Chairman
E. B. Yeager
M. F. Quaely
E. M. Sherwood
Ralph Roberts

The two other Vice-Presidents, Henry B. Linford and Frank L. LaQue, since they were elected for three-year terms, will automatically become first and second Vice-President, respectively.

The above slate will be voted on in the fall ballot-by-mail election, and the successful candidates will assume office in the spring of 1960 at the Chicago Meeting of the Society.

Ralph A. Schaefer

Presidential Candidate

Ralph A. Schaefer, director of research and product development of the Bunting Brass and Bronze Co. at Toledo, Ohio, was born in Grafton, Ohio, in 1913. He received all his college degrees from Western Reserve University in Cleveland, Ohio, receiving his Ph.D. in physical chemistry in 1941.

Dr. Schaefer's entire professional career until his recent appointment at the Bunting Brass and Bronze Co. was with the Cleveland Graphite Bronze Co. and its allied enterprises. He joined this company as a research chemist in 1936 and was director of research from 1946 to 1952.

In 1952, the Clevite Corp. was merged with Cleveland Graphite Bronze and other enterprises. After this consolidation, the corporation created a centralized research and development division with Dr. Schaefer as vice-president. In 1955, he was promoted to the position of technical advisor to the president.

Late in 1958, Dr. Schaefer joined the Bunting Brass and Bronze Co. to initiate and administer an intensified research and development program. He is well known for his research and development contributions in the sleeve bearing field. He holds numerous patents and is the author of many published articles in the general field of electrodeposition and metallurgy as applied to the sleeve bearing industry.

For the past twenty years, Dr. Schaefer has been a member of The Electrochemical Society. He has served as Chairman of the Electrodeposition Division and of the Cleveland Section. He was a contributor and a member of the Editorial Board of the Second Edition of "Modern Electroplating." He has served on the Ways and Means Committee for over ten years and is its present Chairman.

He is currently senior Vice-President of our Society, past president of the American Electroplater's Society, and a member of the American Chemical Society, American Institute of Mining and Metallurgical Engineers, American Society for Testing Materials, Sigma Xi, and a number of other professional organizations.

Walter J. Hamer

Vice-Presidential Candidate

Walter J. Hamer is chief of the Electrochemistry Section of the National Bureau of Standards, Washington, D. C. He was born in Altoona, Pa., in 1907. After receiving his undergraduate training at Juniata College in Huntingdon, Pa., he

received his Ph.D. degree in physical chemistry from Yale University in 1932. He then returned to Yale for two years as a U.S. Navy postdoctorate Research Fellow. In July 1934, he accepted a position as research associate in physical chemistry at M.I.T., which position he held until November 1935 when he joined the staff of the National Bureau of Standards.

Dr. Hamer is the author or coauthor of a substantial number of articles dealing with various aspects of electrochemistry. He has conducted research on electrolytes, fused salts, primary and secondary batteries, and on standard cells. He has published a series of papers on the lead-acid storage battery, one on dry cells, and another on pH standards. At the National Bureau of Standards, one of his main responsibilities is the maintenance of the nation's primary standard of electromotive force.

During World War II, Dr. Hamer worked as an electrochemist first for the Office of Scientific Research and Development and then for the Manhattan Project. He served as battery consultant to the Dept. of Defense in 1952-1954, and is a member or officer of subcommittees on batteries of the Society of Automotive Engineers, the American Institute of Electrical Engineers, and the American Standards Association. Dr. Hamer is a member of the Commission on Electrochemistry of The International Union of Pure and Applied Chemistry, and is technical advisor on primary batteries to the U. S. National Committee of the International Electrotechnical Commission. He holds memberships in the American Association for the Advancement of Science, Alpha Chi Sigma, Sigma Xi, American Institute of Electrical Engineers, American Physical Society, Faraday Society, American Chemical Society, and the Washington Academy of Sciences, and is president of the Yale Chemists' Association.

Dr. Hamer, a member of The Electrochemical Society since 1937, has been active in its affairs. He was Chairman of the Theoretical Electrochemistry Division in 1951-1953 and has served on committees of the Division. He was a member of the Executive Board of the Battery Division in 1954-1956. In 1951, he organized and contributed to the bicentennial issue of the JOURNAL devoted to the Theoretical Electrochemistry Division; and has conducted a number of Society symposia. He is Editor of the Society's Monograph on "The Structure of Electrolytic Solutions" published in 1959 by John Wiley & Sons. Dr. Hamer is a member of the Society's Honors and Awards Committee, and represents the Society on the American Standards Association Committees Y10 and Y32 which deal with letter symbols and abbreviations and standardization of graphical symbols.

John R. Musgrave

Vice-Presidential Candidate

John R. Musgrave, chief of Technical Service in the Research Laboratories of the Chemical Division of The Eagle-Picher Co. at Joplin, Mo., was born at Reading, Pa., in 1906. He received his degree in chemical engineering at Lafayette College in 1927. Following a period of industrial research, he entered the graduate school of the University of Toronto. There he received the Ph.D. degree, majoring in physical chemistry, in 1933. Shortly after the completion of his graduate work, he became affiliated with the Eagle-Picher Research Labs., where he is, at present, in charge of Technical Service for the Chemical Division.

Dr. Musgrave's research activities cover work on thermal insulation, storage batteries, paint, corrosion, instrumentation, diatomaceous earth, and rare metals. He has been active in the development of high-purity germanium for semiconductor work, as well as gallium. He holds several patents, and is the author or coauthor of technical papers on storage battery technology, particle-size determination (in the subsieve range), germanium, cadmium, and gallium.

Dr. Musgrave joined The Electrochemical Society in 1941 and has been particularly active in the Battery and Electronics Divisions. He has been Secretary-Treasurer and Chairman of the Electronics Division and has participated in the development of the rare metals and semiconductor symposia. He has been Chairman of the Membership Committee and is, at present, a member of the Honors and Awards Committee of the Society. He is also a member of a number of other scientific organizations.

Alan U. Seybolt

Vice-Presidential Candidate

Alan U. Seybolt is research metallurgist at the General Electric Research Laboratory, Schenectady, N. Y. He was born in Westfield, N. Y., in 1910, but spent most of his early years in Springfield, Mass. After obtaining a Ph.D. degree in metallurgy at Yale in 1936, he was for several years research metallurgist at Battelle Memorial Institute in Columbus, Ohio. In 1943, he went to Los Alamos, N. Mex., to become associated with the wartime atomic bomb project. After the war, he returned east and, in 1947, joined the Knolls Atomic Power Lab. of the General Electric Co. in Schenectady, N. Y. In 1952, he became associated with this company's Research Lab., also in Schenectady.

Manuscripts and Abstracts for Spring 1960 Meeting

Papers are now being solicited for the Spring Meeting of the Society, to be held at the Lasalle Hotel in Chicago, Ill., May 1, 2, 3, 4, and 5, 1960. Technical sessions probably will be scheduled on Electric Insulation (including a Symposium on "Electrolytic Capacitors"), Electronics (including Luminescence and Semiconductors), Electrothermics and Metallurgy (including a symposium on "High-Purity Vanadium" and a round table on "Methods of Reducing Iron Ores"), Industrial Electrolytics, and Theoretical Electrochemistry.

To be considered for this meeting, triplicate copies of abstracts (*not exceeding 75 words in length*) must be received at Society Headquarters, 1860 Broadway, New York 23, N. Y., *not later than January 4, 1960. Please indicate on abstract for which Division's symposium the paper is to be scheduled, and underline the name of the author who will present the paper.* Complete manuscripts should be sent in triplicate to the Managing Editor of the JOURNAL at the same address.

* * *

The Fall 1960 Meeting will be held in Houston, Texas, October 9, 10, 11, 12, and 13, 1960, at the Shamrock Hotel. Sessions will be announced in a later issue.

Dr. Seybolt's technical interests in recent years have centered in the physical chemistry of metals, with particular reference to gases in metals, phase diagrams, and the oxidation of metals. He has published many technical papers in these fields and, with J. E. Burke, wrote a book, "Procedures in Experimental Metallurgy."

He has been active for several years in the Electrothermics and Metallurgy Division of The Electrochemical Society and has just finished a two-year term as Chairman of this Division. Prior to joining this Division in 1955, he was Chairman of the Rare Metals Group of the Electronics Division, which was amalgamated with the Electrothermics Division toward the end of 1954 to create the present combined Electrothermics and Metallurgy Division. Other society memberships include: the American Society for Metals; the American Institute of Mining, Metallurgical, and Petroleum Engineers; the Institute of Metals; and the Iron and Steel Institute.

Burns, Heise, Mathers, and Linford Honored at Philadelphia

At the Annual Banquet on May 5, 1959, during the Philadelphia Meeting of The Electrochemical Society, Certificates of Honorary Membership were presented by President Sherlock Swann, Jr., to Robert M. Burns, George W. Heise, and Frank C. Mathers, in recognition of distinguished service and for significant contributions to the science of electrochemistry. The awarding of the Certificates was accompanied by the following citations.

R. M. Burns

G. W. Heise

Robert Martin Burns

Dr. Burns was born in Longmont, Colo., in 1890. He graduated from the University of Colorado in 1915 and remained for the M.A. which he received in 1916. During this period, he was an instructor in chemistry. His studies were interrupted by the First World War, in which he served as a Second Lieutenant in the Chemical Warfare Service. After his discharge in 1919, he entered Princeton University where he received the Ph.D. in 1921. Although he did his thesis work with Dr. H. S. Taylor in catalysis, he learned electrochemistry in Dr. G. A. Hulett's lectures.

After graduation, he was with the Barrett Co. for a year and then left to become a member of the Engineering Department of the Western Electric Co., which in 1925 became the Bell Telephone Laboratories. Actually, he was rejoining the company for which he had worked from 1904-1910 before he went to college. He was made chemical director in 1945. In 1951, he was appointed chemical coordinator. He reached the age for retirement in 1955 and, then, became scientific advisor to the Stanford Research Institute and to the Sprague Electric Co. He is, at present, director of the European Office of the Stanford Research Institute.

In the Bell Telephone Laboratories, Dr. Burns created an atmosphere for basic research and organized research groups in many fields related to communication, such as battery components, capacitors, magnetic materials, electronic devices, insulators, and piezoelectric materials. He also organized a group of specialists in experimental techniques to aid in the research. He, himself, is an authority in the field of corrosion.

He has been very much interested in professional societies and has been chairman of the New York Section of the American Chemical Society and of several groups in the field of corrosion. He is a Fellow of the American Association for the Advancement of Science. He is a member of Phi Beta Kappa, Sigma Xi, Tau Beta Pi, Kappa Delta Phi, and Alpha Chi Sigma, of which he has been national president. He has been particularly active in the affairs of our own Society, which he joined in 1922. In 1926, he became Chairman of the Committee on Local Sections and, in 1931, was elected Treasurer of the Society, in which office he served until he was elected President in 1943. In 1947, when Dr. Fink retired, he became Secretary. At that time, the Secretary was also Editor. Dr. Burns carried on this work for two years. In 1950, he became consultant to the Editorial Staff and, in 1951, Chairman of the Publication Committee, in which position he remained until 1957. He was instrumental in the change from preprints to abstracts of articles for meetings, and from the TRANSACTIONS appearing twice a year to the present monthly JOURNAL.

Dr. Burns has received many honors: the D.Sc. from the University of Colorado in 1945, the Perkin Medal of the Society of Chemical Industry in 1952, the Willis R. Whitney Award of the National Association of Corrosion Engineers in 1953, and the Acheson Award of our own Society in 1956.

He has worked with quiet, calm wisdom and an unassuming attitude.

George William Heise

Mr. Heise was born in 1888 in Milwaukee, Wis. He received the B.S. degree in chemistry from the University of Wisconsin. For the next two years, he taught at Grinnell College, Iowa, and at DePaul University in Chicago where he was head of the Department of Physics. In 1911, he returned to the University of Wisconsin to work with Dr. Louis J. Kahlenberg, receiving the M.S. degree in 1912. He continued graduate studies as Fellow in Chem-

F. C. Mathers

H. B. Linford

istry until 1913. Mr. Heise was certainly in an electrochemical environment at that time for, besides Dr. Kahlenberg, Dr. O. P. Watts and Dr. C. F. Burgess were on the staff.

In 1913, he joined the staff of the Philippine Bureau of Science as a physical chemist, becoming chief of the Section on Physical Chemistry and acting chief of the Division of Inorganic Chemistry.

In 1917, he volunteered for active military duty and served as Captain in the Quartermaster Corps. He was transferred later to the Chemical Warfare Service as director of Nitrogen Fixation Research at the Saltville, Va., plant.

After his discharge from the Army in 1919, he accepted a position with the National Carbon Co. where he became head of a department and later associate director of research. He reached the retirement age in 1953, but is still a consultant for the company. He is also chairman of the Panel on Primary Batteries of the Committee on Undersea Warfare of the National Research Council.

Mr. Heise has carried out research in several different fields, but his chief interest has been in the primary battery, on which he is an authority, and related electrochemical subjects. He and his group at the National Carbon Research Laboratories were responsible for the preparation and use of a special manganese dioxide and other improvements in the dry cell, for the development of the air cell battery and other systems with gas electrodes, for porous carbon and graphite electrodes for electrosynthesis, and for improvements in anodes for the brine cell. During the Second World War, he was head of a group which developed highly effective carbons for gas masks and catalysts for oxidation. His approach to a problem was always fundamental and he knew the literature. Further, he had the ability to translate the results of research into commercial realities. He is the author of some 45 technical papers and holds about 85 patents, many duplicated in foreign countries.

He is a member of the American Chemical Society, and a Fellow of the American Association for the Advancement of Sicence, Faraday Society, Society of Chemical Industry, Sigma Xi, Phi Lambda Upsilon, and Alpha Chi Sigma. He received the Certificate of Merit of the Cleveland Chemical Profession in 1953, and the Citation of Honor from Indiana Technical College in 1958.

He joined The Electrochemical Society in 1925 and took the Chairmanship of the Committee on Local Sections in 1931. He helped to found the Cleveland Section and became its Chairman. Since that time, he has served in many capacities, as a member of committees and in elective office. He was a Vice-President in 1934 and 1946, and President in 1947-1948. He was given the Acheson Award in 1954. He was the first Chairman of the Investment Advisory Panel. Currently, he is the Editor of the Monograph on Primary Batteries sponsored by the Battery Division.

He always has been ready with good counsel when called upon.

Frank Curry Mathers

Dr. Mathers was born in Bloomington, Ind., in 1881. He received the A.B. degree in 1903 at Indiana University. He continued on as an instructor, at the same time doing graduate work in electroplating with Dr. O. W. Brown for the A.M. degree which he received in 1905. He then took leave of absence to go to Cornell University where he received the Ph.D., in 1907, in inorganic chemistry with Dr. L. M. Dennis. He took all of Dr. Wilder D. Bancroft's courses and carried out some laboratory work with him. After this training, Dr. Mathers was ready to begin a career in electrochemistry. He rejoined the staff at Indiana University in 1907 as an assistant professor of inorganic chemistry. He was made an associate professor in 1913 and a professor in 1923. In 1946-1947, he was interim head of the Department of Chemistry. He was made emeritus professor in 1950.

The first meeting of the Society which Dr. Mathers attended was in St. Louis in the fall of 1904. He saw there some of the founders about whom he had been reading and was very much impressed. He became a member himself that same year. He first became officially active in the affairs of the Society in 1917 when he was made a member of the Technical Committee on Electroplating in the days before the Electrodeposition Division was created. He was elected President of the Society in 1940. He is a member of Alpha Chi Sigma, Phi Lambda Upsilon, and Sigma Xi.

He has devoted his life to teaching and research. His first research was on the electroplating of lead from its perchlorate, after finding that perchlorates of the heavy metals were unusually stable. This work, published in our TRANSACTIONS in 1910, was the beginning of a series of studies on perchlorates. During the First World War, he was asked to come to Washington to prepare fluorine by Dr. Bancroft, who was then a Major in the Chemical Warfare Service. He designed a cell, which has been named after him, for its preparation by the electrolysis of potassium hydrogen fluoride. A modification of this process is being operated to make fluorine which is used in the preparation of uranium fluoride for the atomic reactor. Most of his research, which has been carried out independently and with students, has been on electroplating. He developed a process for the plating of tin and found that aluminum could be plated successfully from a bath of aluminum halides and aromatic hydrocarbons. In the field of finishing, he discovered a process for oxidizing silver. He has been the author of more than 130 papers in the TRANSACTIONS of the Society and has participated in the discussion of a great many of them. In addition to his academic work, he spent many summers working in the industry.

Dr. Mathers has been characterized by one of his former students as an excellent and demanding teacher, considerate of students who did their best but very hard on those who did not. He continually brought new, unusual, and interesting facts to the attention of his students. In addition to chemistry, he expected them to keep abreast of national

affairs, and it was not uncommon for him to ask them about happenings in Congress.

He still goes to his office every day and is happy to advise those who come to him.

Henry B. Linford

Dr. Henry B. Linford, professor of chemical engineering at Columbia University, New York City, also was presented by President Swann with a Certificate reading as follows.

"In grateful recognition of many years of faithful and distinguished service and unselfish devotion to the interests and welfare of The Electrochemical Society, Incorporated, this scroll is hereby presented to Dr. Henry B. Linford as a token of our genuine appreciation of his outstanding contributions to the progress and building of the Society during his tenure of office as Secretary."

Dr. Linford, who at present is Vice-President of the Society, held the post of Secretary from the spring of 1949 to the spring of 1958, when he took office as Vice-President. He served concurrently as Vice-President and Interim Secretary from May 1958 to January 1959 when he was succeeded as Secretary by I. E. Campbell.

Young Authors' Prize for 1958

At the Annual Banquet held on Tuesday, May 5, during the Philadelphia Meeting of The Electrochemical Society, the Young Author's Prize of $100 was presented to Milton Stern of the Union Carbide Metals Co. Dr. Stern was selected

Milton Stern

for the award in recognition of his paper "The Mechanism of Passivating-Type Inhibitors" which was published in the November 1958 issue of the JOURNAL. This is the second time that Dr. Stern has won this award, having received it in 1955. He has contributed a number of technical papers on corrosion, electrode kinetics, and physical metallurgy.

Dr. Stern is technical supervisor of the Metals Research Group in Union Carbide's Metals Research Laboratories at Niagara Falls, N. Y. He is responsible for the execution of the research program in corrosion, ceramics, reactive metals, and iron and steel.

Dr. Stern is a graduate of Northeastern University and received both his master's degree and his doctor's degree in physical metallurgy from the Massachusetts Institute of Technology. From 1949-1952, he held a research fellowship sponsored by the Aluminum Co. of America. His technical experience includes two years (1952-1954) as a research associate at M.I.T. In addition to The Electrochemical Society, he is a member of the American Chemical Society; American Institute of Mining, Metallurgical, and Petroleum Engineers; American Society for Metals; and is currently chairman of the Niagara Frontier Section of the National Association of Corrosion Engineers.

Dr. Stern recently announced a major breakthrough in the battle against corrosion. He discovered that a small addition of noble metal such as palladium or platinum to titanium causes the resulting alloy to be resistant to both reducing and oxidizing environments. The new alloy, which has tremendous potential practical applications, was developed by Dr. Stern from purely theoretical considerations of the role of noble metal additions on activity and passivity.

Turner Memorial Award for 1958

The Society's Francis Mills Turner Memorial Award, Sponsored by the Reinhold Publishing Corp., consisting of $100 worth of books, was awarded at the Annual Banquet in Philadelphia to J. Paul Pemsler of Nuclear Metals, Inc., for his paper "Diffusion of Oxygen in Zirconium and Its Relation to Oxidation and Corrosion" which appeared in the June 1958 issue of the JOURNAL.

Dr. Pensler was awarded B.S. and Ph.D. degrees from New York University. His last three years there were spent as a teaching fellow in the Department of Chemistry. He was employed by Goodyear Atomic

J. P. Pemsler

in Oak Ridge, Tenn., in 1954 and returned to their installation at Portsmouth, Ohio, in 1955 to organize and direct activities of the Infrared Spectroscopy Laboratory. Here he engaged in research on the applications of infrared spectroscopy to systems of inorganic fluorides and interhalogens, publishing several papers in this field. He joined the staff of Nuclear Metals, Inc., in 1957 and recently has been appointed group leader of chemical metallurgy.

Dr. Pemsler's recent research has concerned zirconium alloy corrosion, oxygen diffusion in zirconium and hafnium, dispersion fuel elements, extrusion lubricants, ternary refractory carbides, simulation of reactor excursions by chemical reactions, beryllium intermetallic compounds, and the thermodynamics of gases in metals.

He is a member of the American Chemical Society, Sigma Xi, and Phi Lambda Upsilon.

Section News

Boston Section

The 17th meeting of the Boston Section of the Society was held Wednesday, May 20, 1959, at the Arthur D. Little Research Laboratories at Acorn Park. Dr. L. B. Rogers of M.I.T. spoke on "Initial Stages of Electrodeposition." For several years, Dr. Rogers has been studying the behavior of the first few layers of electrodeposited elements using radioactivity.

He stated that depositions involving only a fraction of monolayer were first reported nearly 50 years ago. These studies were directed toward obtaining standard potentials for polonium and protactinium, newly discovered radioactive elements, which were found in minute amounts. In recent years, the ready

availability of other radioactive nuclides has made possible an extension to many other elements. Up to the present time, electron diffraction has been the chief tool for examining the effect of the electrode surface on the deposit. It now appears that much useful information can be obtained from plots of potential vs. the fraction of the surface covered with deposit. The closer the lattice dimensions of the electrode material and deposit, the less cathodic the potential required for initial deposition. The effect can still be observed after many layers of deposit. In addition to providing useful information to electroplaters, the significant difference in deposition behavior between the first few layers and those that follow may be important considerations in electrolytic purifications of elements and in analytical separations involving trace amounts.

A proposed change in the Bylaws of the Section was favorably voted on, to the effect that the office of the Secretary-Treasurer be made two separate offices. New officers elected for the term 1959-1960 are as follows:

Chairman—H. C. Gatos, Lincoln Lab., Lexington, Mass.
Vice-Chairman—H. H. Homer, Sylvania Electric Products Inc., Salem, Mass.
Secretary—Herbert Bandes, Arthur D. Little, Inc., Mass.
Treasurer—H. L. Creamer, Mallinckrodt Chemical Works, Mass.
Councilor—Charles Levy, Watertown Arsenal, Watertown, Mass.

L. B. Rogers continues as Councilor (his two-year term expires in 1960).

R. A. Peak,
Retiring Secretary-Treasurer

Council of Local Sections

The new officers of the Council of Local Sections, elected during the Philadelphia Meeting of the Society in May, for the 1959-1960 term are:

Chairman—K. S. Willson, 3785 W. 33 St., Cleveland 9, Ohio
Vice-Chairman—A. J. Cornish, Westinghouse Research Labs., Beulah Rd., Churchill Boro., Pittsburgh 35, Pa.
Secretary—J. C. White, 4205 Woodberry St., University Park, Hyattsville, Md.
Council Representative on Board of Directors—M. F. Quaely (two-year term, 1959-1961)

C. A. Hampel continues as Council Representative on the Board. His term will expire in 1960.

San Francisco Section

The third meeting of the 1958-1959 season was held on January 28, 1959, at the University of California Men's Faculty Club. The speaker was Dr. L. F. Yntema, retired vice-president and director of research of Fansteel Metallurgical Corp. His subject was "The Refractory Metals, Their Properties and Uses."

Dr. Yntema first presented a review of the history and properties of the refractory metals; tungsten, tantalum, molybdenum, and columbium. Then he discussed the various uses of these metals in relation to their properties. Following this, he covered methods of preparation of these metals and the alloying of them. Dr. Yntema emphasized that the usefulness of the refractory metals will be increased by alloying. He stated that alloys of these metals will have better mechanical and chemical resistance properties at elevated temperatures than the pure metals, and predicted that the upper temperature limits of application of the refractory metals alloys will be extended to approximately three-fourths of the melting points of the pure metals.

The speaker at the fourth meeting on March 25 was Dr. G. B. Adams, Jr., senior scientist at the Missiles and Space Division of Lockheed Aircraft Corp. His subject was "Kinetics of Formation of Thin Metal Oxide Films."

Dr. Adams began by reviewing the theory of kinetics of formation of very thin insulating metal oxide films and various experimental methods previously used to study the kinetics of formation of both thin and thick films. Then he described experimental tests of the theory with zirconium and niobiun using low-potential chronopotentiometric techniques. Following this, he discussed several applications of the low-potential chronopotentiometric technique used to study the kinetics of formation of thin films.

R. E. De La Rue,
Vice-Chairman

Notice to Members and Subscribers
(Re Changes of Address)

To insure receipt of each issue of the JOURNAL, please be sure to give us your old address, as well as your new one, when you move. Our records are filed by states and cities, not by individual names. The Post Office does not forward magazines.

New Members

In June 1959, the following were elected to membership in The Electrochemical Society by the Admissions Committee:

Active Member Sponsored by a Sustaining Member

W. D. Moxgan, Foote Mineral Co., Knoxville, Tenn. (Electrodeposition)

Active Members

R. A. Baker, Bell Telephone Labs., Inc., Rm. 1A-369, Murray Hill, N. J. (Theoretical Electrochemistry)
E. O. A. Baumann, Technical University "Fridericiana" Karlsruhe; Mail add: Kaiserstr. 12, Karlsruhe, West Germany (Electric Insulation, Electronics)
R. P. Beatty, C.B.S.-Hytron; Mail add: 28 Priscilla Ave., Chelmsford, Mass. (Electronics)
M. G. Bohar, Lansdale Tube Co., Spring City, Pa. (Electronics)
J. J. Birdcell, P. R. Mallory & Co., Inc.; Mail add: 617 Brewer Place, Greenwood, Ind. (Battery, Corrosion, Electric Insulation, Electronics, Electrothermics & Metallurgy)
J. R. Black, Motorola, Inc.; Mail add: 5356 E. Lafayette Blvd., Phoenix, Ariz. (Electronics)
J. B. Bravo, Foote Mineral Co.; Mail add: 10 Roberts Rd., Malvern, Pa. (Industrial Electrolytic)
C. A. Brown, General Electric Co.; Mail add: 1969 Cliffview Rd., Cleveland 21, Ohio (Electronics)
W. R. Cady, General Electric Co.; Mail add: 105 Castle Rd., North Syracuse, N. Y. (Electronics)
W. H. Corson, II, G. & W. H. Corson, Inc.; Mail add: 9427 Meadowbrook Lane, Philadelphia 18, Pa. (Battery)
T. W. Dakin, Research Labs., Westinghouse Electric Corp., Pittsburgh 35, Pa. (Electric Insulation)
A. P. David, Alcoa Research Labs., Box 772, New Kensington, Pa. (Corrosion)
H. D. Doolittle, Machlett Labs., Inc.; Mail add: 42 Pembroke Dr., Stamford, Conn. (Electronics)
J. J. Dymon, Sylvania Electric Products Inc., 35-22 Linden Place, Flushing 55, N. Y. (Electronics)
E. D. Eich, Anaconda Wire & Cable

Co., Hastings-on-Hudson, N. Y. (Electric Insulation)

C. D. Flanagan, Texas Instruments, Inc.; Mail add: 1152 Oak Hill Ave., Attleboro, Mass. (Electronics)

J. U. Fojt, Texas Instruments, Inc.; Mail add: 4916 Kelton Dr., Dallas 9, Texas (Electronics)

Bernard Fonoroff, C.B.S.-Hytron; Mail add: 8 Saran Ave., Bedford, Mass. (Electronics)

G. K. Gaule, U. S. Army Signal R. & D. Labs.; Mail add: 325 Bath Ave., Long Branch, N. J. (Electronics)

L. E. Gerlach, P. R. Mallory & Co., Inc.; Mail add: 6315 E. Pleasant Run Pkway., S.D., Indianapolis 19, Ind. (Electronics, Electrothermics & Metallurgy)

G. R. Gillooly, General Electric Co.; Mail add: 522A Clearview Dr., Euclid 23, Ohio (Electronics)

H. C. Givens, Silicones Div., Union Carbide Corp.; Mail add: P. O. Box 180, Sistersville, W.Va. (Electronics)

E. J. Goon, National Research Corp.; Mail add: 12 Manor Ave., Burlington, Mass. (Electronics, Electrothermics & Metallurgy)

F. B. Grosselfinger, Hoechst-UHDE Corp.; Mail add: 84 Bourndale Rd., S., Manhasset, N. Y. (Industrial Electrolytic)

R. B. Hand, E. I. du Pont de Nemours & Co.; Mail add: 220 Wellington Rd., Wilmington 3, Del. (Electronics)

G. W. Harrington, Lansdale Tube Co.; Mail add: Abington Court Apts., Apt. E 208, Abington, Pa. (Electronics)

G. L. Hawkins, Hughes Products, Semiconductor Div.; Mail add: 11916 Idaho Ave., Los Angeles 25, Calif. (Electronics, Electrothermics & Metallurgy, Theoretical Electrochemistry)

D. H. Hobbs, Aluminum Co. of Canada Ltd., Arvida, Que., Canada (Industrial Electrolytic)

Seiichi Ishizaka, Scientific Attaché, Embassy of Japan; Mail add: 1324 Juniper St., N.W., Washington 12, D. C. (Industrial Electrolytic)

W. H. Jordon, Jr., Texas Research Associates, 1701 Guadalupe St., Austin 1, Texas (Theoretical Electrochemistry)

Matthew Katz, Astron Corp.; Mail add: 598 Montgomery St., Brooklyn 25, N. Y. (Electric Insulation, Electronics)

E. L. Keltz, Jr., Perkin Engineering Corp.; Mail add: R. D. No. 1, Malvern, Pa. (Industrial Electrolytic)

R. C. Leal, Jr., Bowers-Lth., S.A.; Mail add: Guayana Holandesa 336, Vista Hermosa, Monterrey, N. L., Mexico (Battery)

I. O. Lisk, Canadian General Elec-

ECS Membership Statistics

The following three tables give breakdown of membership as of July 1, 1959. The Secretary's Office feels that a regular accounting of membership will be very stimulating to membership committee activities. In Table I it should be noted that the totals appearing in the right-hand column are *not* the sums of the figures in that line since members belong to more than one Division and, also, because Sustaining Members are not assigned to Divisions. But the totals listed are the total membership in each Section. In Table I, Sustaining Members have been credited to the various Sections.

Table I. *ECS Membership by Sections and Divisions*

Section	Division: Battery	Corrosion	Electric Insulation	Electro-deposition	Electronics	Electro-Organic	Electrotherm-ics & Met.	Industrial Electrolytic	Theoretical Electrochem.	No Division	Total as of 1/1/59	Total as of 7/1/59	Net Change
Boston	19	27	6	38	73	7	27	14	29	6	151	163	+12
Chicago	15	31	4	41	29	9	13	10	22	15	132	129	− 3
Cleveland	50	32	2	53	40	10	31	34	38	13	198	199	+ 1
Columbus, Ohio	2	15	0	14	9	2	25	3	8	4	49	55	+ 6
Detroit	12	19	4	50	10	6	9	6	22	18	91	94	+ 3
India	8	7	2	19	8	6	8	11	15	3	35	36	+ 1
Indianapolis	12	9	6	12	13	5	8	3	7	2	39	45	+ 6
Midland	9	15	0	5	2	3	7	14	11	1	43	42	− 1
Mohawk-Hudson	4	13	14	7	15	1	9	1	19	5	54	64	+10
New York	90	111	27	146	155	33	74	71	105	41	517	543	+26
Niagara Falls	13	25	1	24	11	6	79	68	30	19	183	180	− 3
Ontario-Quebec	9	25	1	16	8	3	39	29	10	14	82	90	+ 8
Pacific Northwest	5	10	0	8	3	1	9	9	9	10	44	42	− 2
Philadelphia	29	28	4	36	73	9	26	20	47	30	185	197	+12
Pittsburgh	2	45	4	26	29	7	41	16	36	10	133	132	− 1
San Francisco	9	13	1	19	19	4	18	22	20	4	71	75	+ 4
S. Calif.-Nevada	19	26	3	32	43	5	22	17	32	10	105	125	+20
Washington-Baltimore	37	37	7	37	24	3	11	9	32	6	129	131	+ 2
U.S. Non-Section	67	92	14	91	88	43	65	78	122	30	408	431	+23
Foreign Non-Section	48	64	7	65	36	31	42	60	76	89	262	273	+11
Total as of Jan. 1, 1959	441	638	103	723	621	190	549	486	656	329	2911		
Total as of July 1, 1959	459	644	107	739	688	194	563	495	690	330		3046	
Net Change	+18	+6	+4	+16	+67	+4	+14	+9	+34	+1			

Table II. *ECS Membership by Grade*

	Total as of 1/1/59	Total as of 7/1/59	Net Change
Active	2538	2627	+ 89
Faraday (Active)	30	32	+ 2
Deutsche Bunsen Gesellschaft (Active)	15	16	+ 1
Delinquent	70	99	+ 29
Active Representative Patron Members	10	10	0
Active Representative Sustaining Members	99	105	+ 6
Total Active Members	2762	2889	+127
Life	17	17	0
Emeritus	49	49	0
Associate	31	27	− 4
Student	46	57	+ 11
Honorary	6	7	+ 1
Total	2911	3046	+135

The figures pertaining to Patron and Sustaining Member Representatives, and Faraday and Deutsche Bunsen Gesellschaft members subscribing to the JOURNAL, have been added to reflect reclassifications and changes in membership status.

Table III. *ECS Patron and Sustaining Membership*

	Total as of 1/1/59	Total as of 7/1/59	Net Change
Patron Member Companies	5	5	0
Sustaining Member Companies	148	153	+ 5

tric Co., Box 525, Weston, Ont., Canada (Electronics, Electrothermics & Metallurgy)

C. M. Little, Diamond Alkali Co.; Mail add: 309 Roosevelt Dr., Mentor, Ohio (Eelctrodeposition, Electrothermics & Metaliurgy)

A. L. MacDonald, Jr., Raytheon Manufacturing Co.; Mail add: 31 Ocean St., Quincy 71, Mass. (Electronics)

H. H. Marvin, Research Lab., General Electric Co., Box 1088, Schenectady, N. Y. (Corrosion, Electrothermics & Metallurgy)

R. E. Meredith, University of California & Lawrence Radiation Lab.; Mail add: 1634½ Delaware St., Berkeley 3, Calif. (Battery, Electrodeposition, Industrial Electrolytic, Theoretical Electrochemistry)

G. H. Morrison, Research Labs., Sylvania Electric Products Inc., Bayside, N. Y. (Electronics)

L. E. Mount, Allegheny Electronic Chemicals; Mail add: P. O. Box 529, Bradford, Pa.

W. R. Nardella, Sperry Gyroscope Co.; Mail add: 46-19 Robinson St., Flushing, N. Y. (Electro-Organic, Theoretical Electrochemistry)

J. F. O'Sullivan, C.B.S.-Hytron; Mail add: 4 Station Ave., Groton, Mass. (Electronics)

F. C. Palilla, Sylvania Electric Products Inc.: Mail add: 60-46 72nd St., Maspeth 78, N.Y. (Electronics)

T. E. Peters, Physics Lab., Sylvania Electric Products Inc., Bayside, N. Y. (Electronics)

R. W. Powers, Research Lab., General Electric Co.; Mail add: 1507 Kingston Ave., Schenectady 8, N. Y. (Theoretical Electrochemistry)

John Pump, Pump Metal Corp. of Canada Ltd.; Mail add: Box 42, R. R. No. 1, Richmond Hill, Ont., Canada

J. G. Quetsch, Jr., Hughes Products; Mail add: 10215 Crenshaw Blvd., Inglewood 4, Calif. (Electronics)

K. S. Quimby, Jr., Texas Instruments, Inc.; Mail add: 6602 Westchester Dr., Dallas 5, Texas (Electronics)

R. A. Quinn, Lockheed Missiles & Space Div.; Mail add: 3358 Kenneth Dr., Palo Alto, Calif. (Electronics, Theoretical Electrochemistry)

E. L. Ralph, Hoffman Electronics Corp., 930 Pitner Ave., Evanston, Ill. (Electrodeposition, Electronics)

W. G. Robson, Marquardt Aircraft Co.; Mail add: 20678 Lemay St., Canoga Park, Calif. (Electrothermics & Metallurgy)

A. N. Sahagen, Hughes Products, Semiconductor Div.; Mail add: 223 Princeton Dr., Costa Mesa, Calif. (Corrosion, Electronics, Electrothermics & Metallurgy)

F. J. Saia, Hughes Aircraft Co.; Mail add: 290 Sierks St., Costa Mesa, Calif. (Electronics)

R. C. Schleck, Fisher Scientific Co.; Mail add: 45 Birkendene Rd., Caldwell, N. J. (Electronics)

H. N. Seiger, AVCO, RAD; Mail add: 32 Pleasant St., North Reading, Mass. (Battery, Theoretical Electrochemistry)

H. V. Seklemian, Metals Research Labs., Union Carbide Metals Co., Box 580, Niagara Falls, N. Y. (Electrodeposition, Electrothermics & Metallurgy)

M. L. Severson, Inland Steel Co.; Mail add: 7814 Walnut Ave., Hammond, Ind. (Electrothermics & Metallurgy)

Shigeo Shionoya, Dept. of Physics, New York University; Mail add: 142-10 Hoover Ave., Jamaica 35, N.Y. (Electronics)

D. W. Smith, E. I. du Pont de Nemours & Co.; Mail add: 2525 Blackwood Rd., Foulk Woods, Wilmington 3, Del. (Electronics, Electrothermics & Metallurgy)

R. B. Spence, Vickers Krebs Ltd.; Mail add: 158 Surrey Dr., Town of Mt. Royal, P.Q., Canada (Industrial Electrolytic)

A. J. Strauss, M. I. T. Lincoln Lab., Lexington 73, Mass. (Electronics)

L. W. Strock, Sylvania Electric Products Inc.: Mail add: 21 Madison Ave., Saratoga Springs, N. Y. (Electronics)

F. M. Sullivan, Robertshaw-Fulton Controls Co., Eastern Research Center, 2920 N. 4th St., Philadelphia 36, Pa. (Electrodeposition)

H. T. Sumsion, Lockheed Missiles & Space Div.; Mail add: 4932 Trent Dr., San Jose 24, Calif. (Electrothermics & Metallurgy)

A. Y. C. Tang, Tang Industries, Inc.; Mail add: 143 Tina Ave., Brockton, Mass. (Electronics)

Charles Thompson, Aerojet-General Corp.; Mail add: 2408 South Mountain Ave., Duarte, Calif. (Electronics)

H. D. Thompson, Great Lakes Carbon Corp., 56th & Pine Ave., Niagara Falls, N. Y. (Industrial Electrolytic)

F. G. Ullman, Physics Research, National Cash Register Co., Dayton 9, Ohio (Electronics)

F. P. Valente, Watertown Arsenal Labs.; Mail add: 61 Pleasant St., Cambridge 39, Mass. (Electrodeposition, Theoretical Electrochemistry)

Daniel Van Rooyen, Westinghouse Research Labs.; Mail add: 350 Iris Dr., Pittsburgh 35, Pa. (Corrosion)

Arthur Van Zee, Owens-Illinois Glass Co.; Mail add: 3430 Inverness Ave., Toledo 7, Ohio (Electronics)

K. D. Wadsworth, I.C.I. (New York) Ltd., 488 Madison Ave., New York 22, N. Y. (Industrial Electrolytic)

C. W. Walters, P. R. Mallory & Co., Inc.; Mail add: 5934 College Ave., Indianapolis 20, Ind. (Electronics)

R. F. Walton, Texas Instruments, Inc.; Mail add: P. O. Box 2944, Main U. S. Post Office, Dallas 21, Texas (Electrodeposition)

R. D. Weaver, Delco-Remy Div., General Motors Corp.; Mail add: 3016 E. Fifth St., Anderson, Ind. (Electro-Organic)

A. C. Wilbur, Glenn L. Martin Co.; Mail add: 121 West Belcrest Rd., Bel Air, Md. (Electronics)

K. L. Wing, Olin Mathieson Chemical Corp.; Mail add: P. O. Box 15, McIntosh, Ala. (Industrial Electrolytic)

Marcel Zundel, Vickers Krebs Ltd.; Mail add: 6272 Av. de Vimy, Montreal, Que., Canada (Industrial Electrolytic)

By action of the Board of Directors of the Society, all prospective members must include first year's dues with their applications for membership.

Also, please note that, if sponsors sign the application form itself, processing can be expedited considerably.

Associate Members

A. W. Gover, Texas Instruments, Inc.; Mail add: 1707 "O" Ave., Plano, Texas (Electronics, Industrial Electrolytic)

J. D. Lounsbury, I.B.M., Products Development Labs.; Mail add: 7 Lagrange Ave., Poughkeepsie, N. Y. (Electrodeposition, Theoretical Electrochemistry)

R. W. Stiegler, Jr., Texas Instruments, Inc.; Mail add: 530 N. Manus Dr., Dallas, Texas (Electronics)

Student Associate Members

L. S. Lemanski, Polytechnic Institute of Brooklyn; Mail add: International Nickel Co., Inc., 30 Oak St., Bayonne, N. J. (Corrosion)

J. D. E. McIntyre, Dept. of Chemistry, Rensselaer Polytechnic Institute, Troy, N. Y. (Theoretical Electrochemistry)

Reinstatements to Active Membership

R. E. Carr, Dow Chemical Co.; Mail

add: 4010 Lowell Court, Midland, Mich. (Industrial Electrolytic)

P. H. Eisenberg, Raytheon Manufacturing Co.; Mail add: 54 Wyckoff St., Hicksville, N. Y. (Electrothermics & Metallurgy)

M. A. Prieto, American Potash & Chemical Corp.; Mail add: 15734 Wilmaglen Dr., Whittier, Calif. (Battery, Electrodeposition, Electrothermics & Metallurgy, Industrial Electrolytic, Theoretical Electrochemistry)

R. A. Ruscetta, General Electric Co.; Mail add: 719 Rickenbaker Rd., Columbia, S. C. (Electric Insulation)

Transfer from Associate to Active Membership

J. P. Pischel, Mallory Battery Co.; Mail add: 13355 Carrington Ave., Cleveland 35, Ohio (Battery)

Deceased Members

Wilfred Meyer, Berlin-Charlottenburg, Germany

George Smolak, Somerville, N. J.

C. K. Sterrett, Portland, Ore.

John Sumner, Montreal, Que., Canada

M. J. Udy, Niagara Falls, N. Y.

F. W. Woodman, Lake Charles, La.

Personals

Julian Glasser and **William E. Few**, Chattanooga, Tenn., are now associated as consultants in chemical and metallurgical activities, offering personal services to industry and government. Julian Glasser was formerly technical director at Cramet Inc., Chattanooga, and has been operating a personal consulting practice for the past year. William E. Few was formerly technical assistant to the general sales manager, Alloy and Metal Div., Tennessee Products and Chemical Corp., Nashville, Tenn.

E. G. F. Arnott, of the Lamp Div., Westinghouse Electric Corp., Bloomfield, N. J., has asked to be relieved of the administrative duties of his position as director of research for reasons of personal health. He will continue to be active in the division as research-engineering consultant. Mr. Arnott joined Westinghouse in 1933, and in 1940 transferred to the Lamp Div. Research Dept. He is credited with many significant contributions to the success of the division.

Edward B. Saubestre has been promoted to technical director of Enthone, Inc., New Haven, Conn. Dr. Saubestre was associated with Sylvania Electric Products Inc., Bayside, N. Y., before joining Enthone in October 1958 as assistant to the research director. As technical director, he will direct the new Enthonics laboratory, including research, development, and technical service activities.

Maurice Friedman has been appointed vice-president and general manager of the General Instrument Corp.'s Semi-Conductor Division, with plant and headquarters at Newark, N. J. Mr. Friedman, a specialist in semiconductor design and engineering, has headed the division since its formation in 1955. He has spent nearly 20 years in the development and production of electronic and electrochemical components, and holds 19 U. S. and foreign patents in these fields.

Samuel Ruben, inventor of the Mallory mercury battery which powered the radios of the Explorer and Pioneer IV satellites, recently was awarded an honorary doctor of science degree at Butler University's 104th annual commencement. Mr. Ruben attracted international attention when mercury batteries enabled U. S. satellites to transmit messages back to earth from over 400,000 miles in space. The original mercury cells, invented by Mr. Ruben during World War II, were developed and produced by P. R. Mallory & Co., Inc., for use in the famous "handie-talkie" and "walkie-talkie." Since the war, they have been widely used in tiny hearing aids, transistor radios, and pocket recorders. Mr. Ruben is head of Ruben Laboratories in New Rochelle, N. Y.

George Smolak

George Smolak, manager of the Johns-Manville Pipe and Board Dept., Somerville, N. J., died in Somerset Hospital on April 11, 1959. He was 59 years old.

A native of New York City, Mr. Smolak graduated from the University of Idaho as a mining engineer in 1922, and received a master's degree in metallurgical engineering there in 1924.

He received a research fellowship from the U. S. Bureau of Mines at the University of Idaho in 1923, and worked with Idaho companies until 1925 when he joined the General Electric Co. in Schenectady, N. Y., as a research chemist.

In 1927, Mr. Smolak joined the staff of Johns-Manville in Nashua, N. H., going from there to Somerville, N. J., in 1930 to the company's Asbestos Cement Products research center. He became section chief in 1943 and assistant manager of the Pipe and Board Dept. in 1952.

Mr. Smolak was credited with the development of standards of shingle manufacture for Johns-Manville, and with writing the first shingle manufacturing specifications. He also developed the Salem shingle, the first shingle using a wood texturing process, and introduced the improvement of ebony.

He was a member of many professional organizations, including: The Electrochemical Society which he joined in February 1931, the American Chemical Society, American Association for the Advancement of Science, Sigma Psi Fraternity, American Waterworks Association, Society of Chemical Industries, and was a former member of the American Institute of Mining and Metallurgical Engineers.

Maurice C. Taylor

Maurice C. Taylor, owner and director of the Taylor Research Laboratories, Niagara Falls, N. Y., died on June 6, 1959 in Memorial Hospital at the age of 65. He had been in poor health for about a year as the result of a heart attack.

Mr. Taylor was born in Howe, Ind., on February 28, 1894. He studied at Purdue University, receiving his B.S. degree in 1918. During the First World War, he served as a second lieutenant in the Chemical Warfare Service, doing research on poisonous gases at Edgewood Arsenal, Md.

In 1919, he became associated with Mathieson Alkali Works, Inc., as a research chemist, and advanced to resident director of research and development. He retired in 1949 to organize his own laboratories.

He was the inventor or co-inventor of more than 25 products, and author of a number of technical publications dealing with the chlor-alkali industry.

In 1957, Mr. Taylor was awarded the honor scroll of the Niagara Chapter, American Institute of Chemists, "in recognition of his significant contributions to the Niagara Frontier chemical industry and for service to the organization." This was the third time in the Chapter's 25-year history that the award had been made.

Mr. Taylor had been a member of The Electrochemical Society since May 1926. He also was a member of the American Chemical Society, Chemical Society of London, and a fellow of the American Institute of Chemists.

Committees of The Electrochemical Society, Inc., 1959-1960

Admissions Committee

	Term expires
Louis Weisberg, Chairman	Spring 1961
L. I. Gilbertson	Spring 1962
M. F. Quaely	Spring 1963

Publication Committee

H. H. Uhlig, Chairman
C. V. King, Editor of JOURNAL
Norman Hackerman, Technical Editor of JOURNAL
H. A. Laitinen, Editor of Monographs and Special Publications
I. E. Cambell, Secretary

Ways and Means Committee

R. A. Schaefer, Chairman

H. B. Linford	M. F. Quaely
F. L. LaQue	A. C. Haskell
Norman Hackerman	Milton Janes

Finance Committee

L. I. Gilbertson, Chairman

I. E. Campbell	F. L. LaQue
R. A. Schaefer	F. P. Peters

Membership Committee (Personal)

F. W. Koerker, Chairman

Membership Committee (Contributing)

J. T. Owen, Chairman

Honors and Awards Committee

	Term expires
H. M. Scholberg, Chairman	Nov. 1959
R. M. Hunter, Chairman-Elect	Nov. 1960
E. M. Sherwood	Nov. 1960
J. R. Musgrave	Nov. 1961
Abner Brenner	Nov. 1961
H. C. Froelich	Nov. 1962
W. J. Hamer	Nov. 1962
L. O. Case	Nov. 1963
C. L. Faust	Nov. 1963

Palladium Medal Award Committee

	Term expires
H. A. Laitinen, Chairman	Jan. 1960
T. P. May	Jan. 1960
E. B. Yeager	Jan. 1960
H. A. Liebhafsky	Jan. 1962
A. L. Ferguson	Jan. 1962

F. M. Becket Memorial Award Committee

	Term expires
G.M. Butler	1960
I. E. Campbell	1960
L. H. Juel	1961
R. R. Rogers	1961
E. M. Sherwood, Chairman	1962
J. H. Westbrook	1962

Perkin Medal Award Committee

	Term expires
Sherlock Swann, Jr., Chairman	Year ending 1959
Norman Hackerman	Year ending 1959
Alternates: L. I. Gilbertson and C. V. King	
W. C. Gardiner, Chairman	Year ending 1960
Sherlock Swann, Jr.	Year ending 1960
Alternates: L. I. Gilbertson and C. V. King	

Investment Advisory Panel

	Term expires
A. K. Graham, Chairman	Spring 1960
R. M. Hunter	Spring 1961
Hans Thurnauer	Spring 1962
B. F. Field	Spring 1963
E. G. Enck	Spring 1964

Committee for Administration of the Corrosion Handbook Fund

F. L. LaQue—Board Representative
R. M. Burns—Representative of Editorial Advisory Board of Corrosion Handbook
M. A. Streicher, Chairman—Corrosion Division Chairman
H. H. Uhlig—Editor of Corrosion Handbook

Nominating Committee

Charles L. Faust, Chairman

E. B. Yeager	E. M. Sherwood
M. F. Quaely	Ralph Roberts

Resolutions Committee

H. B. Linford

William Blum	Harry R. Copson

Representatives of The ECS to Other Societies

American Association for the Advancement of Science
G. W. Heise—Term expires Spring 1960
Harry Alsentzer—Term expires Spring 1961

American Standards Association
Sectional Committee C-18—C. K. Morehouse
Y-10 and Y-32—W. J. Hamer
C-40—Eugene Willihnganz
C-42—W. C. Vosburgh
C-67—Guy Fetterley
C-34.1—W. E. Gutzwiller

Inter-Society Corrosion Committee

F. W. Fink	K. G. Compton

National Academy of Sciences—National Research Council Advisory Board for the Office of Critical Tables
E. B. Yeager—Term expires June 30, 1961

National Research Council—Division of Chemistry and Chemical Technology
Norman Hackerman—Term expires June 30, 1961

Book Reviews

Metal Finishing Abstracts, Vol. 1, No. 1, Jan./Feb. 1959. Published by Robert Draper Ltd., 85 Udney Park Rd., Teddington, Middlesex, England. 44 pages. Annual subscription (six issues): by surface mail, $15.00; by air mail, $20.00.

This first issue of a new bimonthly publication is in compact abstract form a world-wide coverage of the metal finishing literature. The abstracts are conveniently grouped under 20 separate headings which are: Metal Cleaning, Pickling and Etching, Mechanical Treatments, Electro- and Chemical Polishing, Electroplating, Chemical Plating, Anodic Oxidation, Chemical Conversion Coatings, Hot Dip Metal Coatings, Diffusion Coatings, Organic Finishing, Organic Coatings, Plastics and Rubber, Vitreous Enamels and Ceramic Coatings, Tests and Analyses, Regeneration and Waste Disposal, Corrosion and Electrochemistry, and Miscellaneous.

This publication should be of considerable value to those in the metal finishing industries who wish to keep abreast of new developments in the field.

Henry S. Myers

EDTA Titrations; An Introduction to Theory and Practice, by H. A. Flaschka. Published by Pergamon Press Inc., New York City, 1959. 138 pages; $6.50.

The tremendous increase in the analytical applications of ethylene diamine tetraacetic acid (more than 1200 papers which have appeared since 1930 and through 1958) definitely warrants a compilation of the properties and uses of this remarkable reagent. Dr. Flaschka, who has been a major contributor in this field, has done an admirable job in presenting this subject in a clear and concise manner.

This book can serve as an introductory textbook for classroom use and as a practical laboratory manual for the routine determination of many of the elements. There is a brief but adequate treatment of complex formation and a discussion of the stability constants. Directions for several demonstration experiments, which can serve to illustrate the properties of EDTA, are carefully described.

Chapters on titration curves, metal indicators and end-point detection, on various types of titrations and on the selectivity of titrations, are included. Also, there are directions for the preparation of standard solutions of EDTA, reagents, and other solutions. Examples of many types of titrations, such as direct and back-titrations, polarographic, potentiometric, and photometric titrations are given.

In the Appendix are found 52 interesting questions on EDTA and 12 numerical problems with answers. Each chapter has up-to-date references and there is an author and subject index.

This small book should serve to stimulate further interest in the use of EDTA as an analytical reagent.

Barnet Naiman

Semiconductors. Edited by N. B. Hannay. Published by Reinhold Publishing Corp., New York City, 1959. 770 pages; $15.00.

The chemist working in the field of semiconductors finds that most of the available reference works in this field are written from the point of view of the physicist or the engineer. This volume (which is the American Chemical Society Monograph 140) is written for the chemist. It consists of 17 chapters, each constituting an article on a given topic by a distinguished researcher. The emphasis is on the chemical aspects of semiconducting materials, although the basic physics is also treated. While many of the contributions constitute valuable reviews, several chapters contain material not available elsewhere. The chapter by Howard Reiss and C. S. Fuller on Diffusion Processes in Germanium and Silicon, the chapter on Organic Semiconductors by C. G. Garrett, and the contribution by J. F. Dewald on Semiconductor Electrodes struck this reviewer as unusually valuable.

This book would be an important addition to the library of chemists who would like to introduce themselves to this exciting field. It would be indispensable to any chemist directly connected with semiconductor work.

Benson R. Sundheim

Surface Phenomena in Chemistry and Biology. Edited by J. F. Danielli, K. G. A. Pankhurst, and A. C. Riddiford. Published by Pergamon Press Inc., New York City, 1958. 330 pages; $10.00.

Most of the 23 essays and articles in this fascinating little book are not directly connected with electrochemistry, as such, and even the articles which do have some pertinence are mainly of interest to the theoretician. Nevertheless, I would make the book required collateral reading for all students of electrochemistry.

The individual articles are interesting, informative, and well-documented discussions of particular aspects of surface chemistry and biology, as one would expect from such authors as Alexander, Davies, Frumkin, Rideal, Schulman, and Riddiford. But more than this, the collection in one volume of articles on such diverse topics as "Surface Structure in Liquid Crystals," "Heterogeneity of Metal Surfaces," and "The Surface Behavior of Mycobacterium Phlei" is of value in itself. The reader gains an understanding of the problems and methods of the man working the other side of the same street and perhaps a sharper insight into his own problems. Books like this are valuable antidotes against the disease of overspecialization.

The articles of most direct interest are those on hydrogen bonding in surface films, monolayers of long chain ions, detergency in the atomic energy industry, the adsorption of thallous ions and thallium atoms at the mercury-solution interface, and the heterogeneity of metal surfaces. Each article has its own bibliography, some more extensive than others, through 1957.

H. W. Salzberg

Two New Volumes Available in ECS Series

The Electrochemical Society is pleased to announce the availability of the following two new volumes in The Electrochemical Society Series:

Semiconductor Abstracts, 1956 Issue, Volume IV, Abstracts of Literature on Semiconducting and Luminescent Materials and Their Applications, edited by E. Paskell. Price: $12.00. (A review of the 1956 Issue appears on page 131C of the May JOURNAL.)

Also available is **The Structure of Electrolytic Solutions,** edited by Walter J. Hamer; based on a symposium held in Washington, D. C., in May 1957, sponsored by The Electrochemical Society, New York, and The National Science Foundation, Washington, D. C. Price: $18.50. The subjects covered include a wide range of topics relating to the properties of electrolytic solutions, and represent the significant items under investigation in the present age.

Both volumes are available from the publisher, John Wiley & Sons, Inc., 440 Fourth Ave., New York 16, N. Y. *A 33 1/3% discount is offered*

to Electrochemical Society members only and can be obtained by ordering through Society Headquarters, 1860 Broadway, New York 23, N. Y.

News Items

New ECS Sustaining Members

The following recently became Sustaining Members of The Electrochemical Society:

Exmet Corp., Tuckahoe, N. Y.

Foote Mineral Co., Paoli, Pa.

Rheem Semiconductor Corp., Mountain View, Calif.

Three Point One Four Corp., Yonkers, N. Y.

Thirteenth Annual Power Sources Conference

The Thirteenth Annual Power Sources Conference, sponsored by the U. S. Army Signal R & D Laboratory, was held on April 28, 29, and 30, in Atlantic City, N. J. A complete summary of the papers presented will appear in the September JOURNAL.

Max E. Bretschger Recipient of 1959 Schoellkopf Award

Dr. Max E. Bretschger, winner of the 1959 Schoellkopf Award, discussed "Forty Years of Progress in the Manufacture of Electrolytic Hydrogen Peroxide" in accepting his award on May 19, 1959. He related his most interesting background, both in Europe and in this country, in the development of more efficient methods for producing hydrogen peroxide. He particularly emphasized the necessity for a strong research and development program to maintain technological pace with economic requirements. He also cited the urgent need for more efficient utilization of scientific and technically trained manpower.

The Award is presented annually by the Western New York Section of the American Chemical Society. Dr. Bretschger received the medal for ". . . his outstanding leadership in research and development resulting in the production of concentrated hydrogen peroxide by the ammonium persulfate process, and for his guidance and planning in the establishment and growth of technical education at the two year college level."

Dr. Bretschger is now semiretired, holding the position of senior technical advisor to the Becco Chemical Division of Food Machinery and Chemical Corp.

The Award was presented by J. Fred Schoellkopf, IV, great-grandson of the original Award donor, at the Tuesday evening Award Dinner held at the Continental Inn in Buffalo, N. Y.

French Scientist Cited by Westinghouse for New Light Source

A Westinghouse citation for outstanding scientific achievement was presented on May 7 to a French scientist, Professor Georges Destriau (center) who discovered the phenomenon of electroluminescence, man's newest light source. Presenting the citation are F. M. Sloan, Westinghouse vice-president (left), and Dr. R. M. Zabel, Westinghouse lamp division engineering manager.

Professor Destriau, a Westinghouse consultant, visited the United States to present a paper before The Electrochemical Society meeting in Philadelphia. Electroluminescence, the production of visible light by direct application of an electric field to a phosphor material, was first discovered by the University of Paris professor in 1936.

New Fuel Cell Developed at G.E. Research Laboratory

W. Thomas Grubb and Leonard W. Niedrach of the General Electric Research Laboratory at Schenectady, N. Y., recently described a new design of fuel cell which they have developed.

The broad principles of this device are common to all fuel cells, but the type described is novel in employing an *ion exchange membrane* as an electrolyte. This has an advantage over aqueous electrolytes, in that the electrolytically conducting ions are "locked in" and cannot be leached from the cell. These membranes also reject water when they reach saturation and, therefore, no difficulty is experienced from dilution effects. These features combine to simplify the operation of the cell because they provide built-in controls for maintaining the electrolyte concentration and the water balance.

In addition, the electrolyte may be *acidic*, consisting of a cation exchange resin in its hydrogen form. The use of an acidic electrolyte makes it possible to use gases containing carbon dioxide, e.g., air.

In cells using caustic electrolytes, such as potassium hydroxide, the hydroxyl ion is the charge carrier, and the water produced by the net cell reaction forms at the fuel electrode. In the present device, the hydrogen ion is the charge carrier, and the water forms at the oxidant electrode. This is advantageous when the cell is operated on air, since the water can be disposed of by controlled evaporation.

Among the other features that should be noted are the following: the solid polymer electrolyte makes possible very compact cell structure, operation on static heads of gas is possible, no moving parts are involved, and close tolerances are not involved in the construction of the cell.

A number of cells have been operating continuously for from 75 to 100 days, and these tests have not yet been concluded. One cell has operated for more than 100 days, and is still running. Two cells have been operated with their cathodes exposed to the air; one of them is still running after more than 75 days. Portions of these tests have

The Lepel line of induction heating equipment represents the most advanced thought in the field of electronics as well as the most practical and efficient source of heat yet developed for numerous industrial applications.

If you are interested in induction heating you are invited to send samples of the work with specifications. Our engineers will process and return the completed job with full data and recommendations without any cost or obligations

FLOATING ZONE FIXTURE FOR METAL REFINING AND CRYSTAL GROWING

A new floating zone fixture for the production of ultra-high purity metals and semi-conductor materials. Purification or crystal growing is achieved by traversing a narrow molten zone along the length of the process bar while it is being supported vertically in vacuum or inert gas. Designed primarily for production purposes, Model HCP also provides great flexibility for laboratory studies.

Features

- A smooth, positive mechanical drive system with continuously variable up, down and rotational speeds, all independently controlled.
- An arrangement to rapidly center the process bar within a straight walled quartz tube supported between gas-tight, water-cooled end plates. Placement of the quartz tube is rather simple and adapters can be used to accomodate larger diameter tubes for larger process bars.
- Continuous water cooling for the outside of the quartz tube during operation.
- Assembly and dis-assemby of this system including removal of the completed process bar is simple and rapid.

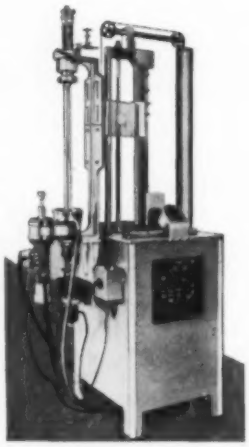

Model HCP

Electronic Tube Generators from 1 kw to 100 kw.
Spark Gap Converters from 2 kw to 30 kw.

WRITE FOR THE NEW LEPEL CATALOG . . . . 36 illustrated pages packed with valuable information.

All Lepel equipment is certified to comply with the requirements of the Federal Communications Commission.

LEPEL HIGH FREQUENCY LABORATORIES, INC.
55th STREET and 37th AVENUE WOODSIDE 77, NEW YORK CITY, N. Y.

been conducted at current densities of 30 ma/cm², although most of the operation has been at lower current densities.

The cells have been operated mainly on commercially available hydrogen and oxygen at room temperature and normal atmospheric pressure. Thermal efficiences over 60% have been obtained.

Because of the thinness of the cell itself and the small size of the gas chambers, the performance of the cell in terms of net power per unit weight (or per unit volume) is attractive. Power densities of the order of 1 to 2 kw per ft³ have been calculated on the basis of present data.

Flexible Inorganic Films Provide High-Temperature Electrical Insulation

Many potentially important applications of electrical circuitry at high temperatures are at present hindered by the lack of high-quality flexible wire insulation. Recent discoveries at Bell Telephone Laboratories indicate that fluoride coatings can be formed on copper, aluminum, and other metal wires which will provide exceptionally high insulation value at elevated temperatures, while retaining flexibility and freedom from porosity.

According to a paper by Drs. Steward S. Flaschen and Paul D. Garn, the insulating coatings are formed directly on freshly cleaned copper or aluminum by exposing them to oxidizing carriers of fluorine such as hydrogen fluoride or elemental fluorine at temperatures from 300° to 600°C. The thickness of the resulting copper fluoride and aluminum fluoride films depends on the temperature at which they are formed, the concentration of fluorine, and the time of exposure. Aluminum forms a fluoride film 1μ thick in a few minutes at 550°C. These films remain adherent when bent repeatedly at 90° angles.

Electrical insulation values are very high for both copper and aluminum films, being in the order of 10^{10} and 10^{11} ohms at room temperature for films in the order of 1 to 2 μ thick, between probe electrodes ¼ in. in diameter. The films retain their excellent insulating properties at high temperatures. For example, aluminum fluoride films exhibit resistances of about 7×10^5 ohms at temperatures as high as 500°C.

The aluminum fluoride films show excellent resistance to oxidation even above 600°C. They also show

no tendency to hydrate or dissolve on exposure to high humidity. The insulation does not break down even at 450 v at 500°C.

The best organic insulating coatings cannot be used continuously above 300°C. Inorganic insulators are generally porous and nonflexible, although some may be used as high as 830°C. Insulating fluoride coatings should be satisfactory almost up to the melting point of the conductor.

Chemical Industries Prepare for 27th Biennial Exposition

More than 450 manufacturers had already engaged space in June for displays at the 27th Exposition of Chemical Industries, representing a large proportion of the entire area available on the four floors of the New York Coliseum, where the Exposition will be held November 30 to December 4, 1959.

Since 1915, this biennial Exposition has provided a market place for the practical advancement of all the mechanical arts, since the penetration of chemistry is universal throughout industry. Displays include chemical processing equipment, chemical materials, and the metals, plastics, and other substances employed in mechanical construction of every kind, as well as functional units and component parts.

Visitors register from the entire United States and from many points north and south of the border, as well as from overseas—from some 40 foreign countries, according to the latest analysis. Registered admissions, exclusive of exposition personnel, totalled upward of 40,000 at the last Exposition, two years ago.

Admission is by invitation and registration only. The general public will not be admitted.

Transistor Diodes Spearhead Electronic Advance

"Transistor diodes, tiny 'circuits within themselves' which outperform their conventional transistor counterparts, are spearheading an important new advance in electronics," declared William Shockley, co-inventor of the transistor, in an opening lecture on May 21 at the International Convention on Transistors and Associated Semiconductor Products in London, England.

Four-layer transistor diodes are the first commercially available examples of solid-state circuitry. They can be used to replace more complex transistor circuitry, saving space and weight, or to replace relays or switches, eliminating moving parts in applications of transistor diodes ranging from household electrical appliances to computers and missile control systems.

Dr. Shockley said the diodes are based on "new principles of transistor operation which permit internal control action in place of the external control required for conventional transistors." Because of this simplification, he said, transistor diodes require only two wire connections instead of the three used by transistors. Whereas some circuits previously required two or more transistors as well as other components and connections, this is now done within a single silicon chip smaller than a typewritten period on a piece of paper.

The four-layer transistor diode, now in its second year of commercial production, is doing many important jobs, he reported. He cited its "outstanding performance" in a new high-speed digital computer which takes approximately one millionth of a second to extract any one of 80,000 bits of information from its magnetic memory cores.

Recent experiments indicate that within two to three years transistor diodes will attain power levels from 10 to 100 times higher than related transistors with comparable frequencies and efficiencies, Dr. Shockley predicted.

Bright Star Industries to Expand Electrolytic Manganese Dioxide Manufacturing Facilities

Bright Star Industries, manufacturers of dry batteries and flashlights, broke ground in June for a new building to enable the company to double its output of electrolytic manganese dioxide. This material is a basic ingredient of dry batteries, especially high-voltage types. The new building will be located at the Clifton, N. J., factory of Bright Star Industries, adjoining the present Electrolytic Manganese Dioxide Plant. Also included will be a new analytical laboratory to handle the increased work for the quality control laboratories due to the new expanded facilities.

NCE Research Foundation Directors Announced

The trustees of Newark College of Engineering recently announced the names of 15 men who will serve as the Board of Directors of a newly established Newark College of Engi-

Since 1861
AMES has been making these
SILVER SALTS
to YOUR specifications

Silver Nitrate
Silver Cyanide
Silver Chloride
Silver Sulfate
Monovalent Silver Oxide
Divalent Silver Oxide

And now for your Battery
Silver Flour
and
for powder metallurgy
Nodular Silver

M. AMES CHEMICAL WORKS, INC.
17-19 Rogers Street
Glen Falls, New York
Phone 2-4394

neering Research Foundation, made possible by the recent gift to NCE of $300,000 by Thomas M. Cole, president of the Federal Pacific Electric Co. of Newark.

Dr. Edward F. Weston, chairman of the college board, stated that, in accordance with the articles of incorporation, eight of the directors are closely related to the college in one capacity or another and seven are representatives of industry and the professions.

Dr. James B. Fisk, president of Bell Telephone Laboratories, will serve as chairman of the new board, Dr. Weston said. The officers of the foundation, who are also board members, are Dr. Robert W. Van Houten, president of NCE, president; Walther H. Feldman, president of Worthington Corp., vice-president; Dr. Donald C. Luce, president of Public Service Electric & Gas Co., vice-president; Dr. Robert G. Cowan, president of National Newark & Essex Banking Co., treasurer; and William Hazell, dean of administration at NCE, assistant secretary. Dr. Joseph Joffe, professor of chemical engineering at NCE, and director of research for the foundation, will serve as secretary.

The board also includes Roy H. Anderson, manager of research, Singer Manufacturing Co., an alumnus; Mr. Cole; Frederick Frelinghuysen, a partner in the law firm of Pitney, Hardin, and Ward; George W. Jernstedt, manager of headquarters manufacturing planning, Westinghouse Electric Corp., an alumnus; Kenneth H. Klipstein, executive vice-president, American Cyanamid Co.; Dr. Charles L. Mantell, chairman, Dept. of Chemical Engineering, Dr. Irving P. Orens, chairman, Graduate Division, and Dr. Frederick A. Russell, chairman, Dept. of Electrical Engineering, all of Newark College of Engineering; and Dr. Weston, who is chairman of the board, retired, of the Weston Electrical Instrument Corp., now the Weston Division of Daystrom, Inc. Dr. Cowan and Dr. Luce are also members of the college's board of trustees.

The foundation has as its three main objectives the creation of opportunities for the professional development of the teaching staff of Newark College of Engineering by providing its members with broadly fundamental research activities in science and engineering; the attraction of capable young engineering graduates to the engineering teaching profession by offering them a combined program of education, teaching, and research; and the development of programs at the college to assist secondary school teachers of science and mathematics in their own professional advancement.

The college expects to have approximately 25 faculty research projects under way by September, Dr. Weston said, and will be ready to institute its various instructional programs at the same time.

Liquid Hydrogen Plant to be Built at Torrance, Calif.

Union Carbide Corp.'s division, Linde Co., will build a liquid hydrogen producing plant at Torrance, Calif. Construction of the plant will be completed in one year.

The National Aeronautics and Space Administration recently awarded a contract for the supply of liquid hydrogen, under the terms of which Linde will supply NASA up to 3,300,000 pounds of liquid hydrogen per year.

The most advanced cryogenic container designs and insulating techniques will be used in the construction of trailers to transport the

CHEMIST

M.S., B.S. with 2 to 5 years' experience in Electro Chemistry and/or Electro Plating. Work involves Bench Research in Plating.

Excellent employee benefits and professional advancement in a growing medium-sized corporation.

Submit complete resume including salary requirements to:

Recruiting Department
300 Union Commerce Building
Cleveland 14, Ohio

DIAMOND ALKALI COMPANY

GROWTH OPENINGS IN RESEARCH

International Resistance Company

One of the fastest growing companies in the electronics field requires 3 Senior Research Managers.

MANAGER, CERAMIC RESEARCH
strong background in ceramic materials for the electronics industry.

MANAGER, SEMI-CONDUCTOR RESEARCH
capable of leading basic studies in thin film semi-conductor field.

MANAGER, APPLIED SEMI-CONDUCTOR & MICROMINIATURIZATION
background in integrated mollecular circuitry important.

All positions require a PhD or equivalent and a proven record of accomplishment, HIGH SALARIES are commensurate with record.

FOR DETAILS IN CONFIDENCE
PLEASE CALL COLLECT—WAlnut 2-2166 (Ext. 357 Phila.)
or write Technical Employment

IRC
INTERNATIONAL RESISTANCE COMPANY
401 North Broad St., Philadelphia 8, Pa.

liquid hydrogen. These large (7800-gal capacity) trailers will be fabricated at the Linde factory in Tonawanda, N. Y. Not only is the Tonawanda factory rich in cryogenic construction techniques and experience, but it is adjacent to Linde's low-temperature research and engineering laboratories where advanced work on cryogenic equipment design has been going on for more than 30 years.

Employment Situations

Positions Available

Engineers (Aeronautical, Electrical, Electronic, Industrial, General, Mechanical, and Power Plant), **Electronic Scientists, Metallurgists, Physicists, Technologists**—Vacancies exist for professional personnel in the above positions. Starting salaries range from $4490 per annum to $10,130 per annum. The Naval Air Material Center is currently engaged in an extensive program of aeronautical research, development, experimentation, and test operations for the advancement of Naval aviation. Experimental work is also being conducted in the guided missile field. Personnel are needed for work on projects involving modification, overhauling, and testing of aeronautical equipment, materials, accessories, power plants, launching and arresting devices, and for modification and structural testing of aircraft. Also, for work involving the basic design of catapults, launchers, arresting gear and their component parts; test and development work at shore stations and on board U. S. Navy ships; evaluation of new equipment and establishment of performance parameters, and applied research on the many problems relevant to this field.

Interested persons should file an Application for Federal Employment, Standard Form 57, with the Industrial Relations Dept., Naval Air Material Center, Naval Base, Philadelphia 12, Pa. Applications may be obtained from the above address, or information as to where they are available may be obtained from any first or second class post office.

Research Chemists—Our new and modern division in San Fernando Valley, Calif., has permanent positions for creative photochemists, electrochemists, and physical chemists for research and long-range military and nonmilitary investigation into the use of thermal, electrochemical, and photochemical power for space vehicle applications. Please submit résumé. All replies confidential. Sundstrand Turbo, 10445 Glenoaks Bldg., Pacoima, Calif. (A Division of Sundstrand Corporation).

Electronic Engineers and Physicists—For research or engineering in silicon and other semiconductor materials, developing methods and instruments for measuring physical properties, automatic control equipment for manufacture and evaluating new materials. Expanding activity offers good opportunities in St. Louis Research and Engineering Center. Replies held in confidence. Write to Dept. M-101, W. R. Hayes, Asst. Director of Personnel, Inorganic Division, Monsanto Chemical Co., St. Louis 66, Mo.

ELECTRO CHEMIST

Graduate chemist needed with experience with electrolytic equipment and high temperature electrolysis. Also desire experience with electroplating processes.

Dynamic organization can offer excellent opportunity and tremendous potential to ambitious person. Full benefit program offered. Age to 45.

Send resume to attention of Employment Manager:

THE BRUSH BERYLLIUM COMPANY
Elmore, Ohio

Advertiser's Index

M. Ames Chemical Works, Inc. 229C
The Brush Beryllium Company 231C
Diamond Alkali Company 230C
E. I. du Pont de Nemours & Company (Inc.) 182C
Enthone, Incorporated ..... Cover 4
Grace Electronic Chemicals, Inc. ..... -87C
Great Lakes Carbon Corp., Electrode Division ..... Cover 2
International Resistance Company 230C
Keithley Instruments, Inc. 186C
Lepel High Frequency Laboratories, Inc. 228C
Lockheed Missiles & Space Division 231C
E. H. Sargent & Company 184C
Stackpole Carbon Company 183C

Expanding the Frontiers of Space Technology in

SOLID STATE ELECTRONICS

■ At Lockheed Missiles and Space Division, solid state electronics encompasses a wide range of activities. Solid state physics concerns itself with theoretical and experimental work in the areas of thermoelectric and radiant energy conversion; paramagnetic resonance studies in solids, ferromagnetics and ferroelectrics; transport processes in solids; electroluminescent and other phosphors; radiation effects in semiconductors; and other related topics.

In solid state devices, the basic work applies to the evaluation of environmental effects, and the study of new components based on ferrites, ferroelectrics, thin films, semiconductors, intermetallic compounds, and other solid state materials.

Advanced development work in high-energy batteries and fuel cells has resulted in a method for converting chemical energy directly into electrical power that promises a fuel utilization of almost 100% and an energy conversion efficiency of 70% or better.

ENGINEERS AND SCIENTISTS

Lockheed Missiles and Space Division programs reach far into the future and deal with unknown and challenging environments. If you are experienced in one of the above areas, or in related work, you are invited to share in the rewards of a company that has an outstanding record of achievement, and make an important individual contribution to your country's progress in the race for space. Write: Research and Development Staff, Dept. H-26, 962 W. El Camino Real, Sunnyvale, California. U.S. citizenship required.

Lockheed

MISSILES AND SPACE DIVISION

Systems Manager for the Navy POLARIS FBM; DISCOVERER SATELLITE; Army KINGFISHER; Air Force Q-5 and X-7

SUNNYVALE, PALO ALTO, VAN NUYS, SANTA CRUZ, SANTA MARIA, CALIFORNIA
CAPE CANAVERAL, FLORIDA
ALAMOGORDO, NEW MEXICO • HAWAII

The Electrochemical Society

INSTRUCTIONS TO AUTHORS OF PAPERS

Address all correspondence to the Editor, JOURNAL OF THE ELECTROCHEMICAL SOCIETY, 1860 BROADWAY, NEW YORK 23, N. Y.

FORM

Manuscripts submitted for publication should be in triplicate to expedite review. They should be typewritten, double-spaced, with 2½-4 cm (1-1½ in.) margins.

Title should be brief, followed by the author's name and his business or university connection.

Abstract of about 100 words should state the scope of the paper and give a brief summary of results.

ILLUSTRATIONS

Drawings will be reduced to column width, 8.3 cm (3¼ in.), after reduction should have lettering at least 0.15 cm (1/16 in.) high. Original drawings in India ink on tracing cloth or white paper are preferred. Curves may be drawn on coordinate paper only if the paper is ruled in blue. All lettering must be of lettering-guide quality. See sample drawing on reverse page.

Photographs must be glossy prints and mounted flat.

Captions for all figures must be included on a separate sheet. Captions and figure numbers should not appear in the body of the figure.

General—Figures should be used only when necessary. Omit drawings or photographs of familiar equipment. Figures from other publications are to be used only when the publication is not readily available, and should always be accompanied with written permission for reprinting.

SYMBOLS

If more than a few symbols are used, these should be defined in a list at the end of the paper, for example:

$a, b \ldots$ = empirical constants of Brown equation
f_i = fugacity of pure ith component, atm
D_e = bulk diffusion coefficient, cm^2/sec

REFERENCES

Literature and patent references should be listed at the end of the paper on a separate sheet, in the order in which they are cited. They should be given in the style adopted by *Chemical Abstracts*. For example:

R. Freas, *Trans. Electrochem. Soc.*, **40**, 109 (1921).

H. T. S. Britton, "Hydrogen Ions," Vol **1**, p. 309, D. Van Nostrand Co., New York (1943).

H. F. Weiss (To Wood Conversion Co.), U. S. Pat. 1,695,445, Dec. 18, 1928.

UNITS OF MEASUREMENT

Metric units should be used throughout but, where desirable, English units may be given in parentheses.

Corrosion rates in the metric system should preferably be expressed as milligrams per square decimeter per day (mdd), and in the English system as inches penetration per year (ipy).

In reporting electrode potentials, the sign of the standard Zn/Zn^{++} electrode potential should be taken as negative; Cu/Cu^{++} as positive.

ABBREVIATIONS

Abbreviations should conform with the American Standards Association's list of "Abbreviations for Scientific and Engineering Terms."

GENERAL

Authors should be as brief as is consistent with clarity, and must omit all material which can be regarded as familiar to specialists in the particular field.

The use of proprietary names, trade-marks, and trade names should be avoided if possible. If used, these should be capitalized so that the owner's legal rights are not jeopardized.

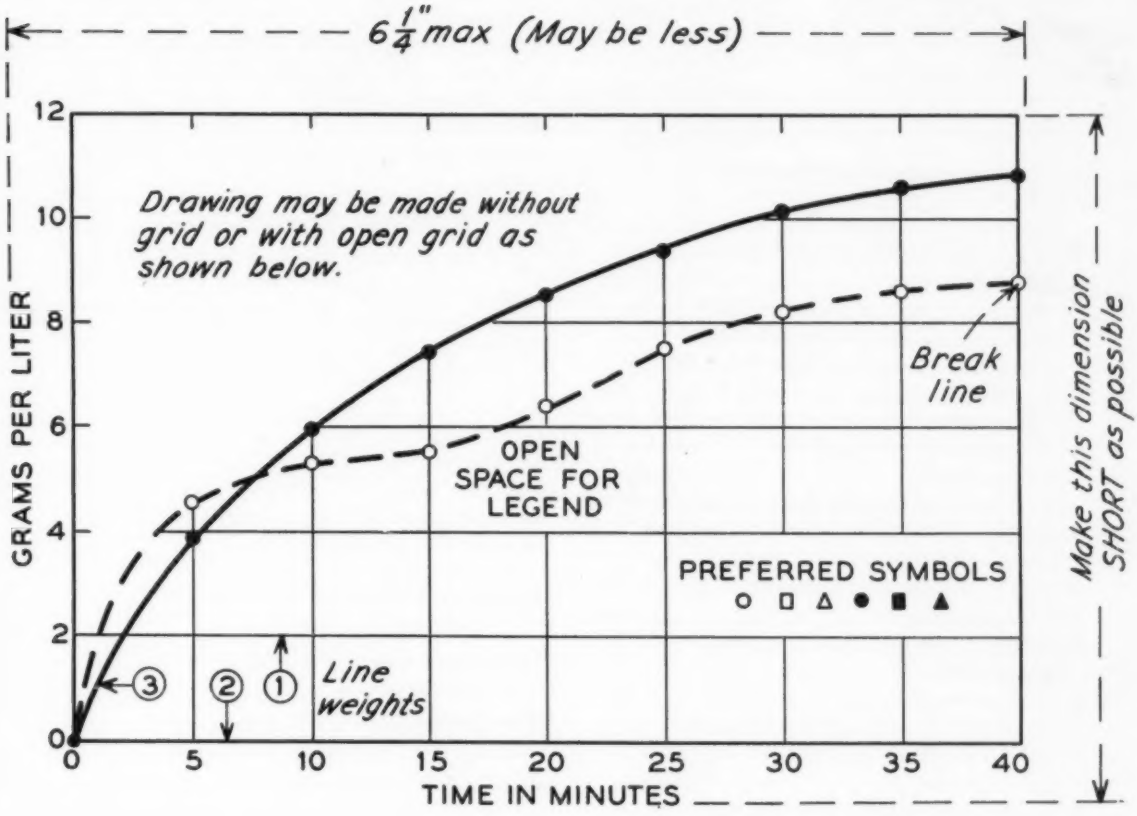
6 1/4" max (May be less)
Drawing may be made without grid or with open grid as shown below.
GRAMS PER LITER
TIME IN MINUTES
Break line
OPEN SPACE FOR LEGEND
PREFERRED SYMBOLS
Line weights
Make this dimension SHORT as possible

Remarks: Line weight 2 is used for borders and zero lines. When several curves are shown, each may be numbered and described in the caption. Lettering shown is approximately ⅛ in. In plotting current or potential as ordinate, increasing negative values should go down.

SAMPLE CURVE DRAWING FOR REDUCTION TO $\frac{1}{2}$ SIZE

The Electrochemical Society

Patron Members

Aluminum Co. of Canada, Ltd.,
Montreal, Que., Canada
International Nickel Co., Inc.,
New York, N. Y.
Olin Mathieson Chemical Corp.,
Niagara Falls, N. Y.
Industrial Chemicals Div., Research
and Development Dept.
Union Carbide Corp.
Divisions:
Union Carbide Metals Co.,
New York, N. Y.
National Carbon Co., New York, N. Y.
Westinghouse Electric Corp., Pittsburgh, Pa.

Sustaining Members

Air Reduction Co., Inc.,
New York, N. Y.
Ajax Electro Metallurgical Corp.,
Philadelphia, Pa.
Allen-Bradley Co., Milwaukee, Wis.
Allied Chemical & Dye Corp.
General Chemical Div., Morristown, N. J.
Solvay Process Div., Syracuse, N. Y.
(3 memberships)
Allied Research Products, Inc.,
Detroit, Mich.
Alloy Steel Products Co., Inc., Linden, N. J.
Aluminum Co. of America,
New Kensington, Pa.
American Machine & Foundry Co.,
Raleigh, N. C.
American Metal Climax, Inc.,
New York, N. Y.
American Potash & Chemical Corp.,
Los Angeles, Calif. (2 memberships)
American Zinc Co. of Illinois,
East St. Louis, Ill.
American Zinc, Lead & Smelting Co.,
St. Louis, Mo.
American Zinc Oxide Co., Columbus, Ohio
M. Ames Chemical Works, Inc.,
Glens Falls, N. Y.
Auto City Plating Company Foundation,
Detroit, Mich.
Basic Inc., Maple Grove, Ohio
Bell Telephone Laboratories, Inc.,
New York, N. Y. (2 memberships)
Bethlehem Steel Co., Bethlehem, Pa.
(2 memberships)
Boeing Airplane Co., Seattle, Wash.
Burgess Battery Co., Freeport, Ill.
(4 memberships)
C & D Batteries, Inc., Conshohocken, Pa.
Canadian Industries Ltd., Montreal, Que.,
Canada
Carborundum Co., Niagara Falls, N. Y.
Catalyst Research Corp., Baltimore, Md.
Chrysler Corp., Detroit, Mich.
Ciba Pharmaceutical Products, Inc., Summit,
N. J.
Columbian Carbon Co., New York, N. Y.
Columbia-Southern Chemical Corp.,
Pittsburgh, Pa.
Consolidated Mining & Smelting Co. of
Canada, Ltd., Trail, B. C., Canada
(2 memberships)
Continental Can Co., Inc., Chicago, Ill.
Cooper Metallurgical Associates, Cleveland,
Ohio
Corning Glass Works, Corning, N. Y.
Crane Co., Chicago, Ill.
Diamond Alkali Co., Painesville, Ohio
(2 memberships)
Dow Chemical Co., Midland, Mich.
Wilbur B. Driver Co., Newark, N. J.
(2 memberships)
E. I. du Pont de Nemours & Co., Inc.,
Wilmington, Del.
Eagle-Picher Co., Chemical Div., Joplin, Mo.
Eastman Kodak Co., Rochester, N. Y.
Electric Auto-Lite Co., Toledo, Ohio
Electric Storage Battery Co.,
Philadelphia, Pa.
Englehard Industries, Inc., Newark, N. J.
(2 memberships)
The Eppley Laboratory, Inc., Newport, R. I.
(2 memberships)
Erie Resistor Corp., Erie, Pa.
Exmet Corp., Tuckahoe, N.Y.
Fairchild Semiconductor Corp., Palo Alto,
Calif.
Federal Telecommunication Laboratories,
Nutley, N. J.
Food Machinery & Chemical Corp.
Becco Chemical Div., Buffalo, N. Y.
Westvaco Chlor-Alkali Div., South
Charleston, W. Va.
Foote Mineral Co., Paoli, Pa.
Ford Motor Co., Dearborn, Mich.
General Electric Co., Schenectady, N. Y.
Chemistry & Chemical Engineering
Component, General Engineering
Laboratory
Chemistry Research Dept.

(Sustaining Members cont'd)

General Electric Co. (cont'd)
- General Physics Research Dept.
- Metallurgy & Ceramics Research Dept.

General Motors Corp.
- Brown-Lipe-Chapin Div., Syracuse, N. Y. (2 memberships)
- Guide Lamp Div., Anderson, Ind.
- Research Laboratories Div., Detroit, Mich.

General Transistor Corp., Jamaica, N. Y.
Gillette Safety Razor Co., Boston, Mass.
Gould-National Batteries, Inc., Depew, N. Y.
Grace Electronic Chemicals, Inc., Baltimore, Md.
Great Lakes Carbon Corp., New York, N. Y.
Hanson-Van Winkle-Munning Co., Matawan, N. J. (3 memberships)
Harshaw Chemical Co., Cleveland, Ohio (2 memberships)
Hercules Powder Co., Wilmington, Del.
Hill Cross Co., Inc., New York, N. Y.
Hoffman Electronics Corp., Evanston, Ill.
Hooker Chemical Corp., Niagara Falls, N. Y. (3 memberships)
Houdaille Industries, Inc., Detroit, Mich.
Hughes Aircraft Co., Culver City, Calif.
International Business Machines Corp., Poughkeepsie, N. Y.
International Minerals & Chemical Corp., Chicago, Ill.
Jones & Laughlin Steel Corp., Pittsburgh, Pa.
K. W. Battery Co., Skokie, Ill.
Kaiser Aluminum & Chemical Corp.
- Chemical Research Dept., Permanente, Calif.
- Div. of Metallurgical Research, Spokane, Wash.

Kennecott Copper Corp., New York, N. Y.
Keokuk Electro-Metals Co., Keokuk, Iowa
Libbey-Owens-Ford Glass Co., Toledo, Ohio
P. R. Mallory & Co., Indianapolis, Ind.
McGean Chemical Co., Cleveland, Ohio
Merck & Co., Inc., Rahway, N. J.
Metal & Thermit Corp., Detroit, Mich.
Metals and Controls Corp., Attleboro, Mass.
Minnesota Mining & Manufacturing Co., St. Paul, Minn.
Monsanto Chemical Co., St. Louis, Mo.
Motorola, Inc., Chicago, Ill.
National Cash Register Co., Dayton, Ohio
National Lead Co., New York, N. Y.
National Research Corp., Cambridge, Mass.
National Steel Corp., Weirton, W. Va.
New York Air Brake Co., Vacuum Equipment Div., Camden, N. J.
Northern Electric Co., Montreal, Que., Canada
Norton Co., Worcester, Mass.
Olin Mathieson Chemical Corp., Niagara Falls, N. Y.
- High Energy Fuels Organization (2 memberships)

Pennsalt Chemicals Corp., Philadelphia, Pa.
Phelps Dodge Refining Corp., Maspeth, N. Y.
Philco Corp., Philadelphia, Pa.
Philips Laboratories, Inc., Irvington-on-Hudson, N. Y.
Pittsburgh Metallurgical Co., Inc., Niagara Falls, N. Y.
Poor & Co., Promat Div., Waukegan, Ill.
Potash Co. of America, Carlsbad, N. Mex.
Radio Corp. of America, Harrison, N. J.
Ray-O-Vac Co., Madison, Wis.
Raytheon Manufacturing Co., Waltham, Mass.
Reynolds Metals Co., Richmond, Va. (2 memberships)
Rheem Semiconductor Corp., Mountain View, Calif.
Schering Corporation, Bloomfield, N. J.
Shawinigan Chemicals Ltd., Montreal, Que., Canada
Speer Carbon Co.
- International Graphite & Electrode Div., St. Marys, Pa. (2 memberships)

Sprague Electric Co., North Adams, Mass.
Stackpole Carbon Co., St. Marys, Pa.
Stauffer Chemical Co., New York, N. Y.
Sumner Chemical Co., Div. of Miles Laboratories, Inc., Elkhart, Ind.
Sylvania Electric Products Inc., Bayside, N. Y. (2 memberships)
Tennessee Products & Chemical Corp., Nashville, Tenn.
Texas Instruments, Inc., Dallas, Texas
Three Point Four Corp., Yonkers, N. Y.
Titanium Metals Corp. of America, Henderson, Nev.
Udylite Corp., Detroit, Mich. (4 memberships)
Universal-Cyclops Steel Corp., Bridgeville, Pa.
Upjohn Co., Kalamazoo, Mich.
Victor Chemical Works, Chicago, Ill.
Western Electric Co., Inc., Chicago, Ill.
Wyandotte Chemicals Corp., Wyandotte, Mich.
Yardney Electric Corp., New York, N. Y.

ONE new dry acid does NINE jobs better

ENTH-ACID 82

A free-flowing powdered blend of acid salts, activators and surfactants. Water soluble. Packed in non-returnable containers. Less expensive than 50% muriatic acid, superior activating and wetting ability. No special equipment needed. No special handling or safety problems. Non-fuming at room temperatures. Produces cleaner activated surfaces that allow shorter plating times.

1. Strips chromium rapidly without current
2. Prevents cloudy, stained nickel plate
3. Provides good adhesion on zinc die castings, copper and brass
4. Descales heat-treated, welded, or brazed steel without attack
5. Allows re-nickel plating on top of old passive nickel plate
6. Dissolves red rust
7. Activates steel prior to plating or phosphating
8. Prepares cast iron for plating
9. Removes soldering flux

Write today for complete technical data. Enthone, Inc., 442 Elm Street, New Haven, Conn.

ASARCO

ANOTHER PRODUCT OF Enthonics RESEARCH

ENTHONE

A Subsidiary of American Smelting and Refining Company